U.S. Department
of Commerce

Volume 94
Number 2
April 1996

Fishery Bulletin

U.S. Department of Commerce
Ronald H. Brown
Secretary

National Oceanic and Atmospheric Administration
D. James Baker
Under Secretary for
Oceans and Atmosphere

National Marine Fisheries Service
Rolland A. Schmitten
Assistant Administrator
for Fisheries

Fishery Bulletin

Scientific Editor
Dr. John B. Pearce

Editorial Assistant
Kimberly T. Murray
Northeast Fisheries Science Center
National Marine Fisheries Service, NOAA
166 Water Street
Woods Hole, Massachusetts 02543-1097

Editorial Committee
Dr. Andrew E. Dizon National Marine Fisheries Service
Dr. Harlyn O. Halvorson University of Massachusetts, Dartmouth
Dr. Ronald W. Hardy National Marine Fisheries Service
Dr. Linda L. Jones National Marine Fisheries Service
Dr. Richard D. Methot National Marine Fisheries Service
Dr. Theodore W. Pietsch University of Washington
Dr. Joseph E. Powers National Marine Fisheries Service
Dr. Fredric M. Serchuk National Marine Fisheries Service
Dr. Tim D. Smith National Marine Fisheries Service

Managing Editor
Sharyn Matriotti
National Marine Fisheries Service
Scientific Publications Office
7600 Sand Point Way NE, BIN C15700
Seattle, Washington 98115-0070

The *Fishery Bulletin* (ISSN 0090-0656) is published quarterly by the Scientific Publications Office, National Marine Fisheries Service, NOAA, 7600 Sand Point Way NE, BIN C15700, Seattle, WA 98115-0070. Second class postage is paid in Seattle, Wash., and additional offices. POSTMASTER send address changes for subscriptions to Fishery Bulletin, Superintendent of Documents, Attn: Chief, Mail List Branch, Mail Stop SSOM, Washington, DC 20402-9373.

Although the contents have not been copyrighted and may be reprinted entirely, reference to source is appreciated.

The Secretary of Commerce has determined that the publication of this periodical is necessary in the transaction of the public business required by law of this Department. Use of funds for printing of this periodical has been approved by the Director of the Office of Management and Budget.

For sale by the Superintendent of Documents, U.S. Government Printing Office, Washington, DC 20402. Subscription price per year: $27.00 domestic and $33.75 foreign. Cost per single issue: $13.00 domestic and $16.25 foreign. **See back page for order form.**

The *Fishery Bulletin* carries original research reports and technical notes on investigations in fishery science, engineering, and economics. The Bulletin of the United States Fish Commission was begun in 1881; it became the Bulletin of the Bureau of Fisheries in 1904 and the Fishery Bulletin of the Fish and Wildlife Service in 1941. Separates were issued as documents through volume 46; the last document was No. 1103. Beginning with volume 47 in 1931 and continuing through volume 62 in 1963, each separate appeared as a numbered bulletin. A new system began in 1963 with volume 63 in which papers are bound together in a single issue of the bulletin. Beginning with volume 70, number 1, January 1972, the *Fishery Bulletin* became a periodical, issued quarterly. In this form, it is available by subscription from the Superintendent of Documents, U.S. Government Printing Office, Washington, DC 20402. It is also available free in limited numbers to libraries, research institutions, State and Federal agencies, and in exchange for other scientific publications.

U.S. Department
of Commerce
Seattle, Washington

Volume 94
Number 2
April 1996

Fishery Bulletin

Contents

Articles

199 **Baelde, Pascale**
Biology and dynamics of the reproduction of blue-eye trevalla, *Hyperoglyphe antarctica* (Centrolophidae), off Tasmania, southern Australia

212 **Brodziak, Jon K. T., and William K. Macy III**
Growth of long-finned squid, *Loligo pealei,* in the northwest Atlantic

237 **Caillouet, Charles W., Jr., Donna J. Shaver, Wendy G. Teas, James M. Nance, Dickie B. Revera., and Andrea C. Cannon**
Relationship between sea turtle stranding rates and shrimp fishing intensities in the northwestern Gulf of Mexico: 1986–1989 versus 1990–1993

250 **DeMartini, Edward E., Frank A. Parrish, and Denise M. Ellis**
Barotrauma-associated regurgitation of food: implications for diet studies of Hawaiian pink snapper, *Pristipomoides filamentosus* (family Lutjanidae)

257 **Dorsey, Suzanne E., Edward D. Houde, and John C. Gamble**
Cohort abundances and daily variability in mortality of eggs and yolk-sac larvae of bay anchovy, *Anchoa mitchilli,* in Chesapeake Bay

268 **Fortier, Louis, and Ann Villeneuve**
Cannibalism and predation on fish larvae by larvae of Atlantic mackerel, *Scomber scombrus:* trophodynamics and potential impact on recruitment

282 **Krieger, Kenneth J., and Michael F. Sigler**
Catchability coefficient for rockfish estimated from trawl and submersible surveys

The National Marine Fisheries Service (NMFS) does not approve, recommend, or endorse any proprietary product or proprietary material mentioned in this publication. No reference shall be made to NMFS, or to this publication furnished by NMFS, in any advertising or sales promotion which would indicate or imply that NMFS approves, recommends, or endorses any proprietary product or proprietary material mentioned herein, or which has as its purpose an intent to cause directly or indirectly the advertised product to be used or purchased because of this NMFS publication.

289 **Laidig, Thomas E., Keith M. Sakuma, and Mary M. Nishimoto**
Description of pelagic larval and juvenile stripetail rockfish, *Sebastes saxicola* (family Scorpaenidae), with an examination of larval growth

300 **Lavaniegos, Bertha E.**
Vertical distribution of euphausiid life stages in waters adjacent to Baja California

313 **Newman, Stephen J., David McB. Williams, and Garry R. Russ**
Variability in the population structure of *Lutjanus adetii* (Castelnau, 1873) and *L. quinquelineatus* (Bloch, 1790) among reefs in the central Great Barrier Reef, Australia

330 **Perkins, Peter C., and Elizabeth F. Edwards**
A mixture model for estimating discarded bycatch from data with many zero observations: tuna discards in the eastern tropical Pacific Ocean

341 **Sminkey, Thomas R., and John A. Musick**
Demographic analysis of the sandbar shark, *Carcharhinus plumbeus,* in the western North Atlantic

348 **Somerton, David, A., and William Donaldson**
Contribution to the biology of the grooved and triangle Tanner crabs, *Chionoecetes tanneri* and *C. angulatus,* in the eastern Bering Sea

358 **Zimmerman, Mark, and Pamela Goddard**
Biology and distribution of arrowtooth, *Atheresthes stomias,* and Kamchatka, *A. evermanni,* flounders in Alaskan waters

Notes

371 **Bertram, Douglas F.**
Size-dependent predation risk in larval fishes: mechanistic inferences and levels of analysis

374 **Franks, James S., Nikola M. Garber, and James R. Warren**
Stomach contents of juvenile cobia, *Rachycentron canadum,* from the northern Gulf of Mexico

381 **Read, Andrew J., John R. Nicolas, and James E. Craddock**
Winter capture of a harbor porpoise in a pelagic drift net off North Carolina

385 *Erratum*

386 *Subscription form*

Biology and dynamics of the reproduction of blue-eye trevalla, *Hyperoglyphe antarctica* (Centrolophidae), off Tasmania, southern Australia

Pascale Baelde

Marine Resources Division, Department of Primary Industry and Fisheries
Nubeena Crescent, Taroona, Tasmania 7053, Australia

Abstract.—The reproduction of blue-eye trevalla, *Hyperoglyphe antarctica*, off Tasmania, southern Australia, is studied in detail through analysis of gonad maturation, spawning location and season, size at maturity, fecundity, and spawning frequency.

Results show that the fecundity of blue-eye trevalla is determinate, and it has a high annual fecundity which increases exponentially with the length of females (to a maximum of about 11 million oocytes). Females are partial spawners and possibly spawn all their oocytes in 3 or 4 large batches, the size of batches increasing with the length of females. Both sexes reach sexual maturity at large sizes, 71.3 and 61.6 cm fork length for females and males, respectively. One major spawning ground was identified off Tasmania where blue-eye trevalla aggregate from October to May. Smaller fish join the aggregation first, at early stages of gonad maturation, whereas larger fish appear to join the aggregation later, just prior to spawning. Spawning takes place at the end of summer–autumn (early March to early May).

Manuscript accepted 21 November 1995.
Fishery Bulletin 94:199–211 (1996).

Blue-eye trevalla, *Hyperoglyphe antarctica* (Centrolophidae) are widely distributed in the southern oceans, from New Zealand to southern Australia, South Africa, and the southern Indian Ocean (Haedrich, 1967; McDowall, 1982). In Australia, they are found from central New South Wales to southern western Australia (Fig. 1) and on offshore seamounts. The fishery has developed off southeast Australia, particularly off Tasmania (Fig. 1). Fishing is traditionally done with drop-lines on hard sea bottom associated with the continental shelf break, at depths between 300 and 500 m. Commercial landings are relatively small (about 800 metric tons per year), but blue-eye trevalla is an excellent table fish and fresh fish fetch high prices on the domestic market.

In the late 1980's, a conflict arose between traditional line fishermen and trawl fishermen who intended to develop mid-water trawling techniques to target blue-eye trevalla. At that time, there was limited information on the biology and size of the resource, and it was feared that mid-water trawling would increase fishing effort to unsustainable levels. As a result, a research program was implemented in 1991 to study the biology of blue-eye trevalla off Tasmania. Anecdotal information on the breeding season of this species was available from Jones[1] in South Australia and from Horn and Massey (1989) in New Zealand; no fecundity study had been undertaken. In this paper the reproductive biology (gonad maturation, size at maturity, spawning frequency, and fecundity) and the composition and dynamics of the main spawning aggregation are studied in detail, and a discussion is provided on some of the implications for the fishery.

Materials and methods

Sampling

Blue-eye trevalla were collected on board commercial vessels during drop-line fishing operations, between November 1991 and July 1993. Drop-lines are polypropylene lines that are anchored with a weight to the sea bottom at depths between 300 and 500 m and that are supported vertically by boys. Ten to 15 lines are used during fishing, each carrying about 100 hooks. At least one sample was obtained each

[1] Jones, G. K. 1988. The biological status of the deepsea trevalla (*Hyperoglyphe antarctica*) offshore line fishery in South Australian waters. Department of Fisheries, South Australia, discussion paper, April 1988, 15 p.

month from most fishing grounds around Tasmania (Fig. 1). A sample represented the total catch made during one fishing trip (of 1–3 day duration) on the same ground. Fish were examined individually as they were hauled on deck, and the entire catch (or the majority of it) was processed during each fishing trip (representing between 50 and 500 fish). Fish were measured (fork length [FL]) to the nearest cm below the true length, sexed, and staged macroscopically by using the maturity stages described in Table 1 (adapted from Hunter and Macewicz, 1985, a and b; Schaefer, 1987; West, 1990). To calculate the gonadosomatic index (GSI), ovaries and testes were collected to be weighed in the laboratory to the nearest 0.1 g. The GSI was calculated as the proportion of gonad weight divided by body weight with the following length-weight relationship: Log (*gutted weight*) = 3.081 × Log (*fork length*) –4.385, where weight is in g and length in cm (Baelde, unpubl. data). For later histological examination and measurement of whole oocytes, ovaries at various stages of maturity were preserved in Davidson's solution immediately after the catch. Nearly all mature ovaries (stages 4 to 6, Table 1) were preserved.

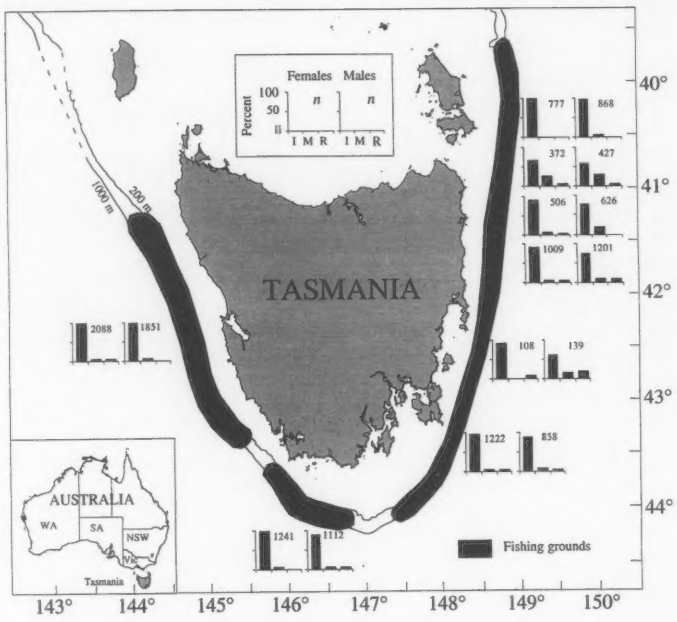

Figure 1

Proportions (as a percentage) by sex of immature (I), mature (M), and resting (R) blue-eye trevalla, *Hyperoglyphe antarctica*, in samples collected from major fishing grounds around Tasmania. I = stages 1 to 3 for females, 1 to 2 for males; M = stages 4 to 6 for females, 3 and 4 for males; and R = stages 7 and 8 for females, stage 5 for males. Depth contours in meters. WA = Western Australia, SA = South Australia, Vic = Victoria, and NSW = New South Wales. Numbers in graphs are the number of fish sampled.

Histological staging of ovaries

A total of 447 ovaries were examined histologically to check macroscopic staging and to note the presence of atretic oocytes and postovulatory follicles (see description in Table 1; Fig. 2; Fig. 3, A and B). Ovary sections were stained in haematoxylin and eosin and ovaries were staged on the basis of the most advanced type of oocytes present, regardless of their abundance (West, 1990).

Size at maturity

The average size at maturity ($FL_{0.5}$) was the size at which 50% of the fish caught during the breeding season were mature (i.e. stages 4 to 6 for females, and stages 3 and 4 for males). For each sex, the proportion (p) of mature individuals, by 1-cm fork length intervals, was fitted to the logistic function

$$p = e^{(a+bFL)} / \left(1+e^{(a+bFL)}\right)$$

by using generalized linear models (Genstat 5 Reference Manual). The average size at maturity was also estimated for length and maturity data collected off the east coast of Tasmania during the 1950's (Cowper and Downie[2]).

Spawning frequency and fecundity

Hunter et al. (1992) have identified three main factors that can affect fecundity estimates: 1) the rate of atresia in reducing the number of oocytes spawned; 2) the occurrence of previous spawnings (as shown by the presence of postovulatory follicles); and 3) the accurate identification of which oocytes to include in estimating fecundity. These three factors were examined as shown below.

Rate of atresia The proportion of atretic oocytes was determined in ovaries at various stages of maturity

[2] Cowper, T. R., and R. J. Downie. 1995. CSIRO, Division of Fisheries and Oceanography, Cronulla, New South Wales, Australia. Unpubl. data.

Table 1

Female and male blue-eye trevalla, *Hyperoglyphe antarctica,* maturity stages based on macroscopic and histological examination. Adapted from Hunter and Macewicz (1985, a and b); Schaefer (1987); West (1990); Hunter et al. (1992); Davis and West (1993).

Females

Stage	Macroscopic description	Histological description	Oocyte development
1 **Immature**	Small thread-like ovaries, pink and translucent;	Chromatin nucleolar stage: very small oocytes, nucleus surrounded by a thin layer of dark-blue-stained cytoplasm;	
2 **Early developing**	Oocytes not visible, ovaries pink and translucent; *First-time developing females:* ovaries up to 10 cm long, 1 cm across, ovary wall thin and transparent; *Redeveloping females:* ovaries up to 20 cm long, 5 cm across, flaccid, ovary wall thick, whitish, and opaque;	Perinucleolar stage: oocyte size increases slightly as dark-blue-stained cytoplasm thickens, nucleoli appear at the periphery of nucleus;	Cytoplasm homogeneous, brownish and transparent, comparatively large dark nucleus;
3 **Developing**	Small oocytes becoming visible, still translucent, ovaries occupy less than 20% of body cavity;	Cortical alveoli stage: appearance of cortical alveoli in pale-blue-stained cytoplasm, pink-stained zona radiata distinguishable, oil vesicles appearing, lampbrush chromosomes often visible in the nucleus;	Oocytes more or less spherical, cytoplasm thickened, darker, granular, but still translucent, nucleus still visible;
4 **Late developing (yolked)**	Small opaque oocytes clearly visible, marked increase in ovary size (20% to 100% of body cavity) and change from pink to yellow-orange color, ovary wall thin and transparent;	Yolk stage: marked increase in oocyte size, cytoplasm filled with pink-stained yolk granules, cortical alveoli and oil vesicles increase in size and number; degenerating postovulatory follicles visible if spawning has started;	Oocytes dark, completely opaque, size increasing with development, nucleus occluded; degenerating postovulatory follicles visible if spawning has started;
5 **Ripe**	Ovary size as in previous stage, large transparent (hydrating) oocytes visible among smaller opaque oocytes;	Nuclear migration stage: migration of nucleus to periphery of oocyte, fusion of yolk granules into yolk plates; fusion of oil vesicles into the oil droplet; degenerating postovulatory follicles visible if spawning has started;	Occurrence of partly translucent oocytes (hydrating), yolk plates visible;degenerating postovulatory follicles visible if spawning has started;
6 **Running-ripe**	Ovary size as in previous stage, hydrated oocytes larger, easily expressed from ovaries;	Hydration stage: further increase in size of oocytes, all yolk granules fused into a few plates;	Occurrence of very large, almost totally translucent oocytes, oil droplet visible;
7 **Spent**	Ovaries flaccid, occupy about 20% of body cavity, greyish ovary wall thickened and wrinkled, some residual oocytes visible within translucent material;	Postovulatory follicles clearly visible, no yolked oocytes left except for a few undergoing atresia; structure of ovaries generally loose, hydrated oocytes may be present in lumen;	Postovulatory follicles visible, remaining yolked oocytes at early stage of atresia;

continued

Table 1 (continued)

Females (continued)

Stage	Macroscopic description	Histological description	Ooycte development
8 Resting	Aspect of ovaries as in previous stage, not accurately distinguishable.	Oocytes at stages 2 and 3 predominate, no trace of postovulatory follicles left, advanced atresia of remaining yolked oocytes, hydrated oocytes sometimes still present in lumen.	Very small oocytes (stages 2 and 3) predominate, advanced atresia of remaining yolked oocytes.

Males

Stage	Macroscopic description
1 Immature	Testes very small, flat, and threadlike;
2 Early developing	Testes increase in size, rounder in shape;
3 Developing	Size of testes increases further, lobed in formation and marked groove in the middle of each testis visible, creamy or white milt sometimes present;
4 Late developing to running-ripe	Testes very large and multilobed, white or pinkish, sometimes bloodshot, free-flowing milt;
5 Spent and resting	Testes much smaller, very bloodshot, milt sometimes present, become thinner, brownish and rubbery as they regress to resting stage.

by using samples preserved in Davidson's solution. Only early stages of atresia (stages alpha and beta as described by Hunter and Macewicz, 1985b) were considered (Fig. 3, B, C, and D); oocytes at later stages of atresia are too difficult to identify with commonly used histological techniques.

Occurrence of postovulatory follicles The presence of postovulatory follicles in ovaries was used to identify females that had begun to spawn. In addition, examination of morphological changes in postovulatory follicles after ovulation (as described by Hunter and Macewicz, 1985b; Schaefer, 1987; Macewicz and Hunter, 1993) provided information on spawning frequency. Postovulatory follicles were classified into two types according to the degree of resorption visible in histological sections. Type-1 postovulatory follicles (Fig. 3A) were more recent, presenting an involuted zona radiata with numerous folds and an open cavity, as well as granulosa cells aligned within the zona radiata; type-2 postovulatory follicles were small, had fewer involutions, and showed a much more reduced follicular cavity; at that stage the zona radiata has thickened markedly and the granulosa cells are disorganized. When present in ovaries, 50 postovulatory follicles were randomly measured (along the perimeter) with NIH image analysis software.

Staging and measurement of whole oocytes Staging and measurement of whole oocytes was used to assess whether the fecundity of blue-eye trevalla is determinate or indeterminate, that is, whether yolk formation is completed before spawning starts or continues after (Hunter et al., 1985). This information is needed to know whether the annual fecundity of blue-eye trevalla can be estimated from a standing stock of yolked oocytes (i.e. vitellogenic) present in ovaries. Subsamples of ovaries preserved in Davidson's solution were mixed in small jars with water and 3-mm glass beads and shaken manually to dissociate the oocytes. All ovaries used had been previously staged histologically, and histological sections were used to stage corresponding whole oocytes under a microscope (see description in Table 1 and Fig 3, C and D, adapted from West, 1990; Hunter et al., 1992; Davis and West, 1993). Fifty oocytes were measured (along the maximum diameter) for 135 females at various stages of maturity. Figure 3D also shows whole, preserved postovulatory follicles of type 1 (type 2 were too small to be properly dissected and photographed).

Fecundity estimation Only ovaries that showed no sign of previous spawnings (absence of postovulatory follicles), no sign of major atresia, and in which oocytes were fully yolked (as indicated by their diam-

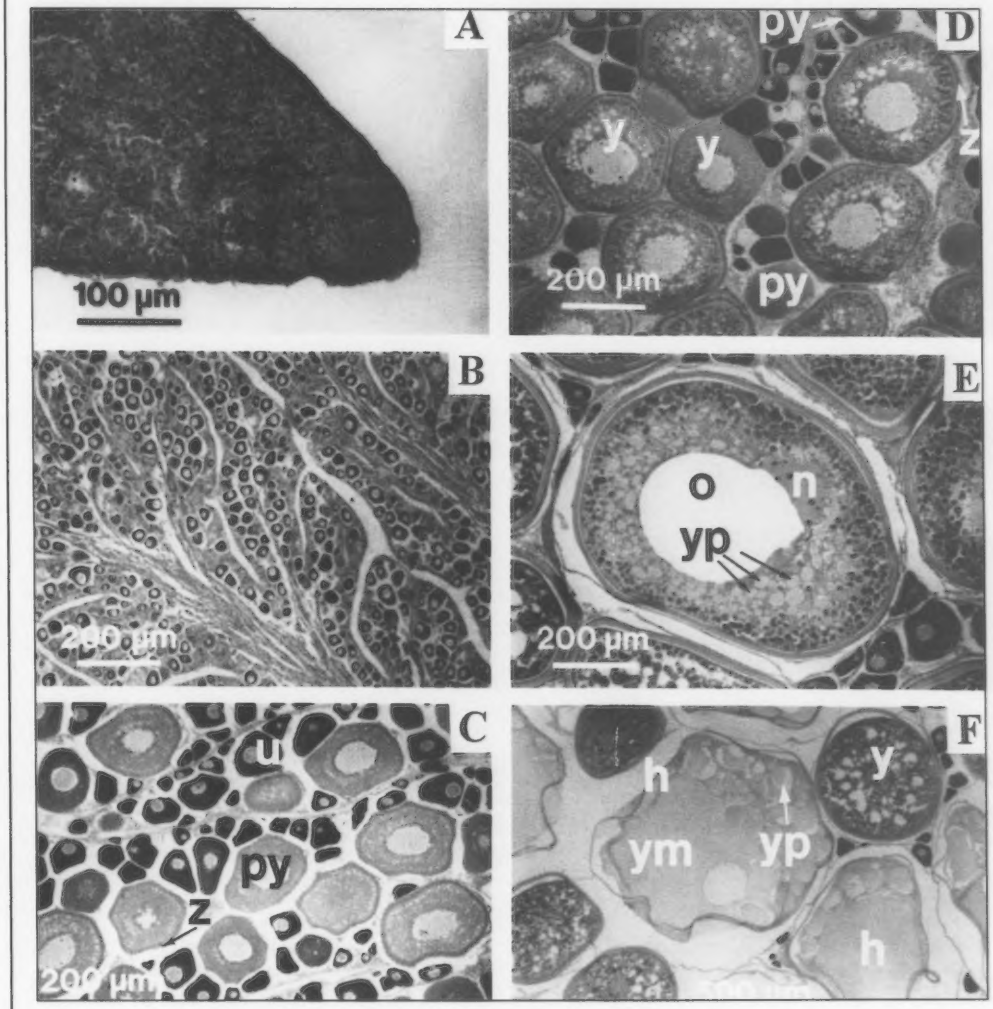

Figure 2

Histological sections showing ovary maturation stages of blue-eye trevalla, *Hyperoglyphe antarctica*. (**A–F**) represent stages 1–6 successively. (D) shows an "early stage 4" characterized by the nonuniform size of yolked oocytes. h = hydrating oocyte (irregular shape due to loss of fluid during histological processing); n = nucleus; o = oil droplet; py = partially yolked oocyte; u = unyolked oocyte; y = yolked oocyte; ym = yolk mass (fusion of yolk plates); yp = yolk plate; z = zona radiata.

eter, see below) were used to estimate the annual fecundity of blue-eye trevalla. Before estimating fecundity, a check was made that the oocytes were uniformly distributed within the ovaries. From five fish, the number of oocytes per gram was compared between subsamples taken across the ovaries (near the periphery and near the center) and along the ovaries (within the anterior, median, and posterior regions). ANOVA showed no differences between subsamples across the ovaries (F=0.68, df=1,4, P=0.42), or between subsamples along the ovaries (F=0.74, df=2,8, P=0.49). Oocytes were then routinely dissociated and counted from three weighed subsamples taken randomly within the ovaries.

Batch fecundity was estimated for eight ripe females by estimating the number of hydrated oocytes;

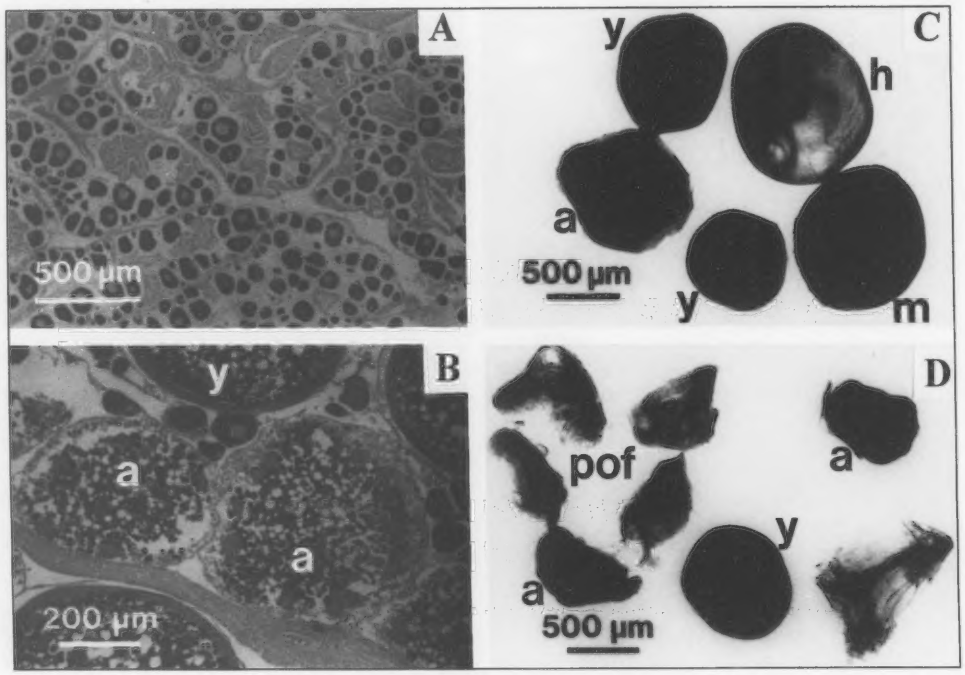

Figure 3

Histological sections of the ovary of blue-eye trevalla, *Hyperoglyphe antartica*. (**A**) Histological section of ovary at stage 7 showing type-1 postovulatory follicles. (**B**) Histological section showing two yolked oocytes at early alpha-stage atresia (a) and a healthy yolked oocyte (y). (**C**) and (**D**) show whole preserved oocytes. (C) shows an oocyte at alpha-stage of atresia (a), stage-4 yolked oocytes (y), a stage-5 oocyte (m) (yolked plates only faintly visible in this photo), and a hydrating oocyte (h) with oil droplet. (D) shows postovulatory follicles (pof) of type 1 and yolked oocytes at an early stage of atresia (a).

only ovaries in which hydrated oocytes formed a well-defined mode were used. Also, the number of yolked oocytes remaining in partially spent ovaries was determined for 24 females.

Results

Gonad maturation

Ovaries at stages 1 and 2 could not be distinguished accurately by macroscopic examination and were grouped together in the analyses, as were stages 7 and 8. GSI values varied greatly within maturity stages (Table 2) and could not be used alone to assess the development of ovaries. Macroscopic staging of the testes was more difficult than that for the ovaries (Table 1). The main criterion used to assess male maturity development, based on the presence or absence of milt, was not consistent. As already observed by Horn and Massey (1989) in New Zealand, milt was sometimes present in small, developing testes but absent in large testes.

Histological examination of stage-4 ovaries led to the distinction, within this stage, of ovaries at an early stage of yolk formation. These ovaries were characterized by a great variation in the size of oocytes (Fig. 2D) compared with the uniform size of fully yolked oocytes. They will be referred to as "early stage 4" in the text. Partially spent ovaries (i.e. stage-4 or stage-5 ovaries containing postovulatory follicles and which were not identifiable macroscopically) will be referred to as stages 4^* and 5^*.

Spawning location and season

Mature fish of both sexes (stages 4–6 for females and stages 3–4 for males) were caught mostly off the northeast coast of Tasmania, at about 41°S (Fig. 1), but a few were occasionally caught in other areas.

Table 2

Range and median value of female gonadosomatic index (GSI) by stage of maturity for blue-eye trevalla, *Hyperoglyphe antarctica*. * indicates partially spent ovaries (presence of postovulatory follicles). Standard deviations are in parentheses. *n* = sample size.

	Gonadosomatic index		
Stage	Range	Mean	*n*
1+2	0.2–1.1	0.4 (0.2)	58
3	0.3–2.0	0.8 (0.3)	203
Early 4	1.6–12.0	5.2 (2.5)	19
4	3.3–19.5	10.2 (3.1)	92
4*	3.3–15.9	9.5 (3.8)	18
5	8.9–19.4	13.9 (4.7)	5
5*	5.1–14.8	10.0 (3.5)	6
6	20.6	—	1
7	1.6–3.8	2.5 (0.6)	8
8	0.7–2.5	1.5 (0.4)	66
Atretic	0.7–8.1	1.8 (1.6)	21

Table 3

Average size at maturity ($FL_{0.5}$) by sex, and 95% confidence limits for blue-eye trevalla, *Hyperoglyphe antarctica*. Data were fitted to the logistic equation shown in text. Results are shown for data collected during the current study and for data collected in the mid 1950's before the fishery developed (from Cowper and Downie's unpubl. data). CL = confidence limits.

	n	*a*	*b*	$FL_{0.5}$	95% CL
Current data					
Females	1803	–29.86	0.419	71.3	70.7–71.9
Males	1613	–21.06	0.342	61.6	61.2–62.1
Cowper and Downie's data					
Females	813	–23.79	0.341	69.8	69.2–70.3
Males	498	–24.05	0.397	60.6	59.6–61.4

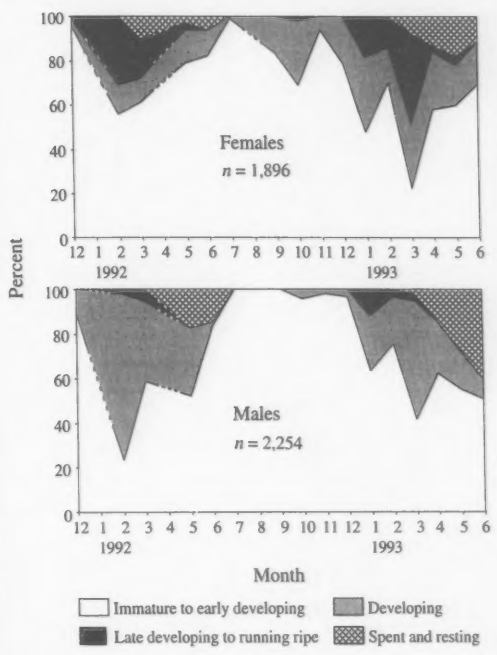

Figure 4

Monthly proportions (as a percentage) of maturity stages by sex for blue-eye trevalla, *Hyperoglyphe antarctica*. *n* = sample size.

Off northeast Tasmania, and over the 20-month sampling period, mature fish were caught in small numbers between October and December; then their abundance increased markedly between January and March (Fig. 4). Stage-4 females caught from October to December 1992 were at early stage of yolk formation (early stage 4) with a low GSI ranging from 1.6 to 2.3. GSI values then increased to a mean of 5.6 (with a standard deviation [SD] of ±2.3) in January, 8.0 (±2.9) in February, and 9.4 (±2.7) in March, 1993. In both 1992 and 1993, ripe (stage-5) and partially spent (stage-4* and stage-5*) females were caught from early March to early May; females in postspawning condition (stages 7 and 8) were caught from mid-March, their maximum abundance occurring in May and June (66.3% of the total 445 postspawning females examined). Thus, maturation of ovaries spanned several months, from October to February, and actual spawning apparently took place from early March to early May.

Size at maturity

The smallest mature female observed during the present study was 59 cm FL, and the smallest mature male was 52 cm FL. The estimated average sizes at maturity were 71.3 and 61.6 cm FL for females and males, respectively (Table 3; Fig. 5). These sizes were very similar to those estimated from data collected in the mid 1950's (Table 3).

Rate of atresia

The rate of atresia for both unyolked and yolked oocytes was generally low (atretic oocytes represented between 1 and 10% of all oocytes when present). However, a few ovaries presented a high level of atresia (about 90%) of their yolked oocytes. These atretic

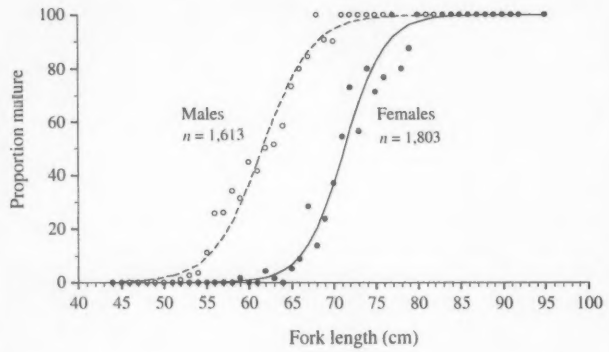

Figure 5

Relative abundance of mature individuals of blue-eye trevalla, *Hyperoglyphe antarctica* (stages 4–6 for females, stages 3–4 for males) by 1-cm size intervals. Data were fitted to the logistic equation shown in text. Black dots represent females; white dots represent males; and n = sample size.

ovaries were of two types. The first type consisted of small ovaries with abundant white oocytes visible macroscopically within a translucent, pinkish mass of unyolked oocytes. Histological examination later revealed that the white oocytes were oocytes at an early stage of yolk formation and were undergoing atresia. This type of ovary was observed in May and June 1992 and 1993, and represented 64% of all yolked ovaries examined during these periods. It was always observed in preadult females at size below the average size at maturity (mean FL=63.6 cm [±3.2 cm SD]).

Only two females presented the second type of atretic ovaries; they had large ovaries (GSI of 6.9 and 8.1) and nearly all fully yolked oocytes were at an early stage of atresia. These atretic oocytes could not be detected macroscopically, but they were recognizable microscopically in preserved samples (Fig. 3, C and D). The two females were caught during the spawning period in March 1993; they represented only 1.2% of all mature ovaries examined histologically.

Occurrence of postovulatory follicles

Postovulatory follicles were found in 16.8% of all mature ovaries examined (n=167). They were never found in ovaries at early stage of yolk formation. Both type-1 and type-2 postovulatory follicles were usually present in stage 4*, whereas only type-2 postovulatory follicles were found in hydrating ovaries (stage 5*) (Fig. 6).

Measurement of whole oocytes

As maturation progressed, a clear gap appeared between unyolked and yolked oocytes (Fig. 7, A–D), showing that the fecundity of blue-eye trevalla is determinate. The recruitment of oocytes from the reserve of unyolked oocytes was completed when the average diameter of yolked oocytes reached about 650 μm (Fig. 7E). Unyolked oocytes present in these ovaries were at stage 2 and had a diameter of less than 100 μm (the gap in size between unyolked and yolked oocytes was clear and unyolked oocytes were no longer measured in most advanced ovaries). The diameter of yolked oocytes then increased slightly to about 700 μm (Fig. 7G) before migration of the nucleus and hydration began (Fig. 7. H–I). After a batch was spawned, formation of a new batch began from the remaining pool of yolked oocytes, showing migration of nucleus and hydration (Fig. 7, J–K). The mean oocyte diameter of stage-4 ovaries used to construct graphs E to G ranged from 500 to 770 μm (having an overall mean of 640 [±60 SD] μm, n=81). Hydrating oocytes observed during the present study were about 1.3 mm (Fig. 7I).

Fecundity

Because fecundity was found to be determinate, annual fecundity was estimated from the standing stock

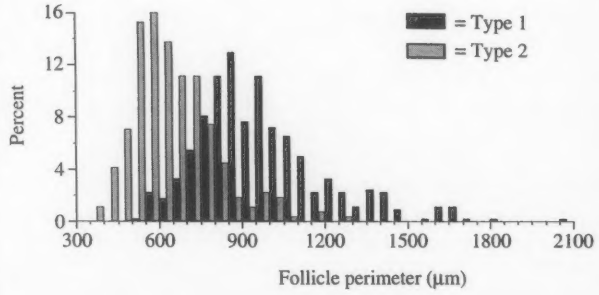

Figure 6

Frequency distributions of the perimeter (micrometers) of type-1 and type-2 postovulatory follicles (pooling of measurements from 16 ovaries) for blue-eye trevalla, *Hyperoglyphe antarctica*.

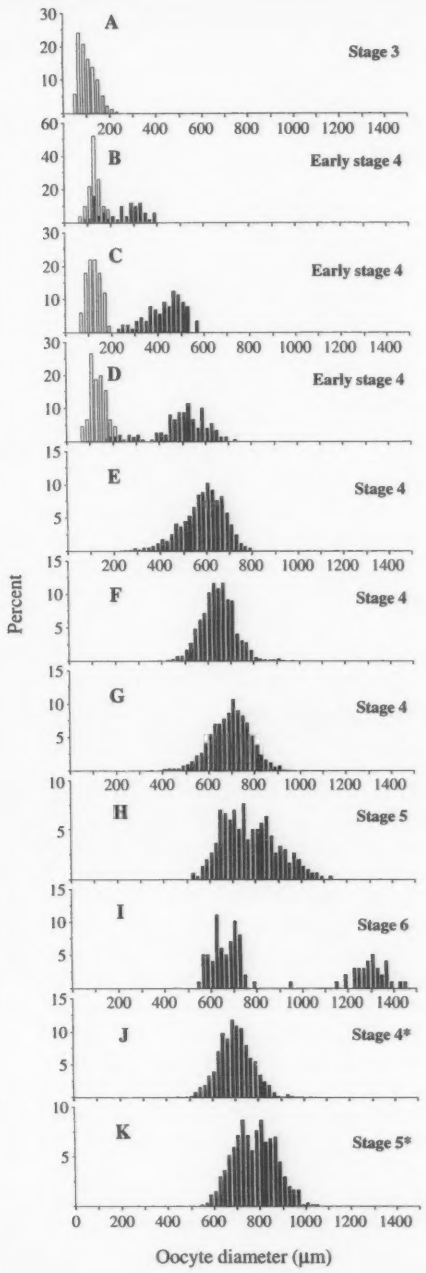

Figure 7

Frequency distribution of oocyte diameter by stage of maturity (measurements from several ovaries pooled in each graph) for blue-eye trevalla, *Hyperoglyphe antarctica*. White and black bars represent independent measurements of unyolked and yolked oocytes, respectively (unyolked oocytes were not measured in stage-4 ovaries from graph E). * = partially spent ovaries.

of yolked oocytes in stage-4 and stage-5 ovaries (Fig. 7, E–H). The fecundity (F) ranged from 1.3 to 11.0 million oocytes per fish, and although varying considerably at given length (Fig. 8), it showed a significant exponential increase with the length (FL) of females, following the equation

$$F = 4.2 \times 10^{-8} \times FL^{4.22},$$

where F is in millions and FL in cm. The linear regression between log-transformed data was statistically significant: F=110.6, df=82; P<0.001, R^2=0.57. Multiple regression analysis showed that the variation in average diameter of yolked oocytes between mature females (as illustrated in Fig. 7, E–H) did not affect fecundity estimates (Table 4). The average relative fecundity was 480 oocytes (±125 SD) per g (gutted weight) and did not show clear trends with the size of fish.

Batch fecundity estimated for ripe females ranged from 0.5 to 2.4 million oocytes (n=8) and also increased with length (Fig. 9). The number of yolked oocytes left in partially spent ovaries ranged from 0.6 to 7.9 million (Fig. 8), with a median value at 2.4 million (n=24).

Spawning aggregation

The bulk of the commercial catch for blue-eye trevalla consisted of small (<55 cm FL), immature fish year

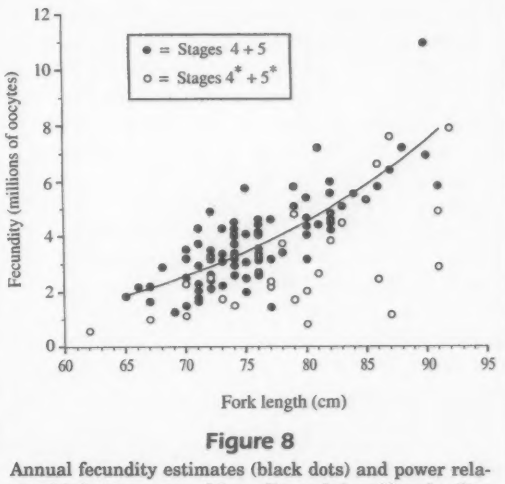

Figure 8

Annual fecundity estimates (black dots) and power relationship between annual fecundity and size of females (line drawn from equation $F = 4.2 \times 10^{-8} \times FL^{4.22}$) for blue-eye trevalla, *Hyperoglyphe antarctica*. Fecundity estimated for partially spent ovaries is also shown (white dots) but was not included in the regression analysis.

Table 4

Multiple regression between log-transformed annual fecundity, fork length (FL, cm), and mean oocyte diameter (micrometers) for blue-eye trevalla, *Hyperoglyphe antarctica*. Sample size = 84, SE = Sampling error.

Source	Partial coefficient	SE	t	P (2-tail)
Constant	–3.942	2.263	–1.742	0.086
Log (*FL*)	4.059	0.437	9.291	0.000
Log (oocyte diameter)	0.228	0.302	0.757	0.451

round, and the proportion of larger fish increased during the breeding season (Fig. 10). The proportion of these large fish (both sexes) increased in catches from 31.1% during the "nonspawning period" (May to December) to 61.3% during the "spawning period" (January to April).

Examination of size composition and sexual maturity data for females >55 cm FL allowed broad distinction of three groups of fish in commercial catches during the breeding season (Fig. 10): 1) preadult females at size below the average size at maturity (i.e. <69 cm FL), most in the developing stage of maturity, but only a few of which would spawn during the current spawning period; 2) females just reaching size at maturity (i.e. between 69 and 75 cm FL), ranging from developing to ripe stages of maturity, about half of which would spawn for the first time during the current spawning period; and 3) large females (i.e. >75 cm FL), most in the fully developed stage of maturity and likely to spawn. Preadult females were caught all around Tasmania from November to May; first-time spawners were caught mainly off the northeast coast of Tasmania and were more abundant between January and April; largest females were also caught primarily off the northeast coast of Tasmania but only during a brief period, from early March to early May, and quickly disappeared from catches afterward (very few were caught in postspawning condition).

For males, several groups could also be distinguished (Fig. 10), although not as clearly as those for females, because of their generally more compact length-frequency distributions.

Preadult females (<69 cm FL) represented as much as 45.6% of all three groups defined above. Similarly, 31.5% of males >55 cm FL had not reached the average size of sexual maturity. In addition, first-time spawners (i.e. mature females at ≤75 cm FL and mature males at ≤65 cm FL) represented as much as 56.7 and 75.9% of all mature females and males, respectively.

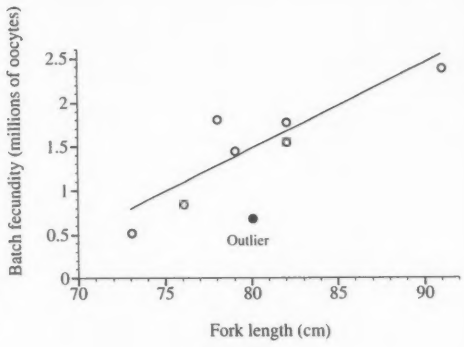

Figure 9

Linear relationship between batch fecundity and size of females for blue-eye trevalla, *Hyperoglyphe antarctica*. Line drawn from the equation *Batch Fec.*= 0.097 × *FL* – 6.28 (F=20.2, df=5, P<0.001, R^2=0.80. R^2 increased from 0.65 to 0.80 when the outlier was excluded from the regression).

Discussion

Ovary maturation, spawning frequency, and fecundity

Maturation of ovaries appears to be group-synchronous for blue-eye trevalla, spanning from spring to summer (October–February) and followed by a brief spawning period in late summer–autumn (early March–early May). As observed for other fish species (Hunter and Macewicz, 1985b), the occurrence of atretic ovaries marks the end of spawning. The timing of spawning coincides well with the discovery, in June 1991 and May 1993, of a few juvenile blue-eye trevalla among floating seaweed off the Tasmanian east coast (Last et al., 1993). These juveniles ranged in size from about 30 to 60 mm standard length and were estimated to be about 2.5 to 3 months old on the basis of daily ring counts of otoliths (Proctor[3]).

Blue-eye trevalla reach sexual maturity at a large size, and according to yet unvalidated age data,[4] females are about 11–12 years old and males about 8–9 years old at sexual maturity. The bulk of immature fish in commercial catches are about 3 to 4 years old. Analysis of data collected in the 1950's showed

[3] Proctor., C. 1994. CSIRO, Division of Fisheries, Hobart, Tasmania. Personal commun.

[4] Morison, S. 1995. Victorian Fisheries Research Institute, Department of Conservation and Natural Resources, P.O. Box 114, Queenscliff 3225, Australia. Unpubl. data.

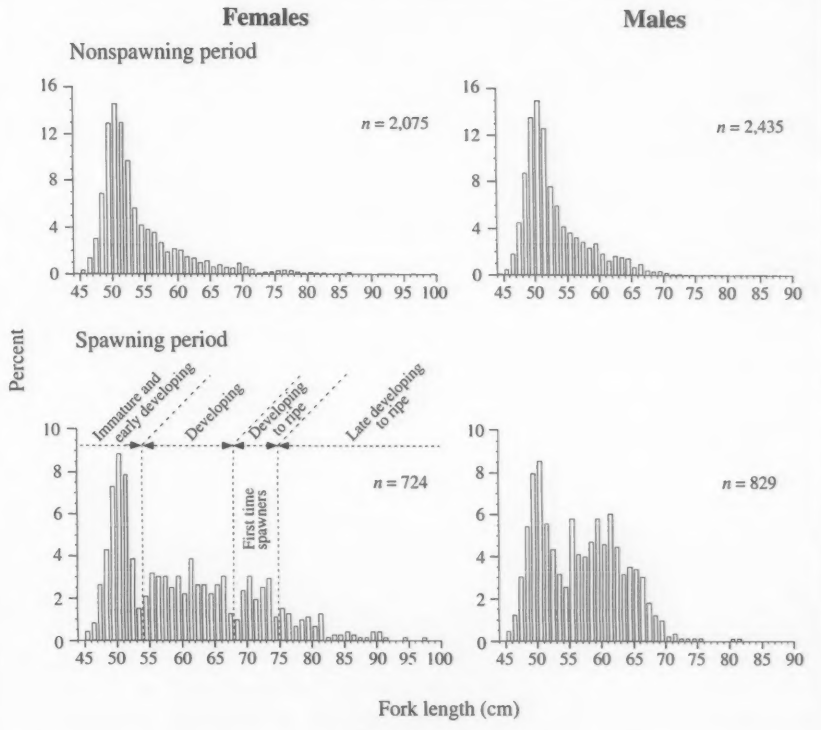

Figure 10

Comparison by sex of frequency distributions between "nonspawning" (May to December) and "spawning" (January to April) periods (years combined) for blue-eye trevalla, *Hyperoglyphe antarctica*. For females, most common maturity status is indicated for different size groups (see text). *n* = sample size.

that there had been no changes in the size at maturity of blue-eye trevalla since the fishery began.

The fecundity of blue-eye trevalla is clearly determinate; several batches of ripe oocytes are formed successively from a standing stock of yolked oocytes. Comparison of annual and batch fecundities suggests that females spawn all their oocytes in 3 or 4 large batches. Several studies (e.g. Macewicz and Hunter, 1993; Oda et al., 1993) have shown that postovulatory follicles usually persist in fish ovaries for short periods (days). The cooccurrence of postovulatory follicles and ripe oocytes in ovaries of blue-eye trevalla also suggests that hydration and ovulation of successive batches could take place within a short period. However, multiple samples taken at short intervals during spawning would be required to age postovulatory follicles accurately.

The average relative fecundity of blue-eye trevalla appears to be fairly high when compared with other middle slope species (e.g. hoki, *Macruronus novaezelandiae* off southern Australia [520 oocytes/g[5]] and sablefish, *Anoplopoma fimbria* off Oregon [110 oocytes/g [Macewicz and Hunter, 1994]). The rate of atresia in ovaries appears to be negligible, and, in the present study, it did not affect fecundity estimates (although this would not necessarily be true for all spawning seasons). The fact that female blue-eye trevalla are partial spawners constitutes more of a problem for estimating fecundity, even more so because spawning batches are large. Partially spent females cannot be identified macroscopically, and to avoid underestimating annual fecundity, it is necessary to check microscopically for the presence of postovulatory follicles in every female before estimating the number of oocytes.

[5] Bulman, C. CSIRO, Division of Fisheries, Hobart, Tasmania. Personal commun.

Composition and dynamics of the spawning aggregation

Blue-eye trevalla in spawning condition were mostly caught off the northeast coast of Tasmania, which may be a major spawning ground. However, the occasional occurrence of mature blue-eye trevalla on nearly all other Tasmanian fishing grounds, including an offshore seamount 120 miles south of Tasmania (data not included), and the presence of spawning aggregations off New South Wales (Rowling[6]) and South Australia (Jones[7]) indicate that spawning takes place on several grounds within southern Australia. The fact that no genetic difference was found between blue-eye trevalla collected off New South Wales, Tasmania, and South Australia (Bolch et al., 1993) further supports the view of a widely distributed spawning activity. Horn and Massey (1989) also believed that blue-eye trevalla spawned on many grounds in New Zealand.

During his work on hoki spawning aggregations, Langley (1993) identified several spawning groups arriving successively and then leaving the spawning ground. The situation is different for blue-eye trevalla, where the three groups of females identified in the summer aggregation seemed to correspond to progressive arrivals of different size (or age) groups and not to commuting spawning groups, spawning taking place at the end of summer. Older females join the aggregation just before spawning and leave shortly after; younger females (first-time spawners) aggregate earlier and stay on the grounds for some time after spawning.

The presence of preadults in the aggregation (i.e. at size below the average size at maturity and, thus, not all capable of spawning) suggests that this summer aggregation off northeast Tasmania is related to both feeding and spawning behaviors. Blue-eye trevalla feed mainly on the pelagic tunicate *Pyrosoma atlanticum* (Winstanley, 1978), and Cowper (1960) noted a maximum incidence of *Pyrosoma* in the stomachs of blue-eye trevalla during the summer. As observed for Atlantic cod, *Gadus morhua* (Swain, 1993), it is possible that blue-eye trevalla off northeast Tasmania migrate between deeper wintering grounds and shallower feeding and spawning summer grounds. The presence of preadult fish on other Tasmanian fishing grounds during spring and summer indicates that feeding aggregations are not restricted to the northeast coast of Tasmania. Winstanley (1979) also noted that blue-eye trevalla off Victoria probably move from deeper to shallower depths in spring.

The spawning population observed in commercial catches was young and the majority were first-time spawners. Larger fish used to be caught by drop-line in the early years of the fishery (Baelde, unpubl. data), and it is not known whether their low proportion in current catches reflects a lower vulnerability to line fishing (owing to age- or size-specific change in distribution and aggregating behavior), or reflects a significant decline in abundance owing to fishing. In addition, it is believed that there is one stock of blue-eye trevalla in southern Australia, and, as shown for other fish species with a wide geographic distribution (Schaefer, 1987; Bell et al., 1992; Rijnsdorp, 1993; Clark et al., 1994), size at maturity, spawning season, and fecundity could vary significantly between areas. Differences in the time of spawning and the size of spawners have already been observed between New South Wales and Tasmania.[6]

This study points out that a proper estimate of the spawning biomass of blue-eye trevalla stock off southern Australia would require fishery-independent surveys (i.e. identification of other spawning grounds and analysis of the age-specific movements of fish during spawning) to determine more accurately the structure and abundance of the spawning population.

[6] Rowling, K. 1994. Fisheries Research Institute, P.O. Box 21, Cronulla, New South Wales, Australia. Personal commun.

[7] Jones, G. K. 1985. An exploratory dropline survey for deepsea trevalla (*Hyperoglyphe antarctica*) in continental slope waters off South Australia. Department of Fisheries, South Australia, Fisheries Research Paper 15, 20 p.

Acknowledgments

This project would not have been possible without the assistance of commercial drop-line fishermen, and I thank them all. I also thank L. Hick, F. Ewing, and A. Brown for their technical assistance at various stages of the project, R. Kennedy for helping with generalized linear models techniques, and finally J. Lyle, G. West, and K. Rowling for reviewing early drafts of the manuscript. This study was partly funded by the Fishing Industry Research Development Council (Project No 91/20).

Literature cited

Bell, J. D., J. M. Lyle, C. M. Bulman, K. J. Graham, G. M. Newton, and D. C. Smith.
1992. Spatial variation in reproduction, and occurrence of non-reproductive adults, in orange roughy, *Hoplostethus atlanticus* Collett (Trachichthyidae), from south-eastern Australia. J. Fish. Biol. 40:107–122.

Bolch, C. J. S., N. G. Elliot, and R. D. Ward.
1993. Enzyme variation in south-eastern Australian samples of the blue-eye or blue-eye trevalla, *Hyperoglyphe*

antarctica Carmichael 1818 (Teleostei: Stromateoidei). Aust. J. Mar. Freshwater Res. 44:687–697.

Clark, M. R., D. J. Fincham, and D. M. Tracey.
1994. Fecundity of orange roughy (*Hoplostethus atlanticus*) in New Zealand waters. N.Z. J. Mar. Freshwater Res. 28:193–200.

Cowper, T. R.
1960. Occurrence of *Pyrosoma* on the continental slope. Nature (London) 187:878–79.

Davis, T. L. O., and G. J. West.
1993. Maturation, reproductive seasonality, fecundity, and spawning frequency in *Lutjanus vittus* (Quoy and Gaimard) from the North West Shelf of Australia. Fish. Bull. 91:224–236.

Haedrich, R. L.
1967. The stromateoid fishes: systematics and a classification. Bull. Mus. Comp. Zool., Harvard Univ. 135:31–139.

Horn, P. L., and B. R. Massey.
1989. Biology and abundance of alfonsino and bluenose off the lower east coast North Island, New Zealand. N.Z. Minist. Agric. Fish. Fish. Tech. Rep. 15, 32 p.

Hunter, J. R., and B. J. Macewicz.
1985a. Measurement of spawning frequency in multiple spawning fishes. *In* R. Lasker (ed.), An egg production method for estimating spawning biomass of pelagic fish: application to the northern anchovy, *Engraulis mordax*, p. 79–94. U.S. Dep. Commer., NOAA Tech. Rep NMFS 36.
1985b. Rates of atresia in the ovary of captive and wild northern anchovy, *Engraulis mordax*. Fish. Bull. 83:119–136.

Hunter, J. R., N. C. H. Lo, and R. J. H. Leong.
1985. Batch fecundity in multiple spawning fishes. *In* R. Lasker (ed.), An egg production method for estimating spawning biomass of pelagic fish: application to the northern anchovy, *Engraulis mordax*, p. 67–77. U.S. Dep. Commer., NOAA Tech. Rep. NMFS 36.

Hunter, J. R., B. J. Macewicz, N. Chyan-huei Lo, and C. A. Kimbrell.
1992. Fecundity, spawning, and maturity of female Dover sole *Microstomus pacificus*, with an evaluation of assumptions and precision. Fish. Bull. 90:101–128.

Langley, A. D.
1993. Spawning dynamics of hoki in the Hokitika Canyon. N.Z. Fish. Tech. Rep. 34, 29 p.

Last, P., C. Bolch, and P. Baelde.
1993. Discovery of juvenile blue-eye. Aust. Fish. 52(8): 16–17.

Macewicz, B. J., and J. R. Hunter.
1993. Spawning frequency and batch fecundity of jack mackerel, *Trachurus symmetricus*, off California during 1991. CalCOFI Rep. 34:112–121.
1994. Fecundity of sablefish, *Anoplopoma fimbria*, from Oregon coastal waters. CalCOFI Rep. 35:160–174.

McDowall, R. M.
1982. The centrolophid fishes of New Zealand (Pisces: Stromateoidei). J. R. Soc. N.Z. 12:103–142.

Oda, D. L., R. J. Lavenberg, and J. M. Rounds.
1993. Reproductive biology of three species of *Paralabrax* (Pisces: Serranidae). CalCOFI Rep. 34:122–132.

Rijnsdorp, A. D.
1993. Relationship between juvenile growth and the onset of sexual maturity of female north sea plaice, *Pleuronectes platessa*. Can. J. Fish. Aquat. Sci. 50:1617–1631.

Schaefer, M. B.
1987. Reproductive biology of black skipjack, *Euthynnus lineatus*, an eastern Pacific tuna. IATTC Bulletin 19:169–260.

Swain, D. P.
1993. Age- and density-dependent bathymetric pattern of Atlantic cod (*Gadus morhua*) in the southern Gulf of St. Laurence. Can. J. Fish. Aquat. Sci. 50:1255–1264.

West, G.
1990. Methods of assessing ovarian development in fishes: a review. Aust. J. Mar. Freshwater Res. 41:199–222.

Winstanley, R. H.
1978. Food of the trevalla *Hyperoglyphe antarctica* (Richardson) off south-eastern Australia (Note). N.Z. J. Mar. Freshwater Res. 12(1):77–79.
1979. Exploratory droplining for deepsea trevalla *Hyperoglyphe porosa* off Victoria. Fisheries and Wildlife Division Paper 23, East Melbourne, Victoria 3002, Australia, 17 p.

Growth of long-finned squid, *Loligo pealei*, in the northwest Atlantic

Jon K. T. Brodziak
Northeast Fisheries Science Center
National Marine Fisheries Service, NOAA
Woods Hole, Massachusetts 02543-1097
Present address: Northwest Fisheries Science Center at
Hatfield Marine Science Center, Newport, Oregon 97365

William K. Macy III
Graduate School of Oceanography
University of Rhode Island
Narragansett, Rhode Island 02882

Abstract.–The application of statolith ageing techniques to long-finned squid, *Loligo pealei*, suggests that this species has a life span of less than one year and grows more rapidly than previously thought. In this study we provide direct estimates of growth for long-finned squid in the northwest Atlantic based on a data set of 353 animals aged by counting putative daily statolith increments. We examine empirical patterns in length and weight at age and estimate parameters of a general growth model. The results indicate that growth rate increases rapidly as squid age and that growth in length and weight is exponential. Although there is substantial heterogeneity in *L. pealei* size at age, sexual dimorphism is evident: males grow more rapidly than do females and achieve larger sizes. Back-calculated hatching dates show that *L. pealei* spawning is not restricted to spring through late-autumn, as previously supposed, but occurs during winter months as well. Differences between growth rates of squid hatched during June–October and November–May are suggested and lend support to the hypothesis that growth can be influenced by seasonal environmental conditions. We discuss the practical implications of our findings for the assessment and management of the long-finned squid stock in the northwest Atlantic.

Manuscript accepted 25 October 1995.
Fishery Bulletin 94:212–236 (1996).

The long-finned squid, *Loligo pealei* (also known as the longfin inshore squid (FAO, 1984), is a pelagic schooling loliginid distributed in continental shelf and slope waters from Newfoundland, Canada (Dawe et al., 1990), to the Gulf of Venezuela (Summers, 1983). A substantial commercial fishery exists in the northwest Atlantic where annual landings averaged 17,300 metric tons (t) during 1963–92, and totalled 22,300 t in 1993 for an ex-vessel value of approximately $30 million (NEFSC, 1995). Recent advances in the use of statolith increments to age squid directly and recent increases in fishing effort in the northwest Atlantic have led to a renewed interest in the life history of this species, and, in particular, its growth rate.

Several estimates of the growth rate of *L. pealei* have been made by comparing modes of length-frequency distributions (Verrill, 1881; Summers, 1968, 1971; Cohen, 1976; Mesnil, 1977; Whitaker, 1978; Lange, 1980; Lange and Sissenwine, 1980; Macy, 1980; Hixon et al., 1981). These studies generally have suggested that growth rate, measured by change in dorsal mantle length (ML), ranged from 10 to 24 mm per month, and that growth rate was dependent upon sex, hatching date, and season (Hixon et al., 1981). Sexual dimorphism was evident; males attained larger sizes than did females (Summers, 1971). Seasonal effects on growth were also suggested; higher growth rates occurred during summer months and lower rates during winter months (Mesnil, 1977). Latitudinal differences in age structure and mean size of *L. pealei* have also been proposed (Summers, 1971), namely that mean size has been suggested to be greater at higher latitudes. These studies, combined with the observed maximum size of approximately 46.5 cm mantle length (Summers, 1968), were consistent with a maximum life span of roughly three years in the northwest Atlantic, a value that was assumed for stock assessment (NEFSC, 1988).

The inferred growth rates of *L. pealei*, based on length-frequency analyses, should be viewed cautiously because they have not been supported by direct ageing data (Caddy, 1991). In general, growth rates of squid might be expected to vary with prey availability (O'Dor et al., 1980), temperature (Forsythe, 1993), and population density

(Dawe, 1988). Squid populations with protracted spawning seasons, such as that of *L. pealei* (Summers, 1971; Macy, 1980), can be composed of numerous broods or microcohorts that may experience different growth and survival rates (Caddy, 1991). As a result, length-frequency samples may consist of several microcohorts with differing growth rates. Migration of microcohorts with differing hatching dates and growth rates to and from an area (e.g. *Illex illecebrosus*, Dawe and Beck[1]; *Illex argentinus*, Arkhipkin, 1993a) may also substantially influence the size composition of a local population, and may bias growth estimates based on length-frequency data (Hatfield and Rodhouse, 1994). Further, postspawning mortality of squid may also influence local size composition if the sampled area is a spawning ground. For these reasons, analysis of length-frequency data may be inadequate in representing the potentially complicated pattern of individual growth within a squid population. Therefore, it is highly desirable to have a method to age individual squid directly.

Statolith ageing techniques (Jereb et al., 1991) have recently provided useful information on the age, growth, and population structure of several squid species (Rodhouse and Hatfield, 1990a; Jackson and Choat, 1992; Arkhipkin, 1993, a and b; Arkhipkin and Nekludova, 1993; Hatfield and Rodhouse, 1994). Ageing of squid, based on counts of fine increments presumed to have daily periodicity, was first developed for *Illex illecebrosus* (Lipinski, 1978) and *Loligo opalescens* (Spratt, 1979) in the late 1970's. Subsequently, studies of several species have indicated that increments within statolith microstructure are formed daily (Dawe et el., 1985; Hurley et al., 1985; Lipinski, 1986; Jackson, 1990, a and b; Jackson et al., 1993), although the mechanisms that regulate increment formation have not yet been determined (Jackson, 1994a).

The application of statolith ageing techniques to *L. pealei* suggests that this species has a life span of less than one year and grows more rapidly than previously thought (Macy, 1995; Macy[2]). In this study we provide estimates of growth rate for *L. pealei* in the northwest Atlantic based on a data set of 353 animals aged by counting putative daily increments on statoliths. We examine empirical patterns in length and weight at age and estimate parameters of a general growth model proposed by Schnute (1981) by squid sex and season of hatching. We discuss some practical implications of our findings for the assessment and management of the stock in the northwest Atlantic.

Materials and methods

Sampling

Data used in this growth study consisted of 353 squid collected during 1991–93. Squid samples were obtained from catches of a commercial fishing vessel[3] and from inshore research surveys in the northwest Atlantic (Table 1; Fig. 1). Samples were flash frozen and stored for subsequent analysis. Basic measurements of mantle length (ML) (to the nearest mm), wet weight (g), and morphometric characters needed to assess maturity stage according to the scheme of Macy (1982a) were taken. Statoliths were dissected from all animals and stored dry in plastic 96-well immunoassay microplates. Statoliths were randomly selected from representative size categories of squid on the basis of observed length-frequency distributions for male, female, and squid of indeterminate sex.

Statolith preparation

Statoliths were prepared by mounting them in a thermoplastic medium (Crystal Bond, Aremco Products; cf. Secor et al., 1991) and by grinding both anterior and posterior surfaces in a manner similar to that described by Jackson (1990a). Several steps were required to prepare a statolith for ageing (Fig. 2). First, a small piece of mounting medium was placed on a petrographic slide (26 × 46 mm) and melted with a hot-air gun. The statolith was then placed in the fluid medium with its concave anterior side down and allowed to cool (Fig. 2B). Material was ground from the exposed convex posterior surface (Fig. 2C) with a graded sequence (12 μm to 3 μm) of water-lubricated abrasive films (Imperial Brand lapping film, 3M Co.) to reveal the nucleus. Progress was monitored throughout the grinding procedure with a stereoscopic dissecting microscope. When the nucleus was clearly revealed, the exposed surface was polished with 0.3-μm aluminum oxide polish (Buehler micropolish) in water on a felt lapidary pad, rinsed with deionized water, and cleaned ultrasonically. After the posterior face was ground, the mounted

[1] Dawe, E. G., and P. C. Beck. 1992. Population structure, growth, and sexual maturation of short-finned squid at Newfoundland, Canada, based on statolith analysis. ICES Council Meeting, Shellfish Committee/K, 33 p.

[2] Macy, W. K., III. 1992. Preliminary age determination of the squid, *Loligo pealei*, using digital imaging. ICES, Shellfish Committee Council Meeting (mimeo), 9 p.

[3] FV *Huntress*, Deep Sea Fish Co., Point Judith, RI.

Table 1

Sample sizes of indeterminate-sex, female, and male long-finned squid, *Loligo pealei*, by collection date, location, source, and sampling gear. In the location field the map code refers to Figure 1. D.E.M. = Department of Environmental Management.

Collection dates	Location (map code)	Source	Sampling gear	Number of squid			
				Indeterminate-sex	Female	Male	Total
1991							
10 Apr	Block Island Sound (1)	Pt. Judith Fishermen's Coop.	Otter trawl[1]	—	7	7	14
10 May	Vineyard Sound (2)	Marine Biological Lab.	Otter trawl[2]	—	2	2	4
13–15 May	Block Island Sound (1)	Rhode Island D.E.M.	Otter trawl[3]	—	1	6	7
16–18 May	Narragansett Bay (1)	W.K. Macy	Dip net[4]	—	1	3	4
22 May	Block Island Sound (1)	Rhode Island D.E.M.	Otter trawl[3]	12	20	12	44
17–18 Jul	Narragansett Bay (1)	Rhode Island D.E.M.	Otter trawl[3]	31	8	6	45
31 Jul	Narragansett Bay (1)	W.K. Macy	Dip net[4]	—	1	2	3
15 Oct	Block Island Sound (1)	Rhode Island D.E.M.	Otter trawl[3]	28	25	27	80
1992							
1 Jan	Hudson Canyon (3)	F/V *Huntress*	Otter trawl[1]	—	—	1	1
9 Jan	Block Canyon (4)	F/V *Huntress*	Otter trawl[1]	—	—	5	5
31 Jan–2 Feb	Block Canyon (4)	F/V *Huntress*	Otter trawl[1]	—	—	2	2
17 Feb	Block Canyon (4)	F/V *Huntress*	Otter trawl[1]	—	—	1	1
11 Mar	Wilmington Canyon (5)	F/V *Huntress*	Otter trawl[1]	—	—	5	5
6–14 May	Narragansett Bay (1)	Univ. Rhode Island	Otter trawl[5]	—	27	23	50
7 Oct	Narragansett Bay (1)	Rhode Island D.E.M.	Otter trawl[3]	4	22	14	40
1993							
7 Feb	Hudson Canyon (3)	F/V *Huntress*	Otter trawl[1]	—	2	4	6
25 Feb–8 Mar	Hudson Canyon (3), Baltimore Canyon (6), and Lydonia Canyon (7)	F/V *Huntress*	Otter trawl[1]	1	22	19	40

[1] Mesh size not reported.
[2] 32-mm mesh.
[3] 6-mm mesh.
[4] Hand-held dip net with SCUBA gear.
[5] 19-mm mesh. Graduate School of Oceanography, Univ. Rhode Island, trawl survey described in Jeffries and Johnson (1974).

statolith was reheated to soften the medium and turned over with a pair of probes constructed of insect pins so that the anterior face could be ground (Fig. 2, C (2) and D). The statolith was oriented with the dorsal dome elevated and the anterior face was carefully ground. When the nucleus was clearly revealed, the anterior face was polished and cleaned.

Because the statolith of *L. pealei* grows outward from the oval-shaped nucleus in a curved manner (Fig. 2, A and B), a second grinding and polishing of the posterior surface (Fig. 2E) was generally needed to reveal the entire sequence of growth increments from the nucleus to the lateral dome (LD) margin. Because of this curvature, no single sectioning plane could have exposed all layers equally well. As a result, the use of the typical two-sided grinding method (Jackson, 1990a; Jereb et al., 1991) would have produced increments that were difficult to resolve. To circumvent this difficulty, the posterior surface was ground a second time (Fig. 2E) at a slightly different angle to approximate the curved statolith growth plane. For squid smaller than 2 cm ML, however, a single grinding of each surface was usually sufficient to reveal the statolith microstructure. After the second posterior grinding, the mounted statolith was reheated, and a thin film of fluid medium was smeared over the uppermost ground surface to improve transparency. As the medium cooled, the LD margin was elevated so that the last-ground plane was approximately parallel to the surface of the slide (Fig. 2F); this was done to improve the clarity of statolith microstructure under a 40× objective lens.

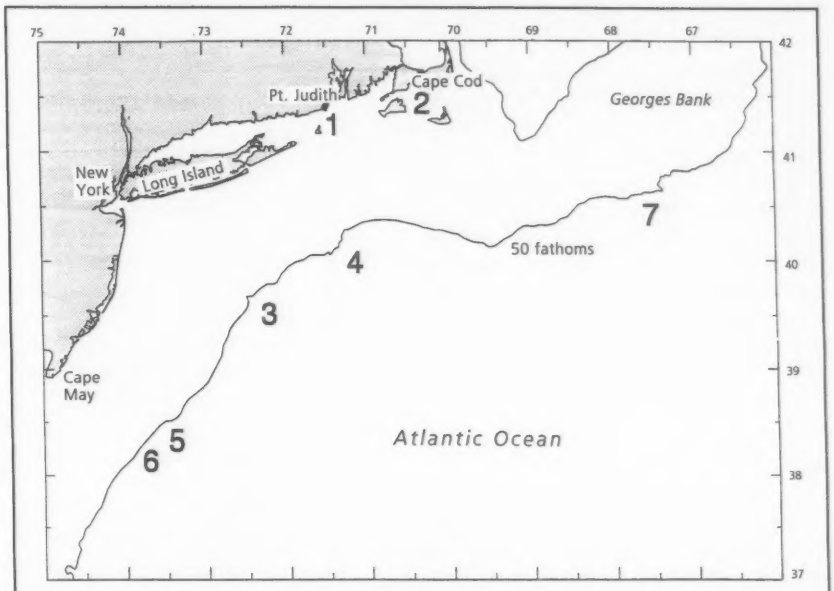

Figure 1

Collection sites for long-finned squid, *Loligo pealei*, samples off the northeast coast of the United States.

Statolith ageing

A video image processing system with high-resolution monochrome video camera (MTI-Dage 65, Newvicon) mounted on a compound microscope (Zeiss Universal) was used to count increments (Macy, 1995). Because of the low contrast seen in *L. pealei* statolith microstructure, image enhancement was employed to identify growth marks. Statolith increments were counted by using transmitted light with the microscope stage condenser (brightfield) set to the smallest aperture to obtain maximum depth of field. A rotatable polarizing filter was also placed above the field condenser to improve contrast between increments. Within a prepared *L. pealei* statolith, a series of paired bands that alternate from light to dark is observable in the LD, beginning at the nucleus and continuing to the LD margin. Two fractures that radiate outward from the nucleus are also apparent. These fractures are not the result of statolith preparation because they are also found in unprepared statoliths. In this study, the successive circumferential light bands in the statolith (appearing black in enhanced images) were counted and will be referred to hereafter as "growth increments."

Counting began with the first check or natal ring (Lipinski, 1986; Natsukari et al., 1988, Saleh-Eddine, 1991), which is a distinct oblong-shaped mark roughly the same size (100–120 μm) as the major axis length of a statolith from a *L. pealei* embryo. Although prehatching increments can sometimes be observed (Saleh-Eddine, 1991; Macy, 1995), their periodicity, if any, is unknown. Typically, counting proceeded along a series of transects extending outward from the first check across the LD to the edge. Up to six fields of view were used to enumerate the increments.

The consistency of increment counts between the reader of this study and another experienced reader was evaluated post hoc by using a sample of 76 *L. pealei* collected during 1994. Three statistical tests were applied to determine the consistency between age readings (cf. Campana et al., 1995): a linear regression analysis of paired counts; a paired t-test; and a paired Wilcoxon rank test. Results of the linear regression of one reader's counts on the other's indicated that the regression slope was not significantly different from 1 (b=1.046, σ_b=0.033, P=0.17) and that the regression intercept was not significantly different from 0(a=1.655, σ_a=4.697, P=0.73). This suggested that the readers' age determinations were consistent. Results of the paired t-test, however, indicated a significant mean paired difference of 7.6 days (σ=2.1, P<0.001). Similarly, results of the Wilcoxon signed rank test indicated a significant median paired difference (P<0.001) existed between

readers. The results of the statistical tests were equivocal but suggested that there was a potential bias between the readers' counts. However, the apparent bias was relatively small and did not suggest that there were substantial differences between the readers' recognition of increments.

An examination of *L. pealei* marked with oxytetracycline supported the hypothesis that statolith increments are formed daily (Macy, 1995). In particular, one marked squid that did grow appreciably during a 21-d period was found to have a total of 21 statolith increments (Macy, 1995). To date, the daily increment hypothesis has been verified by statolith marking for several squid species, including *Illex illecebrosus* (Dawe et al., 1985), *Alloteuthis subulata* (Lipinski, 1986), *Loligo opalescens* (Jackson, 1994b), *Sepioteuthis lessoniana* (Jackson, 1990a; Jackson et al., 1993), *Loliolus noctiluca* and *Loligo chinensis* (Jackson, 1990b), *Todarodes pacificus* (Nakamura and Sakurai, 1991), *Abralia trigonura* (Bigelow, 1992), *Ommastrephes bartramii* (Bigelow and Landgraf, 1993), *Onychoteuthis borealjaponica* (Bigelow, 1994), and validation is in progress for *Loligo plei*.[4] The daily increment hypothesis has also been verified by using laboratory-reared squid of known age for *Loligo opalescens* (Jackson, 1994b) and for *Sepioteuthis lessoniana* (Jackson et al., 1993), both loliginids, and is considered to be the best working hypothesis for statolith increment formation in *L. pealei* on the basis of limited marking data and by analogy with other loliginid species.

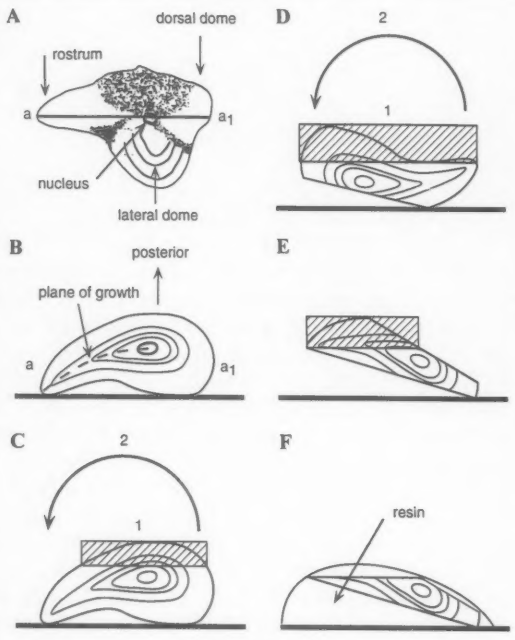

Figure 2

(**A**) Schematic view of posterior face of *Loligo pealei* statolith with a ventro–dorsal cross section indicated from points a to a_1. (**B**) Cross section [a, a_1] from (A) showing the curved plane where growth increments are counted. (**C**) After initial grinding removes the cross-hatched area to reveal the nucleus (1), the statolith is turned over (2). (**D**) After the anterior side of the statolith is oriented with the dorsal dome elevated and the cross-hatched material removed (1), the statolith is turned over again to show the posterior face (2). (**E**) The lateral dome is elevated while the resin cools and the cross-hatched material is removed. (**F**) The polished statolith is covered with molten resin and allowed to cool with the lateral dome elevated.

Month of hatching was backcalculated for all samples by subtracting the estimated age, based on statolith analysis, from the date of sample collection. Samples were categorized by sex (indeterminate, female, and male) and maturity stage (immature, maturing, and mature) to examine whether size at age was related to maturity stage. Samples were also categorized by month and year of hatching to examine monthly and seasonal patterns in size at age. Average monthly growth rates of individual squid were computed to examine individual variation in growth, where the growth rate in length was ML (mm) divided by age (months), and the growth rate in weight was total wet weight (g) divided by age. Summary statistics of the average monthly growth rate of individuals in ML and in weight were computed for squid categorized by sex, maturity stage, hatch month, and hatch year. Variances of growth rate in length and weight were log-transformed and tested for homogeneity by sex, maturity, hatch month, and hatch year by using Bartlett's test for homogeneity of variances (Sokal and Rohlf, 1981). Unplanned multiple comparison tests appropriate for equal variances and unequal samples sizes (Sokal and Rohlf, 1981) and for unequal variances and sample sizes (Games and Howell, 1976; Day and Quinn, 1989) were applied to test whether growth rate in length and weight differed by sex, maturity stage, hatch month, and hatch year.

Growth model

We applied the general growth model of Schnute (1981) to quantify the relationship between length

[4] Jackson, G. 1994. Department of Marine Biology, James Cook Univ., Townsville, Queensland 4811, Australia. Personal commun.

and weight at age for *L. pealei*. This flexible model includes asymptotic, linear, exponential, and other growth curves as particular cases. The complete set of size-at-age data consisted of the 353 squid that were aged. Size data for the i^{th} individual were denoted as (t_i, y_i), where t_i was observed age in months, and y_i is either observed length in centimeters or weight in grams. Additionally, t_{max} and t_{min} denoted the maximum and minimum observed age in months for any subset of the size-at-age data. In the most general case, the Schnute model has four parameters: α, β, y_{min}, and y_{max}. The parameters α and β determine the shape of the growth curve, whereas the parameters y_{min} and y_{max} are the predicted sizes of the youngest and oldest individuals in the subset of weight-at-age data. That is, $y_{min} = Y(t_{min})$ and $y_{max} = Y(t_{max})$, where Y is the growth model.

There are four general forms for the Schnute growth model. The most general form (case I) gives size (Y) at age (t) as

$$Y(t) = \left\{ (y_{min})^{\beta} + \left((y_{max})^{\beta} - (y_{min})^{\beta}\right) \frac{1-\exp\left[-\alpha(t-t_{min})\right]}{1-\exp\left[-\alpha(t_{max}-t_{min})\right]} \right\}^{\frac{1}{\beta}}. \quad (1)$$

In Equation 1, it is assumed that $\alpha \neq 0$ and $\beta \neq 0$ and that $y_{min} > 0$ and $y_{max} > 0$. A second form (case II) sets the β parameter to be 0 in the differential equation defining $Y(t)$. The resulting 3-parameter model is

$$Y(t) = y_{min} \exp\left[\ln\left(\frac{y_{max}}{y_{min}}\right) \frac{1-\exp\left[-\alpha(t-t_{min})\right]}{1-\exp\left[-\alpha(t_{max}-t_{min})\right]} \right], \quad (2)$$

where $\alpha \neq 0$ and $y_{min} > 0$, and $y_{max} > 0$. A third form (case III) sets the α parameter to be 0 in the differential equation defining $Y(t)$. This gives

$$Y(t) = \left\{ (y_{min})^{\beta} + \left((y_{max})^{\beta} - (y_{min})^{\beta}\right) \frac{t-t_{min}}{t_{max}-t_{min}} \right\}^{\frac{1}{\beta}}, \quad (3)$$

where $\beta \neq 0$ and $y_{min} > 0$, and $y_{max} > 0$. The fourth form (case IV) sets both α and β parameters to be 0. The resulting 2-parameter model is

$$Y(t) = y_{min} \exp\left[\ln\left(\frac{y_{max}}{y_{min}}\right) \frac{t-t_{min}}{t_{max}-t_{min}} \right], \quad (4)$$

where $y_{min} > 0$ and $y_{max} > 0$.

Two possible error structures were considered for estimating parameters of the Schnute model: additive and multiplicative. The additive error structure consisted of an additive normal term, where, for each data point,

$$y_i = Y(t_i) + \sigma\varepsilon_i, \quad (5)$$

whereas the multiplicative error structure consisted of a lognormally distributed term where, for each data point,

$$y_i = Y(t_i)\exp\left[\sigma\varepsilon_i\right]. \quad (6)$$

The random variables ε_i were independent and identically distributed standard normal random variables, and the variance term σ^2 was a positive constant. These two error structures differed in how individual size at age varied about the growth curve. Use of the additive error term implied that the model error in predicting individual size at age was invariant with respect to age. In contrast, the use of a multiplicative error term implied that the model error in predicting individual size at age was scaled with size so that more heterogeneity could be expected in size at age as age increased.

Least-squares estimates of growth parameters under the additive error structure were computed by minimizing the residual sum of squares, R_A, where

$$R_A(y_{min}, y_{max}, \alpha, \beta) = \sum_{i=1}^{n} \left[y_i - Y(t_i, y_{min}, y_{max}, \alpha, \beta)\right]^2, \quad (7)$$

Similarly, least-squares estimates of parameters under the multiplicative error structure were computed by minimizing the residual sum of squares R_M, where

$$R_M(y_{min}, y_{max}, \alpha, \beta) = \sum_{i=1}^{n} \left[\ln\left(\frac{y_i}{Y(t_i, y_{min}, y_{max}, \alpha, \beta)}\right) \right]^2. \quad (8)$$

We used SAS to compute least-squares estimates of parameters for the growth models (SAS Institute Inc., 1989). For the additive error structure, the nonlin-

ear regression model was given by Equation 5, whereas for the multiplicative error structure, the nonlinear regression model was

$$z_i = \ln\left(Y(t_i)\right) + \sigma\varepsilon_i, \quad (9)$$

where $z_i = \ln(y_i)$ was the log-transformed size of the i^{th} squid in the data set.

We estimated parameters of the Schnute growth model for several subsets of the length-at-age and weight-at-age data to assess the adequacy of the additive and multiplicative error structures. The goodness of fit of the additive and the multiplicative error structures was compared by testing whether the residuals of estimated growth curves were normally or lognormally distributed with the Shapiro-Wilk test (Shapiro and Wilk, 1965). In particular, parameters for case I of the growth model were estimated for the set of pooled-sex samples (n=353) by using the additive and the multiplicative error structures. The set was then partitioned into immature squid of indeterminate sex (n=76), female (n=131), and male (n=146) samples, and parameters for case I were estimated. We also partitioned the set into samples with hatching dates from June to October (n=145) and from November to May (n=208), and parameters for case I were estimated. Last, female and male samples were partitioned into samples with hatching dates from June to October (n_F=61 and n_M=76) and from November to May (n_F=70 and n_M=70), and parameters of case I were estimated. Overall, growth curves for case I were estimated for each of 10 subsets of the length-at-age and weight-at-age data.

We then estimated parameters for cases II, III, and IV of the Schnute growth model for each of the 10 subsets of size-at-age data using the best error structure. For each subset of size-at-age data, the estimated growth curves were compared on the basis of two criteria. First, an estimated growth curve was rejected if at least one of its parameters was not significantly different from 0 at the 5% level of significance. Second, if more than one growth curve had significant parameters, an analysis of variance of the residual sum of squares (RSS) for full and reduced parameter cases was used to select the best fit on the basis of the variance ratio described by Schnute (1981; see also Bigelow 1994). A comparison between cases II and IV tested whether the hypothesis α=0 was acceptable, and a comparison between cases III and IV tested whether the hypothesis that β=0 was acceptable. Cases II and III were compared on the basis of the lowest RSS. For each of the 10 subsets of data, one growth curve was selected as the best relationship between length at age and weight at age.

Results

Month of hatching

Long-finned squid hatched during all months of the year (Table 2). The fact that some samples hatched during December–April indicated that *L. pealei* were successfully reproducing during the winter. Given this, our data show that *L. pealei* from the northwest Atlantic have the capacity to spawn throughout the year.

The frequency distribution of hatch month of *L. pealei* samples grouped by collection season (Fig. 3) indicated that several microcohorts were present within seasonal collections. For the winter collections (Fig. 3A), most squid were hatched during June–September. Considerable variability in squid size was apparent in the length-frequency distribution (ML ranged from 6.3 to 44.0 cm [μ=19.3, σ=11.1]). Most squid in the spring collections (Fig. 3B) were hatched during August–November. Again, considerable variability in squid size was apparent (ML ranged from 1.8 to 40.8 cm [μ=16.6, σ=9.0]). For the summer collections (Fig. 3C), most of the squid were hatched during December–March, with the exception of 17 juvenile squid of indeterminate sex from the 17 July 1991 Rhode Island Department of Environmental Management survey that hatched during May. In comparison to the winter and spring collections, there was less variability in squid size within the summer collections (ML ranged from 1.3 to 16.3 cm [μ=5.0, σ=3.5]). Most of the squid in the fall collections (Fig. 3D) were hatched during March–May and ML

Table 2

Summary of the number of *Loligo pealei* samples by back-calculated month and year of hatching.

Hatching month	Year			Totals
	1990	1991	1992	
January	—	11	—	11
February	—	10	—	10
March	—	28	17	45
April	—	39	16	55
May	—	39	8	47
June	—	12	4	16
July	4	6	19	29
August	7	7	18	32
September	7	17	6	30
October	18	20	—	38
November	25	6	—	31
December	9	—	—	9
Totals	70	195	88	353

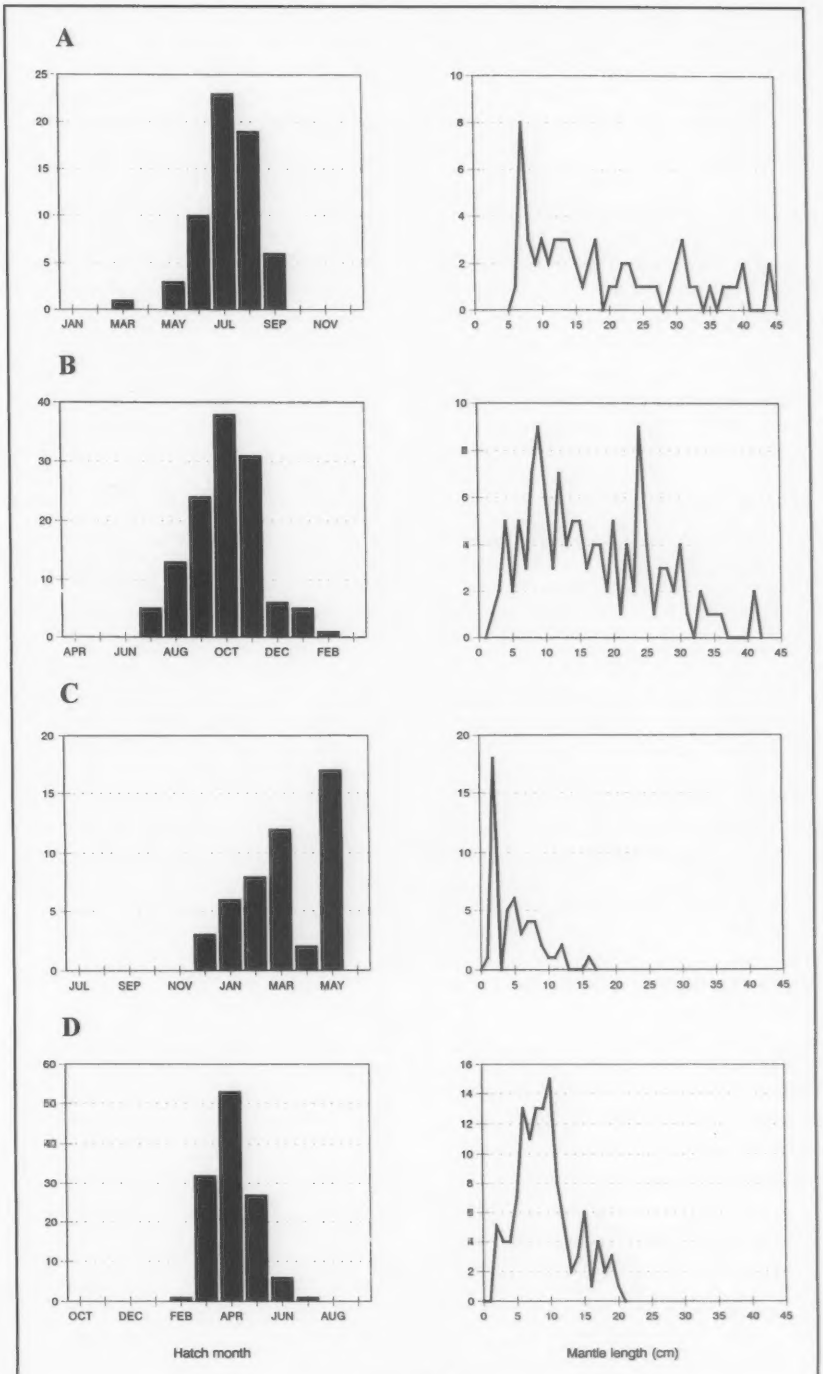

Figure 3

Frequency distributions of hatching month and mantle length of *Loligo pealei* collected during (A) winter, (B) spring, (C) summer, and (D) fall.

ranged from 1.8–20.0 cm (μ=9.1, σ=4.1). Squid size in the fall collections was more variable than in the summer collections and less variable than in the winter and spring collections.

Patterns in size at age

The average monthly growth rate in ML and weight suggested that individual growth of *L. pealei* was associated with maturity stage (Table 3) because higher growth rates were apparent for more advanced maturity stages. Relatively large coefficients of variation for the monthly growth rate indicated that the pattern of individual growth was highly variable, especially in terms of weight. Monthly growth rates of indeterminate-sex squid averaged 8.8 mm per month in ML (4.6–15.4 mm/month) and averaged 0.9 g per month in weight (0.1–3.0 g/month). Monthly growth rates of females averaged 18.2 mm per month in ML (8.8–36.6 mm/month) and averaged 9.5 g per month in weight (1.0–40.2 g/month). Monthly growth rates of males averaged 25.9 mm per month in ML (9.6–64.0 mm/month) and averaged 21.4 g per month in weight (1.5–98.2 g/month). The average growth rates in length of females and males were more than twice the average rates for indeterminate-sex squid. Similarly, the average growth rates in weight of females and males were more than 10 times the average rate for indeterminate-sex squid. For males, the average growth rates by length and by weight were 1.4 and 2.2 times greater than for females. Overall, these data indicated that individual growth was highly variable and was related to maturity stage and sex.

Average growth rates were tested for significant differences by sex and maturity stage by using unplanned multiple comparisons procedures. First, squid were categorized as indeterminate-sex, female, or male. With respect to maturity stage, squid were categorized as mature if they were maturing or mature; otherwise they were categorized as immature (Table 2). Bartlett's homogeneity of variance test was then applied to the sex and maturity stage groups. The natural logarithmic transformation was applied to the growth-rate data to stabilize variance prior to testing for differences. The null hypothesis of homogeneous variances for growth rate in length was rejected for the samples grouped by sex (X^2= 40.42>>$\chi^2_{0.05[2]}$=5.99) but was accepted for the samples grouped by maturity stage (X^2=0.40 < $\chi^2_{0.05[1]}$=3.84). The null hypothesis of homogeneous variances for growth rate in weight was rejected for the samples grouped by sex (X^2=9.35>>$\chi^2_{0.05[2]}$=5.99) and by maturity stage (X^2=26.46>>$\chi^2_{0.05[1]}$=3.84). Because variances were inherently heteroscedastic and sample sizes were unequal, the unplanned comparison test of Games and Howell (1976) (Day and Quinn, 1989) was applied to test for differences among group means of log-transformed length-at-age data categorized by sex. The group means of indeterminate-sex and female squid ($|Y_I - Y_F| = 0.71 > MSD_{0.05[I,F]} = 0.14$), indeterminate-sex and male squid ($|Y_I - Y_M| = 1.00 > MSD_{0.05[I,M]} = 0.16$), and female and male squid ($|Y_F - Y_M| = 0.30 > MSD_{0.05[F,M]} = 0.16$) were significantly different at the 5% level. For the length-at-age data categorized by maturity stage, the Tukey-Kramer comparison test (Sokal and Rohlf, 1981) was used because variances were homogeneous. The immature

Table 3

Average monthly growth rates and coefficients of variation (CV) in parentheses for long-finned squid, *Loligo pealei*, in length (millimeters per month) and weight (grams per month) and average age (months) by sex and maturity stage.

Sex category and maturity stage	mm per month Average (CV)	g per month Average (CV)	Age (months) Average (CV)	*n*
Indeterminate-sex				
Immature	8.8 (25%)	0.9 (87%)	4.4 (35%)	76
Female				
Immature	15.8 (29%)	5.8 (70%)	6.2 (14%)	88
Maturing	20.0 (24%)	11.3 (73%)	7.0 (16%)	20
Mature	26.1 (21%)	22.1 (44%)	7.5 (13%)	23
Male				
Immature	16.5 (30%)	6.6 (85%)	6.2 (10%)	60
Maturing	21.3 (24%)	12.2 (64%)	6.6 (16%)	15
Mature	34.9 (31%)	35.8 (65%)	7.4 (11%)	71

and mature groups means were significantly different at the 5% level ($|Y_I - Y_M| = 0.78 > MSD_{0.05[I,M]} = 0.08$). Because variances were heteroscedastic for the weight-at-age data grouped by sex and by maturity stage, the Games and Howell test was applied. The group means of indeterminates and females ($|Y_I - Y_F| = 2.47 > MSD_{0.05[I,F]} = 0.46$), indeterminates and males ($|Y_I - Y_M| = 3.08 > MSD_{0.05[I,M]} = 0.50$), and females and males ($|Y_F - Y_M| = 0.62 > MSD_{0.05[F,M]} = 0.40$) were significantly different at the 5% level. Similarly, the immature and mature group means were significantly different at the 5% level ($|Y_I - Y_M| = 2.13 > MSD_{0.05[I,M]} = 0.32$). Overall, the average growth rates in length and weight were found to be significantly different by sex and maturity stage.

The pattern of growth of *L. pealei* analyzed by month of hatching was also highly variable (Table 4). For indeterminate-sex squid, average growth in ML ranged from 5.9 (June-hatched) to 11.2 (September-hatched) mm/month, whereas average growth in weight ranged from 0.2 (July-hatched) to 1.9 (September-hatched) g/month. No seasonal pattern was apparent in the average growth rate for indeterminate-sex squid. However, few samples of indeterminate-sex squid hatched during July to December were available, and comparisons of growth rate by season of hatching were not possible. For females, average growth in ML ranged from 11.1 (December-hatched) to 22.5 (October-hatched) mm/month whereas average growth in weight ranged from 2.2 (December-hatched) to 19.5 (June-hatched) g/month. Average growth rates were generally higher for squid hatched from June to October when the average growth rate in weight exceeded 10 g/month. For males, average growth in ML ranged from 13.9 (December-hatched) to 40.9 (June-hatched) mm/month whereas growth in weight ranged from 3.4 (December-hatched) to 53.3 (June-hatched) g/month. Average growth rates of males were generally highest for squid hatched from June to October when the average growth rate in weight exceeded 20 g/month. Overall, these data suggested that the highest average growth rates were achieved by adult squid hatched from June to October.

The average growth rates by hatch month were also tested for significant differences by using unplanned multiple-comparisons procedures where the natural logarithmic transformation was applied to stabilize variance. The null hypothesis of homogeneous variances for the samples grouped by hatch month was rejected for growth in length ($X^2 = 44.41 >> \chi^2_{0.05[11]} = 19.67$) and in weight ($X^2 = 75.71 >> \chi^2_{0.05[11]} = 19.67$). A total of 16 pairs of group means for growth rate in length were significantly different at the 5% level (Table 5): July–January; July–February; July–March; July–April; July–May; July–November; July–December; September–April; September–May; September–December; October–January; October–March; October–April; October–May; October–November; and October–December. Overall, these tests indicated that there were significant differences between growth rates of squid hatched during November–May and July–October. Similarly, for growth rate in weight, a total of 16 pairs of group means for growth rate in length were significantly different at the 5% level (Table 6): July–January; July–February; July–March; July–April; July–May; July–November; July–December; August–May; September–April; September–May; September–December; October–March; October–April; October–May; October–November; and October–December. Overall, these tests indicated that there were significant differences between growth rates of squid hatched during November–May and July–October.

There was no consistent pattern in growth of *L. pealei* analyzed by year of hatching (Table 7). For indeterminate-sex squid, average growth in ML was lowest in 1990 (8.5 mm/month) and highest in 1992 (12.3 mm/month), whereas average growth in weight was lowest in 1991 (0.7 g/month) and highest in 1992 (2.2 g/month). For females, average growth in ML and weight was lowest in 1992 (16.3 mm/month and 7.2 g/month) and highest in 1990 (21.5 mm/month and 15.2 g/month). For males, average growth in ML and weight was lowest in 1992 (21.9 mm/month and 13.2 g/month) and highest in 1991 (27.8 mm/month and 25.0 g/month). Overall, these data suggested that growth rates varied by sex among years.

The average growth rates by hatch year were also tested for significant differences by using unplanned multiple-comparisons procedures where the natural logarithmic transformation was applied to stabilize variance. The null hypothesis of homogeneous variances for the samples grouped by hatch year was rejected for growth in length ($X^2 = 26.12 >> \chi^2_{0.05[2]} = 5.99$) and weight ($X^2 = 47.90 >> \chi^2_{0.05[2]} = 5.99$). The group means of 1990 and 1991 hatched squid were significantly different in length ($|Y_{1990} - Y_{1991}| = 0.28 > MSD_{0.05[1990,1991]} = 0.26$) and weight ($|Y_{1990} - Y_{1991}| = 0.93 > MSD_{0.05[1990,1991]} = 0.67$), but no general trend in growth by year was apparent.

Growth model

The additive and the multiplicative error structures were compared by testing whether the residuals of estimated case-I growth curves were normally or log-normally distributed. For 8 out of 10 subsets of length-at-age data, the hypothesis of an additive normal error structure was rejected at the 5% level. In contrast, the hypothesis of a multiplicative log-

Table 4

Average monthly growth rates and coefficients of variation (CV) for long-finned squid, *Loligo pealei*, in length (millimeters per month) and weight (grams per month) and average age (months) by sex and month of hatching.

Sex category and hatching months	mm per month Average (CV)	g per month Average (CV)	Age (months) Average (CV)	*n*
Indeterminate-sex				
January	8.3 (27%)	0.6 (58%)	4.2 (9%)	5
February	9.6 (16%)	1.1 (57%)	4.7 (11%)	7
March	10.6 (13%)	1.4 (29%)	5.1 (27%)	10
April	8.7 (24%)	1.1 (71%)	5.6 (22%)	15
May	8.8 (26%)	0.6 (141%)	3.0 (45%)	25
June	5.9 (18%)	0.3 (43%)	4.0 (6%)	6
July	6.1	0.2	3.4	1
September	11.2	1.9	6.2	1
November	8.7 (9%)	1.3 (29%)	6.1 (2%)	3
December	8.4 (23%)	0.9 (74%)	5.3 (3%)	3
Female				
January	13.2 (9%)	3.2 (27%)	6.0 (6%)	4
March	15.7 (25%)	5.6 (80%)	5.9 (21%)	16
April	17.2 (33%)	6.7 (68%)	5.8 (6%)	25
May	18.4 (30%)	8.0 (100%)	5.4 (19%)	12
June	19.5 (75%)	19.5 (128%)	7.7 (6%)	2
July	21.2 (21%)	15.9 (66%)	7.8 (8%)	9
August	17.9 (32%)	10.9 (78%)	7.4 (10%)	15
September	19.4 (32%)	11.4 (70%)	7.2 (12%)	17
October	22.5 (31%)	14.7 (74%)	6.9 (6%)	18
November	15.7 (43%)	6.3 (130%)	6.3 (3%)	12
December	11.1	2.2	6.7	1
Male				
January	19.6 (46%)	9.1 (100%)	6.0 (7%)	2
February	20.5 (22%)	8.2 (12%)	6.1 (22%)	3
March	20.8 (30%)	13.0 (74%)	6.8 (14%)	19
April	17.1 (28%)	6.9 (79%)	5.9 (5%)	15
May	21.9 (55%)	15.6 (141%)	5.7 (18%)	10
June	40.9 (19%)	53.3 (37%)	7.8 (11%)	8
July	35.5 (36%)	41.8 (66%)	7.6 (7%)	19
August	27.9 (53%)	25.4 (105%)	7.4 (12%)	17
September	33.1 (27%)	29.4 (47%)	7.5 (9%)	12
October	29.6 (36%)	21.1 (62%)	6.9 (5%)	20
November	17.4 (46%)	7.8 (157%)	6.1 (5%)	16
December	13.9 (16%)	3.4 (43%)	5.9 (12%)	5
Pooled-sex				
January	12.1 (45%)	3.1 (140%)	5.2 (19%)	11
February	12.8 (45%)	3.2 (108%)	5.1 (20%)	10
March	16.8 (37%)	7.8 (106%)	6.1 (21%)	45
April	14.9 (40%)	5.2 (93%)	5.8 (12%)	55
May	14.0 (61%)	5.6 (215%)	4.2 (42%)	47
June	25.1 (72%)	29.2 (101%)	6.4 (31%)	16
July	30.1 (44%)	32.3 (82%)	7.5 (13%)	29
August	23.2 (53%)	18.6 (115%)	7.4 (11%)	32
September	24.6 (41%)	18.3 (77%)	7.3 (11%)	30
October	26.2 (37%)	18.1 (68%)	6.9 (5%)	38
November	16.0 (47%)	6.6 (154%)	6.2 (4%)	31
December	11.8 (28%)	2.5 (66%)	5.8 (12%)	9

normal error structure could not be rejected for any subset of the length-at-age data. Similarly, for all 10 subsets of weight-at-age data, the hypothesis of an additive normal error structure was rejected at the 5% level, whereas the hypothesis of a multiplicative lognormal error structure could not be rejected for any subset. As a result, the multiplicative error structure was considered to be the best assumption for modelling variability in size at age.

Although the residuals from the curves estimated with the multiplicative error structure conformed to model assumptions, the parameters of these curves were imprecisely determined. In particular, the case-I curve was rejected for each subset of length-at-age and weight-at-age data because there was at least one parameter that was not significantly different from 0. Thus, the 4-parameter form of the Schnute model had more parameters than necessary to characterize *L. pealei* growth.

For the length-at-age growth curves, most of the case-II and case-III curves were rejected because their parameters were not significant. As a result, there were only 3 instances where comparison of RSS was used to select the best curve. The best curve for pooled-sex samples hatched during June–October was the case-II curve which was selected over the case-IV curve because the hypothesis $\alpha=0$ was rejected ($f=14.98 > 3.91=F_{0.05}(1,142)$). The best curve

Table 5

Results of Games and Howell test of differences between means of log-transformed growth rate in length by hatch month of long-finned squid, *Loligo pealei*. Absolute values of differences between means are given below the diagonal and corresponding values of the maximum significant difference at the 5% level are given above the diagonal. Significantly different means are indicated with an asterisk.

	Jan	Feb	Mar	Apr	May	Jun	Jul	Aug	Sep	Oct	Nov	Dec
Jan	—	0.94	0.77	0.77	0.78	1.41	0.81	0.80	0.80	0.77	0.77	0.86
Feb	0.06	—	0.77	0.77	0.79	1.41	0.81	0.80	0.80	0.77	0.77	0.86
Mar	0.34	0.28	—	0.37	0.44	1.32	0.52	0.49	0.47	0.39	0.40	0.63
Apr	0.21	0.15	0.13	—	0.44	1.32	0.52	0.49	0.48	0.39	0.41	0.63
May	0.09	0.03	0.25	0.12	—	1.33	0.56	0.54	0.53	0.46	0.47	0.65
Jun	0.45	0.39	0.11	0.24	0.36	—	1.34	1.34	1.33	1.32	1.32	1.36
Jul	**0.89***	**0.83***	**0.55***	**0.68***	**0.80***	0.44	—	0.60	0.60	0.53	0.55	0.70
Aug	0.62	0.56	0.28	0.41	0.53	0.17	0.27	—	0.56	0.51	0.52	0.68
Sep	0.70	0.64	0.36	**0.49***	**0.61***	0.25	0.19	0.08	—	0.50	0.51	0.67
Oct	**0.79***	0.73	**0.45***	**0.58***	**0.70***	0.34	0.10	0.17	0.09	—	0.43	0.64
Nov	0.28	0.22	0.06	0.08	0.19	0.16	**0.60***	0.33	0.41	**0.50***	—	0.64
Dec	0.01	0.05	0.33	0.19	0.08	0.43	**0.87***	0.60	**0.68***	**0.77***	0.27	—

Table 6

Results of Games and Howell test of differences between means of log-transformed growth rate in weight by hatch month for long-finned squid, *Loligo pealei*. Absolute values of differences between means are given below the diagonal and corresponding values of the maximum significant difference at the 5% level are given above the diagonal. Significantly different means are indicated with an asterisk.

	Jan	Feb	Mar	Apr	May	Jun	Jul	Aug	Sep	Oct	Nov	Dec
Jan	—	2.85	2.38	2.41	2.52	3.94	2.47	2.42	2.42	2.37	2.41	2.61
Feb	0.18	—	2.23	2.22	2.37	3.85	2.31	2.28	2.27	2.21	2.22	2.48
Mar	1.14	0.96	—	1.02	1.49	3.53	1.33	1.20	1.19	0.94	1.02	1.78
Apr	0.78	0.60	0.36	—	1.48	3.53	1.32	1.18	1.17	0.93	1.00	1.80
May	0.21	0.39	1.35	1.00	—	3.62	1.69	1.61	1.60	1.43	1.48	2.00
Jun	1.32	1.14	0.18	0.54	1.53	—	3.59	3.57	3.56	3.50	3.53	3.65
Jul	**2.61***	**2.43***	**1.47***	**1.83***	**2.83***	1.30	—	1.47	1.46	1.26	1.32	1.90
Aug	1.94	1.76	0.80	1.16	**2.16***	0.62	0.67	—	1.33	1.14	1.21	1.85
Sep	2.07	1.89	0.93	**1.29***	**2.29***	0.75	0.54	0.13	—	1.13	1.20	1.84
Oct	2.22	2.04	**1.08***	**1.44***	**2.44***	0.90	0.39	0.28	0.15	—	0.93	1.77
Nov	1.02	0.84	0.12	0.24	1.23	0.30	**1.59***	0.92	1.05	**1.20***	—	1.80
Dec	0.23	0.05	0.91	0.56	0.44	1.09	**2.39***	1.72	**1.85***	**1.99***	0.79	—

Table 7

Average monthly growth rates and coefficients of variation (CV) for long-finned squid, *Loligo pealei*, in length (millimeters per month), weight (grams per month), and average age (months) by sex and year of hatching.

Sex category and hatching year	mm per month Average (CV)	g per month Average (CV)	Age (months) Average (CV)	*n*
Indeterminate-sex				
1990	8.5 (16%)	1.1 (48%)	5.7 (8%)	6
1991	8.5 (23%)	0.7 (89%)	4.2 (37%)	65
1992	12.3 (17%)	2.2 (20%)	5.4 (17%)	5
Totals	8.8 (25%)	0.9 (87%)	4.4 (35%)	76
Female				
1990	21.5 (42%)	15.2 (87%)	6.7 (10%)	24
1991	18.4 (27%)	9.0 (72%)	6.5 (19%)	61
1992	16.3 (31%)	7.2 (95%)	6.5 (14%)	46
Totals	18.2 (34%)	9.5 (91%)	6.5 (16%)	131
Male				
1990	27.5 (47%)	22.7 (89%)	6.9 (13%)	40
1991	27.8 (46%)	25.0 (102%)	6.8 (16%)	69
1992	21.9 (40%)	13.2 (94%)	6.7 (12%)	37
Totals	25.9 (47%)	21.4 (102%)	6.8 (14%)	146
Pooled-sex				
1990	23.8 (52%)	18.3 (100%)	6.8 (13%)	70
1991	18.4 (62%)	11.9 (156%)	5.8 (30%)	195
1992	18.0 (39%)	9.4 (106%)	6.6 (14%)	88
Totals	19.4 (56%)	12.5 (136%)	6.2 (24%)	353

for female samples hatched during November–May was the case-IV curve which was selected over the case-II curve because the hypothesis α=0 was accepted (f=2.68 < 3.98=$F_{0.05}$(1,67)). The best curve for male samples hatched during June–October was the case-II curve which was selected over the case-IV curve because the hypothesis α=0 was rejected (f=5.46 > 3.97=$F_{0.05}$(1,73)). For each of the 7 other subsets of length-at-age data, case IV yielded the best growth curve (Table 8).

Case-IV curves were the best growth models for length at age of pooled-sex samples (Fig. 4A) and pooled-sex samples hatched during November–May (Fig. 5A). In general, the case-IV growth curves are power functions that represent unbounded accelerating growth with a theoretical minimum size. In particular, case-IV curves are what Schnute termed "T^{th} power" growth curves, where size (G) at age (T) is proportional to some positive constant K>1 raised to the T^{th} power. That is, $G \propto K^T = \exp[T \ln(K)]$, so that size increases exponentially as age increases. In contrast, the case-II curve was chosen for pooled-sex samples hatched during June–October (Fig. 5A). For these samples, growth in length appeared nearly linear over the range of data, although there was some indication of a slight decrease in growth rate past 250 days of age.

For the length-at-age data partitioned by sex, case-IV curves were also the best growth models, with one exception. Exponential growth in length was evident for indeterminate-sex (Fig. 6A), female (Fig. 7A), and male (Fig. 7A) samples. Similarly, growth in length was exponential for female samples hatched during June–October and during November–May (Fig. 8A) and for male samples hatched during November–May (Fig. 9A). In contrast, growth in length for males hatched during June–October was not exponential (Fig. 9A) and growth rate decreased between 200 and 250 days of age.

For the subsets of the weight-at-age growth data, most of the case-II and case-III curves were rejected because their parameters were not significant and there were only 4 instances where comparison of RSS was used to select the best curve. The best curve for pooled-sex samples was the case II curve which was selected over the case-IV curve because the hypothesis α=0 was rejected (f=4.30 > 3.87=$F_{0.05}$(1,350)). The best curve for indeterminate-sex samples was the case-II curve which was selected over case-IV curve because the hypothesis α=0 was rejected (f=5.61 >

Table 8

Summary of best growth curves for long-finned squid, *Loligo pealei*, length (cm) at age (months).

Data set	Sample size	Growth curve	r^2	α	β	t_{min}	y_{min}	t_{max}	y_{max}
Pooled-sex samples	353	IV	0.97	—	—	1.6427	1.3670	9.7249	47.1939
Indeterminate-sex samples	76	IV	0.97	—	—	1.6427	1.5267	6.8993	7.3841
Female samples	131	IV	0.98	—	—	4.0739	6.1918	9.2320	21.2922
Male samples	146	IV	0.98	—	—	4.4353	5.4317	9.7249	57.8786
Pooled-sex samples hatched Jun–Oct	145	II	0.98	0.2867	—	3.4497	1.4801	9.2320	30.6814
Pooled-sex samples hatched Nov–May	208	IV	0.97	—	—	1.6427	1.5796	9.7249	37.4441
Female samples hatched Jun–Oct	61	IV	0.99	—	—	5.4209	8.8066	9.2320	22.5526
Female samples hatched Nov–May	70	IV	0.98	—	—	4.0739	6.9978	8.6078	13.8768
Male samples hatched Jun–Oct	76	II	0.99	0.8284	—	5.6509	6.1309	9.1335	32.5621
Male samples hatched Nov–May	70	IV	0.98	—	—	4.4353	5.9896	9.7249	36.6641

$3.97=F_{0.05}(1,74)$). The best curve for pooled-sex samples hatched during June–October was the case-II curve which was selected over the case-IV curve because the hypothesis $\alpha=0$ was rejected ($f=18.64 > 3.91=F_{0.05}(1,142)$). The best curve for pooled-sex samples hatched during November–May was the case-III curve which was selected over case-IV curve because the hypothesis $\alpha=0$ was rejected ($f=6.82 > 3.89=F_{0.05}(1,205)$). For each of the 6 other subsets of length-at-age data, case IV yielded the best growth curve (Table 9).

For the weight-at-age data, case-II growth curves were chosen for pooled-sex samples (Fig. 4B) and pooled-sex samples hatched during June–October (Fig. 5B). Although these curves are sigmoidal and eventually approach an asymptote (cf. Schnute, 1981), it is important to note that the asymptotes are not approached within the range of data for the estimated curves and that growth is nearly exponential for the observed ages. In contrast, a case-III growth curve was chosen for pooled-sex samples hatched during November–May (Fig. 5B). This growth curve is not asymptotic and consists of an initial period of decelerated growth followed by a period of accelerated growth after a certain size is reached.

Case-IV growth curves were chosen for every data set where the weight-at-age data were partitioned by sex, with one exception. Growth in weight was exponential for female and male samples (Fig. 7B). Similarly, exponential growth was evident for female samples hatched during June–October and during November–May (Fig. 8B) and for male samples hatched during June–October and during November–May (Fig. 9B). In contrast, a case-II curve was chosen for indeterminate-sex squid (Fig. 6B), although growth rate was effectively exponential for the observed ages. In this case, the estimated curve would approach an asymptote outside the range of possible sizes for *L. pealei* that lack identifiable sexual characteristics.

For adult squid, the estimated growth curves indicated sexual dimorphism. Length-at-age curves for female (L_F) and male (L_M) samples were

$$L_F(d) = 2.3343e^{0.0079d}$$
$$L_M(d) = 0.7470e^{0.0147d}, \quad (10)$$

where L is mantle length in centimeters and age (d) is measured in days (Fig. 7A). Similarly, weight-at-age curves for female (W_F) and male (W_M) samples were

$$W_F(d) = 1.1446e^{0.0182d}$$
$$W_M(d) = 0.1316e^{0.0311d}, \quad (11)$$

Table 9

Summary of best growth curves for long-finned squid, *Loligo pealei*, weight (g) at age (months).

Data set	Sample size	Growth curve	r^2	α	β	t_{min}	y_{min}	t_{max}	y_{max}
Pooled-sex samples	353	II	0.94	0.0577	—	1.6427	0.1813	9.7249	783.6477
Indeterminate-sex samples	76	II	0.85	0.2058	—	1.6427	0.1985	6.8993	11.2208
Female samples	131	IV	0.96	—	—	4.0739	10.9940	9.2320	192.8125
Male samples	146	IV	0.97	—	—	4.4353	8.7765	9.7249	1314.8945
Pooled-sex samples hatched Jun–Oct	145	II	0.96	0.3038	—	3.4497	0.3545	9.2320	365.0887
Pooled-sex samples hatched Nov–May	208	III	0.92	—	0.1315	1.6427	0.1820	9.7249	323.5635
Female samples hatched Jun–Oct	61	IV	0.97	—	—	5.4209	23.7236	9.2320	222.6014
Female samples hatched Nov–May	70	IV	0.96	—	—	4.0739	14.1734	8.6078	78.0026
Male samples hatched Jun–Oct	76	IV	0.97	—	—	5.6509	39.6333	9.1335	681.9745
Male Samples hatched Nov–May	70	IV	0.97	—	—	4.4353	10.1822	9.7249	633.1753

where weight (W) is in grams and age (d) is measured in days (Fig. 7B). These curves gave instantaneous daily growth rates of 0.8% and 1.5% in length and of 1.8% and 3.1% in weight for females and males, respectively. Thus, female growth in length and weight was generally slower than that for males.

The estimated growth curves also indicated differences in growth rate between hatching seasons for both sexes. Length-at-age curves for female squid hatched during June–October ($L_{F,JO}$) and female squid hatched during November–May ($L_{F,NM}$) were (Fig. 8A):

$$L_{F,JO}(d) = 2.3116e^{0.0081d}$$
$$L_{F,NM}(d) = 3.7828e^{0.0050d}. \quad (12)$$

Weight-at-age curves for female squid hatched during June–October ($W_{F,JO}$) and female squid hatched during November–May ($W_{F,NM}$) were (Fig. 8B):

$$W_{F,JO}(d) = 0.9820e^{0.0193d}$$
$$W_{F,NM}(d) = 3.0617e^{0.0124d}. \quad (13)$$

These curves gave instantaneous daily growth rates of 0.8% and 0.5% in length and of 1.9% and 1.2% in weight for females hatched during June–October and during November–May, respectively. Thus, female growth rate in length and weight was generally more rapid for June–October hatched squid.

Differences in growth rate between hatching seasons were also evident for male squid. In particular, male growth in length (Fig. 9A) was more rapid at younger ages (≤225 d) for June–October hatched squid than for November–May hatched squid. In contrast, male growth in length was estimated to be more rapid at older ages (>225 d) for November–May hatched squid than for June–October hatched squid (Fig. 9A). However, this comparison should be viewed with caution because the sample size of older males hatched during November–May available for estimating the length-at-age curve was small. Weight-at-age curves (Fig. 9B) for male squid hatched during June–October ($W_{M,JO}$) and male squid hatched during November–May ($W_{M,NM}$) were

$$W_{M,JO}(d) = 0.3917e^{0.0268d}$$
$$W_{M,NM}(d) = 0.3190e^{0.0256d}. \quad (14)$$

These curves gave instantaneous daily growth rates of 2.7% and 2.6% of body weight for males hatched

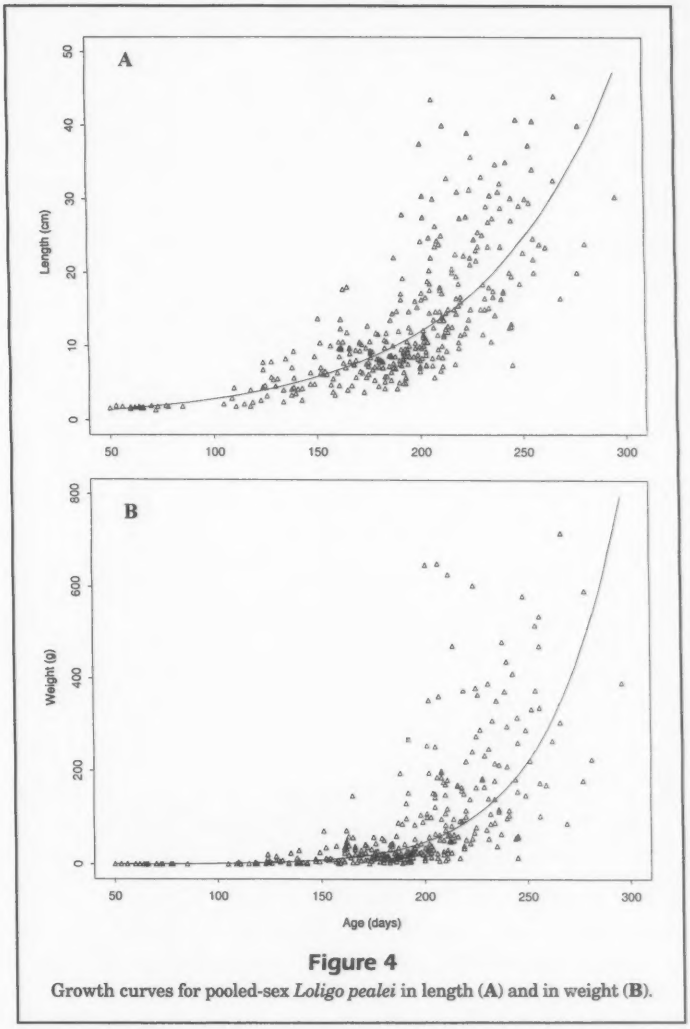

Figure 4

Growth curves for pooled-sex *Loligo pealei* in length (**A**) and in weight (**B**).

during June–October and during November–May, respectively. Overall, female growth in length and weight and male growth in weight were more rapid for June–October hatched squid. Male growth in length was also more rapid at younger ages for squid hatched during June–October than for squid hatched during November–May.

The selected growth curves indicated that *L. pealei* growth was dependent upon maturity stage, sex, and hatching season. Indeterminate-sex squid grew more slowly than adults whereas males grew more rapidly than females. Further, squid hatched during June–October grew more rapidly than squid hatched during November–May.

Discussion

Growth rates obtained in this study were generally higher than those reported in Hixon et al. (1981, Tables 1 and 2) but were lower than those in studies of cultured *L. pealei*. In particular, average monthly growth rates for males reported in this study (26 mm/month and 21 g/month) were lower than those reported by Hanlon et al. (1983) who found average growth rates of 44 mm/month and 37 g/month in a sample of 6 male *L. pealei* raised in a closed sea-water system. Additionally, Hanlon et al. (1987) reported an instantaneous daily growth rate of roughly 2% in ML for 10 *L. pealei* raised in a closed sea-water sys-

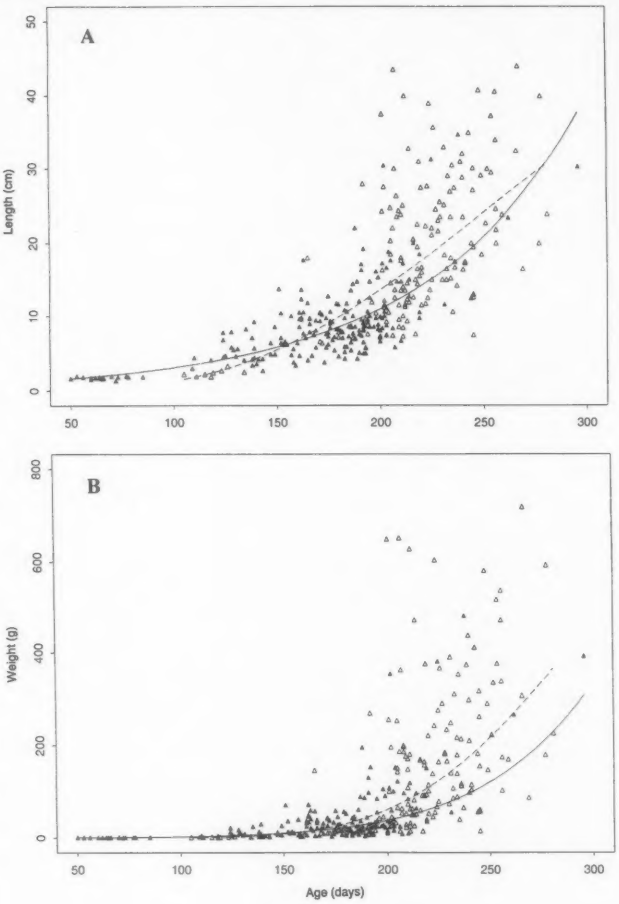

Figure 5

Growth curves for pooled-sex *Loligo pealei* hatched during June–October (dashed line and open triangles) and during November–May (solid line and solid triangles) in length (**A**) and in weight (**B**).

tem whereas the estimated growth curve for pooled-sex samples in this study indicated a growth rate of 1.4%. While the lower growth rates of wild squid were likely due to the better growth conditions experienced by the cultured squid, it should be noted that the largest squid in this study, a 44-cm male, was only 2.5 cm smaller than the largest reported *L. pealei*[5] (Summers, 1968). The fact that this 9-month-old male could have achieved the maximum reported size if it grew for one more month at average male growth rate suggested that it was unlikely that the lifespan of *L. pealei* exceeded 1 year.

Although a comprehensive growth model for squid has not yet been determined (Jackson, 1994a), we suggest that the Schnute model is a viable choice given its flexibility. In addition, we recommend the methods used to select the best form of the growth model because they provide an objective basis for evaluating alternative forms. Even though there was substantial heterogeneity in *L. pealei* size at age, the estimated growth curves for pooled sexes indicated that *L. pealei* growth in length and weight was effec-

[5] Based on a total of 55,616 length-frequency measurements, the maximum size of *L. pealei* taken in the domestic commercial fishery during 1972–91 was 45 cm (Northeast Fisheries Science Center, Woods Hole, MA, unpubl. data).

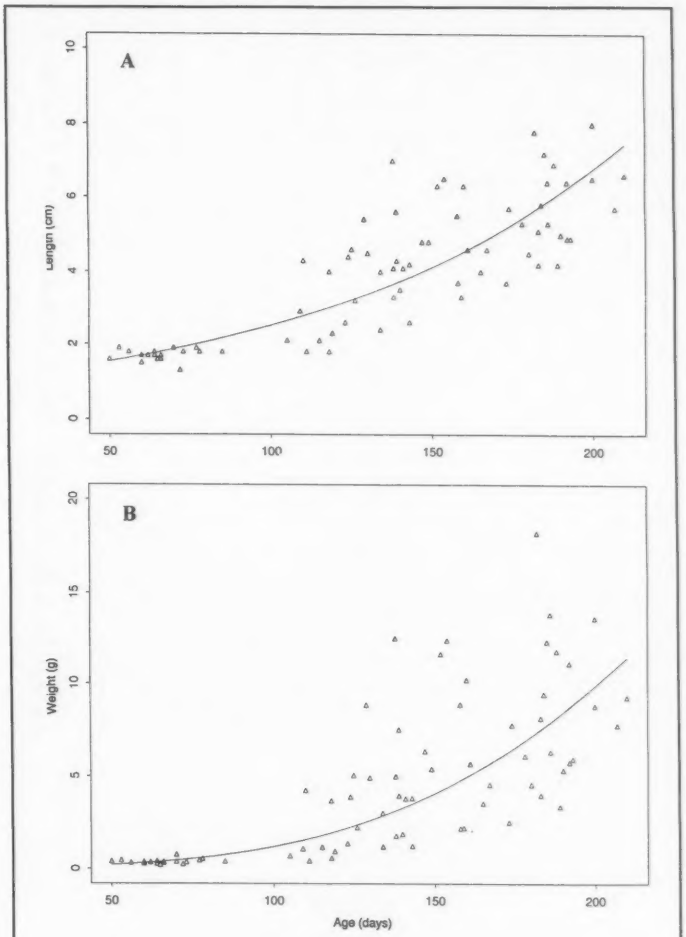

Figure 6

Growth curves of indeterminate-sex *Loligo pealei* in length (**A**) and in weight (**B**).

tively exponential, which is consistent with the findings of Forsythe and Van Heukelem (1987).

It is important to account for individual heterogeneity in size at age when determining a growth curve because the use of mean values for size classes can obscure the pattern of individual growth (Alford and Jackson, 1993). In this study, growth curves were estimated by using size-at-age data for individual squid. We found that the use of a multiplicative lognormal error term provided an adequate statistical framework for estimating growth curves despite substantial heterogeneity in squid size at age. In general, a growth curve with a multiplicative lognormal error term will be more appropriate than an additive normal error term when size-at-age distributions are skewed because prediction error scales with size at age under the lognormal assumption. Regardless, it is recommended that researchers use residual patterns to evaluate the adequacy of an assumed error structure for estimating a growth curve.

The fact that some *L. pealei* were hatched during December–April was unexpected because the protracted spawning season of *L. pealei* in the northwest Atlantic had previously been considered to extend from roughly April to November (Lange, 1982). McMahon and Summers (1971) found that embryonic development of *L. pealei* was related to water temperature. In their study, the average development time required before hatching was 26.7 days for wa-

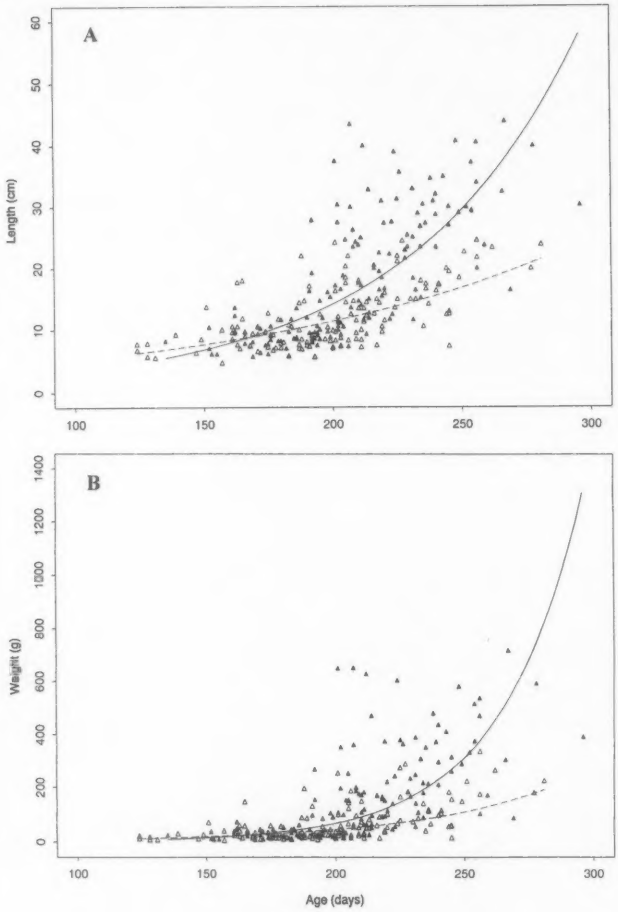

Figure 7

Growth curves for female (dashed line and open triangles) and male (solid line and solid triangles) *Loligo pealei* in length (**A**) and in weight (**B**).

ter temperatures of 12.0–18.0°C, 18.5 days for water temperatures of 15.5–21.3°C, and 10.7 days for water temperatures of 21.5–23.0°C. During winter, *L. pealei* move offshore to the edge of the continental shelf to avoid cooler inshore waters (Lange, 1982). Assuming that squid hatched during December–April encountered water temperatures of 9.0–13.0°C that are characteristic of the convergence zone at the edge of the continental shelf (Bowman, 1977), it would have taken about 1 month for them to develop to the hatching stage. Although our results indicated that winter spawning occurred, further research will be needed to evaluate the relative contribution of winter-hatched squid to the population's dynamics.

Our results lend support to the hypothesis that growth of *L. pealei* can be influenced by seasonal environmental variation and month of hatching. Empirical differences in growth rates between June–October and November–May hatched squid were apparent for both females and males. Further, significant differences in growth rate were detected between squid hatched during November–May and July–October. These differences were also evident in estimated growth curves. The notion that *L. pealei* growth can be influenced by hatching season and its associated temperature regime is consistent with the results of Rodhouse and Hatfield (1990b) who found an apparent effect of seasonal environmental varia-

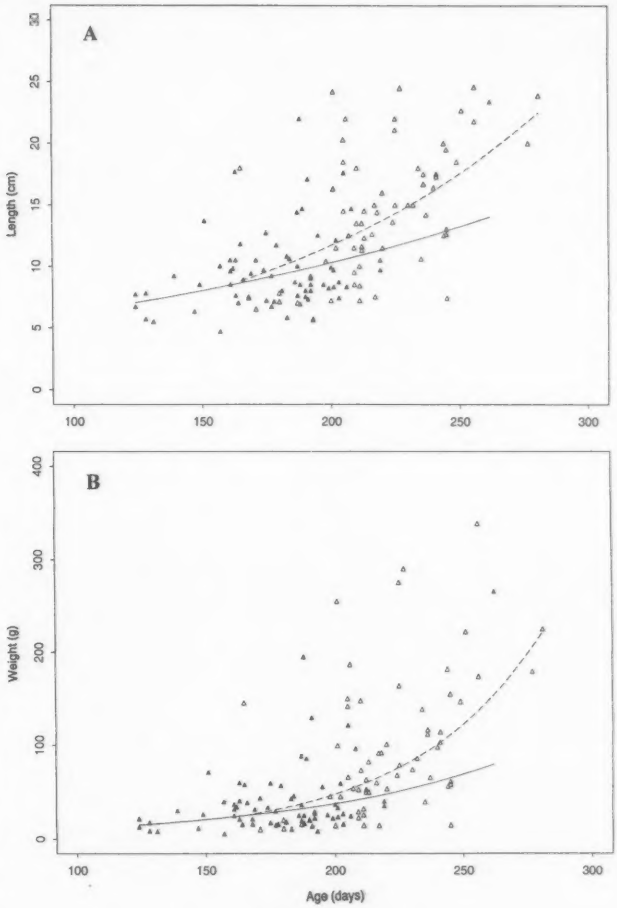

Figure 8

Growth curves for female *Loligo pealei* hatched during June–October (dashed line and open triangles) and during November–May (solid line and solid triangles) in length (**A**) and in weight (**B**).

tion on the growth rate of the Argentine short-finned squid, *Illex argentinus*. Using statolith ageing techniques, they found that older short-finned squid hatched during cooler months apparently grew more slowly than younger squid hatched during warmer months. They speculated that the faster growth of the younger cohort was due to the generally warmer temperatures experienced by hatchlings. Similarly, Forsythe (1993) conducted a simulation study to examine the potential effects of seasonal temperature regimes on the growth of juvenile cephalopods. He showed that small temperature changes could have a substantial effect on the growth of juvenile squid under certain conditions. Overall, further research to estimate directly the potential effect of temperature on the growth rate of *L. pealei* would help to quantify the potential yield from this resource on a seasonal basis.

The fact that the growth rate of *L. pealei* was found to be associated with maturity stage also has potential implications for the management of the resource. Empirical differences in growth rate by maturity stage were consistent for both females and males; on average, growth rates in length and weight were lowest for immature squid and highest for mature squid. Significant differences in growth rate by length

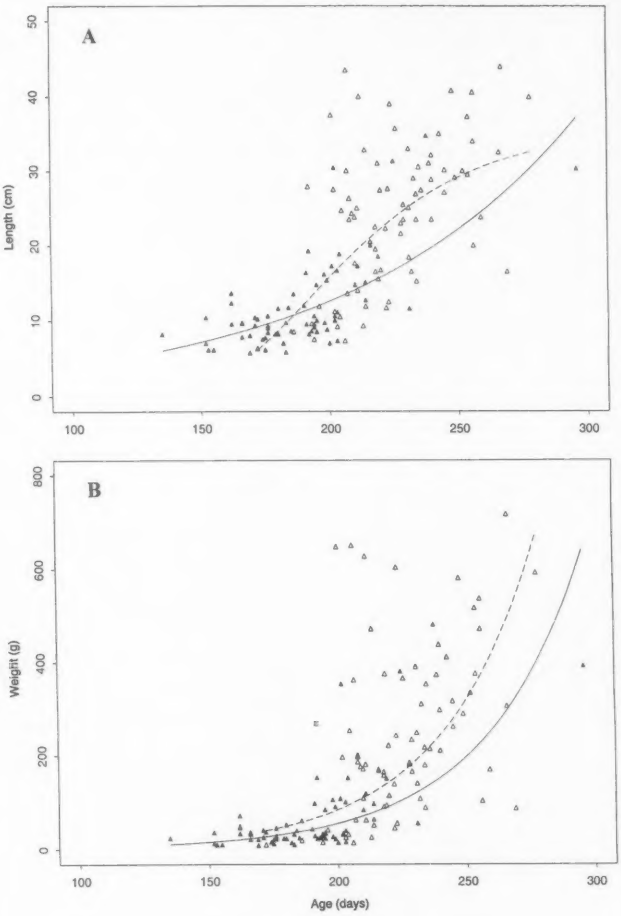

Figure 9

Growth curves for male *Loligo pealei* hatched during June–October (dashed line and open triangles) and during November–May (solid line and solid triangles) in length (**A**) and in weight (**B**).

and weight were also detected between immature and mature squid. In general, intensive harvest of slow-growing immature squid has the potential to reduce fishery production through a decrease in yield per recruit.

No clear effect of hatch year on growth rate was detected in this study. However, these data were not collected for the purpose of examining yearly differences in growth rates, and any annual effects were likely confounded by the effects of hatch month, sex, and maturity stage. Further research conducted with more extensive multi-year collections will likely be needed to ascertain the importance of annual effects on growth rate.

The estimated growth curves for indeterminate-sex squid indicated that their pattern of growth was exponential as suggested by Hanlon et al. (1987) who examined growth rates of juvenile *L. pealei* in closed-system aquaria. Growth of indeterminate-sex squid in weight was less rapid than that for adults and would be predicted to slow outside the range of observed ages, when these juveniles would develop identifiable sexual characteristics. In contrast, growth of indeterminate-sex squid in length was roughly 1.0% per day. In comparison, growth curves for females and males indicated exponential growth with instantaneous daily growth rates of 0.8% to 1.5%

in ML and 1.8% to 3.1% in weight. The exponential growth of *L. pealei* throughout their life cycle is consistent with the fact that squid have high gross-growth efficiency and are metabolic maximizers in comparison with teleosts (O'Dor and Webber, 1986).

The difference between growth rate in weight of indeterminate-sex squid and adults suggests that there may be a body size above which growth rate increases substantially. This critical size could be related to changes in diet because *L. pealei* undergo an ontogenetic shift in prey selection from crustaceans to fish and other squid as they grow (Vovk, 1972; Macy, 1982b; Vovk, 1985; Anderson and Griswold, 1988). Alternatively, this difference could be the result of a shift from somatic to gonadal growth as squid mature (Macy, 1995), although this seems less likely given the substantial variability in size at maturity of *L. pealei* (Macy, 1980). Regardless of the cause, understanding the implications of the rapid growth of adults and its relationship to maturity stage will be important for predicting how the population structure will respond to exploitation. Over the longterm, it is conceivable that intensive exploitation of an annual semelparous species, such as *L. pealei*, could lead to strong selective pressure for a smaller average size at maturity. Such a reduction in average size at maturity could diminish the reproductive potential of the population (cf. Murphy et al., 1994), and this could lower resilience to environmental fluctuations by reducing the genetic variation in the population.

The implications of these estimates of growth for *L. pealei* in the northwest Atlantic are substantial for the assessment and management of this resource. The short lifespan for this species, combined with the rapid growth of adults and the capacity to spawn year-round, implies that the stock will respond rapidly to environmental variation and fishing pressure. As a result, monitoring the stock for in-season management would likely require several assessments throughout the year.

New management measures are being developed for the long-finned squid stock to reflect the improved understanding of its growth and pattern of reproduction (MAFMC[6]). At present, management of the stock is based on a level of total allowable catch that cannot be exceeded (MAFMC[7]) and on an overfishing definition that has been characterized as "risky" (Rosenberg et al. 1994). A preliminary analysis of some of the weight-at-age data presented in this study indicated that the annual level of maximum sustainable yield, based upon average recruitment and an initial estimate of maximum yield per recruit, could be roughly 36,000 t (NEFSC[8]). This interim estimate was 18% lower than the estimate of 44,000 t, which was based on a presumed two-year lifespan (Sissenwine and Tibbetts, 1977) that has been used as the maximum optimum yield for the stock (MAFMC[7]). However, this estimate appears overly optimistic because landings above 36,000 t have occurred only once, in 1973, when 37,600 t were landed. Regardless, any revision of the annual level of sustainable yield for the stock will need to account for the seasonal patterns of growth and spawning, the potential discarding of juveniles, and variability in stock-recruitment dynamics. Further, it would be more appropriate to estimate sustainable yield and to develop an overfishing definition on a seasonal, rather than an annual, basis for this short-lived species. In contrast to the current quota-based harvesting strategy, a constant harvest-rate strategy that includes a proportional escapement target (Beddington et al., 1990) on a seasonal basis may be a useful management approach.

If the long-finned squid stock is managed on a seasonal basis, revised stock assessment procedures are likely to require rapid collection of catch and effort data and efficient data analysis during periods of peak fishing activity. Real-time assessment procedures have been used to monitor the short-finned squid stock in Falkland Islands waters during the fishing season to achieve proportional escapement goals (Rosenberg et al., 1990), and the use of a constant harvest-rate strategy is a potential option for management of the long-finned squid resource. Although a constant harvest-rate strategy can be overly restrictive in years of good recruitment and result in a loss of yield, it can also jeopardize the stock when recruitment is poor. Therefore, assessment procedures that permit in-season adjustment of the harvest rate would likely be necessary to maintain an adequate level of spawning biomass if management is conducted on a seasonal basis.

As with any renewable resource, long-term management of the long-finned squid stock will involve a balance of the risks and benefits of harvesting the resource. Because long-finned squid are semelparous and likely live for less than 1 year, the risk of re-

[6] Mid-Atlantic Fishery Management Council. 1995. Amendment 5 to the fishery management plan and the final environmental impact statement for the Atlantic mackerel, squid, and butterfish fisheries. MAFMC, Dover, DE.

[7] Mid-Atlantic Fishery Management Council. 1992. 1993–1994 allowable biological catch, optimum yield, domestic annual harvest, domestic annual processing, joint venture processing, and total allowable level of foreign fishing recommendations for Atlantic mackerel, *Loligo*, *Illex*, and butterfish. MAFMC, Dover, DE.

[8] Northeast Fisheries Science Center. 1994. Report of the 17th Northeast Regional Stock Assessment Workshop. NEFSC Ref. Doc. 94–06, Woods Hole, Massachusetts, 124 p.

cruitment overfishing is substantial for this stock. Further, because growth appears to be nearly exponential throughout its life cycle, the risk of growth overfishing is also considerable. On the other hand, harvesting impacts may be difficult to evaluate unless stock response to environmental variation, density-dependence in growth and survival, and community-level interactions with competitors and predators are better understood. Owing to its short lifespan, the immediate benefits of harvesting the long-finned squid resource are probably best measured by average seasonal yield and its variance, and an adaptive approach to management may be needed to ensure sufficient spawning escapement and to foster efficient utilization of this resource.

Acknowledgments

We would like to thank the Captain and the crew of the FV *Huntress* and scientists at the Rhode Island Department of Environmental Management and the National Marine Fisheries Service for their assistance in sample collection. We also thank Frank Almeida, Ann Durbin, Roger Hanlon, James Weinberg, and two anonymous reviewers for their constructive comments on an earlier draft of the manuscript. This work was partially supported by Grant NA89AA-D-SG082 from the National Marine Fisheries Service of the National Oceanic and Atmospheric Administration (NOAA) to the University of Rhode Island Sea Grant College Program.

Literature cited

Alford, R. A., and G. D. Jackson.
1993. Do cephalopods and larvae of other taxa grow asymptotically? Am. Nat. 141:717–728.

Anderson, J., and C. A. Griswold.
1988. The feeding ecology of juvenile long-finned squid, *Loligo pealei*, off the Northeast coast of the United States. U.S. Dep. Commer., NOAA, NMFS, MARMAP Contrib. FED/NEFSC 88-08, Narragansett, RI, 20 p.

Arkhipkin, A.
1993a. Age, growth, stock structure and migratory rate of pre-spawning short-finned squid *Illex argentinus* based on statolith ageing investigations. Fish. Res. 16:313–338.
1993b. Statolith microstructure and maximum age of *Loligo gahi* (Myopsida: Loliginidae) on the Patagonian Shelf. J. Mar. Biol. Assoc. U.K. 73:979–982.

Arkhipkin, A., and N. Nekludova.
1993. Age, growth, and maturation of the loliginid squids *Alloteuthis africana* and *A. subulata* on the West African Shelf. J. Mar. Biol. Assoc. U.K. 73:949–961.

Beddington, J. R., A. A. Rosenberg, J. A. Crombie, and G. P. Kirkwood.
1990. Stock assessment and the provision of management advice for the short fin squid fishery in Falkland Islands waters. Fish. Res. 8:351–365.

Bigelow, K. A.
1992. Age and growth of paralarvae of the mesopelagic squid *Abralia trigonura* based on daily growth increments in statoliths. Mar. Ecol. Prog. Ser. 82:31–40.
1994. Age and growth of the oceanic squid *Onychoteuthis borealjaponica* in the North Pacific. Fish. Bull. 92:13–25.

Bigelow, K. A., and K. C. Landgraf.
1993. Hatch dates and growth of *Ommastrephes bartramii* paralarvae from Hawaiian waters as determined from statolith analysis. *In* T. Okutani, R. K. O'Dor, and T. Kubodera. (eds.), Recent advances in cephalopod fisheries biology, p. 15–24. Tokai Univ. Press, Tokyo, Japan.

Bowman, M. J.
1977. Hydrographic properties. MESA New York Bight Atlas Monograph 1. New York Sea Grant Institute, Albany, New York, 78 p.

Caddy, J. F.
1991. Daily rings on squid statoliths: an opportunity to test standard population models? *In* P. Jereb, S. Ragonese, and S. von Boletzky (eds.), Squid age determination using statoliths: proceedings of the international workshop held at the Instituto di Technologia della Pesce e del Pescato (ITPP-CNR): Mazara del Vallo, Italy, 9–14 October 1989, p. 53–66. NTR-ITPP Spec. Publ., Vol. 1.

Campana, S. E., M. C. Annand, and J. I. McMillan.
1995. Graphical and statistical methods for determining the consistency of age determinations. Trans. Am. Fish. Soc. 124:131–138.

Cohen, A. C.
1976. The systematics and distribution of *Loligo* (Cephalopoda, Myopsida) in the western Atlantic with descriptions of two new species. Malacologia 15:299–367.

Dawe, E. G.
1988. Length-weight relationships for short-finned squid in Newfoundland and the effect of diet on condition and growth. Trans. Am. Fish. Soc. 117:591–599.

Dawe, E. G., R. K. O'Dor, P. H. Odense, and G. V. Hurley.
1985. Validation and application of an ageing technique for short-finned squid (*Illex illecebrosus*). J. Northwest Atl. Fish. Sci. 6:107–116.

Dawe, E. G., J. C. Shears, N. E. Balch, and R. K. O'Dor.
1990. Occurrence, size, and sexual maturity of long-finned squid (*Loligo pealei*) at Nova Scotia and Newfoundland, Canada. Can. J. Fish. Aquat. Sci. 47:1830–1835.

Day, R. W., and G. P Quinn.
1989. Comparisons of treatments after an analysis of variance in ecology. Ecol. Monogr. 59:433–463.

FAO (Food and Agriculture Organization of the United Nations).
1984. FAO species catalogue. Vol. 3: cephalopods of the world. FAO Fish. Synop. 125, 277 p.

Forsythe, J. W.
1993. A working hypothesis of how seasonal temperature change may affect the field growth of young cephalopods. *In* T. Okutani, R. K. O'Dor, and T. Kubodera (eds.), Recent advances in cephalopod fisheries biology, p. 133–143. Tokai University Press, Tokyo, Japan.

Forsythe, J. W., and W. F. Van Heukelem.
1987. Growth. *In* P. R. Boyle (ed.), Cephalopod life cycles, Vol. 2, p. 135–136. Academic Press, London, England.

Games, P. A., and J. F. Howell.
1976. Pairwise multiple comparison procedures with unequal n's and/or variances: a Monte Carlo study. J. Educ. Stat. 1:113–125.

Hanlon, R. T., R. F. Hixon, and W. H. Hulet.
1983. Survival, growth, and behavior of the loliginid squids *Loligo plei, Loligo pealei,* and *Lolliguncula brevis* (Mollusca: Cephalopoda) in closed sea water systems. Biol. Bull. 165:637–685.

Hanlon, R. T., P. E. Turk, P. G. Lee, and W. T. Yang.
1987. Laboratory rearing of the squid *Loligo pealei* to the juvenile stage: growth comparisons with fishery data. Fish. Bull. 85:163–167.

Hatfield, E. M. C., and P. G. Rodhouse.
1994. Migration as a source of bias in the measurement of cephalopod growth. Antarct. Sci. 6:179–184.

Hixon, R. F., R. T. Hanlon, and W. H. Hulet.
1981. Growth and maximal size of the long-finned squid *Loligo pealei* in the Northwestern Gulf of Mexico. J. Shellfish Res. 1:181–185.

Hurley, G. V., P. H. Odense, R. K. O'Dor, and E. G. Dawe.
1985. Strontium labelling for verifying daily growth increments in the statolith of the short-finned squid (*Illex illecebrosus*). Can. J. Fish. Aquat. Sci. 42:380–383.

Jackson, G. D.
1990a. Age and growth of the tropical nearshore loliginid squid *Sepioteuthis lessoniana* determined from statolith growth-ring analysis. Fish. Bull. 88:113–118.
1990b. The use of tetracycline staining techniques to determine statolith growth ring periodicity in the tropical squids *Loliolus noctiluca* and *Loligo chinensis*. Veliger 33:389–393.
1994a. Application and future potential of statolith increment analysis in squids and sepiods. Can. J. Fish. Aquat. Sci. 51:2612–2625.
1994b. Statolith age estimates of the loliginid squid *Loligo opalescens*(Mollusca: Cephalopoda): corroboration with culture data. Bull. Mar. Sci. 54:554–557.

Jackson, G. D., and J. H. Choat.
1992. Growth in tropical cephalopods: an analysis based on statolith microstructure. Can. J. Fish. Aquat. Sci. 49:218–228.

Jackson, G. D., A. I. Arkhipkin, V. A. Bizikov, and R. T. Hanlon.
1993. Laboratory and field corroboration of age and growth from statoliths and gladii of the loliginid squid *Sepioteuthis lessoniana* (Mollusca: Cephalopoda). *In* T. Okutani, R. K. O'Dor, and T. Kubodera (eds.), Recent advances in cephalopod fisheries biology, p. 189–199. Tokai Univ. Press, Tokyo, Japan.

Jeffries, H. P., and W. C. Johnson.
1974. Seasonal distributions of bottom fishes in the Narragansett Bay area: seven-year variations in abundance of winter flounder (*Pseudopleuronectes americanus*). J. Fish. Res. Board Can. 31:1057–1066.

Jereb, P., S. Ragonese, and S. von Boletzky (eds.).
1991. Squid age determination using statoliths: proceedings of the international workshop held at the Instituto di Technologia della Pesce e del Pescato (ITPP-CNR); Mazara del Vallo, Italy, 9–14 October 1989. N.T.R.-I.T.P.P. Spec. Publ., Vol. 1, 127 p.

Lange, A. M. T.
1980. The biology and population dynamics of squids *Loligo pealei* (LeSueur) and *Illex illecebrosus* (LeSueur) from the Northwest Atlantic. M.S. thesis, Univ. of Washington, Seattle, 178 p.
1982. Long-finned squid, *Loligo pealei*. *In* M. D. Grosslein, and T. R. Azarovitz (eds.), Fish distribution, p. 133–135. MESA New York Bight Atlas Monograph 15, New York Sea Grant Institute, Albany, New York, NY.

Lange, A. M. T., and M. P. Sissenwine.
1980. Biological considerations relevant to the management of squid, *Loligo pealei* and *Illex illecebrosus*, of the Northwest Atlantic. Mar. Fish. Rev. 42(7–8):23–38.

Lipinski, M.
1978. The age of squid, *Illex illecebrosus*, from their statoliths. Int. Comm. Northwest Atl. Fish. Res. Doc. 78/II/15, 4 p.
1986. Methods for the validation of squid age from statoliths. J. Mar. Biol. Assoc. U.K. 66:506–526.

Macy, W. K., III.
1980. The ecology of the common squid *Loligo pealei* Le Sueur, 1821 in Rhode Island waters. Ph.D. diss., Univ. Rhode Island, Kingston, RI, 236 p.
1982a. Development and application of an objective method for classifying long-finned squid, *Loligo pealei*, into sexual maturity stages. Fish. Bull. 80:449–459.
1982b. Feeding patterns of the long-finned squid, *Loligo pealei*, in New England waters. Biol. Bull. 162:28–38.
1995. Digital image processing to age long-finned squid using statoliths. *In* D. H. Secor, J. M. Dean, and S. E. Campana (eds.), Fish otolith research and application, p. 283–302. Univ. S. Carolina Press, Columbia, SC.

McMahon, J. J., and W. C. Summers.
1971. Temperature effects on the developmental rate of squid (*Loligo pealei*) embryos. Biol. Bull. 141:561–567.

Mesnil, B.
1977. Growth and life cycle of squid, *Loligo pealei* and *Illex illecebrosus*, from the Northwest Atlantic. Northwest Atl. Fish. Org. Res. Doc. 76/VI/65.

Murphy, E. J., P. G. Rodhouse, and C. P. Nolan.
1994. Modelling the selective effects of fishing on reproductive potential and population structure of squid. ICES J. Mar. Sci. 51:299–313.

Nakamura, Y., and Y. Sakurai.
1991. Validation of daily growth increments in statoliths of Japanese common squid *Todarodes pacificus*. Nippon Suisan Gakkaishi 57:2007–2011.

Natsukari, Y., T. Nakanose, and K. Oda.
1988. Age and growth of loliginid squid *Photololigo edulis* (Hoyle, 1885). J. Exp. Mar. Biol. Ecol. 116:177–190.

NEFSC (Northeast Fisheries Science Center).
1988. Status of fishery resources off the northeastern United States for 1988. Dep. Commer., NOAA Tech. Memo NMFS-F/NEC–63.
1995. Status of fishery resources off the northeastern United States for 1993. U.S. Dep. Commer., NOAA Tech. Memo NMFS-F/NEC, Woods Hole, MA, 138 p.

O'Dor, R. K., and D. M. Webber.
1986. The constraints on cephalopods: why squid aren't fish. Can. J. Zool. 64:1591–1605.

O'Dor, R. K., R. D. Durward, E. Vessey, and T. Amaratunga.
1980. Feeding and growth in captive squid, *Illex illecebrosus*, and the influence of food availability on growth in the natural population. Int. Comm. Northwest Atl. Fish. Sel. Pap. 6:15–21.

Rodhouse, P. G., and E. M. C. Hatfield.
1990a. Age determination in squid using statolith growth increments. Fish. Res. 8:323–334.
1990b. Dynamics of growth and maturation in the cephalopod *Illex argentinus de Castellanos*, 1960 (Teuthoidea: Ommastrephidae). Philos. Trans. R. Soc. Lond. B. Biol. Sci. 329:229–241.

Rosenberg, A. A., G. P. Kirkwood, J. A. Crombie, and J. R. Beddington.
1990. The assessment of stocks of annual squid species. Fish. Res. 8:335–350.

Rosenberg, A., P. Mace, G. Thompson, G. Darcy, W. Clark, J. Collie, W. Gabriel, A. MacCall, R. Methot, J. Powers, V. Restrepo, T. Wainwright, L. Botsford, and K. Stokes.
1994. Scientific review of definitions of overfishing in U.S. fishery management plans. U.S. Dep. Commer., NOAA Tech. Memo NMFS-F/SPO-17, 205 p.

Saleh-Eddine, N.
1991. Age and growth of inshore juvenile Massachusetts long-finned squid, *Loligo pealei* (Lesueur, 1821), using daily increments in statoliths. M.S. thesis, Univ. Rhode Island, Kingston, RI, 61 p.

SAS (SAS Institute, Inc.)
1989. SAS/STAT user's guide, Version 6, 4th ed., vol. 2. Cary, NC, 846 p.

Schnute, J.
1981. A versatile growth model with statistically stable parameters. Can. J. Fish. Aquat. Sci. 38:1128–1140.

Secor, D. H., J. M. Dean, and E. H. Laban.
1991. Manual for otolith removal and preparation for microstructural examination. Electric Power Research Institute and Bell-Baruch Institute for Marine Biology and Coastal Research, Columbia, SC, 85 p.

Shapiro, S. S., and M. B. Wilk.
1965. An analysis of variance test for normality (complete samples). Biometrika 52:591–611.

Sissenwine, M. P., and A. M. Tibbetts.
1977. Simulating the effect of fishing on squid (*Loligo* and *Illex*) populations of the northeastern United States. ICNAF Sel. Pap. 2:71–84.

Sokal, R. R., and F. J. Rohlf.
1981. Biometry, 2nd ed. W. H. Freeman, San Franciso, CA, 859 p.

Spratt, J. D.
1979. Age and growth of the market squid *Loligo opalescens* Berry, from statoliths. CALCOFI Rep. 20:58–64.

Summers, W. C.
1968. The growth and size distribution of current year class *Loligo pealei*. Biol. Bull. 135(2):366–377.
1971. Age and growth of *Loligo pealei*, a population study of the common Atlantic coast squid. Biol. Bull. 141:189–201.
1983. *Loligo pealei*. *In* Cephalopod life cycles, vol. I, p. 115–142. Academic Press, London, England.

Verrill, A. E.
1881. The cephalopods of the north-eastern coast of America, part II. Trans. Connecticut Academy Sci., vol. 5, New Haven, CT.

Vovk, A. N.
1972. Feeding habits of the North American squid, *Loligo pealei* Les. [O. pitanii severoamerikanskogo kal'mar *Loligo pealei* Les]. Tr. Atl. Nauchno-Issled. Inst. Rybn. Khoz. Okeanog. 42:141–151. Fish. Mar. Serv. Canada Transl. Ser. 3304, 14 p.
1985. Feeding spectrum of longfin squid (*Loligo pealei*) in the Northwest Atlantic and its position in the ecosystem. NAFO Sci. Counc. Stud. 8:33–38.

Whitaker, J. D.
1978. A contribution to the biology of *Loligo pealei* and *Loligo plei* (Cephalopoda: Myopsida) off the southeastern coast of the United States. M.S. thesis, College of Charleston, SC, 186 p.

Relationship between sea turtle stranding rates and shrimp fishing intensities in the northwestern Gulf of Mexico: 1986–1989 versus 1990–1993

Charles W. Caillouet Jr.
Galveston Laboratory, Southeast Fisheries Science Center
National Marine Fisheries Service, NOAA
4700 Ave. U, Galveston, Texas 77551–5997

Donna J. Shaver
Padre Island National Seashore, National Biological Service
United States Department of the Interior
9405 South Padre Island Drive, Corpus Christi, Texas 78418

Wendy G. Teas
Miami Laboratory, Southeast Fisheries Science Center
National Marine Fisheries Service, NOAA
75 Virginia Beach Drive, Miami, Florida 33149

James M. Nance
Dickie B. Revera
Andrea C. Cannon
Galveston Laboratory, Southeast Fisheries Science Center
National Marine Fisheries Service, NOAA
4700 Avenue U, Galveston, Texas 77551–5997

Abstract.—This paper tested the null hypothesis that the statistical relationship between monthly sea turtle (species combined) stranding rates (strandings per 100 km of accessible shoreline) and monthly shrimp fishing intensities (days fished per 100 km^2) in the northwestern Gulf of Mexico was the same in 1990–93 as in 1986–89. The expectation was that regulations requiring use of turtle excluder devices (TED's) in shrimp trawls during 1990–93 would reduce the incidental catch of sea turtles and thereby diminish or eliminate the statistical relationship between stranding rates and fishing intensities. Significant positive correlations were detected between the log-transformed stranding rates and fishing intensities for shrimping landward of the 20-fathom (36.6-m) contour in 1990–93. The null hypothesis was not rejected; therefore TED regulations did not result in diminishing or eliminating the statistical relationship between sea turtle stranding rates and shrimp fishing intensities in the northwestern Gulf. Various hypotheses were suggested as possible explanations.

Manuscript accepted 4 October 1995.
Fishery Bulletin 94(2):237–249 (1996).

Endangered Species Act amendments of 1988 mandated an independent review of scientific and technical information pertaining to conservation of sea turtles and the causes and significance of turtle mortality, including that caused by commercial trawling (National Research Council, 1990). Incidental capture of sea turtles in shrimp trawls was identified as the most important human-associated source of mortality in juvenile, subadult, and breeding sea turtles in coastal waters. It was concluded that shrimping could be compatible with sea turtle conservation if adequately controlled, especially through mandatory use of turtle excluder devices (TED's) at most places and times of year. Federal regulations requiring use of TED's by offshore (seaward of the COLREG's demarcation line [the boundary used by the U.S. Coast Guard to distinguish inshore from offshore waters]) shrimp trawlers longer than 25 ft were published in 1987 (Federal Register, vol. 52, no. 124, p. 24247–24262, 28 June 1987). These regulations did not require TED's in "try nets" (small trawls towed and retrieved intermittently during shrimping operations to sample abundance of shrimp), and TED's were used only sporadically in the northwestern

Gulf until 1990 (McDonald, 1990; Henwood et al., 1992; Crouse, 1993b; Weber et al.[1]; Crouse et al.[2]). Therefore, 1986–89 can be considered pre-TED years, for the most part. In contrast, 1990–93 were years during which TED regulations were in effect.

Caillouet et al. (1991) examined the statistical relationship between monthly sea turtle stranding rates (species combined) and monthly shrimp fishing intensities in the northwestern Gulf of Mexico during 1986–89. They detected significant statistical relationships between stranding rates and fishing intensities in some offshore depth intervals within 0 to 15 fathoms (fm) (27.4 m) in two geographic zones of the northwestern Gulf: the upper coast defined as shrimp statistical subareas 17–18, and the lower coast defined as subareas 19–21 (Fig. 1; see Kutkuhn, 1962).

In this paper, we used the approach of Caillouet et al. (1991) to determine whether or not the statistical relationships they detected between monthly sea turtle stranding rates and monthly shrimp fishing intensities during 1986–89 continued to exist after TED regulations had been promulgated. We tested the null hypothesis that the statistical relationship between monthly sea turtle stranding rates and fishing intensities in two geographic zones of the northwestern Gulf was the same in 1990–93 as in 1986–89. The expectation was that regulations requiring use of TED's in shrimp trawls during 1990–93 would reduce the incidental catch of sea turtles and thereby diminish or eliminate the statistical relationship between sea turtle stranding rates and fishing intensities.

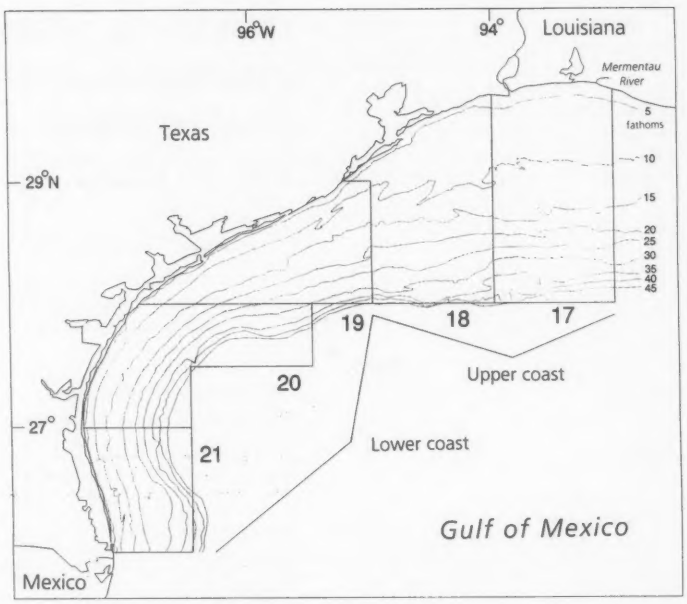

Figure 1

Boundaries of the upper coast (shrimp statistical subareas 17–18) and lower coast (subareas 19–21), and ten depth intervals of the northwestern Gulf of Mexico (see Kutkuhn, 1962; Patella, 1975).

Materials and methods

A data set (subareas 17–21) containing 2,445 sea turtle records was obtained from the Sea Turtle Stranding and Salvage Network (STSSN) headquarters, National Marine Fisheries Service (NMFS) Miami Laboratory, Miami, Florida. It contained records not only of sea turtle strandings but also of turtles caught or entangled in commercial and recreational fishing gears.

Stranded sea turtles, whether live or dead, exhibit no known external or internal signs of capture in shrimp trawls. To our knowledge, only mark-recapture studies have provided direct evidence that some tagged sea turtles captured incidentally in shrimp trawls have become stranded (e.g. Manzella et al., 1988; Fontaine et al., 1989). When examination of stranded sea turtles provides evidence of other causes of death, then capture in shrimp trawls may be ruled out; however, the remaining strandings still lack definite explanation. Strandings that had no explanation were the focus of our analyses.

Prior to our analyses, we deleted 890 records (419 from 1986 to 1989 and 471 from 1990 to 1993) based on codes in data fields named LAT, LONG, NOTE1, NOTE2,... NOTE6, HEADSTART, and TYPEREP (Table 1). The following categories of records were deleted:

[1] Weber, M., D. Crouse, R. Irvin, and S. Indicello. 1995. Delay and denial: a political history of sea turtles and shrimp fishing, 46 p. Center for Marine Conservation, 1725 DeSales St. NW. No. 500, Washington, D.C., 20036.

[2] Crouse, D. T., M. Donnelly, M. J. Bean, A. Clark, W. R. Irvin, and C. E. Williams. 1992. The TED experience: claims and reality, 17 p. A report by the Center for Marine Conservation, Environmental Defense Fund, and National Wildlife Federation. Center for Marine Conservation, 1725 DeSales St. NW, No. 500, Washington, D.C., 20036

Table 1

Frequencies of codes in data fields NOTE1–NOTE6, HEADSTART, TYPEREP, LONG and LAT of records deleted from the STSSN data for shrimp statistical subareas 17–21 and years 1986–93 prior to correlation analyses.[1]

Field	Code	Description	Frequency
NOTE1–NOTE6			
	01	Caught on hook and line	77
	02	Found in dredge hopper	0
	06	Power plant entrapment	3
	08	Cold stun related	69
	11	Entangled in fishing line	13
	13	Entangled in fishing net	4
	15	Found trapped in sunken wreckage	0
	18	Apparent propeller wounds, probably boat strike	53
	22	Caught in shrimp trawl	19
	24	Hook in mouth	17
	28	Entangled in debris, entangled on reef	0
	29	Rope tied to flipper(s) or neck, or both, or to body	13
	36	Emaciated	8
	40	NMFS Galveston Laboratory head-start	261
	41	Nature of wounds suggests entanglement in gill net, net of unknown type, trap line of unknown type, or line of unknown type	2
	43	Nature of wounds suggests bang stick	0
	44	Skull or head only	7
	45	Florida Department of Natural Resources head-start	2
	46	Butchered	6
	48	Entangled in a nonfishing gear medium	17
	51	Caught in a set net	0
	54	Blow to skull	1
	55	Live, adult turtle found flipped on beach	2
	56	Entangled in crab or lobster trap line	0
	58	Caught on trot line	1
	59	Caught in gill net	3
	60	Caught in fish trap	0
	61	Caught in fishing net of unknown type	0
	62	Miami Seaquarium head-start	0
	63	Caught in trawl not targeting shrimp	0
	64	Caught in cast net	0
	65	Catch method unknown	2
	68	Caught in drift net	0
	70	Posthatchling young of the year	165
	73	Nesting female, butchered apparently for eggs	0
	76	Stingray barb embedded in flesh or carapace	0
	80	Nature of wounds suggests crab or lobster trap line entanglement	0
	81	Living tag or apparent living tag noted	42
	82	Spear gun wounds	0
	83	Guts or part(s) only, probable butchering	0
	84	Apparent natural mortality in adult female on a nesting beach	0
	87	Guts or part(s) only, cause unknown	4
	88	Possible boat collision, but not from propeller	1
	90	Constriction wounds or marks on flippers or neck	6
	93	Caught in pound net	0
	95	Monofilament or steel line protruding from mouth or cloaca	1
	96	Probable dredge kill	1
	99	Additional tags applied this capture	0
	AE	Hook in flipper or other soft body part, but not in mouth	7
	AF	Monofilament line found in digestive tract upon necropsy or X-ray	2
	AG	Turtle has tag; number was not recorded	1
	AH	Caught in try net	1
	AI	Fishing hook(s) found in digestive tract upon necropsy or X-ray	9
	AJ	Binary coded internal tag verified	1
	AN	Caught in seine net	1
	AO	Caught in abandoned gear	1
	AP	Entangled in rope (not deliberately tied)	5
	AR	Apparent gaff or hook wounds	0
	AV	Caught on long-line	0
	AX	Found trapped in jetty rocks	2
	AZ	Hatchling found in stomach of predator	1
	BB	TED test turtle (captive-reared)	0
HEADSTART			
	H	Head-started Kemp's ridleys or greens	261
	T	Loggerheads captive-reared for TED certification trials	2
TYPEREP			
	I	Incidental catch or capture	109
LONG		East of longitude 93°07'30"W	8
LAT		South of latitude 26°00'00"N	17

[1] The frequencies in this table represent the number of records bearing a particular code, among the 890 records that were deleted. Therefore, the frequencies do not sum to the total records deleted. Zero frequency indicates that no records containing the code were found among the 2,445 records examined, but it was not known, a priori, that these codes were not represented in the data set.

- turtles that occurred south of subarea 21 (south of latitude 26°00'00"N), because they had been assigned erroneously to subarea 21 (Fig. 1);
- turtles that occurred along the coastline of subarea 17, east of longitude 93°07'30"W, which is near the mouth of the Mermentau River (Fig. 1), because access to it by the STSSN was limited by logistics (Caillouet et al., 1991);
- turtles reported as caught or entangled, either intentionally or incidentally, in commercial (including shrimp trawls) or recreational fishing gears;
- head-started turtles (identified by tags; see

Fontaine et al., 1993), because their temporal-spatial distribution was determined in part by when and where they were released (Manzella et al., 1988; Caillouet et al., 1995);
- small, pelagic-stage turtles, because they were not considered vulnerable to incidental capture in trawls;
- strandings for which likely or possible causes had been assigned.

In some cases, particular codes that defined records to be deleted did not occur among the 2,445 records examined (i.e. they had zero frequency, Table 1), but this was not known a priori. The 1,555 records (937 from 1986–89 and 618 from 1990–93) retained for analysis represented strandings of wild sea turtles for which no known or likely cause of mortality had been assigned. As a consequence of more stringent deletion criteria, our re-analyses for 1986–89 were based on 111 fewer sea turtle records than were the analyses of Caillouet et al. (1991).

For each year, monthly sea turtle strandings (species combined, including those identified to species as well as those not identified to species) were summed over subareas within the upper and lower coasts. This produced 96 observations of monthly sea turtle strandings (2 geographic zones × 4 years × 12 months). Each observation was standardized to S, the monthly number of strandings per 100 km of accessible shoreline bordering the Gulf, which was a measure of sea turtle stranding rate.

A set of offshore, monthly shrimp fishing effort (days fished) data for subareas 17–21 during 1986–93 was obtained from the NMFS Galveston Laboratory (Patella[3]). It was not possible to partition shrimp fishing effort within subarea 17 into portions east and west of longitude 93°07'30"W; therefore the eastern boundary of subarea 17 (Fig. 1) marked the eastern boundary of the upper coast in regard to fishing effort. The total fishing effort at depths seaward of 30 fm (54.9 m) represented less than 8% of the total fishing effort in 1986–89 and 1990–93 on the upper and lower coasts (Table 2), but we included depth intervals seaward of 30 fm for comparison with shallower intervals. For 1986–89 and 1990–93, monthly fishing effort was summed over subareas within the upper and lower coasts, by depth interval (0–5, 5–10, ... >45 fathoms; see Kutkuhn, 1962; Patella, 1975). This produced 960 observations of monthly fishing effort (2 geographic zones × 10 depth intervals × 4 years × 12 months). Each observation was standardized to E, the monthly fishing effort per 100 km^2, which was a measure of fishing intensity.

[3] Patella, F. 1994. Galveston Laboratory, Southeast Fish. Sci. Cent., Natl. Mar. Fish. Serv., NOAA, 4700 Ave. U, Galveston, TX 77551-5997. Personal commun.

Table 2

Percentage of shrimp fishing effort (days fished), total shrimp fishing effort, total catch (pounds of shrimp tails), and pounds caught per unit fishing effort on the upper and lower coasts of the northwestern Gulf of Mexico in 1986–89 and 1990–93, by depth interval.[1]

Depth interval		1986–89		1990–93	
(fm)	(m)	Upper Coast[2]	Lower Coast[3]	Upper Coast[2]	Lower Coast[3]
0–5	0.0–9.1	28.3	5.1	21.4	3.3
5–10	9.1–18.3	27.1	13.2	33.9	11.5
10–15	18.3–27.4	16.2	20.4	6.2	23.5
15–20	27.4–36.6	9.8	25.5	24.9	22.9
20–25	36.6–45.7	6.6	17.9	4.8	16.8
25–30	45.7–54.9	5.7	10.0	6.8	14.8
30–35	54.9–64.0	4.4	5.5	1.4	5.6
35–40	64.0–73.2	1.6	1.9	0.4	1.3
40–45	73.2–82.3	0.3	0.4	0.2	0.3
>45	>82.3	0.1	0.1	0.1	0.0
Total fishing effort		150,229	225,427	144,734	210,710
Total pounds caught		75,346,306	103,309,240	65,789,423	108,365,720
Pounds per unit fishing effort		502	458	455	514

[1] Based on data provided by Frank Patella (see Footnote 3 in the text).
[2] Shrimp statistical subareas 17 and 18 (Fig. 1; see Kutkuhn, 1962).
[3] Shrimp statistical subareas 19–21 (Fig. 1; see Kutkuhn, 1962).

Because some observations of S and E were equal to 0 and the data required logarithmic transformation to assure bivariate normality for correlation analyses, 1 was added to all observations of S and E. Tables 3 and 4 show that $\ln(S + 1)$ and $\ln(E + 1)$ had lower coefficients of skewness and kurtosis (both approaching zero) than did S and E, indicating that the log-transformed variables approached normality, whereas the nontransformed variables were not normally distributed.

Forty product-moment correlations (2 periods × 2 geographic zones × 10 depth intervals) between the paired variables $\ln(S + 1)$ and $\ln(E + 1)$ were calculated, each based on 48 observations (12 months × 4 yr) within a depth interval. These correlations were not statistically independent of each other, because each was based on one set of 48 observations of $\ln(S + 1)$ correlated with each of ten sets of 48 observations of $\ln(E + 1)$. Significant, positive correlations detected between $\ln(S + 1)$ and $\ln(E + 1)$ were tested for homogeneity by using chi-square. Finally, 140 product-moment correlations (2 periods × 2 geographic zones × 35 correlations) between pairs of $\ln(E + 1)$ for the ten depth intervals were calculated, each based on 48 observations. These correlations were statistically independent of each other.

Results

Ten significant positive correlations (i.e. correlation coefficients, r, greater than 0 at $P < 0.05$) were detected between the $\ln(S + 1)$ and $\ln(E + 1)$, half of them in 1986–89 (Fig. 2) and the other half in 1990–93 (Fig. 3). These ten correlations involved $\ln(E + 1)$ for some of the depth intervals between 0 and 20 fm

Table 3

Descriptive statistics for S, E, $\ln(S + 1)$, and $\ln(E + 1)$ for the upper and lower coasts of the northwestern Gulf of Mexico during 1986–89.

	S		E		$\ln(S + 1)$		$\ln(E + 1)$	
	Upper	Lower	Upper	Lower	Upper	Lower	Upper	Lower
n	48	48	480	480	48	48	480	480
Mean	3.98	2.72	9.02	12.51	1.09	1.10	1.57	2.01
Variance	40.62	8.87	340.25	283.53	0.91	0.39	1.32	1.39
Skewness coefficient	2.67	2.27	5.33	4.75	0.72	0.69	0.39	–0.27
Kurtosis coefficient	7.72	5.56	35.50	38.77	–0.27	0.31	–0.25	–0.77
Minimum	0.0	0.0	0.0	0.0	0.00	0.00	0.00	0.00
Maximum	30.7	14.4	170.0	197.4	3.46	2.74	5.14	5.29

Table 4

Descriptive statistics for S, E, $\ln(S + 1)$, and $\ln(E + 1)$ for the upper and lower coasts of the northwestern Gulf of Mexico during 1990–93.

	S		E		$\ln(S + 1)$		$\ln(E + 1)$	
	Upper	Lower	Upper	Lower	Upper	Lower	Upper	Lower
n	48	48	480	480	48	48	480	480
Mean	2.86	1.67	8.06	11.05	1.12	0.84	1.31	1.76
Variance	8.07	2.72	356.92	201.81	0.48	0.26	1.44	1.63
Skewness coefficient	1.47	1.92	5.24	1.76	0.20	0.69	0.81	0.05
Kurtosis coefficient	1.87	4.18	35.38	2.95	–0.80	0.02	–0.03	–1.24
Minimum	0.0	0.0	0.0	0.0	0.00	0.00	0.00	0.00
Maximum	11.3	8.1	195.4	77.0	2.51	2.21	5.28	4.36

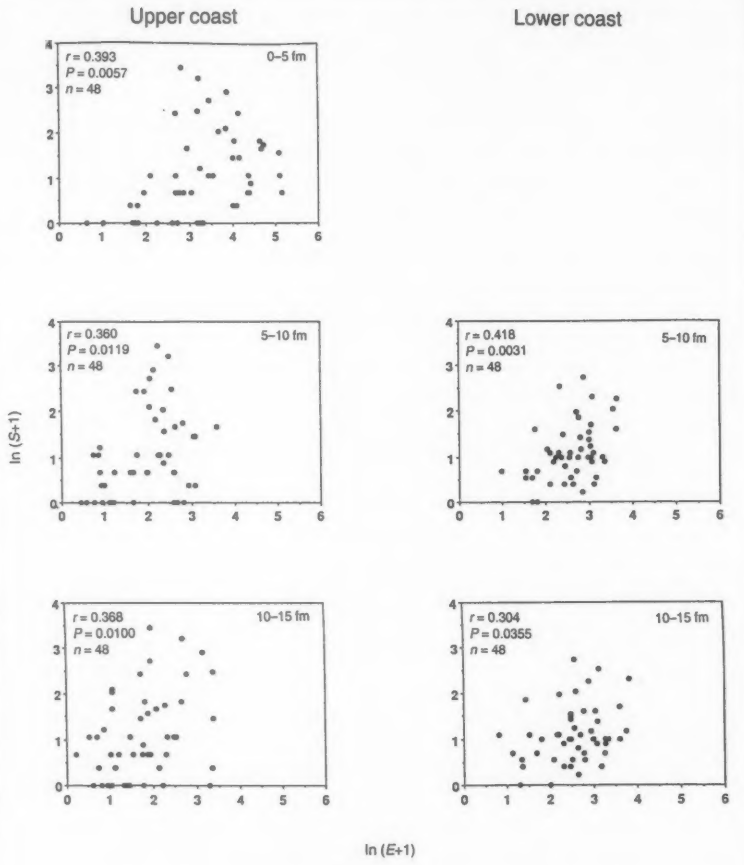

Figure 2

Scatter plots for significant ($P<0.05$), positive correlations between $\ln(S + 1)$ and $\ln(E + 1)$ on the upper coast (shrimp statistical subareas 17–18) and lower coast (subareas 19–21) of the northwestern Gulf of Mexico during 1986–89.

(36.6 m), suggesting that sea turtle stranding rates increased as fishing intensities increased in these depth intervals. The null hypothesis of homogeneity among the ten correlations was not rejected ($\chi^2=9.5$, $P>0.05$), showing that the correlations did not differ significantly from one another. Thus, the null hypothesis that the statistical relationship between monthly sea turtle stranding rates and shrimp fishing intensities in the northwestern Gulf was the same in 1990–93 as in 1986–89 could not be rejected.

Four significant negative correlations between $\ln(S + 1)$ and $\ln(E + 1)$ were also detected for depth intervals seaward of 20 fm. Two occurred on the upper coast, one in 1986–89 for $\ln(E + 1)$ in >45 fm ($r=-0.358$, $P=0.0125$), and one in 1990–93 for $\ln(E + 1)$ in the 35–40 fm depth interval ($r=-0.334$, $P=0.0203$). Two occurred on the lower coast in 1986–89, one for $\ln(E + 1)$ in the 20–25 fm depth interval ($r=-0.431$, $P=0.0022$), and the other in the 25–30 fm depth interval ($r=-0.308$, $P=0.0332$).

A temporal-spatial pattern in monthly fishing intensities was evident from the correlations involving the $\ln(E + 1)$ of the ten depth intervals (Tables 5–8). Significant correlations between the $\ln(E + 1)$ of adjacent depth intervals tended to be positive, showing that monthly fishing intensities in such depth intervals increased or decreased in synchrony. Conversely, monthly fishing intensities in widely separated depth intervals varied in opposite directions, as indicated by significant negative correla-

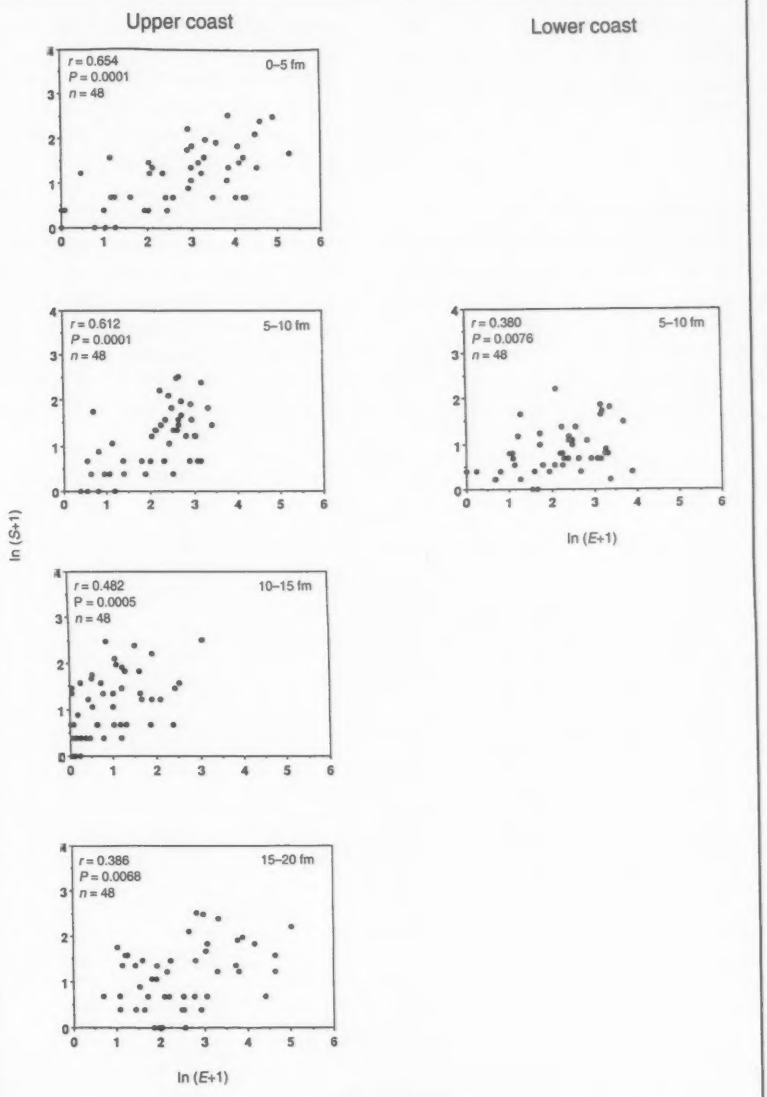

Figure 3

Scatter plots for significant ($P<0.05$), positive correlations between $\ln(S + 1)$ and $\ln(E + 1)$ on the upper coast (shrimp statistical subareas 17–18) and lower coast (subareas 19–21) of the northwestern Gulf of Mexico during 1990–93.

tions. Intermediate depth intervals represented a transition zone, as depicted by a general absence of significant correlations of $\ln(E + 1)$ between these depth intervals and either the shallower or deeper intervals.

In 1986–89 and 1990–93, loggerhead sea turtles, *Caretta caretta,* and Kemp's ridley sea turtles, *Lepidochelys kempii,* occurred most frequently in the strandings, followed by green sea turtles, *Chelonia mydas,* and leatherback sea turtles, *Dermochelys coriacea* (Tables 9 and 10). Strandings of hawksbill sea turtles, *Eretmochelys imbricata,* were equal in number to those of leatherback turtles in 1986–89 (Table 9), but fewer in number than leatherback turtles in 1990–93 (Table 10). Monthly strandings

summed over 1986–89 were highest in April and May (Table 9). Monthly strandings summed over 1990–93 were highest in April and July (Table 10). The total number of strandings decreased from 939 in 1986–89 to 618 in 1990–93.

Discussion

Even though TED regulations were in effect during 1990–93, significant statistical associations continued to exist between sea turtle stranding rates and fishing intensities in some offshore depth intervals within 0 to 20 fm. The 1990–93 period differed somewhat from the 1986–89 period with regard to which depth intervals had significant positive correlations. In 1986–89, significant positive correlations between $\ln(S + 1)$ and $\ln(E + 1)$ were detected on the upper coast only for the 0–5, 5–10, and 10–15 fm depth intervals. However, in 1990–93 on the upper coast, not only were there significant positive correlations for the 0–5, 5–10, and 10–15 fm depth intervals, but also for the 15–20 fm depth interval. On the lower coast, in 1986–89, significant positive correlations occurred between $\ln(S + 1)$ and $\ln(E + 1)$ for the 5–10 and 10–15 fm depth interval, but in 1990–93 only the 5–10 fm depth interval had a significant positive correlation. In addition, the significant positive correlations we detected for the period 1986–89 were somewhat lower (though not significantly) than the comparable ones detected by Caillouet et al. (1991), no doubt the result of excluding 111 more records from the data set, than they did, before conducting our analyses.

Table 5

Correlation coefficients, r, measuring the associations between the $\ln(E + 1)$ of ten depth intervals on the upper coast during 1986–89.

Depth interval	Depth interval (fm)								
	0–5	5–10	10–15	15–20	20–25	25–30	30–35	35–40	40–45
5–10	0.723*[1]								
10–15	0.497*	0.678*							
15–20	0.548*	0.508*	0.679*						
20–25	0.312*	0.237	0.447*	0.695*					
25–30	0.165	0.000	0.304*	0.319*	0.645*				
30–35	–0.142	–0.472*	–0.281	–0.217	–0.168	0.510*			
35–40	–0.447*	–0.505*	–0.300*	–0.276	–0.115	0.256	0.433*		
40–45	–0.372*	–0.459*	–0.213	–0.267	0.010	0.148	0.365*	0.491*	
>45	–0.492*	–0.549*	–0.290*	–0.160	–0.025	–0.162	0.154	0.340*	0.588*

[1] An asterisk indicates that the correlation coefficient, r, was significantly different from zero at $P < 0.05$.

Table 6

Correlation coefficients, r, measuring the associations between the $\ln(E + 1)$ of ten depth intervals on the lower coast during 1986–89.

Depth interval	Depth interval (fm)								
	0–5	5–10	10–15	15–20	20–25	25–30	30–35	35–40	40–45
5–10	0.151								
10–15	0.175	0.379*[1]							
15–20	0.375*	0.147	0.585*						
20–25	0.271	0.108	0.102	0.718*					
25–30	–0.050	0.281	–0.087	0.260	0.629*				
30–35	–0.176	0.116	–0.316*	–0.200	0.138	0.600*			
35–40	–0.143	–0.016	–0.272	–0.445*	–0.387*	0.100	0.447*		
40–45	–0.162	–0.121	–0.251	–0.373*	–0.460*	–0.112	0.317*	0.662*	
>45	0.031	0.040	–0.132	–0.278	–0.393*	–0.053	0.168	0.460*	0.580*

[1] An asterisk indicates that the correlation coefficient, r, was significantly different from zero at $P < 0.05$.

The statistical relationship between stranding rates and fishing intensities persisted despite our using more stringent criteria than did Caillouet et al. (1991) to exclude from the analyses strandings to which possible causes had been assigned. In the absence of significant heterogeneity among the significant positive correlation coefficients, the null hypothesis could not be rejected. Therefore, there was no significant change in the degree of statistical association between sea turtle stranding rates and fishing intensities for some offshore depth intervals within 0 to 20 fm, despite TED regulations, nor was there a significant difference in the degree of this association between the upper and lower coasts.

In 1990–93, as in 1986–89, there was a significant positive correlation between $\ln(S + 1)$ and $\ln(E + 1)$ within 0–5 fm on the upper coast, but not on the lower coast. Depth increases more rapidly with distance from shore on the lower than on the upper coast (Fig. 1). In addition, shrimp move to deeper waters as they migrate southward along the Texas coast each year, accompanied by a corresponding concentration of the shrimping fleet in areas of shrimp abundance. A smaller percentage of fishing effort occurred in the 0–5 fm depth interval on the lower coast than on the upper coast (Table 2).

The significant negative correlations detected between $\ln(S + 1)$ and $\ln(E + 1)$ for some depth intervals seaward of 20 fm probably resulted from a tendency for fishing effort to be concentrated seasonally within certain depth intervals. The pattern of correlations involving fishing intensities in various

Table 7

Correlation coefficients, r, measuring the associations between the $\ln(E + 1)$ of ten depth intervals on the upper coast during 1990–93.

Depth interval	Depth interval (fm)								
	0–5	5–10	10–15	15–20	20–25	25–30	30–35	35–40	40–45
5–10	0.594*[1]								
10–15	0.393*	0.453*							
15–20	0.299*	0.572*	0.528*						
20–25	0.095	0.165	0.153	0.295*					
25–30	–0.100	0.197	–0.048	0.038	0.629*				
30–35	–0.083	–0.135	–0.201	–0.086	0.289*	0.346*			
35–40	–0.416*	–0.314*	–0.390*	–0.255	0.005	0.209	0.109		
40–45	–0.232	–0.179	–0.433*	–0.136	–0.057	0.052	0.174	0.335*	
>45	–0.049	–0.092	0.225	0.001	0.109	0.238	0.117	0.011	–0.029

[1] An asterisk indicates that the correlation coefficient, r, was significantly different from zero at $P < 0.05$.

Table 8

Correlation coefficients, r, measuring the associations between the $\ln(E + 1)$ of ten depth intervals on the lower coast during 1990–93.

Depth interval	Depth interval (fm)								
	0–5	5–10	10–15	15–20	20–25	25–30	30–35	35–40	40–45
5–10	0.550*[1]								
10–15	0.520*	0.838*							
15–20	0.433*	0.636*	0.667*						
20–25	0.238	0.320*	0.439*	0.796*					
25–30	0.130	0.287*	0.347*	0.604*	0.791*				
30–35	–0.305*	–0.234	–0.096	–0.053	0.082	0.389*			
35–40	–0.330*	–0.129	–0.002	–0.202	–0.129	0.196	0.731*		
40–45	–0.256	–0.210	–0.096	–0.231	–0.269	0.026	0.515*	0.668*	
>45	0.117	0.114	0.085	0.145	0.142	0.229	0.266	0.282	0.165

[1] An asterisk indicates that the correlation coefficient, r, was significantly different from zero at $P < 0.05$.

Table 9

Numbers of sea turtle strandings in the northwestern Gulf of Mexico by species and month, summed over years 1986–89.[1]

Species	Jan	Feb	Mar	Apr	May	Jun	Jul	Aug	Sep	Oct	Nov	Dec	Total
Loggerhead (*Caretta caretta*)	9	9	42	144	94	30	41	34	26	24	17	19	489
Kemp's ridley (*Lepidochelys kempii*)	0	6	32	81	47	37	23	44	23	21	15	10	339
Green (*Chelonia mydas*)	0	0	5	7	6	6	1	1	0	3	1	3	33
Leatherback (*Dermochelys coriacea*)	0	0	0	6	4	3	0	1	0	1	3	0	18
Hawksbill (*Eretmochelys imbricata*)	0	1	2	0	1	3	1	1	3	2	2	2	18
Undetermined	0	0	6	6	2	5	8	3	4	4	0	2	40
Total	9	16	87	244	154	84	74	84	56	55	38	36	937

[1] After some records were deleted (see Table 1).

Table 10

Numbers of sea turtle strandings in the northwestern Gulf of Mexico by species and month, summed over years 1990–93.[1]

Species	Jan	Feb	Mar	Apr	May	Jun	Jul	Aug	Sep	Oct	Nov	Dec	Total
Loggerhead (*Caretta caretta*)	8	11	27	50	16	8	48	30	22	15	16	31	282
Kemp's Ridley (*Lepidochelys kempii*)	5	2	18	38	20	17	44	34	38	22	22	11	271
Green (*Chelonia mydas*)	0	2	4	5	2	1	2	1	3	1	2	1	24
Leatherback (*Dermochelys coriacea*)	0	0	0	5	5	2	3	0	0	0	0	0	15
Hawksbill (*Eretmochelys imbricata*)	0	1	0	0	1	1	1	0	2	1	2	0	9
Undetermined	0	0	0	2	2	1	2	0	3	5	0	2	17
Total	13	16	49	100	46	30	100	65	68	44	42	45	618

[1] After some records were deleted (see Table 1).

depth intervals suggested that monthly fishing intensities in contiguous depth intervals increase or decrease in the same direction. This pattern also suggests that monthly fishing intensities are high in deeper waters when they are low in shallower waters, and vice versa, probably in association with the seasonal migrations of shrimp and the fishing fleet (Tables 5–8). Thus, when fishing intensities in depth intervals between 0 and 20 fm were positively associated with strandings, the fishing intensities seaward of 20 fm were low, producing inverse associations with stranding rates.

The pattern of correlations between the $\ln(E + 1)$ of the various depth intervals may have influenced the correlations between $\ln(S + 1)$ and $\ln(E + 1)$. Some of the significant positive correlations detected between $\ln(S + 1)$ and $\ln(E + 1)$ may have resulted from correspondences between stranding rates and fishing intensities, whereas others may have been coincidental. Our analyses determined only that there were significant positive correlations between $\ln(S + 1)$ and $\ln(E + 1)$, but they cannot prove there was a cause and effect relationship between fishing intensities and stranding rates. On the other hand, our results would be consistent with a cause and effect relationship. Although the positive correlations we detected were not significantly heterogeneous, they did tend to decrease in strength with depth, which may suggest a decreasing degree of statistical association between stranding rates and fishing intensities as depth increases. This tendency also could occur if sea turtles injured or killed in deeper waters were less likely to wash ashore than those injured or killed closer to the shoreline (Caillouet et al., 1991).

The significant positive correlations we detected between $\ln(S + 1)$ on $\ln(E + 1)$ were circumstantial evidence of a relation between sea turtle stranding rates and shrimp fishing intensities, but they did not demonstrate that shrimping caused the strandings. Nevertheless, they were consistent with previous findings that sea turtles are caught and killed incidentally in shrimping (National Research Council,

1990) and that some turtles incidentally caught during shrimping operations become stranded (Manzella et al., 1988; Fontaine et al., 1989). The surprising aspect of our findings comes from the expectation that TED regulations would lead to a reduction or elimination of the statistical association between sea turtle stranding rates and fishing intensities in the northwestern Gulf. To explain this continued statistical association, we offer the following hypotheses:

1 legal and properly installed TED's failed to eject all of the sea turtles caught incidentally in shrimp trawls;
2 sea turtles were captured and ejected repeatedly from trawls containing legal and properly installed TED's, and eventually succumbed to the stresses of repeated passage through such trawls;
3 sea turtles were captured incidentally in shrimpers' try nets that had no TED's;
4 violations of TED regulations resulted in incidental capture of sea turtles;
5 nonshrimping causes of sea turtle mortality were in synchrony with shrimping effort.

Legal and properly installed TED's may have failed to eject all of the sea turtles caught incidentally in shrimp trawls (hypothesis 1). Prior to June 1994, supporting floats were not required on bottom-opening hard TED's (Mitchell[4]). Tests by NMFS showed that use of such legal TED's without floats could result in sea turtle mortality (Mitchell[4]). Therefore, NMFS issued new rules to ensure sea turtle escape. Other NMFS studies have shown that sea turtles are sometimes caught in TED-equipped shrimp trawls (Renaud et al., 1990, 1991; Epperly et al., 1995). Each type of TED certified for use by the shrimp industry has been tested under an established scientific protocol (Federal Register, vol. 55, no. 195, p. 41882–41883, 9 October 1990). NMFS-certified TED's that were properly installed and "tuned" (adjusted) were required to be no less than 97% effective in ejecting incidentally captured sea turtles. The actual rate of ejection could vary below 97% under less than ideal shrimp trawling conditions.

There is no evidence that individual sea turtles were captured and ejected repeatedly from certified, properly installed TED's during commercial shrimp trawling operations (hypothesis 2). If they had been, they would have undergone repeated stress. To determine whether sea turtles are captured and ejected repeatedly from TED's during commercial trawling operations, underwater observations would be required and the sea turtles would have to be marked for repeated recognition. During TED certification trials conducted near Panama City, Florida, Kemp's ridley turtles, released into TED-equipped shrimp trawls and submerged for less than 8 min before ejection and surfacing, developed blood acidosis. The acidosis was, for the most part, metabolic (caused by accumulation of lactate) and to a lesser degree respiratory (caused by accumulation of CO_2)(Stabenau et al., 1991). The turtles released excess CO_2 when they hyperventilated after surfacing (Stabenau et al., 1991). Other research showed that at least 20 h were required for complete recovery from lactate acidosis in loggerhead sea turtles caught in shrimp trawls during sea turtle surveys in Port Canaveral Ship Channel, Florida (Lutz and Dunbar-Cooper, 1987). It is doubtful that a sea turtle in a state of severe blood acid-base disequilibrium, resulting from submergence and struggling to escape a shrimp trawl, would dive soon after release from a TED (Stabenau[5]). If it dived, the blood acidosis would be exacerbated. On the other hand, if the turtle remained at or near the surface it could take frequent breaths and recover from the acid-base disturbance. As standard practice, sea turtles submerged in shrimp trawls for less than 10 minutes during TED certification trials are allowed at least 48 h of recovery before being submerged in a second test (Fontaine[6]).

Sea turtles may have been captured incidentally in shrimpers' try nets (hypothesis 3) within which TED's were not required. Even though these small trawls are towed for relatively brief intervals, direct observations aboard shrimp trawlers have shown that sea turtles are caught incidentally in try nets (Renaud et al., 1990, 1991; Mitchell[4]).

Violations of TED regulations have been shown to result in incidental capture of sea turtles in shrimp trawls (hypothesis 4). For example, unprecedented numbers of sea turtles were stranded in Louisiana in 1993 and in Texas in 1994 and 1995, concomitant with concentrations of shrimp trawling. These stranding events were attributed, at least in part, to violations of TED regulations, including, but not limited to, various illegal alterations of TED's (Crouse, 1993a; Shaver, 1994, 1995; Steiner, 1994; Shrimp Trawling in the Southeastern United States Under the Sea Turtle Conservation Regulations, Endan-

[4] Mitchell, J. 1995. Pascagoula Laboratory, Southeast Fish. Sci. Cent., Natl. Mar. Fish. Serv., NOAA, P.O. Drawer 1207, Pascagoula, MS 39568-1207. Personal commun.

[5] Stabenau, E. 1994. Department of Physiology, School of Medicine, East Carolina University, Greenville, NC 27858-4354. Personal commun.

[6] Fontaine, C. 1995. Galveston Laboratory, Southeast Fish. Sci. Cent., Natl. Mar. Fish. Serv, NOAA, 4700 Ave. U, Galveston, TX 77551-5997. Personal commun.

gered Species Act, Section 7 Consultation, Biological Opinion, NMFS, 14 November 1994; Mitchell[4]). As a consequence, NMFS developed an Emergency Response Plan (Federal Register, vol. 60, no. 77, p. 19885–19886, 21 April 1995; Federal Register, vol. 60, no. 85, p. 21741–21745, 3 May 1995). This plan, a resurgence of sea turtle strandings along the Texas coast during the spring 1995 shrimping season (Shaver, 1995), and an ensuing ruling by Judge Samuel B. Kent (*Center for Marine Conservation vs. Brown*, C.V. No. G-94-660, U.S. District Court, Galveston, Texas) led to additional TED restrictions on shrimping seaward to 12 nautical miles.

There is little evidence to support hypothesis 5, that causes of strandings other than incidental capture of sea turtles in shrimp trawls were in synchrony with shrimping. It seems unlikely that a major nonshrimping cause of sea turtle mortality has escaped detection during the many years of study of factors causing sea turtle injury and mortality at sea (National Research Council, 1990; Kemp's Ridley Recovery Team[7]). Prior to our analyses, we deleted stranding records that represented known or likely causes (Table 1), even when some of these causes did not absolutely rule out incidental capture in shrimp trawls (Table 1). The records retained for analysis represented strandings for which no cause was known. Nevertheless, it is possible that causes other than shrimping contributed to the unexplained strandings that were retained for our analyses, because it is known that there are other minor causes of sea turtle mortality, some of which could have been in synchrony with shrimping.

The lower total number of strandings in the northwestern Gulf in 1990–93 as compared with 1986–89 (Tables 9 and 10) would be encouraging were it not for differences in STSSN coverage in 1990–93 and 1986–89. Schroeder (1989), Whistler (1989), and the National Research Council (1990) pointed out that temporal–spatial coverage of sea turtle strandings is rarely uniform because the STSSN depends for the most part on volunteers. During 1986–89, to supplement the efforts of volunteers, universities, and other agencies (Texas A&M University, the University of Texas, National Park Service, U.S. Fish and Wildlife Service, and Texas Parks and Wildlife Department), NMFS Galveston Laboratory personnel conducted systematic surveys at least once a month along accessible shorelines of beaches bordering the Gulf from the Mermentau River to the Rio Grande (Caillouet et al., 1991). During 1990–93, personnel at Galveston Laboratory focused their coverage only on subarea 18 during March–November; STSSN coverage in other areas of the northwestern Gulf in those years depended more on volunteers, universities, and other agencies than was the case in 1986–89. Therefore, the decrease in total number of strandings might have occurred because of a reduction in STSSN coverage, but the mandatory use of TED's and the decrease in total shrimp fishing effort, both on the upper and lower coasts (Table 2), cannot be ignored as possible contributing factors. The statistical association between stranding rates and fishing intensities persisted in 1990–93 despite the reduction in total strandings. It is essential that STSSN coverage of strandings be consistent, both spatially and temporally, to provide data sufficient to assess real trends in sea turtle strandings and to determine their relationship to natural as well as anthropogenic causes.

The statistical association between sea turtle stranding rates and shrimp fishing intensities in the northwestern Gulf is worthy of concern and further attention. Continued strandings of sea turtles demonstrate that the problem of sea turtle mortality at sea has not been solved (Henwood et al., 1992; Shaver, 1994, 1995). It is clear that further efforts will be necessary to solve this problem and thereby speed the recovery of sea turtle populations. Those efforts must include reduction or elimination of human-caused sea turtle mortality at sea (National Research Council, 1990; Henwood et al., 1992).

Acknowledgments

Special thanks are due to all who documented sea turtle strandings in the northwestern Gulf during 1986–93, and especially the National Biological Service, U.S. Dept. of Interior, Corpus Christi, Texas, and the Aquarium of the Americas, New Orleans, Louisiana, for coordinating the collection and processing of stranding data. We greatly appreciated comments and suggestions by Jeffrey Brown, Clark Fontaine, William Jackson, John Mitchell, Charles Oravetz, Erich Stabenau, and anonymous reviewers of the manuscript.

Literature cited

Caillouet, C. W., Jr., M. J. Duronslet, A. M. Landry Jr., D. B. Revera, D. J. Shaver, K. M. Stanley, R. W. Heinly, and E. K. Stabenau.
1991. Sea turtle strandings and shrimp fishing effort in the

[7] Kemp's Ridley Recovery Team. 1992. Recovery plan for the Kemp's ridley sea turtle (*Lepidochelys kempii*). Prepared for the Southwest Region, U.S. Fish and Wildlife Service, Albuquerque, New Mexico, and National Marine Fisheries Service, Washington, D.C., 40 p.

Northwestern Gulf of Mexico, 1986–89. Fish. Bull. 89:712–718.

Caillouet, C. W., Jr., C. T. Fontaine, S. A. Manzella-Tirpak, and D. J. Shaver.
1995. Survival of head-started Kemp's ridley sea turtles (*Lepidochelys kempii*) released into the Gulf of Mexico or adjacent bays. Chelonian Conservation and Biology 1(4):285–292.

Crouse, D.
1993a. Tragic mass stranding confirms presence of Kemp's ridley turtles in Louisiana. Marine Turtle Newsletter No. 63, p. 5–6. [Available from BIOSIS, 2100 Arch Street, Philadelphia, PA 19103–1399.]
1993b. Victory! TEDs required in all U.S. shrimp trawls. Marine Turtle Newsletter No., 61, p. 3–5. [Available from BIOSIS, 2100 Arch St., Philadelphia, PA 19103–1399.]

Epperly, S. P., J. Braun, A. J. Chester, F. A. Cross, J. V. Merriner, and P. A. Tester.
1995. Winter distribution of sea turtles in the vicinity of Cape Hatteras and their interactions with the summer flounder trawl fishery. Bull. Mar. Sci. 56:519–540.

Fontaine, C. T., S. A. Manzella, T. D. Williams, R. M. Harris, and W. J. Browning.
1989. Distribution, growth and survival of head started, tagged and released Kemp's ridley sea turtles (*Lepidochelys kempi*) from year-classes 1978–1983. *In* C. W. Caillouet Jr. and A. M. Landry Jr. (eds.), Proceedings of the first international symposium on Kemp's ridley sea turtle biology, conservation and management, p. 124–144. Texas A&M Univ., Sea Grant College TAMU-SG-89-105.

Fontaine, C. T., D. B. Revera, T. D. Williams, and C. W. Caillouet Jr.
1993. Detection, verification and decoding of tags and marks in head started Kemp's ridley sea turtles, *Lepidochelys kempii*. U.S. Dep. Commer., NOAA Tech. Memo. NMFS-SEFC-334, 40 p.

Henwood, T., W. Stuntz, and N. Thompson.
1992. Evaluation of U.S. turtle protective measures under existing TED regulations, including estimates of shrimp trawler related turtle mortality in the wider Caribbean. U.S. Dep. Commer., NOAA Tech. Memo. NMFS-SEFSC-303, 14 p.

Kutkuhn, J. H.
1962. Gulf of Mexico commercial shrimp populations-trends and characteristics, 1956–59. Fish. Bull. 62:343–402.

Lutz, P. L., and A. Dunbar-Cooper.
1987. Variations in the blood chemistry of the loggerhead sea turtle, *Caretta caretta*. Fish. Bull. 85:37–43.

Manzella, S. A., C. W. Caillouet Jr., and C. T. Fontaine.
1988. Kemp's ridley, *Lepidochelys kempi*, sea turtle head start tag recoveries: distribution, habitat, and method of recovery. Mar. Fish. Rev. 50(3):24–32.

McDonald, D.
1990. Shrimpers arrested for non-compliance as efforts to enforce TED regulations intensify. Marine Turtle Newsletter No. 51, p. 10–12. [Available from BIOSIS, 2100 Arch St., Philadelphia, PA 19103–1399.]

National Research Council.
1990. Decline of the sea turtles: causes and prevention. Committee on Sea Turtle Conservation, Board of Environmental Studies and Toxicology, Board on Biology, Commission on Life Sciences, National Research Council, National Academy Press, Wash., D.C., 190 p.

Patella, F.
1975. Water surface area within statistical subareas used in reporting Gulf Coast Shrimp Data. Mar. Fish. Rev. 37(12):22–24.

Renaud, M., G. Gitschlag, E. Klima, A. Shah, D. Koi, and J. Nance.
1991. Evaluation of the impacts of turtle excluder devices (TEDs) on shrimp catch rates in coastal waters of the United States Along the Gulf of Mexico and Atlantic, September 1989 through August 1990. U.S. Dep. Commer., NOAA Tech. Memo NMFS-SEFC-288, 80 p.

Renaud, M., G. Gitschlag, E. Klima, A. Shah, J. Nance, C. Caillouet, Z. Zein-Eldin, D. Koi, and F. Patella.
1990. Evaluation of the impacts of turtle excluder devices (TEDs) on shrimp catch rates in the Gulf of Mexico and South Atlantic, March 1988 through July 1989. U.S. Dep. Commer., NOAA Tech. Memo. NMFS-SEFC-254, 165 p.

Schroeder, B. A.
1989. Marine turtle data base management: National Marine Fisheries Service—Miami Laboratory. *In* C. W. Caillouet Jr. and A. M. Landry Jr. (eds.), Proceedings of the first international symposium on Kemp's ridley sea turtle biology, conservation and management, p. 153–156. Texas A&M Univ., Sea Grant College TAMU-SG-89-105.

Shaver, D. J.
1994. Sea turtle strandings along the Texas coast reach alarming levels. Marine Turtle Newsletter 66:8–9. [Available from BIOSIS, 2100 Arch St., Philadelphia, PA, 19103–1399.]
1995. Sea turtle strandings along the Texas coast again cause concern. Marine Turtle Newsletter 70:2–4. [Available from BIOSIS, 2100 Arch St., Philadelphia, PA 19103–1399.]

Stabenau, E. K., T. A. Heming, and J. F. Mitchell.
1991. Respiratory, acid-base and ionic status of Kemp's ridley sea turtles (*Lepidochelys kempi*) subjected to trawling. Comp. Biochem. Physiol. 99A(1/2):107–111.

Steiner, T.
1994. Shrimpers implicated as strandings soar in the USA. Marine Turtle Newsletter 67:2–5. [Available from BIOSIS, 2100 Arch St., Philadelphia, PA 19103–1399.]

Whistler, R. G.
1989. Kemp's ridley sea turtle strandings along the Texas coast, 1983–1985. *In* C. W. Caillouet Jr. and A. M. Landry Jr. (eds.), Proceedings of the first international symposium on Kemp's ridley sea turtle biology, conservation and management, p. 43–50. Texas A&M Univ., Sea Grant College TAMU-SG-89-105.

Barotrauma-associated regurgitation of food: implications for diet studies of Hawaiian pink snapper, *Pristipomoides filamentosus* (family Lutjanidae)

Edward E. DeMartini
Frank A. Parrish
Denise M. Ellis

Honolulu Laboratory, Southwest Fisheries Science Center
National Marine Fisheries Service, NOAA
2570 Dole Street, Honolulu, Hawaii 96822-2396

Abstract.—Juvenile (128–244 mm fork length) pink snapper, *Pristipomoides filamentosus*, were caught by hook and line from 60–90 m depths offshore of Kaneohe Bay, windward Oahu, Hawaii, during February–August 1994. About one-half of the 180 specimens were intercepted by scuba divers 15–18 m below the sea surface and individually "bagged" live before they were retrieved for the remaining distance to the surface. The other half were retrieved directly by fishing line to the surface ("unbagged"); these latter fish thus remained at a continual risk of prey loss from regurgitation while they were stressed by the full extent of pressure change. The retained stomach contents of bagged and unbagged fish were compared on the basis of volume and type of food and on the size of individual prey items. Bagged samples of juvenile snapper on average retained a 116% (95% CI=70–157%) greater volume of prey than unbagged snapper; bagged snapper also had more types and greater maximum body sizes of prey than did unbagged fish. These results are discussed in terms of designing quantitative diet studies for juvenile snapper and other deep-water physoclistous fishes.

Manuscript accepted 1 November 1995.
Fishery Bulletin 94:250–256 (1996).

The diet and feeding habits of deep-water physoclistous fishes are usually described by using fish collected with gears (hook and line, set lines, trawls, nets, traps) that subject specimens to the stress of large reductions in ambient pressure (barotrauma) as they are retrieved. Numerous studies have derived estimates of stomach fullness, prey consumption or daily ration, and gastric evacuation rates (reviewed by Bromley, 1994) based on collections that include or exclude specimens with empty stomachs. Often overlooked is the distinction between naturally occurring empty stomachs and stomachs that have partially or totally everted their contents as a result of swimbladder expansion during gear retrieval or other procedures of capture (Kohler and Fitzgerald, 1969; Daan, 1973; Durbin et al., 1983; Rice, 1988; Hislop et al., 1991).

The Hawaiian pink snapper or "opakapaka" (*Pristipomoides filamentosus*) represents a major portion of the deep-slope (150–300 m) bottomfishery in Hawaii (Haight et al., 1993a). Juveniles inhabit a shallower (60–90 m), relatively narrow depth zone on insular shelves (Parrish, 1989; Ellis and DeMartini, 1995; Moffitt and Parrish[1]) but, nonetheless, experience barotrauma during conventional collection procedures (Parrish and Moffitt, 1993). Juveniles are discontinuously distributed, and localized patches of occupied habitat have recently persisted for at least five consecutive years (1989–93; Parrish et al.[2]). One hypothesis for the persistence of these patches of juveniles is the localized distribution of prey, which in turn might reflect static substrate characteristics or recurrent patterns of near-bottom water movements. Testing such hypotheses requires describing the diet of juveniles as well as the distribution and availability of prey organisms.

[1] Moffitt, R. B., and F. A. Parrish. 1995. Habitat use and life history of juvenile Hawaiian pink snapper, *Pristipomoides filamentosus*. Honolulu Lab., Southwest Fish. Sci. Cent., Natl. Mar. Fish. Serv., NOAA, 2570 Dole St., Honolulu, HI 96822–2396. Unpubl. manuscript.

[2] Parrish, F. A., E. E. DeMartini, and D. M. Ellis. 1995. Effects of physiography and coastal discharge on the longshore distribution of juveniles of the snapper *Pristipomoides filamentosus* in the Hawaiian Archipelago. Honolulu Lab., Southwest Fish. Sci. Cent., Natl. Mar. Fish. Serv., NOAA, 2570 Dole St., Honolulu, HI 96822–2396. Unpubl. manuscript.

As part of our studies of the foraging and distribution of juvenile pink snapper, we have been developing methods to quantify stomach contents with acceptable accuracy and precision. In this paper we describe and evaluate a method of collecting juvenile snapper for diet analysis that minimizes the problem of subsurface regurgitation of food as specimens are retrieved from depth.

Methods

Fish collection

Juvenile snapper were caught by hook and line from near-bottom depths of 60–90 m, about 3–4 km offshore of Kaneohe Bay, windward Oahu, Hawaii, on nine dates during the period February–August 1994. All fish were captured between about 0900 and 1500 h. On each date, at 15–18 m below the sea surface, about one-half of all fish (randomly selected) were "bagged" by scuba divers (using NOAA NITROX II [64% N_2, 36% O_2] to extend diving periods approximately twofold at these depths). Divers observed fish—underwater visibilities consistently exceeded 30 m—as they were reeled up to 15–18 m and subsequently to the sea surface and noted whether specimens regurgitated food just before or during the bagging process; if they did regurgitate, these fish were left "unbagged" (see below). Median time for collection (1055 h) was the same for both bagged and unbagged fish. Bagged fish were sealed live in individually marked canvas bags before they were retrieved the remaining distance to the surface. The other half of the fish (unbagged) were brought directly to the surface by the fishing line. All fish were reeled in at a rate of about 30 m per minute (Haight et al., 1993b). Once aboard ship, unbagged fish were also packaged individually in marked canvas bags. Fish were stored on ice in a cooler until they were frozen intact in their marked bags at the NMFS Honolulu Laboratory, 2–8 h after capture.

Stomach content analyses

Each frozen fish was thawed, removed from its bag, and the bag everted in the laboratory. The external body surface of each specimen and the inside surface of the bag were rinsed into a black paraffin-bottom dissecting tray. Any prey fragments in the fluid were collected. Gill rakers, esophagus, and pharynx (including vomerine and jaw teeth) of the specimen were examined for prey. Ruptured swim bladders were noted, and extent of stomach eversion according to a stomach eversion index (EvI) was recorded (on a scale from 1 [not everted] to 2 [partially everted] to 3 [fully everted]). Fish were then measured (mm fork length [FL]). Lastly, the stomach was excised and its contents saved, along with any prey items that were free in the coelom as the result of stomach rupture. All prey (regurgitated and present in the stomach) were pooled. Prey were then blotted damp on a paper towel, and a displacement volume (0.01 mL) was measured. Stomachs and prey were fixed in 3.7% formaldehyde (sea water buffered) for 1–2 months, then preserved in 60% EtOH. The eviscerated wet weight (EW) of each snapper was recorded to the nearest gram.

Prey were examined under a dissecting microscope at 8–50×and classified (when possible) to the level of suborder or order. The length (longest axis) of each prey item was recorded to the nearest millimeter.

Identifiable prey were divided a priori into four major types (Bowen, 1983) on the basis of probable microhabitat: 1) crustaceans—mostly shrimps and stomatopods of indeterminate epibenthic or lower water column habitats; 2) benthos—primarily demersal octopods, echinoids, and microgastropods representing mobile epifauna; 3) nekton—actively swimming water column fishes and squids; and 4) jellies—weakly mobile, gelatinous salps and heteropods.

Statistics

A nonparametric bootstrapping procedure was used to evaluate mean prey volume in bagged versus unbagged fish because we were interested in quantifying the magnitude of possible differences in prey volume between the two treatments, even though sampling dates were too few to evaluate normality accurately. The variables used for bootstrapping (n=1,000 iterations; Manly, 1991) were 1) the differences between the date-specific mean prey volumes for bagged and unbagged fish. Because sampling design alone might have incompletely controlled for body size and date effects on prey volume, we further evaluated 2) the differences between predicted and observed prey volumes in unbagged snapper. Predicted values for unbagged fish were calculated on the basis of prey volumes measured for bagged fish of the same weight and date, because prey volumes were positively related to body weight for bagged snapper only (see Results section). Predicted values for bagged fish were derived from stepwise multiple regression of prey volume on sampling date and body weight. For both 1) and 2), date-means were weighted by the number of sample fish on that date.

Standard nonparametric tests (Siegel and Castellan, 1988; SAS, 1988: Proc NPAR1WAY, Proc FREQ)

were used to compare prey composition and prey size between bagged and unbagged fish. All tests were two-tailed (α=0.05). The Bonferroni correction (α'=0.05/m; Manly, 1991, p. 52) was used to control type-I error for $m = 3, 2 \times 2$ chi-squared tests of presence or absence of prey types between treatments. Data were too few to analyze by separate chi-squared tests for each date. A three-way G-test was inappropriate for simultaneous comparisons of prey types because the occurrences of types were interdependent.

Results

Fish specimens

A total of 180 juvenile snapper (88 bagged, 92 unbagged) were collected on the nine sampling dates. From 5 to 40 specimens were collected per date (numbers of bagged and unbagged fish were <15% different on six of the last seven dates). Median size of fish was 176 mm FL (range 128–244 mm) and 98 g eviscerated weight (EW, range 36–289 g). No significant difference existed between bagged and unbagged fish, and growth was clearly evident over the sampling period (Table 1). Few bagged (n=3) and unbagged (n=3) snapper had ruptured swimbladders, and both bagged and unbagged fish had equivalently high indices of stomach eversion (Table 1). Four specimens had completely empty stomachs, and all were unbagged fish. Regurgitated prey were typically evident inside the bags of bagged fish and on gill rakers or elsewhere in the pharynx of both bagged and unbagged fish. Divers witnessed unbagged snapper frequently regurgitating stomach contents between 15–18 m depth and the sea surface, as the volume of gases in swimbladders expanded by more than an atmosphere of pressure, equivalent to 40% of all bladder expansion between depths of 75 and 15 m. Snapper were never seen regurgitating prey below 18 m, although safety considerations precluded prolonged observations by divers at depths >18 m.

Prey volume

From bagged snapper, we collected an average 108% more prey (0.75 ±0.57 mL [SD], versus 0.36 ±0.24 mL for unbagged fish), on the basis of the unadjusted grand means of all nine date-means weighted by their respective sample sizes (Fig. 1; Table 1). The logarithm of prey volume was positively related to the logarithm of fish body weight for bagged fish (P<0.0001) and additionally differed among collection dates (P=0.04; forward stepwise regression, P=0.15 as inclusion level; Proc REG: SAS, 1988; R^2=0.98). Date effects thus represented more than just temporal differences in fish size. A fish body weight effect on prey volume was undetectable (P>0.95) for unbagged fish, for which only collection date was important (R^2=0.93). A general date effect increased monotonically over the sampling period.

Prey volumes for both bagged and unbagged snapper were evaluated on the basis of bootstrapped estimates for the last seven sampling dates on which

Table 1

Summary statistics for juvenile pink snapper, *Pristipomoides filamentosus*, caught by hook and line off Kaneohe Bay, windward Oahu, Hawaii, during February–August 1994. Values for fork length (FL, mm), eviscerated body weight (EW, g), and the stomach eversion index (EvI) are medians for the sampling date; number of fish (n) is the date-specific sample size.

	Bagged					Unbagged				
Sampling date	n	FL	EW	Time caught	EvI	n	FL	EW	Time caught	EvI
09 Feb	1	155	57	0935	3	4	190	118	0920	2
28 Feb	4	168	87	1206	2.5	2	165	98	1006	2
02 Mar	16	150	60	1130	2	16	153	63	1143	2
04 Mar	14	155	64	1120	3	16	187	101	1104	2
15 Jul	9	172	87	1112	2	8	170	84	1105	2
19 Jul	11	173	94	1045	2	12	166	85	1045	2
11 Aug	19	198	138	1050	2	21	202	154	1044	2
16 Aug	6	187	116	1112	3	3	202	150	1025	2
18 Aug	9	184	105	1055	2	10	186	112	1055	2
All dates	88	177	100	1057	2	92	175	97	1050	2

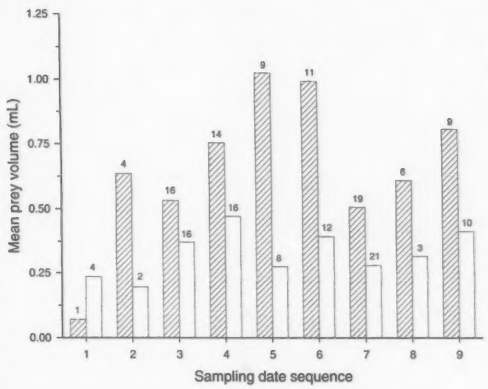

Figure 1

Mean prey volume for bagged (diagonal-line histograms) and unbagged (open histograms) juvenile pink snapper, *Pristipomoides filamentosus*, collected on each of nine dates during February–August 1994. Number of fish sampled is noted above histograms.

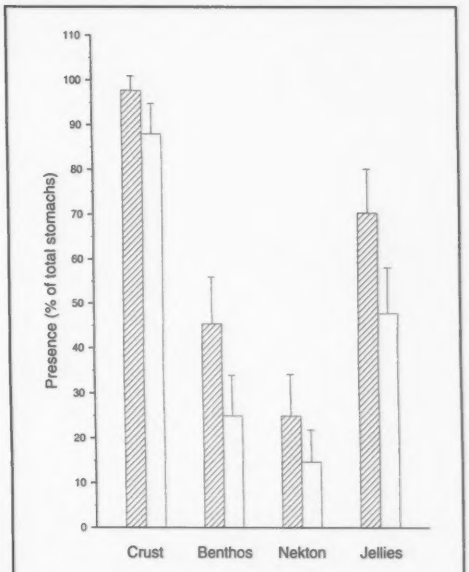

Figure 2

Percentage presence (1 standard error noted) for each of four major identifiable prey types (crustaceans, benthos, nekton, and jellies) for bagged (diagonal-line histograms) and unbagged (open histograms) juvenile pink snapper, *Pristimopoides filamentosus*, collected on nine dates during February–August 1994.

the smaller of the two sample sizes was nontrivial (≥3 fish, Table 1). Prey volumes bootstrapped without fish size and date adjustments averaged 112% (95% CI=72–152%) greater for bagged than for unbagged fish. For unbagged fish, predicted prey volumes (based on predicted values for bagged fish of the same body size and date) averaged 0.64 mL among dates, compared with observed prey volumes that averaged <0.30 mL. Bootstrapped differences of predicted minus observed prey volumes for unbagged snapper averaged +116% (95% CI=70–157%) or were 116% greater for bagged fish. Adjusted bootstrapped estimates thus were slightly larger than the bootstrapped estimates from unadjusted data.

Prey types

Three prey types (crustaceans, benthos, and jellies) were retained with greater relative frequency by bagged versus unbagged samples (2×2 Contingency χ^2 tests, $P<0.01$ for each of the three types; Fig. 2). A greater relative frequency of nekton for bagged (25%) versus unbagged (14%) snapper was only suggestive ($P=0.06$; Fig. 2). The proportion of fish with unidentifiable prey was similar in both bagged (49%) and unbagged (43%) fish (2×2 Contingency χ^2; $P=0.47$). Bagged fish in general retained greater numbers of major prey types (mean=2.9; median and mode=3) than did unbagged fish (mean=2.2; median and mode=2) (2-sample K-S test, $P<0.001$; Fig. 3).

Prey sizes

On average, the maximum size of prey retained by bagged samples was greater than the maximum prey size for unbagged samples (2-sample K-S test, $P<0.001$; Fig. 4). The minimum and median sizes of prey retained were equivalent, however, for bagged and unbagged (2-sample K-S tests, both $P>0.1$). Maximum prey size increased with fish body size for both bagged ($R^2=0.94$) and unbagged ($R^2=0.91$) snapper.

Discussion

Fundamental influences of ingestion

Two factors (fish body weight and date of collection) appear naturally to influence the amounts of prey consumed by juvenile snapper. The positive relation between fish size and prey volume was associated with snapper growth; juveniles averaged 50% greater body weight at the end versus the beginning of the 7-month period of study. Our observation of a monotonic temporal (date) effect in addition to the effect

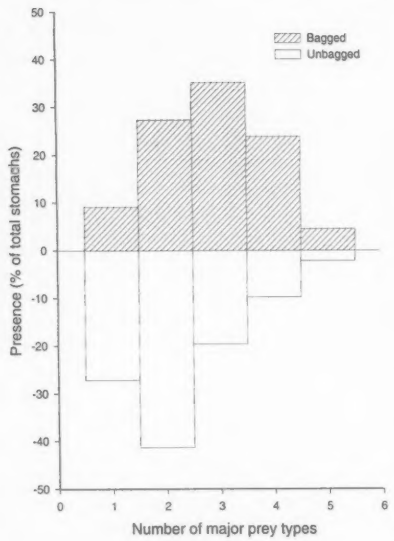

Figure 3

Frequency distributions for the major prey types (five, including unidentifiable category) present in bagged (above horizontal axis) and unbagged (below axis) juvenile pink snapper, *Pristimopoides filamentosus*, collected on nine dates during February–August 1994.

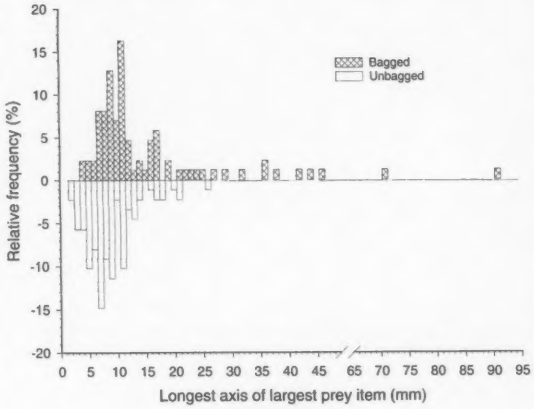

Figure 4

Frequency distributions of maximum prey sizes (all types, including unidentifiable category) for bagged and unbagged juvenile pink snapper, *Pristimopoides filamentosus*, collected on nine dates during February–August 1994.

of body size was not expected. It is possible that the date effect not related to size was caused by increases in the abundance or availability of prey between winter and summer.

In comparisons of prey volumes between bagged and unbagged specimens, the effects of body size and date of collection clearly need to be recognized, and adjustments made. Although this would seem intuitively necessary if sampling design does not control for fish body size and collection date, these factors influenced our results despite the fact that our sampling design specifically controlled for them. The possibility that the effects of body size and collection date may be too large to adjust statistically after-the-fact (if left uncontrolled by basic sampling design) should be taken into account in future studies.

Artifacts of regurgitation

Some food studies of physoclistous marine fishes (e.g. Bowman, 1986) have indicated or have strongly suggested that ingested prey are lost due to stomach eversion resulting from expansion of swimbladders when specimens are retrieved from even moderate (50 m) depths. This appears especially true for piscivores and other predators of large prey that have simple, undifferentiated stomachs (Treasurer, 1988).

Undetected regurgitation can lower the precision of estimates by adding erroneously empty or low-volume samples to the data set. There are also at least three ways in which undetected loss of stomach contents can bias dietary studies. These include 1) underestimates of the amount of food ingested, 2) underestimates of diet composition, including the taxonomic or functional variety of prey, and 3) size-selective regurgitation of prey. The latter can either inflate or reduce the effect of 1) depending on the nature of the size bias, which in turn may influence the precision of the estimates.

Precision of estimates

Total loss of stomach contents due to regurgitation occurred infrequently (4 out of 92 fish). However, the large reduction in prey volume for unbagged fish indicates that partial loss of prey because of regurgitation was a frequent occurrence. Partial prey loss did not inflate the variances of prey volume estimates for unbagged snapper; CV's (mean/SD·100%) of the date-specific estimates of prey volume were equivalent for bagged and unbagged fish (67% and 62%, respectively). Perhaps this reflects an effect of bias—selective loss of large prey—offsetting a decrease in

precision for unbagged fish. Species or collections in which the incidence of partial regurgitation is higher thus may be less precise, depending on whether loss of regurgitated prey is size-selective and in what manner so. High incidence of total regurgitation will be more likely to overwhelm size biases in retention and thereby lower precision.

Quantity and types of prey

Our observations for pink snapper document a general bias toward underestimating the total amount of food ingested by this species if partial or complete regurgitation goes undetected or is ignored. Because the number of different prey detected reflects the amount of material examined, underestimation of quantity should often underestimate prey variety as well, as our data illustrate. The observed underestimation for all four major prey types argues that our a priori classification of types, although subjective, was sufficient to detect a general bias resulting from regurgitation.

Sizes of prey

Size composition of prey can be biased by size-selective regurgitation. In the case of snapper, larger prey items were selectively regurgitated and lost by unbagged specimens. Large prey items might have been more recently ingested, despite likely crepuscular or nighttime periods of peak foraging (Haight et al., 1993b). The observed bias against retaining large prey may explain much of the underestimation of prey volume for unbagged snapper. Fishes with other feeding mechanism structures (e.g. different gill-raker size and spacing) may lack such a size bias, or regurgitation may result in the selective loss of smaller prey. Biases toward retaining larger prey can dampen the effect of regurgitation on underestimation of the total amount of prey.

Implications for diet studies

Depending on the specific research question, future studies of the food and feeding habits of juvenile pink snapper may benefit from the use of specimens collected at depth by divers. If simple comparisons of, say, the relative abundances of major prey types among fish collections are all that is needed, perhaps unbagged fish will suffice. Conversely, if longshore comparisons of large prey—perhaps comprising the bulk of the diet—are necessary, or if field estimates of total food intake or gastric evacuation rates are required, it is obvious that specimens retrieved directly to the sea surface will provide underestimates. Clearly, ingestion estimates for unbagged specimens will need to be adjusted for regurgitation loss, but collection date effects that are strongly nonlinear may make this difficult in practice. Further research is needed to develop methods for quantifying effectively the magnitude of regurgitation if collection date effects are nonmonotonic. Comparisons of diet among unbagged snapper captured at different depths will also be biased in terms of composition and size, as well as in terms of quantity of prey, because the amounts, diversity, and sizes of prey are interrelated and because the magnitude of regurgitation is influenced by extent of pressure change and hence depth of capture.

Bowman (1986) noted the progressive effects of depth on extent of regurgitation for other species. Prior explicit consideration of the interrelated biases resulting from regurgitation, on the composition, size, and quantity of prey has been lacking. The current consensus that diet descriptions require compound measures of both occurrence and bulk or mass data (Hyslop, 1980; Bowen, 1983; but see MacDonald and Green, 1983) reinforces the argument for critically evaluating prey data which may have been affected by barotrauma or other causes.

Acknowledgments

We thank A. Everson, T. Kazama, and K. Landgraf for assistance with diving or fishing operations. We also thank C. Boggs, R. Brodeur, W. Haight, J. Parrish, J. Polovina, M. Seki, and two anonymous reviewers for constructive criticisms of drafts of the manuscript.

Literature cited

Bowen, S. H.
1983. Quantitative description of the diet. *In* L. A. Nielsen, and D. L. Johnson (eds.), Fisheries techniques, p. 325–336. Am. Fish. Soc., Bethesda, MD.

Bowman, R. E.
1986. Effect of regurgitation on stomach content data of marine fishes. Environ. Biol. Fish. 16:171–181.

Bromley, P. J.
1994. The role of gastric evacuation experiments in quantifying the feeding rates of predatory fish. Rev. Fish Biol. Fish. 4:36–66.

Daan, N.
1973. A quantitative analysis of the food intake of North Sea cod, *Gadus morhua*. Neth. J. Sea Res. 6:479–517.

Durbin, E. G., A. G. Durbin, R. W. Langton, and R. E Bowman.
1983. Stomach contents of silver hake, *Merluccius bilinearis*, and Atlantic cod, *Gadus morhua*, and estimation of their daily rations. Fish. Bull. 81:437–454.

Ellis, D. M., and E. E. DeMartini.
1995. Evaluation of a video camera technique for indexing abundances of juvenile pink snapper, *Pristipomoides filamentosus*, and other Hawaiian insular shelf fishes. Fish. Bull. 93:67–77.

Haight, W. R., D. R. Kobayashi, and K. E. Kawamoto.
1993a. Biology and management of deepwater snappers of the Hawaiian Archipelago. Mar. Fish. Rev. 55(2):17–24.

Haight, W. R., J. D. Parrish, and T. A. Hayes.
1993b. Feeding ecology of deepwater lutjanid snappers at Penguin Bank, Hawaii. Trans. Am. Fish. Soc. 122:328–347.

Hislop, J. R. G., A. P. Robb, M. A. Bell, and D. W. Armstrong.
1991. The diet and food consumption of whiting (*Merlangius merlangus*) in the North sea. ICES J. Mar. Sci. 48:139–156.

Hyslop, E. J.
1980. Stomach contents analysis: a review of methods and their application. J. Fish Biol. 17:411–429.

Kohler, A. C., and D. N. Fitzgerald.
1969. Comparison of food of cod and haddock in the Gulf of St. Lawrence and on the Nova Scotia Banks. J. Fish. Res. Board Can. 26:1273–1287.

MacDonald, J. S., and R. H. Green.
1983. Redundancy of variables used to describe importance of prey species in fish diets. Can. J. Fish. Aquat. Sci. 40:635–637.

Manly, B. F. J.
1991. Randomization and Monte Carlo methods in biology. Chapman and Hall, New York, NY, 281 p.

Parrish, F. A.
1989. Identification of habitat of juvenile snappers in Hawaii. Fish. Bull. 87:1001–1005.

Parrish, F. A., and R. B. Moffitt.
1993. Subsurface fish handling to limit decompression effects on deepwater species. Mar. Fish. Rev. 54(3):29–32.

Rice, J. C.
1988. Repeated cluster analysis of stomach contents data—method and application to diet of cod in NAFO Division 3L. Environ. Biol. Fish. 21:263–278.

Siegel, S., and N. J. Castellan Jr.
1988. Nonparametric statistics for the behavioral sciences, 2nd ed. McGraw-Hill, New York, NY, 399 p.

SAS (Statistical Analysis System).
1988. SAS/STAT guide for personal computers, 6th ed. SAS Inst., Cary, NC, 1030 p.

Treasurer, J. W.
1988. Measurement of regurgitation in feeding studies of predatory fishes. J. Fish Biol. 33:267–271.

Cohort abundances and daily variability in mortality of eggs and yolk-sac larvae of bay anchovy, *Anchoa mitchilli*, in Chesapeake Bay

Suzanne E. Dorsey
Chesapeake Biological Laboaratory
Center for Environmental and Estuarine Studies
The University of Maryland System
Solomons, MD 20688-0038

and

Marine Sciences Research Center,
State University of New York at Stony Brook
Stony Brook, NY 11794-5000

Edward D. Houde
Chesapeake Biological Laboratory
Center for Environmental and Estuarine Studies
The University of Maryland System
Solomons, MD 20688-0038

John C. Gamble*
Sir Alister Hardy Foundation for Ocean Science
The Laboratory, Citadel Hill
Plymouth PL1 2PB, England

Abstract.—Eggs and yolk-sac larvae of bay anchovy, *Anchoa mitchilli*, were surveyed at seven sites in Chesapeake Bay on 12 days in July 1991 to estimate abundances and mortality rates of daily cohorts and the relative biomasses of adults that spawned them. An objective was to determine variability in abundance and mortality rates among sites and survey dates. Estimated abundances of eggs spawned each day and their hourly mortality rates were considered in relation to 1) in situ predator abundances, 2) environmental factors, and 3) initial egg and yolk-sac larval abundances. The mean initial abundance of bay anchovy eggs on each day during the 12 experiments was 6,630 eggs/m^2 (427.0/m^3). Mean initial abundance of yolk-sac larvae was 385 larvae/m^2 (24.6/m^3). Mean adult biomass at the survey sites, estimated from the egg productions, was 18.0 g/m^2 (1.16 g/m^3). A correlation analysis indicated that spawning by bay anchovy may be most intense in areas with high zooplankton biomass and where the ctenophore *Mnemiopsis leidyi*, a potential predator on eggs and larvae, was least abundant. Mean cohort instantaneous egg mortality was 0.066 eggs/h; on average, 73% of spawned eggs died before hatching. Yolk-sac larvae incurred a mean cohort instantaneous mortality of 0.053/h, i.e. 64% mortality during the first 24-h posthatch. Together, the mean egg and yolk-sac larval mortality rates indicated that >93% of bay anchovy daily cohorts die within 2 days after egg fertilization and before larvae reach the first-feeding stage. The range of cohort-specific mortality rates at a single station sampled on five consecutive days was equal to that observed at the seven sites. The high abundances, combined with high and variable cohort mortality rates, emphasize the probable importance of the egg and yolk-sac larval stages in the recruitment process of bay anchovy.

Manuscript accepted 11 December 1995.
Fishery Bulletin 94:257–267 (1996).

Most marine and estuarine fishes are highly fecund and spawn pelagic eggs that suffer high mortalities (Dahlberg, 1979; McGurk, 1986; Pepin, 1991). Historically, an estimation of in situ mortality rates of fish eggs and yolk-sac larvae has been problematic because of their temporally and spatially patchy distributions (Fortier and Leggett, 1985; Heath, 1992). However, it is important to obtain such estimates because the magnitude and variability of mortalities potentially can affect recruitment levels and contribute to fluctuations in stock abundance (Houde, 1989a).

Bay anchovy, *Anchoa mitchilli*, is the most abundant fish in estuaries and bays along the east coast of the United States (Hildebrand and Schroeder, 1928; Bigelow and Schroeder, 1953; Houde and Zastrow, 1991). The species is euryhaline and occurs in habitats as diverse as tidal freshwater tributaries and continental shelf waters. In most estuaries, including the Chesapeake Bay, the bay anchovy is an important trophic link between plankton and piscivores (Baird and Ulanowicz, 1989; Luo and Brandt, 1993). Its eggs and larvae dominate summer ichthyoplankton collections from Chesapeake Bay, accounting for 99% of the

* Deceased.

eggs and ~70% of the larvae (Dovel, 1971; Olney, 1983).

Recruitment variability in anchovies is hypothesized to result from variable stage-specific mortality (Lasker 1985b; Smith 1985). If bay anchovy egg and yolk-sac larvae experience both high and variable stage-specific mortalities, the effect on annual recruitment could be substantial. Crude estimates of daily mortality of eggs and yolk-sac larvae ranged from 26% to 97% in Biscayne Bay, Florida, whereas mortality rates of feeding-stage larvae were lower, averaging 30%/d (Leak and Houde, 1987). To obtain reliable estimates of mortality during the short egg and yolk-sac larval stages (about two days total) of bay anchovy, it is necessary to sample repeatedly a daily cohort of eggs or yolk-sac larvae throughout a 24-h period. Our surveys followed that plan during twelve days on Chesapeake Bay in which mortalities were estimated in relation to biotic or abiotic factors that may have affected the rates. By restricting the study to cohorts of eggs and prefeeding yolk-sac larvae, the calculated mortalities must, therefore, have resulted primarily from causes other than starvation.

In Chesapeake Bay, bay anchovy is sexually mature at 40 mm fork length (FL), 10 months after hatching (Zastrow et al., 1991), and seldom lives beyond age 2 (Wang, 1992; Newberger and Houde, 1995). It is a serial spawner (Luo and Musick, 1991; Zastrow et al., 1991) and has a reproductive season in Chesapeake Bay that extends from May until September. Peak spawning occurs in July (Dalton, 1987) when virtually all females spawn nightly (Zastrow et al., 1991). Age-1 females produce most eggs (Zastrow et al., 1991), which hatch into yolk-sac larvae at approximately 20–24 h after fertilization. The yolk-sac larval stage also is short, with a duration of about 24 h (Houde and Zastrow, 1991).

The high abundances, serial spawning, and the presence of a single cohort of eggs on each day for this species allowed for repeated estimates of cohort-specific mortality rates within one season and for investigations into the factors that may affect variability in the rates. The four objectives of the study were as follows: 1) to estimate daily-cohort abundances and variability of bay anchovy eggs and yolk-sac larvae in selected areas of Chesapeake Bay; 2) to estimate mortality rates and variability of daily cohorts of bay anchovy eggs and yolk-sac larvae; 3) to relate densities of two potential predators—the scyphomedusan *Chrysaora quinquecirrha*, and the ctenophore *Mnemiopsis leidyi* (as well as environmental variables)—to anchovy egg and yolk-sac larval mortality rates; and 4) to estimate relative spawning-stock biomasses of bay anchovy at the experimental sites.

Materials and methods

Sampling design

After determining that anchovy eggs were present in test lifts of a plankton net, daily experiments were conducted at seven sites (Fig. 1) to estimate mortality rates of bay anchovy. Once a site had been selected, samples were obtained at 2-h intervals to estimate abundances of eggs and yolk-sac larvae. The sites were defined by the drift patterns of concurrent free-drifting mesocosm studies (Houde et al., 1994), which were initiated when the sites were selected. Each sample for this study was taken adjacent to free-drifting mesocosms. The mesocosms, which were 5 m in length and 1 m in diameter, acted as drogues and were assumed to drift with the water mass that was originally sampled. Each experiment consisted of 8 to 12 duplicate lifts of a plankton net. Water depths at the seven sites generally ranged from 10 to 25 m. Based upon the mesocosm drift tracks (Fig. 2), the mean area of the Bay included in an individual experiment was 59.8 km^2.

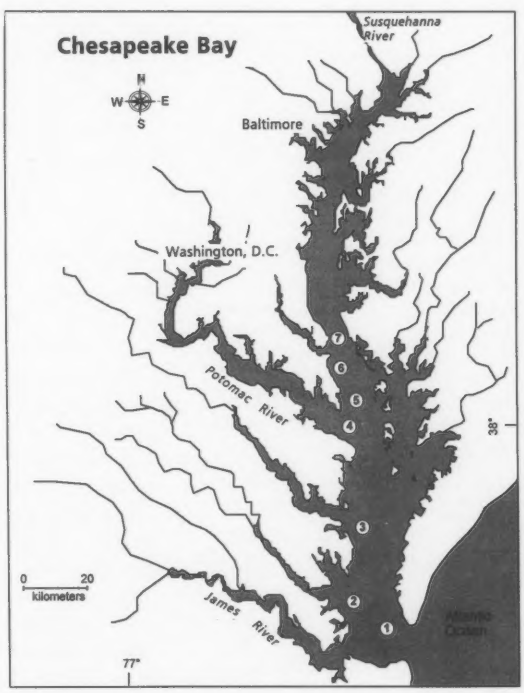

Figure 1
Chesapeake Bay and the seven sampling sites.

Collections

Collections were made from the research vessel RV *Henlopen* during the periods 2–9 July and 18–24 July 1991, the peak of the spawning season for bay anchovy. The lower Chesapeake Bay (sites 1–4) was surveyed on the first cruise and the mid-Bay (sites 5–7) was surveyed on the second cruise (Fig. 1).

Anchovy eggs and larvae were collected in a 40-cm diameter plankton net with 280-μm meshes. A flowmeter in the net mouth was used to determine the volume of water sampled. Vertical lifts of the net from near bottom (never deeper than 25 m) to the surface were made at 1 m/sec. The mean volume sampled in 312 net lifts was 3.00/m^3 (SD=1.38/m^3). Upon collection, samples were immediately preserved in 5% formalin-seawater. At each experimental site, sampling began between 0000 and 0400 h local time, shortly after peak spawning had occurred on each day. Duplicate samples were collected at 2-h intervals until approximately 2100 h. By sampling at 2-h intervals we documented declines in abundances of eggs and yolk-sac larvae from which mortality rates of daily cohorts were estimated. In this way, the level of mortality and its variability were determined for 12 daily cohorts.

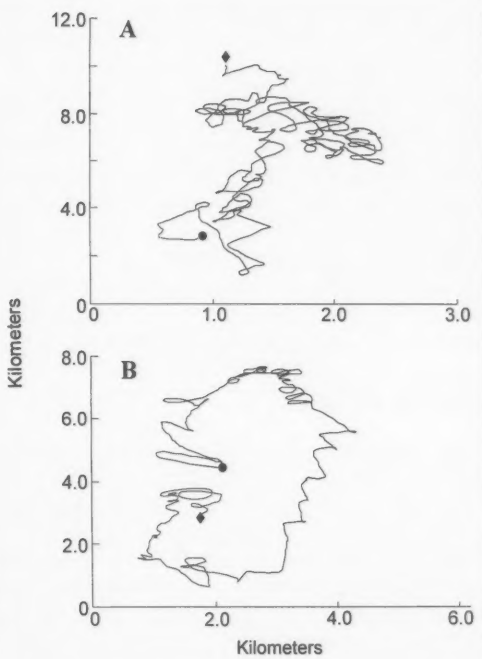

Figure 2

Vessel tracks from two surveys of bay anchovy egg and larval abundance in Chesapeake Bay. Samples were collected every 2 hours on the vessel track. (**A**) Track for site 6, 19 July 1991. (**B**) Track for site 3, 5 July 1991. The locations of sites are illustrated in Figure 1. ♦ = start; • = end.

Abundances of gelatinous predators were estimated from collections in a 60-cm, 280-μm mesh, opening and closing net. Collections were made in partitioned oblique tows: 1) from near-bottom to the pycnocline; and 2) from the pycnocline to the surface. They were made ~12 times daily adjacent to the drifting mesocosm array and concurrent with collections of anchovy eggs and larvae. Total biovolumes of *C. quinquecirrha* and *M. leidyi* >10 mm diameter in each sample were measured immediately upon collection.

Salinity, temperature, dissolved oxygen, and chlorophyll *a* fluorescence were determined from surface-to-bottom casts of a conductivity-temperature-depth (CTD) probe. Mean values during each 24-h experiment were based upon three to five CTD casts. Position data for plankton samples and CTD casts were logged by the vessel's navigation system to delineate drift tracks of the mesocosm deployments and the locations of sampling stations.

In the laboratory, fish eggs and larvae (yolk-sac and older) were removed from all samples. Eggs were identified and counted. Yolk-sac larvae were sorted, identified, and separated on the basis of ≥6 samples from each day's collections.

Settled volumes of zooplankton from the 40-cm net collections, determined from a minimum of three samples each day, were recorded and expressed as mL under 1 m^2 of bay surface. The zooplankton in the 280-μm mesh net potentially represented prey of adult bay anchovy, rather than prey of first-feeding larvae.

Egg and yolk-sac larval abundance

Densities (number/m^3) and abundances (number under 1.0/m^2) of anchovy eggs and yolk-sac larvae in each sample were estimated. Duplicate samples, collected between 0000 and 0600 h, were examined to determine the sample pair on each day which had the maximum abundance of eggs or yolk-sac larvae. Those samples provided an estimate of the mean "initial abundance" for each experiment. The decline in abundance over the next 18 to 20 h was a measure of mortality.

Some yolk-sac larvae are extruded through 280-μm meshes. However, abundances of yolk-sac larvae, which are of uniform length (approximately 2.0 mm), were not adjusted for extrusion in this analysis be-

cause mortality estimates presumably were not affected by consistent proportional losses. Adjustments to estimate actual yolk-sac larval abundances could be obtained by multiplying the uncorrected abundances by 2.3, the adjustment factor derived from paired collections in 280-μm and 53-μm mesh nets (MacGregor, 1994).

Mortality

Because bay anchovy eggs are abundant in Chesapeake Bay and hatch <24 h after being spawned, an intensive ichthyoplankton survey could derive mortality estimates for a daily cohort of eggs or yolk-sac larvae on the basis of the decline in their abundances on a single day. By using this approach, daily mortality rates were estimated. Hourly instantaneous mortality rates of eggs and yolk-sac larvae were estimated from a log-linear fit of the exponential model: $N_t = N_0\, e^{-Zt}$, where N_t is the abundance (number under 1/m^2) of a cohort at time t, N_o is its initial abundance (number under 1 m^2), Z is the instantaneous mortality coefficient (per h), and t is the time elapsed (h) since the initial abundance estimate.

Estimates of daily cohort abundances and mortality rates of eggs and yolk-sac larvae were compared among days, an approach seldom possible in research on species with eggs that have longer development times. Some losses due to diffusion or transport of eggs and larvae out of the sampling areas may have occurred. However, such losses were minimized by the short period over which each cohort was sampled (≤1 d) and because sampling was directed by the drift of mesocosms that tracked the initially sampled water mass.

Egg production and adult biomass

We obtained an estimate of adult biomass from estimates of egg production, knowledge of adult fecundity, and spawning frequency. Egg production, when divided by relative fecundity (mean number of eggs spawned per gram of female), provides an estimate of adult female biomass (Saville, 1964). Biomass of serial-spawning fishes such as bay anchovy can be estimated by single-survey methods of egg production (Lasker, 1985a; Parker, 1985; Eltink[1]). Parker's (1985) formulation to estimate adult biomass is

$$B = E_d / (F_{bw} \times S \times R),$$

where B = adult biomass (g);
E_d = daily egg production;
F_{bw} = mean batch fecundity per female;
S = spawning fraction (i.e. the fraction of females that spawned on the sampling date); and
R = the proportion of the population that is female.

Batch fecundities and spawning fraction of bay anchovy were based upon estimates by Zastrow et al. (1991) who reported that batch fecundity (F_{bw}) was 687.1 ova per gram of ovary-free female weight and that spawning fraction (S) was 1.0 during July in Chesapeake Bay. We assumed that the proportion of adult females (R) was 0.5, on the basis of trawling data (Newberger and Houde, 1995), which indicated a mean female:male ratio of 1.02:1.00. Thus, relative adult biomass (g/m^2) at each site was about twice the relative female biomass.

Predators and other factors

Egg and yolk-sac larval abundances were examined in relation to environmental variables. Possible correlations between egg or yolk-sac larval abundances and biovolumes (mL/m^2) of two gelatinous predators (ctenophore *M. leidyi* and scyphomedusa *C. quinquecirrha*) were analyzed because Cowan and Houde (1992, 1993) and Purcell et al. (1994) indicated that these dominant species were important predators on bay anchovy eggs and larvae. Bay anchovy apparently is not cannibalistic (Klebasko, 1991), and other major predators have not been identified. Possible correlations between egg or yolk-sac larval abundances and zooplankton biomasses also were examined.

Statistical analyses

When assumptions for parametric tests were met, Analysis of Variance (ANOVA) was used to test for differences among daily surveys in initial egg abundances, zooplankton biomasses, and gelatinous predator biovolumes. An ANOVA also was used to determine if means of those variables differed among the five surveys carried out at site 5 (Fig. 1). When ANOVA results were significant, individual means were compared by using the a posteriori Student-Newman-Keuls (SNK) multiple-comparison procedure.

The estimates of hourly instantaneous mortality rates of eggs and yolk-sac larvae were the regression coefficients in the log-linear models relating $\log_e$ abundance to elapsed time. Egg mortality was calculated from collections made between 0200 and 2000 h because eggs hatch in ~20 h. Yolk-sac larval mor-

[1] Eltink, A. 1991. Horse mackerel egg production and spawning stock size in the North Sea in 1990. Int. Counc. Explor. Sea, Council Meeting 1991/H:27, 14 p.

tality was calculated from collections made between 0000 and 2400 h. Each of the duplicate samples was treated as a separate data point in regression analysis. An SNK test was applied following the regression analyses to determine which of the instantaneous mortality rates of eggs and yolk-sac larvae differed significantly from each other. In several cases the estimated mortality coefficients did not differ significantly from zero at the $P = 0.05$ level. These coefficients were retained in our overall analysis of mortality rates and comparisons among sites because we assumed that low, near-zero rates may occur and that such estimates did characterize low rates of loss at some sites.

Pearson product-moment correlation coefficients were calculated for mortality rates and selected biotic variables. Possible correlations between egg or yolk-sac larval mortality rates and initial abundances, zooplankton biomasses, and gelatinous predator biovolumes, were examined.

Results

Hydrography

Mean values of temperature, salinity, oxygen, and chlorophyll *a* fluorescence at 3-m depth are summarized in Table 1. Chlorophyll *a* fluorescence tended to increase in a south-to-north direction. Both temperatures and chlorophyll *a* fluorescence peaked at site 5 (Fig. 1). Depth profiles of salinity and oxygen, although not illustrated, indicated increasing stratification in a south-to-north direction and nearly anoxic conditions near-bottom at sites 5, 6, and 7.

Initial egg abundance and adult biomass

Initial egg abundances of daily cohorts during each of the 12 experiments were high and variable, ranging from 935 to 18,277 eggs/m^2 (Table 2). The mean initial abundance was 6,630 eggs/m^2 (427.0/m^3). The initial abundances of eggs differed significantly among experiment dates (ANOVA, $P<0.0002$) and probably among sites, although most sites were sampled on only one day. The highest initial egg abundance, 18,277 eggs/m^2, was observed at site 7, the northernmost site (Fig. 1).

The mean relative adult biomass (±2 standard error [SE]), estimated from the initial cohort abundances of eggs, was 18.0 g/m^2 (±8.0 SE). Biomass estimates varied widely among experiments and sites, ranging from 2.5 to 49.3 g/m^2 (Table 2).

Initial yolk-sac larval abundance

The mean initial abundance of cohorts of yolk-sac larvae was approximately 17 times less than initial

Table 1

Summary of sampling data for bay anchovy. *Anchoa mitchilli*, in Chesapeake Bay, 3–24 July 1991. Data include estimated relative biomass (B) of adult bay anchovy; mean daily biovolumes (mL/m^2) of *Mnemiopsis leidyi* (CTV), *Chrysaora quinquecirrha* (CHV), and zooplankton (ZP), mean daily temperature (TMP); salinity (SLT); oxygen concentration (OXY); and chlorophyll *a* fluorescence (FLR) at 3-m depth. Identical superscripts on means indicate no significant (P >0.05) difference (SNK pairwise comparison procedure). Locations of sites are indicated in Figure 1.

July date	Site	B g/m^2	CTV mL/m^2	CHV mL/m^2	ZP mL/m^2	TMP °C	SLT PSU	OXY mg/L	FLR mg/m^2
3	1	33.1	0.0^{b}	0.0^{b}	15.3^{ab}	26.4^{a}	22.3^{a}	8.04^{a}	0.82^{b}
4	2	15.0	0.0^{b}	0.0^{b}	16.4^{ab}	26.2^{a}	20.9^{ab}	7.87^{a}	1.53^{b}
5	3	10.6	0.0^{b}	0.0^{b}	17.1^{ab}	26.5^{a}	18.3^{bc}	9.35^{a}	1.10^{b}
7	4	2.5	484.4^{a}	128.4^{a}	7.2^{b}	26.6^{a}	14.6^{cd}	7.47^{a}	1.47^{b}
8	4	5.3	470.8^{a}	36.6^{b}	6.8^{b}	26.6^{a}	14.8^{cd}	6.44^{a}	0.90^{b}
18	7	49.3	32.5^{b}	41.8^{b}	20.3^{a}	27.3^{a}	14.3^{cd}	6.63^{a}	15.7^{ba}
19	6	15.5	24.4^{b}	35.7^{b}	15.0^{ab}	25.2^{a}	13.0^{d}	8.26^{a}	15.8^{ba}
20	5	19.6	30.6^{b}	6.8^{b}	10.6^{ab}	28.0^{a}	15.4^{cd}	6.01^{a}	11.0^{ba}
21	5	35.9	49.39^{b}	18.6^{b}	13.4^{ab}	28.0^{a}	15.4^{cd}	6.42^{a}	18.4^{a}
22	5	5.7	129.0^{b}	19.5^{b}	12.2^{ab}	28.5^{a}	15.3^{cd}	6.92^{a}	15.9^{ba}
23	5	9.2	278.6^{ab}	39.8^{b}	10.6^{ab}	26.6^{a}	13.9^{cd}	7.85^{a}	23.7^{a}
24	5	13.7	368.9^{ab}	22.3^{b}	18.8^{ab}	28.7^{a}	15.6^{cd}	5.41^{a}	25.3^{a}
Mean		18.0	155.7	29.1	13.6	27.1	16.1	7.22	11.0
Standard error		4.0	52.8	10.1	1.2	0.3	0.8	0.31	2.6

mean egg abundance. In the 12 experiments, initial yolk-sac larval abundances ranged from 56 to 781/m^2 with a mean of 385/m^2 (24.6/m^3 SE) (Table 2). Mean abundances differed significantly among experiments (ANOVA, $P<0.002$). The highest abundance of yolk-sac larvae was observed at site 7, where eggs also were most abundant (Table 2).

Table 2

Estimated hourly mortality rates and standard errors (SE) for egg (Z) and yolk-sac larvae (Z_L), initial egg abundances (N_o) and initial yolk-sac larval abundances (NL) of bay anchovy, *Anchoa mitchilli*, on 12 days during the period 3–24 July 1991. Identical superscripts on mortality rates and initial abundances indicate no significant ($P>0.05$) difference (SNK pairwise comparison procedure). Asterisks indicate that regression coefficients of $\log_e$ abundances regressed on time (h), from which Z and ZL estimates were obtained, differed significantly from zero at $P = 0.05$ level.

July date	Site	Z/h	SE_Z/h	N_0/m^2	n	r^2
Eggs						
3	1	$*0.108^{ab}$	0.027	$12{,}214^{bc}$	16	0.54
4	2	0.014^{ab}	0.015	$5{,}521^{d}$	18	0.05
5	3	0.001^{ab}	0.012	$3{,}891^{d}$	19	0.10
7	4	0.049^{a}	0.027	935^{d}	20	0.15
8	4	$*0.062^{ab}$	0.021	$1{,}966^{d}$	20	0.32
18	7	$*0.081^{b}$	0.020	$18{,}277^{a}$	19	0.50
19	6	0.042^{ab}	0.055	$5{,}708^{cd}$	19	0.04
20	5	$*0.080^{ab}$	0.013	$7{,}245^{bcd}$	20	0.67
21	5	0.020^{ab}	0.027	$13{,}237^{ab}$	20	0.02
22	5	$*0.100^{a}$	0.021	$2{,}118^{d}$	20	0.55
23	5	$*0.045^{b}$	0.012	$3{,}402^{d}$	20	0.44
24	5	$*0.185^{b}$	0.028	$5{,}044^{cd}$	20	0.77
Mean		0.066		6,630		
Standard error		0.014		1,462		

July date	Site	Z_L/h	SE_{ZL}/h	NL/m^2	n	r^2
Yolk-sac larvae						
3	1	$*0.057^{ab}$	0.049	422^{bc}	7	0.18
4	2	0.040^{b}	0.048	222^{d}	8	0.11
5	3	0.082^{b}	0.064	614^{ab}	9	0.19
7	4	$*0.177^{ab}$	0.018	162^{cd}	6	0.96
8	4	0.017^{ab}	0.052	56^{d}	7	0.02
18	7	$*0.036^{b}$	0.009	781^{a}	11	0.66
19	6	0.022^{ab}	0.019	605^{ab}	8	0.19
20	5	0.022^{a}	0.028	380^{bcd}	6	0.14
21	5	0.058^{ab}	0.027	430^{bc}	9	0.39
22	5	$*0.072^{ab}$	0.015	289^{bcd}	11	0.72
23	5	0.028^{b}	0.018	364^{bcd}	8	0.27
24	5	0.030^{ab}	0.021	299^{bcd}	8	0.25
Mean		0.053		386		
Standard error		0.012		56.7		

Gelatinous predator biovolumes

The above-pycnocline biovolumes of gelatinous zooplankters were highly variable among experiments, ranging from 0 to 612.8 mL/m^2 (Table 1). Ctenophore *M. leidyi* biovolumes ranged from 0 to 484.4 mL/m^2 and scyphomedusan *C. quinquecirrha* biovolumes ranged from 0 to 128.4 mL/m^2. The mean biovolume of *M. leidyi* was 4 times higher than that of *C. quinquecirrha*. Biovolumes of each species were highest at site 4 (ANOVA, $P<0.0001$), near the mouth of the Potomac River (Table 1; Fig. 1).

Zooplankton biomass

Zooplankton biovolumes from the 280-μm net ranged from 6.8 to 20.3 mL/m^2, mean = 13.6 mL/m^2. The two lowest zooplankton biovolumes (ANOVA, $P<0.02$) were observed at site 4 (Table 1; Fig. 1), where gelatinous zooplankton biovolumes were highest. The highest zooplankton biovolume occurred at site 7, coincident with highest anchovy egg and yolk-sac larvae abundances.

Egg and yolk-sac larvae mortality rates

The overall mean instantaneous mortality rate for eggs was 0.066/h. The estimates, which ranged from 0.001 to 0.185/h, represent stage-specific (20-h) mortalities of 2% to 98%. The highest egg mortality rates (>0.10/h) were estimated on 3, 22, and 24 July (Figs. 3 and 4; Table 2). If only the seven rates judged to be significantly different from zero ($P<0.05$) are included in the analysis, the mean mortality was 0.094/h (SE=0.017).

The overall mean mortality rate of yolk-sac larvae was 0.053 larva/h. The yolk-sac larval rates, which ranged from 0.017 to 0.177/h, represent daily mortality rates of 33.5 to 98.6%. The highest yolk-sac larval mortality rates (>0.07/h) were estimated on 5, 7, and 22 July. If only the four rates judged to be significantly different from zero ($P<0.05$) are included in the analysis, the mean mortality rate was 0.077/h (SE=0.035/h).

The mortality estimates differed among the daily surveys. Rates were estimated with low precision, possibly because the eggs and larvae were distributed in patches within each sampling site. The standard errors of yolk-sac larval mortality rates were relatively high at sites between the mouth of the Chesapeake Bay and the Potomac River (sites 1–4)

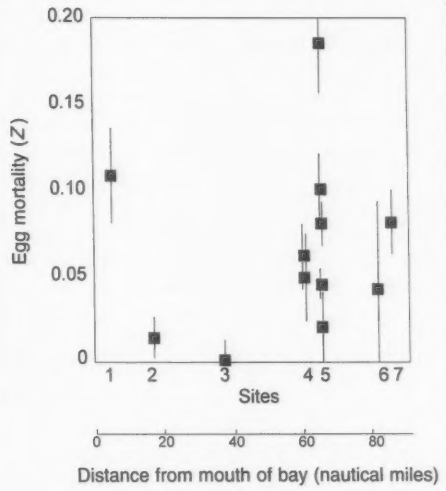

Figure 3

Instantaneous mortality rates (Z/h) of bay anchovy eggs collected at seven sites in Chesapeake Bay, July 1991. Locations of sites are illustrated in Figure 1. Vertical bars represent ±1 SE.

compared with sites farther north (Table 2; Fig. 1). Observed variability in mortality rates was approximately equal for eggs and yolk-sac larvae. Coefficients of variation (ratio of standard deviation to mean) were 0.73 and 0.79 for eggs and yolk-sac larvae, respectively.

The regression coefficients, which were the estimates of mortality rates, did not differ significantly from zero at the $\alpha = 0.05$ level in five of the twelve $\log_e$ egg abundance-on-time regressions and eight of the twelve yolk-sac larva regressions. The yolk-sac larval regressions were based upon relatively few data points, which contributed to their lower precision (Table 2). The nonsignificant ($P>0.05$) mortality coefficients corresponded to low, near-zero regression coefficients. Although not significantly different from zero, these coefficients were presumed to estimate mortality rates.

Correlations

There were several simple correlations among organism abundances, biovolumes, and mortality rates (Table 3). Most notable were 1) the positive correlation between yolk-sac larval mortality rate and *C. quinquecirrha* biovolume ($P<0.01$); 2) the positive correlations between egg abundance, yolk-sac larval abundance, and zooplankton biovolume ($P<0.05$); and 3) the negative correlations between both egg and yolk-sac larval abundances and *M. leidyi* biovolume ($P<0.05$).

Discussion

Daily cohorts of bay anchovy were demonstrated to suffer high and variable mortality during egg and yolk-sac larval stages. Our estimates of mortality rates indicate both day-to-day and regional variability in Chesapeake Bay. At site 5, which was sampled on five consecutive days, the range of egg mortality rates exceeded the range observed over all remaining sites. The high variability at a single site suggests that environmental conditions were changing daily. Variability in initial egg abundances indicated that numbers of adult spawners in the area also were changing on a daily basis.

Our egg-stage mortality rates ranged from 2% to 98%, and averaged 73%. Recent experiments in free-drifting mesocosms (Houde et al., 1994) conducted at the same sites and dates of surveys reported here have also provided estimates of mortality of bay anchovy eggs and yolk-sac larvae. The mesocosms, which included gelatinous predators, provided mean estimates of mortality that were essentially identical to those reported here. In Great South Bay, New York, Castro and Cowen (1991) reported that seasonal mortality rates of combined bay anchovy eggs and yolk-sac larvae ranged from 70% to 98%/d. If eggs in Great South Bay hatched in 20 h, the mortality rates on eggs alone may have ranged from 63.0% to 96.5%/d. In Biscayne Bay, Florida, Leak and Houde (1987) compared seasonal abundances of eggs and yolk-sac larvae of bay anchovy and estimated that

Table 3

Matrix of correlation coefficients for bay anchovy, *Anchoa mitchilli*, where *Z* is hourly egg mortality rate, *ZL* is hourly yolk-sac larvae mortality rate, *N* is initial abundance of eggs, *NL* is initial abundance of yolk-sac larvae, CTV is biovolume in mL/m^2 of *M. leidyi*, CHV is biovolume in mL/m^2 of *C. quinquecirrha*, ZP is zooplankton biovolume in mL/m^2. Asterisks indicate significant correlation ($P<0.05$).

	Z	*ZL*	*N*	*NL*	CTV	CHV
ZL	–0.19					
N	+0.07	–0.28				
NL	–0.12	–0.20	+0.66*			
CTV	+0.29	+0.30	–0.57*	–0.68*		
CHV	–0.04	+0.67*	–0.28	–0.26	+0.68*	
ZP	+0.22	–0.30	+0.58*	+0.70*	–0.59*	–0.49

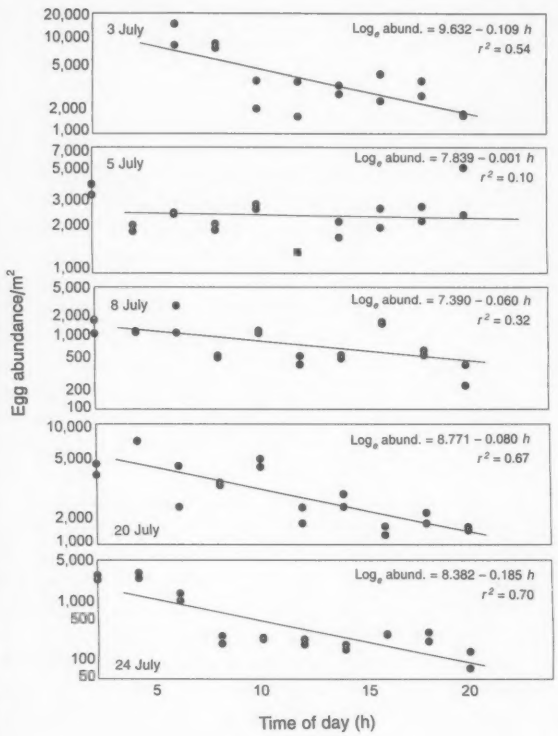

Figure 4

Regressions of $\log_e$ abundances on elapsed time in hours (t) for five experimental surveys of bay anchovy eggs in Chesapeake Bay during July 1991. The five regressions are examples which demonstrate the method to obtain mortality rates of eggs and yolk-sac larvae for the 12 surveys summarized in Table 2.

mean daily egg mortality was 86%, with a range of 26% to 97%.

Egg mortality rates of bay anchovy obviously are high. But, they are lower than predicted at their temperature of development (27°C), based upon Pepin's (1991) temperature-dependent mortality model, $Z = 0.030\ e^{0.18T}$, in which Z is the daily instantaneous mortality rate for marine fish eggs and T is temperature (°C). At 27°C the model predicts a mortality of $Z = 3.91$ (=0.16/h), a rate more than twice our mean estimate of $Z = 1.58$/d (=0.066/h). Pepin's (1991) model for marine fish eggs predicts mortality rates of $Z = 2.81$ to 4.63/d for temperatures in the range 25.23°C to 27.99°C which were observed during this study. These predicted mortality rates are higher than all except one of our estimated rates and are also higher than rates estimated for bay anchovy eggs by Leak and Houde (1987) in Biscayne Bay, Florida. Castro and Cowen (1991) determined mortality of bay anchovy eggs and yolk-sac larvae at lower average temperatures in Great South Bay. At their two-year mean of 23.4°C, they estimated a mean mortality rate of 2.36/d, a value rather close to Pepin's (1991) model-predicted 2.02/d. Pepin (1991) had suggested that species with short development times (i.e. high temperatures) may have lower than predicted daily mortality rates because of their relatively short exposure to predators.

Mortality rates for bay anchovy eggs are higher and perhaps more variable than rates reported for eggs of other anchovy species. Only the Peru anchoveta, *Engraulis ringens*, has been reported to experience similar daily egg mortality rates, a consequence of cannibalism by adult anchoveta and of high predation rates by other pelagic fish (Smith et al., 1989). The reported stage-specific egg mortalities of other anchovies, while high, probably do not exceed 50% to 60% (Dorsey and Houde[2]) and appear to be considerably lower than rates estimated for bay anchovy.

Instantaneous mortality rates for bay anchovy eggs also are higher than rates reported for most teleost fishes (Houde, 1989b; Houde and Zastrow, 1993). However, if stage-specific mortalities are compared, rather than daily rates, the bay anchovy resembles many fishes. For example, Harding et al. (1978) estimated that the mean mortality rate for plaice, *Pleuronectes platessa*, eggs was $Z = 0.075$/d in the Southern Bight of the North Sea at mean temperature 5.65°C. Egg-stage duration of plaice is about 22 days (Coombs et al., 1990). Thus, the stage-specific egg mortality is $Z_{cum} = 1.65$, equivalent to 81%, and similar to that of bay anchovy (Z_{cum}=1.32) despite the more than 20-fold difference in hourly rates (0.003 for plaice, 0.066 for bay anchovy).

Yolk-sac larvae are essentially embryos free of the chorion, and their expected mortality may be more comparable to eggs than to feeding-stage larvae. Our estimated mortality rates of bay anchovy yolk-sac larvae ranged from $Z = 0.41$ to 4.24/d (33.5 to 98.5%/d). The mean rate was $Z = 1.27$/d (72.0%/d), a value nearly equal to the egg-stage mortality rate. Because the yolk-sac larval stage of bay anchovy is approximately one day in duration, the daily mortality rate is

[2] Dorsey, S. E., and E. D. Houde. 1992. Daily variability in mortality of bay anchovy, *Anchoa mitchilli*, eggs in Chesapeake Bay. Int. Counc. Explor. Sea, Pelagic Fish Committee, Council Meeting 1992/H:17, 11 p.

equivalent to a stage-specific rate. At 27°C, the mean stage-specific mortality of bay anchovy yolk-sac larvae (Z=1.27) is higher than the mortality predicted (Z=0.77) from the temperature-dependent model of Pepin (1991) for yolk-sac larvae of marine fishes.

There was a high degree of spatial and temporal variability in the abundances of bay anchovy eggs. The initial abundances of eggs varied among days (i.e. experiments) and probably among sites. Because repeated experiments were carried out only at sites 4 and 5, it was not possible to critically analyze among-site differences in egg abundances or their mortality rates. Some of the variation may be explained by adult distributions and spawning strategy; Luo and Musick (1991) hypothesized that bay anchovy spawns preferentially in areas with plentiful adult food. Our study supports their hypothesis because zooplankton biovolumes were positively correlated with initial anchovy egg abundances. Additionally, the two lowest initial egg abundances in our study occurred at site 4, which also had lowest zooplankton biovolumes; the highest egg abundance was observed at site 7, where highest zooplankton biovolume occurred.

Our estimates of relative adult biomasses may be considerably higher than actual mean biomasses of bay anchovy in Chesapeake Bay because we had selected survey sites with high egg abundances. Our criterion for selecting sampling sites was the obvious presence of bay anchovy eggs in test tows. This criterion probably accounts for the high biomass estimates. Our mean biomass estimate, 1.16 g/m^3 (18.0 g/m^2), equates to approximately one adult anchovy per m^3. In a concurrent study of bay anchovy in the mid and upper Chesapeake Bay, acoustics-adjusted trawl abundances in July 1991 indicated a mean adult biomass of 0.58 g/m^3 (Wang and Houde, 1995).

Initial mean abundance of cohorts of yolk-sac larvae, uncorrected for the extrusion of a fraction of larvae through the 280-m net meshes, equaled 385.4/m^2 (24.6 [±6.0]/m^3). This unadjusted abundance was approximately 17 times lower than the initial mean abundance of egg cohorts. If yolk-sac larvae abundances were adjusted upward by the factor (2.3) required to correct them (MacGregor, 1994), the difference between initial egg and yolk-sac larvae abundances reduces to a factor of 5.8. The observed mean initial abundance of yolk-sac larvae, after adjustment, based upon our mean egg mortality rate (0.066/h), was still only 50% of that expected. However, because eggs hatch at ca. 2000 h and the initial yolk-sac larval abundance was estimated at ca. 0230 h, continuing mortality would have caused further declines in yolk-sac larval numbers for 6.5 h before samples were taken. Applying the mean yolk-sac larval mortality rate (0.053/h) to the 6.5-h period further reduced the mean discrepancy, although initial numbers of yolk-sac larvae were still 30% lower than expected. The cause of the remaining discrepancy, if real, was not identified but could have resulted if a fraction of the sampled eggs were infertile or dead.

Estimated biovolumes of two gelatinous predators of bay anchovy eggs and larvae, *M. leidyi* and *C. quinquecirrha*, were variable, probably patchy on temporal and spatial scales. Both have been demonstrated to be major consumers of bay anchovy eggs and larvae (Cowan and Houde, 1993; Purcell et al., 1994). There was a significant correlation between mortality of yolk-sac larvae and *C. quinquecirrha* biovolume (Table 3). Biovolumes of the two jellyfishes were highest at site 4, where lowest zooplankton biovolumes and lowest anchovy egg and larval abundances occurred. At the three southernmost sites (sites 1, 2, and 3 in Table 1), neither *M. leidyi* nor *C. quinquecirrha* were present. Despite their absence, there was no evidence that mortality rates of anchovy eggs or yolk-sac larvae were lower there than at sites with jellyfish present.

Spawning intensity by bay anchovy, indexed by initial abundances of egg cohorts, was lowest at site 4 where the gelatinous predator biovolumes were highest, raising a possibility that anchovy adults might avoid areas where zooplankton have been depleted on account of consumption by gelatinous predators. This suggests a mechanism that may indirectly reduce baywide predation mortality on anchovy eggs and larvae; this, in turn, is supported by the negative correlations between both egg and yolk-sac larval abundances and jellyfish biovolumes. The combined densities of *C. quinquecirrha* and *M. leidyi* were extremely high at site 4, near the mouth of the Potomac River, and possibly caused the depressed zooplankton biovolumes. Purcell (1992) noted that consumption by *C. quinquecirrha* depleted zooplankton in tributaries of Chesapeake Bay, but she reported smaller effects in the mainstem of the Bay.

An important conclusion of our study is that bay anchovy suffers highest mortality during its first two days after being spawned; on average, 73% of all spawned bay anchovy eggs in Chesapeake Bay died before hatching. Of the surviving 27%, approximately 72% perished during the 24-h yolk-sac larval stage. In July 1991 only 7.6%, on average, of each night's egg production survived until the first-feeding stage, which commences 2 days after hatching. Lasker (1985b) and Smith (1985) pointed out that fluctuations in yearly recruitment in engraulids may result from variable stage-specific mortality rates, which can be a consequence of interannual variability in both biotic and abiotic factors. Results of our study suggest that such factors also vary significantly on

much shorter, day-to-day, temporal scales and that interannual recruitment differences in species with life histories similar to bay anchovy could depend upon the variable conditions faced by daily cohorts during each summer's spawning season.

Acknowledgments

Research was supported by National Science Foundation grants OCE87-01304 and OCE92-03307. We thank R. E. Ulanowicz and J. E. Purcell for their reviews of the research in progress. We acknowledge the crew of the RV *Henlopen* for their capable support. L. Fernandez, F. Younger, M. Trice, and S. Leach assisted in the preparation of this manuscript.

Literature cited

Baird, D., and R. E. Ulanowicz.
1989. The seasonal dynamics of the Chesapeake Bay. Ecol. Monogr. 59:329–364.

Bigelow, H. B., and W. C. Schroeder.
1953. Fishes of the Gulf of Maine. U.S. Fish Wild. Serv., Fish Bull, vol. 53, 577 p.

Castro, L., and R. K. Cowen.
1991. Environmental factors affecting the early life history of bay anchovy *Anchoa mitchilli* in Great South Bay, New York. Mar. Ecol. Prog. Ser. 76:235–247.

Coombs, S. H., J. H. Nichols, and C. A. Fosh.
1990. Plaice eggs (*Pleuronectes platessa* L.) in the southern North Sea: abundance, spawning area, vertical distribution, and buoyancy. J. Cons. Int. Explor. Mer 47:133–139.

Cowan, J. H., Jr., and E. D. Houde.
1992. Size-dependent fish predation on marine fish larvae by ctenophores, scyphomedusae, and planktivorous fish. Fish. Oceanogr. 1:113–126.
1993. The relative predation potentials of scyphomedusae, ctenophores, and planktivorous fish on ichthyoplankton in Chesapeake Bay. Mar. Ecol. Prog. Ser. 95:55–65.

Dahlberg, M.
1979. A review of survival rates of fish eggs and larvae in relation to impact assessments. Mar. Fish. Rev. 41:1–12.

Dalton, P. D.
1987. Ecology of bay anchovy (*Anchoa mitchilli*) eggs and larvae in the mid-Chesapeake Bay. M.S. thesis, Univ. Maryland, College Park, MD, 104 p.

Dovel, W. L.
1971. Fish eggs and larvae of the upper Chesapeake Bay. Univ. Maryland, Nat. Res. Inst. Spec. Rep. 4:1–71.

Fortier, L., and W. C. Leggett.
1985. A drift study of larval fish survival. Mar. Ecol. Prog. Ser. 25:245–257.

Harding, D., J. H. Nichols, and D. S. Tungate.
1978. The spawning of plaice (*Pleuronectes platessa* L.) in the southern North Sea and English Channel. Rapp. P.-V. Reun. Cons. Int. Explor. Mer 172:102–113.

Heath, M. R.
1992. Field investigations of the early life stages of marine fish. Adv. Mar. Biol. 28:1–173.

Hildebrand, S. F., and W. C. Schroeder.
1928. Fishes of Chesapeake Bay. U.S. Bur. Fish., Fish. Bull. 43:301–318.

Houde, E. D.
1989a. Subtleties and episodes in the early life of fishes. J. Fish Biol. 35 (Suppl. A):29–38.
1989b. Comparative growth, mortality, and energetics of marine fish larvae; temperature and implied latitudinal effects. Fish. Bull. 87:471–495.

Houde, E. D. and C. E. Zastrow.
1991. Bay anchovy. *In* S. L. Funderburk, J. A. Mihursky, S. J. Jordan, and D. Riley (eds.), Habitat requirements for Chesapeake Bay living resources, 2nd ed., p. 8.1–8.14. Living Resources Subcommittee, Chesapeake Bay Program, Annapolis, MD.
1993. Ecosystem- and taxon-specific dynamic and energetics properties of larval fish assemblages. Bull. Mar. Sci. 53(2):290–335.

Houde, E. D., J. C. Gamble, S. E. Dorsey, and J. H. Cowan Jr.
1994. Drifting mesocosms: the influence of gelatinous zooplankton on mortality of bay anchovy *Anchoa mitchilli* eggs and yolk-sac larvae. ICES J. Mar. Sci. 51:383–394.

Klebasko, M.
1991. Feeding ecology and daily ration of bay anchovy (*Anchoa mitchilli*) in the mid-Chesapeake Bay. M.S. thesis, Univ. Maryland, 103 p.

Lasker, R. (ed.).
1985a. A egg production method for estimating spawning biomass of pelagic fish: application to the northern anchovy, *Engraulis mordax*. *In* R. Lasker (ed.), An egg production method for estimating spawning biomass of pelagic fish: application to the northern anchovy, *Engraulis mordax*, p. 1–3. U.S. Dep. Commer., NOAA Tech. Rep. NMFS 36.
1985b. What limits clupeoid production? Can. J. Fish. Aquat. Sci. 42 (Suppl. 1):31–38.

Leak, J. C., and E. D. Houde.
1987. Cohort growth and survival of bay anchovy *Anchoa mitchilli* larvae in Biscayne Bay, Florida. Mar. Ecol. Prog. Ser. 37:109–122.

Luo, J., and J. Musick.
1991. Reproductive biology of the bay anchovy in Chesapeake Bay. Trans. Am. Fish. Soc. 120:701–710.

Luo, J., and S. B. Brandt.
1993. Bay anchovy, *Anchoa mitchilli*: production and consumption in mid-Chesapeake Bay based on a bioenergetics model and acoustic measures of fish abundance. Mar. Ecol. Prog. Ser. 98:223–236.

MacGregor, J. M.
1994. Temporal and spatial variability in cross-bay distribution and abundance of bay anchovy (*Anchoa mitchilli*) eggs and larvae. M.S. thesis, Univ. Maryland, College Park, MD, 138 p.

McGurk, M.
1986. Natural mortality of marine pelagic fish eggs and larvae: role of spatial patchiness. Mar. Ecol. Prog. Ser. 34:227–242.

Newberger, T., and E. D. Houde.
1995. Population biology of bay anchovy (*Anchoa mitchilli*) in the mid-Chesapeake Bay. Mar. Ecol. Prog. Ser. 116: 25–37.

Olney, J. E.
1983. Eggs and early larvae of the bay anchovy, *Anchoa mitchilli*, and the weakfish, *Cynoscion regalis*, in lower Chesapeake Bay with notes on associated ichthyoplankton. Estuaries 6:20–35.

Parker, K.
1985. Biomass model for the egg production method. *In* R. Lasker (ed.), An egg production method for estimating spawning biomass of pelagic fish: application to the northern anchovy, *Engraulis mordax*, p. 5–7. U.S. Dep. Commer., NOAA Tech. Rep. NMFS 36.

Pepin, P.
1991. Effect of temperature and size on development, mortality and survival rates of the pelagic early life history stages of marine fish. Can. J. Fish. Aquat. Sci. 48:503–518.

Purcell, J. E.
1992. Effects of predation by the scyphomedusan *Chrysaora quinquecirrha* on zooplankton populations in Chesapeake Bay, USA. Mar. Ecol. Prog. Ser. 87:65–76.

Purcell, J. E., D. A. Nemazie, S. E. Dorsey, E. D. Houde, and J. C. Gamble.
1994. Predation mortality of bay anchovy (*Anchoa mitchilli*) eggs and larvae due to scyphomedusae and ctenophores in Chesapeake Bay. Mar. Ecol. Prog. Ser. 114:47–58.

Saville, A.
1964. Estimation of the abundance of a fish stock from egg and larval surveys. Rapp. P.-V. Cons. Int. Explor. Mer 155:164–170.

Smith, P. E.
1985. Year-class strength and survival of 0-group clupeoids. Can. J. Fish. Aquat. Sci. 42 (Suppl. 1):69–82.

Smith, P. E, H. Santander, and J. Alheit.
1989. Comparison of the mortality rates of Pacific sardine, *Sardinops sagax*, and Peruvian anchovy, *Engraulis ringens*, eggs off Peru. Fish. Bull. 87:497–508.

Wang, S.-B.
1992. Abundance, relative biomass, production and energy storage of bay anchovy, *Anchoa mitchilli*, in the Chesapeake Bay. M.S. thesis, Univ. Maryland, College Park, MD, 167 p.

Wang, S.-B., and E. D. Houde.
1995. Distribution, relative abundance, biomass and production of bay anchovy, *Anchoa mitchilli*, in the Chesapeake Bay. Mar. Ecol. Prog. Ser. 121:27–38.

Zastrow, C. E., E. D. Houde, and L. G. Morin.
1991. Spawning, fecundity, hatch-date frequency and young-of-the-year growth of bay anchovy *Anchoa mitchilli* in mid-Chesapeake Bay. Mar. Ecol. Prog. Ser. 73:161–171.

Cannibalism and predation on fish larvae by larvae of Atlantic mackerel, *Scomber scombrus*: trophodynamics and potential impact on recruitment*

Louis Fortier
Ann Villeneuve
GIROQ, Département de biologie, Université Laval
Ste-Foy, Québec G1K 7P4, Canada

Abstract.—Predation and cannibalism during larval life are potential determinants of recruitment and year-class strength in marine fish. We studied predation by larval Atlantic mackerel, *Scomber scombrus*, 3–14 mm in length, on conspecifics and other fish larvae over Sable Island Bank (Scotian Shelf) in July 1991. With increasing length, the diet of mackerel larvae shifted from copepod nauplii to copepods and fish larvae. Mackerel <5 mm selected strongly for copepod nauplii. Mackerel ≥6 mm preyed indifferently on copepods (i.e. in proportion to their abundance in the plankton) but selected strongly for fish larvae. The larval fish prey of Atlantic mackerel larvae comprised conspecifics (66%), yellowtail flounder, *Limanda ferruginea* (18%), silver hake, *Merluccius bilinearis* (12%), and redfish, *Sebastes* spp. (4%) larvae. Predation was stage-specific: only the newly hatched larvae of a given species were ingested. Based on a conservative estimate of the transit time of fish larvae in the gut (24 h), estimates of prey mortality by Atlantic mackerel larvae ranged from 7% to 57%/d (average 31%) of the standing stock of newly hatched larvae of suitable prey size. Piscivory was limited at densities of fish larvae <0.1/m^3. Predation on fish larvae by Atlantic mackerel larvae declined with increasing density of nauplii in the environment and with increasing number of alternative copepod prey ingested. Because the capacity of Atlantic mackerel larvae to digest fish larvae was limited, cannibalism was density independent and predation on other species was depensatory. Hence, despite its potential importance during the first days after hatching, cannibalism and predation by Atlantic mackerel larvae 3–14 mm long do not appear to contribute to the density-dependent regulation of Atlantic mackerel and other prey species.

Manuscript accepted 26 October 1995.
Fishery Bulletin 94:268–281 (1996).

Several lines of indirect evidence suggest that predation is a major determinant of early survival in marine fish (Bailey and Houde, 1989): 1) the high mortality rate of eggs and yolk-sac larvae in the field (Fossum, 1988; Incze and Campbell, 1989); 2) the high estimates of predation mortality obtained by subtracting starvation mortality from total mortality (Hewitt et al., 1985; Leak and Houde, 1987); 3) the vulnerability of fast-growing, healthy larvae to predators in mesocosm experiments (Øiestad, 1985); 4) the wide range of potential predators of prerecruit fish in the sea (Hunter, 1984; Bailey and Houde, 1989); and 5) the variety of spawning strategies that can be interpreted as reducing the vulnerability of eggs and larvae to predators (Bailey and Houde, 1989). A recent field study comparing concurrent measurements of predation mortality and total mortality confirmed that predators such as medusae can have a significant impact on the early survival of bay anchovy, *Anchoa mitchilli*, in Chesapeake Bay (Purcell et al., 1994). Yet, in most ecosystems, the actual predators of fish larvae, the trophodynamics between predators and fish larvae, and the role of predation in regulating year-class strength remain unclear (Hunter, 1984; Anderson, 1988; Bailey and Houde, 1989; Heath, 1992).

Scombrid larvae often prey on the larval stages of their own and other fish species (Hunter and Kimbrell, 1980; Jenkins et al., 1984; Finucane et al., 1990; Young and Davis, 1990). In particular, Atlantic mackerel, *Scomber scombrus*, larvae capture fish larvae sometimes more than half their own length (Grave, 1981). The diet of Atlantic mackerel larvae changes markedly during ontogeny. First-feeding larvae may be phytophagous, young post-yolk-sac larvae feed primarily on copepod nauplii and copepodites, and Atlantic mackerel >6.5 mm in length add conspecifics and other fish larvae to their diet (Grave, 1981; Peterson and Ausubel, 1984; Ware and Lambert, 1985).

Because the probability of encounter between planktonic larvae increases with increasing density, Grave (1981) proposed that intracohort cannibalism could be a simple mechanism for the density-dependent regulation of year-class strength in Atlantic mackerel. In the present study, we examined the diet of Atlantic mackerel larvae and their selectivity for prey on Sable Island Bank (Scotian Shelf) in July

* Contribution to the research program of GIROQ (Groupe interuniversitaire de recherches océanographiques du Québec).

1991. Cannibalism and predation on other fish larvae were studied in relation to larval fish density and the availability and consumption of alternative invertebrate prey. In particular, we searched for evidence that cannibalism and piscivory by Atlantic mackerel larvae were density dependent. Finally, we evaluated the potential impact of predation by Atlantic mackerel larvae on the early survival of fish larvae.

Methods

In spring, the northern component of the Northwest Atlantic stock of Atlantic mackerel migrates from the New England Continental Shelf and the Scotian Shelf towards the southern Gulf of St. Lawrence where the bulk of spawning takes place from early June to mid-August (Sette, 1943, 1950). Some spawning also takes place along the coast of Nova Scotia (Sette, 1943; Berrien et al., 1981). During a 27-month series of monthly ichthyoplankton surveys on Emerald, Western, and Sable Island banks (Fig. 1), Atlantic mackerel larvae were captured offshore, primarily over Sable Island Bank, in June, July, and August of 1991 and 1992. The larvae ranged from 2.7 to 13.7 mm standard length (SL)(unpreserved), corresponding to an approximate age span of 4 to 16 days (D'Amours et al., 1990). These lengths and ages indicate that the shallow waters west of Sable Island constitute a spawning ground for the species. The present study focuses on the trophodynamics of Atlantic mackerel larvae sampled in July 1991.

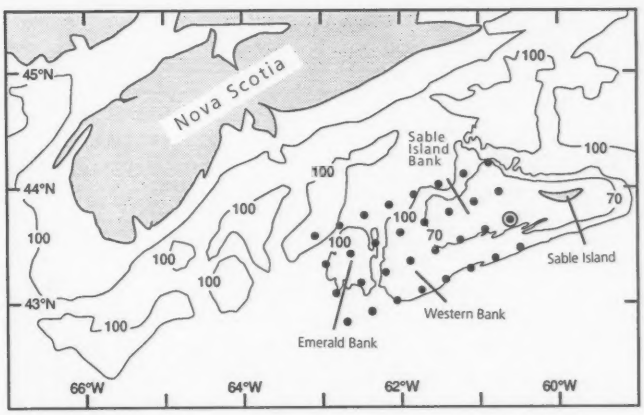

Figure 1

Location of the 32 rectangular midwater trawl (RMT) stations sampled for Atlantic mackerel, *Scomber scombrus*, larvae and their prey from 18 to 23 July 1991 on Emerald, Western, and Sable Island banks (Scotian Shelf). The vertical distribution of fish larvae was studied with the multi-net sampler on 24 and 25 July at the station marked with a circled black dot. Isobaths are in meters.

Sampling

Atlantic mackerel larvae and their prey were sampled from 18 to 23 July 1991 over a grid of 32 stations covering part of Emerald, Western, and Sable Island banks (Fig. 1). Three different plankton nets mounted on a rectangular midwater trawl (RMT) were used to collect young fish and zooplankton simultaneously. A main net (8-m^2 sweeping section, 1,600-μm mesh) captured juvenile fish; an intermediate net (2-m^2 sweeping section, 333-μm mesh) collected fish larvae and mesozooplankton; and a small net (0.0075-m^2 mouth, 64-μm mesh) sampled the microzooplankton prey of fish larvae. The RMT was towed once at each station in a multiple oblique trajectory from 0 to 75 m (or 5 m from the bottom at stations shallower than 75 m) for an average (± standard deviation [SD]) of 17 (±5) min at a speed of approximately 2 knots (1 m/s). A CTD (conductivity, temperature, and depth) probe and flowmeters linked to a computer allowed real-time monitoring of depth, water column temperature and salinity, and the volume of water filtered by each net.

On 24 July, a multi-net sampler (Eastern Marine Services E-Z-Net) mounted with 10 identical nets (1-m^2 mouth, 333-μm mesh) was used to determine the vertical distribution of fish larvae at the grid station (52-m depth) where the greatest density of fish larvae was found with the RMT (Fig. 1). Six casts were made at intervals of approximately four hours from 2115 h on 24 July to 2000 h on 25 July 1991. For each cast, 4 depth intervals of 10 m were sampled twice in the following order: 40–30, 30–20, 20–10, 10–0, 0–10, 10–20, 20–30, and 30–40 m. Nets were also opened on the downward (0–40 m) and upward (40–0 m) trajectories of the cast, providing two depth-integrated samples. The multi-net system was equipped with the same real-time monitoring system as that used on the RMT.

Most fish larvae (70%) were sorted immediately at sea and preserved in 95% ethanol. The remainder of the plankton sample, including undetected fish larvae, was preserved in 4% buffered formalin. A subset of 50 Atlantic mackerel larvae were videotaped on the ship for determination of morphometrics before preservation. Twenty-six of these (3.3 to 13.7 mm fresh SL) were preserved in ethanol and 24 (3.3 to 13.3 mm fresh SL) in formalin.

In the laboratory, all fish larvae remaining in the preserved samples were sorted and identified. All undamaged mackerel

larvae (n=1,667) were measured to the nearest 0.1 mm SL. Standard length of mackerel larvae preserved in ethanol and formalin was corrected for shrinkage by using the relationships between fresh and preserved measurements obtained from the subset of larvae videotaped at sea (r^2=0.98). The standard length of a random subset of the 3 other dominant larval fish species (51 silver hakes, 467 yellowtail flounders, 200 redfishes, preserved in ethanol) was measured. Mackerel lengths represent fresh measurements except those used for comparison with other species, in which case all lengths are ethanol-preserved measurements.

Gut content analysis

Undamaged Atlantic mackerel larvae were selected for gut content analysis. The digestive tract was separated from the body and dissected under a light microscope. Whenever possible, prey were identified and measured. The position of the prey in the tractus (foregut, midgut, and reargut) and the state of digestion of the prey (slightly, partly, and well digested) were noted. Because crustacean prey were flattened dorso-ventrally, cephalothorax length, rather than width, was measured. Fish larvae were particularly damaged by digestion and only a small proportion of them (36 out of 710) could be identified and measured directly under the light microscope.

Indirect identification of some digested fish larvae was based on discriminant analysis of their otoliths. To establish the discriminant function, between 18 and 29 ethanol-preserved specimens of each of the four dominant larval fish species sampled in July 1991 (Atlantic mackerel, silver hake, yellowtail flounder, and redfish), ranging in size from hatching length to 10 mm, were selected from the plankton collections and measured. The sagittae and lapilli of each fish were extracted and 8 measurements were taken on each of the 4 otoliths: longest and shortest diameter (LD and SD); longest and shortest radius (LR and SR); surface and perimeter (SU and PE); and longest and shortest diameter of nucleus (LN and SN). The discriminant function used 15 measures and ratios of measures (LR_S/LR_L, LN_S, SU_S/SU_L, PE_S/SU_S, PE_S/LD_L, SN_S/LN_L, SR_S/SD_L, LD_S/LR_L, SD_S/SD_L, LR_S/SU_L, SD_S/SR_S, SD_S/SN_L, SD_L, LN_S/SN_L, SR_S/SU_L), in order of decreasing discriminatory power, where the subscripts S and L refer to the sagitta and the lapillus, respectively (from the same side of the fish). The discriminant function, which was validated by using the known larvae, correctly classified between 67% and 89% of the larvae of each species (Table 1).

The discriminant function was used to identify an additional 38 (out of 710) digested fish larvae for which one undamaged sagitta and one undamaged lapillus (from the same side of the fish) were recovered. The length of identified fish larvae was back-calculated on the basis of the best polynomial regression between one of the otolith dimensions and the ethanol-preserved standard length for the known specimens of the species (LD_S, r^2=0.87 for Atlantic mackerel; LD_S, r^2=0.93 for silver hake; SR_S, r^2=0.80 for yellowtail flounder; SD_S, r^2=0.75 for redfish).

Table 1

Validation of the linear discriminant function used to identify fish larvae found in the gut of larval Atlantic mackerel, *Scomber scombrus*, sampled from 18 to 23 July 1991, southwest of Sable Island (Scotian Shelf). The discriminant function is based on the morphometry of the otoliths of known larvae (see text). Successful identification is the percentage of larvae of a given species correctly identified by the discriminant function. Type-1 error is the proportion of fish larvae incorrectly assigned to another species (H_0 rejected when it is true). Type-2 error is the proportion of fish larvae identified as a given species that were actually of another species (H_0 accepted when it is false).

	Silver hake	Yellowtail flounder	Atlantic mackerel	Redfish
Successful identification (%)	78	89	71	67
Type-1 error (%)	22	11	29	33
Type-2 error (%)	8	29	28	31
Sample size	54	38	58	36

Zooplankton were identified, enumerated, and measured in the RMT collections (64-μm and 333-μm net samples) that contained Atlantic mackerel larvae. The selectivity of Atlantic mackerel larvae for a category of prey was estimated by using Chesson's α (Chesson, 1978):

$$\alpha_j = (d_j / p_j) / \left(\sum d_i / p_i \right), \text{ for } i = 1,\ldots N,$$

where α_j is the selectivity for prey taxon j, N is the number of prey taxa, d_j and p_j are the frequencies of prey taxon j in the diet and the plankton respectively, and d_i and p_i are the same frequencies for the ith prey taxon. Copepod eggs in the diet of large fish larvae may have reflected the ingestion of egg-bearing females and, accordingly, eggs were not considered in the calculation of selectivity indices. Following Fortier and Harris (1989), α_j was first computed for each individual Atlantic mackerel larva captured in the RMT and then averaged by length classes (<5, 5 to <6, 6 to <7, 7 to <8, ≥9 mm). Variations in α reflect changes in the preference of the predator. α is not

affected by changes in the abundance of potential prey and is thus suitable for describing ontogenetic variations in prey selectivity and for comparing or averaging selectivity among stations with different prey densities (Pearre, 1982). A value of $\alpha_j > 1/N$ indicates that prey j is selected for, whereas $\alpha_j < 1/N$ indicates that the prey is rejected.

All dissected mackerel larvae (feeding and nonfeeding) were included in the determination of diurnal patterns of feeding activity. Larvae with empty guts occurred primarily during late-night and early-morning hours (0000–0800 h). These larvae were excluded from the calculations of feeding ratios (mean number of prey organisms per gut of feeding mackerel) or of piscivory (proportion of feeding mackerels with at least one fish larva in the gut). Note that the calculation of a feeding ratio for Atlantic mackerel larvae feeding on fish larvae was meaningless because the gut of mackerel larvae seldom (3% of all cases) contained more than one fish larva.

Results

Zooplankton and fish larvae

Copepods numerically dominated the zooplankton (Table 2). The cyclopoid *Oithona similis*, harpacticoid copepods, and the calanoid *Pseudocalanus* sp. were particularly abundant. The low mean densities of copepod eggs and nauplii (<2/L) may reflect the wide depth interval sampled by the RMT (0–75 m) because these organisms are often concentrated at the pycnocline or in the surface mixed layer.

Representatives of at least 18 genera of fish were collected (Table 2). Silver hake, yellowtail flounder, Atlantic mackerel, and redfish made up the bulk (98%) of the larval fish assemblage. Atlantic mackerel, silver hake, and yellowtail flounder larvae were found primarily over the shallow area of Sable Island Bank (Fig. 2). Redfish larvae were more evenly distributed in the sampling area than were the other species. Vertically, Atlantic mackerel, yellowtail flounder, and redfish larvae aggregated in the surface layer (<20 m) at night and moved deeper in the water column during the day (Fig. 3). In the morning and afternoon, Atlantic mackerel were concentrated in the thermocline at 10–20 m, whereas yellowtail flounder and redfish were found in or below the thermocline. At 2000 h, all four species were most abundant in the thermocline. During the day, the newly-hatched silver hake larvae were found primarily in the surface layer (0–20 m). Too few larvae were captured at night to confirm any diel migration pattern in this species.

Table 2

Mean density (± standard deviation) and percent composition of the zooplankton and larval fish assemblages at stations where Atlantic mackerel larvae, *Scomber scombrus*, were captured (n=14) from 18 to 23 July 1991, southwest of Sable Island (Scotian Shelf).

	Density	Percent
Invertebrates (no./m³)		
Copepods		
Oithona similis	2,048 ±1,226	29
Copepod nauplii	1,642 ±978	23
Harpacticoids	973 ±565	14
Copepod eggs	606 ±597	8
Pseudocalanus sp.	506 ±452	7
Temora longicornis	168 ±278	2
Calanus finmarchicus	153 ±163	2
Centropages sp.	85 ±107	1
Metridia lucens	12 ±20	<1
Eurytemora hirundoides	2 ±5	<1
Acartia sp.	1 ±2	<1
Calanus hyperboreus	<1	<1
Metridia longa	<1	<1
Tintinnids	690 ±838	10
Bivalve larvae	198 ±306	3
Gastropods	64 ±60	1
Appendicularians	29 ±39	<1
Polychaete larvae	6 ±15	<1
Chaetognaths	2 ±3	<1
Euphausiids	2 ±3	<1
Amphipods	1 ±3	<1
Decapod larvae	1 ±1	<1
Gelatinous zooplankton	<1	<1
Ichthyoplankton (no. 100/m³)		
Merluccius bilinearis, silver hake	17 ±52	37
Limanda ferruginea, yellowtail flounder	12 ±30	27
Scomber scombrus, Atlantic mackerel	11 ±23	24
Sebastes spp.,[1] redfish	4 ±10	10
Glyptocephalus cynoglossus, witch flounder	<1	<1
Melanogrammus aeglefinus, haddock	<1	<1
Scophthalmus aquosus, spotted flounder	<1	<1
Mallotus villosus, capelin	<1	<1
Ammodytes sp., sand lance	<1	<1
Hippoglossoides platessoides, American plaice	<1	<1
Lophius americanus, goosefish	<1	<1
Stichaeus punctatus, Arctic shanny	<1	<1
Urophycis sp., hake	<1	<1
Ulvaria subbifurcata, radiated shanny	<1	<1
Others[2]	1 ±1	2

[1] Includes *Sebastes mentella* and *Sebastes fasciatus*.
[2] Includes unidentified fish larvae, pleuronectids, gonostromatids, stichaeids, and *Cyclopterus lumpus* (lumpfish) in order of decreasing average density.

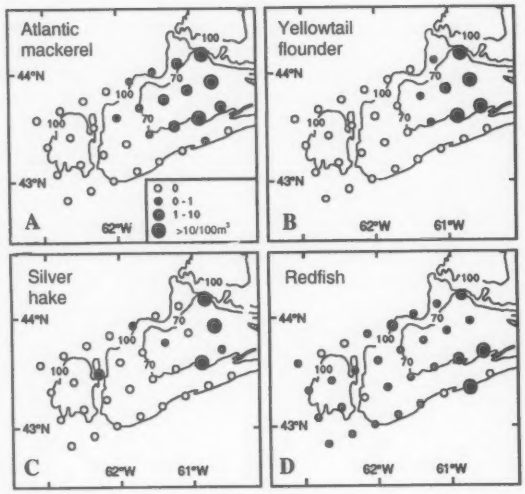

Figure 2

Distribution of the four most abundant species of fish larvae sampled with a rectangular midwater trawl (RMT) from 18 to 23 July 1991 on Emerald, Western, and Sable Island banks (Scotian Shelf).

Diet and feeding patterns in Atlantic mackerel larvae

The diet of Atlantic mackerel larvae changed markedly during early ontogeny (Table 3). Small larvae (<5 mm) fed almost exclusively on copepod nauplii. With increasing length, their diet shifted from nauplii to copepods (copepodites and adults) and fish larvae. Copepod eggs did not contribute substantially (<1% of the prey) to the diet of mackerel larvae <7 mm that preyed mainly on copepod nauplii. The increased proportion of copepod eggs in the diet of larvae ≥7 mm may have reflected the ingestion of egg-bearing female copepods such as *O. similis* or *Pseudocalanus* sp. Appendicularians were present in small proportion (<5%) in the diet of all length classes of larvae. The importance of fish larvae in the diet increased with the length of Atlantic mackerel larvae. The smallest Atlantic mackerel larva that had preyed on another fish larva was 3.3 mm (fresh SL).

The mean cephalothorax length of the copepod prey of Atlantic mackerel larvae increased threefold over the range of lengths studied (<5 to ≥9 mm, Table 3). Feeding incidence was high (≥75%) in all length classes of mackerel. The feeding ratio (all prey types considered) tended to decrease with length, a reflection of the increasing frequency of large prey such as fish larvae. The incidence of predation on fish larvae increased with larval mackerel size, from 12% in the smallest length class (<5 mm) to 69% in the largest length class (≥9 mm).

The mean number of invertebrate prey in the gut of Atlantic mackerel larvae was relatively constant from the second half of the night to late afternoon (1.9–3.5 prey per gut) and then jumped to 13 prey at dusk or soon after (Fig. 4A). This sharp increase in the number of invertebrate prey at dusk may represent an increase in copepod availability as the latter pass through the layer containing mackerel larvae during their nycthemeral migration towards the surface. The percentage of dissected Atlantic mackerel larvae with at least one fish larva in the gut tended to increase from the morning (<30%) to the afternoon and late evening (40–60%) (Fig. 4B).

The gut of Atlantic mackerel larvae usually contained no more than one fish larva (97% of cases). Forty-four percent (314 out of 710) of mackerel larvae containing a larval fish prey also contained at least one invertebrate prey. Most fish larvae were found in the midgut of Atlantic mackerel larvae throughout the diurnal period (Fig. 5A). The frequency of fish larvae in the foregut remained relatively constant during daylight hours, increased at dusk, and decreased in the second half of the night. Occurrence in the reargut was maximum in the early morning hours. In general, fish larvae in the gut of mackerel larvae were either partly or well digested (Fig. 5B). The percentage of Atlantic mackerel containing slightly digested fish larvae was low and relatively constant throughout the day. The frequency of partly digested fish larvae was high and tended to increase from early morning to late afternoon, whereas the frequency of well digested fish larvae declined.

Prey selectivity in Atlantic mackerel larvae

Atlantic mackerel larvae of all lengths fed selectively, but selectivity for a given prey type changed during ontogeny (Table 4). Selection for copepod nauplii was high in small larvae (<5 mm) but declined rapidly as predator size increased; larvae ≥7 mm selected against this prey. Despite their numerical importance in the diet, copepods were either selected against by larvae <7 mm or consumed in rough proportion to their availability in the plankton by larger larvae. Selection for fish larvae increased steadily with the length of Atlantic mackerel larvae and preference for this prey type was particularly strong in larvae ≥9 mm (Table 4).

When analyzed by size categories, copepod prey (nauplii + copepodites + copepods) <300 μm in cephalothorax length were selected (among the copepods) by larvae <7 mm, whereas copepods in the range 300–600 μm were selected against or consumed in near

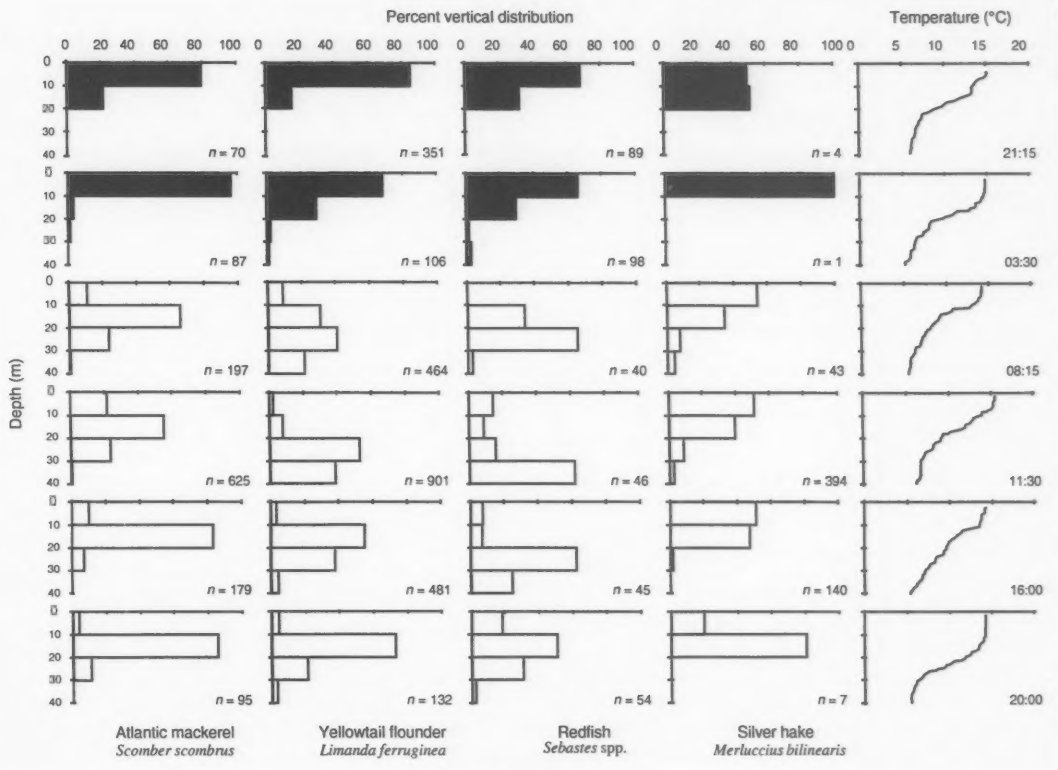

Figure 3

Diel changes in the vertical distribution of the four most abundant species of fish larvae captured with the multi-net sampler (24 and 25 July 1991) at the station (52-m depth) of the sampling grid where the greatest density of fish larvae was found. Black histograms represent nighttime percent distribution and white histograms, daytime percent distribution. Vertical profiles of temperature are shown on the right. Sample size (number of larvae) is given with the vertical distribution and sampling hour with the temperature profile.

proportion to their availability in the plankton by larvae of all lengths. Copepods ≥600 μm were selected for by larvae ≥7 mm (Table 5).

Out of the 710 fish larvae found in the gut of Atlantic mackerel larvae, 36 were identified visually and 38 were identified by discriminant analysis of their otoliths (Table 6). The species composition of the prey identified by either method was similar (Table 6). Assuming that the species composition of the 74 fish larvae identified represented the true composition of the assemblage ingested, conspecifics made up the majority (66%) of the fish larvae preyed upon by Atlantic mackerel larvae. Selectivity for a given species of larval fish prey was calculated for stations where ≥10 larvae were identified in the gut of Atlantic mackerel larvae. The results indicated little selection by mackerel larvae for any species of fish larvae ($\alpha \approx 1/N = 0.25$, where N=4 species) (Table 6).

Atlantic mackerel larvae preyed primarily on newly hatched larvae despite the availability of larger larvae in the plankton (Fig. 6). Only one conspecific prey >5 mm was found in the gut of mackerel larvae despite the availability of conspecifics in the plankton. Except for one larva 9 mm long, yellowtail flounder prey were <6.5 mm. The three redfish prey for which measurements are available were <5.5 mm. Atlantic mackerel apparently did not capture silver hakes >2.5 mm. The lengths of conspecifics, redfish, and silver hake prey corresponded to the range of lengths at hatching for these species (Fig. 6).

Predation by Atlantic mackerel larvae in relation to prey density

There was no consistent relationship between predation on invertebrates by Atlantic mackerel larvae

Table 3

Percent composition of diet and feeding statistics by length classes for larval Atlantic mackerel, *Scomber scombrus*, sampled southwest of Sable Island (Scotian Shelf) from 18 to 23 July 1991.

	Length class (mm)					
Prey taxa	<5	5–<6	6–<7	7–<8	8–<9	≥9
Copepod eggs	<1	<1	<1	18	46	37
Copepod nauplii	89	63	56	23	2	8
Copepods[1]	5	21	30	41	34	34
Appendicularians	4	7	4	5	2	1
Fish larvae	2	9	9	12	14	16
Others[2]	<1	<1	<1	1	2	4
Total number of prey	742	1,655	2,913	1,350	570	227
Total number of mackerel larvae	172	444	523	322	144	62
Feeding incidence (%)	75	87	92	88	88	86
Mean feeding ratio (prey per gut)	5.8	4.3	6.0	4.8	4.5	4.3
Incidence of piscivory (%)	12	39	54	57	63	69
Mean length of copepod prey (μm)[3]	190	253	289	405	657	597

[1] Copepodites and adult copepods.
[2] Include euphausiids, chaetognaths, gastropods, phytoplankton cells, cladocerans, amphipods, euphausiid nauplii, and crab larvae in order of decreasing frequency.
[3] Nauplii, copepodites, and adult copepods.

and the density of these prey in the environment. The feeding ratio for copepod nauplii (mean number of nauplii per gut) was not correlated with the density of nauplii in situ for any length class of Atlantic mackerel larvae ($P \geq 0.33$). The feeding ratio for copepods (copepodites and adults) was negatively correlated with the density of this prey for Atlantic mackerel larvae 6 to <7 mm ($P=0.03$, $n=7$) but not significantly correlated with prey density for other length classes (5 to <6 and ≥7 mm, $P \geq 0.67$).

In RMT collections, the relationship between the incidence of piscivory (proportion of feeding Atlantic mackerel with at least one fish larva in the gut) and the density of fish larvae of suitable prey size (sum of Atlantic mackerels and redfishes ≤5.5 mm, yellowtail flounders ≤6.5 mm, and silver hakes ≤2.5 mm) was adequately described by an Ivlev equation (Fig. 7, A–C). Incidence of piscivory was limited at densities of larval fish prey <0.1 larvae/m^3 and quickly reached a plateau as availability increased. The height of the plateau (maximum incidence of piscivory) increased with predator length. The parameters of the Ivlev equation varied little when the data from the multi-net collections were added to the RMT data set (Fig. 7, D–F).

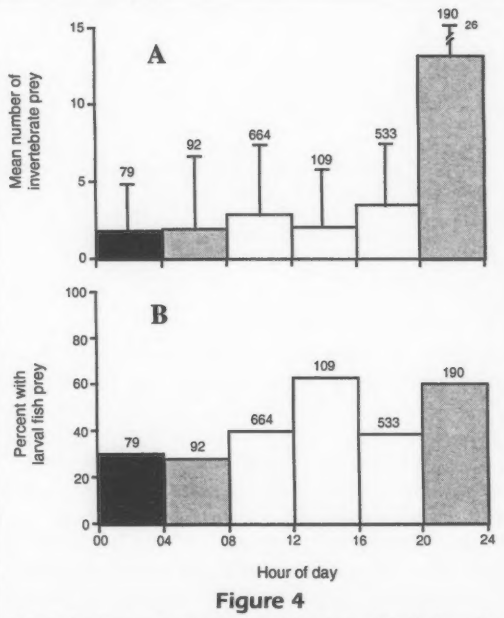

Figure 4

Daily feeding activity of larval Atlantic mackerel, *Scomber scombrus*. (**A**) Mean number (and standard deviation) of invertebrate prey per dissected gut. (**B**) Percentage of dissected mackerel larvae with at least one fish larva in the gut. Black histograms represent nighttime, gray histograms twilight, and white histograms daytime. Number above time class indicates the number of dissected mackerel larvae.

Effect of alternative invertebrate prey on piscivory

In the present study, the absolute predation rate could not be assessed because the transit time for fish larvae

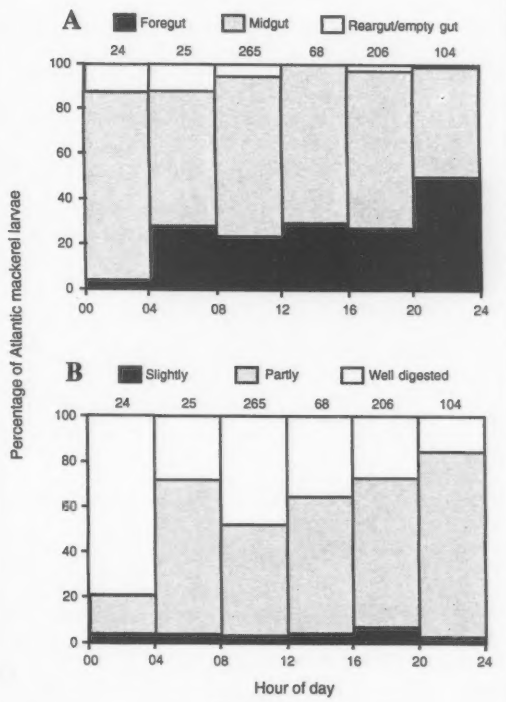

Figure 5

Diel changes in the position (**A**) and state of digestion (**B**) of larval fish prey in the gut of larval Atlantic mackerel, *Scomber scombrus*. Histograms represent the percentage of mackerel larvae with larval fish prey in a given position in gut (A) and the percentage of mackerel larvae with larval fish prey in a given state of digestion (B). Numbers above each time class indicate the number of Atlantic mackerel larvae dissected.

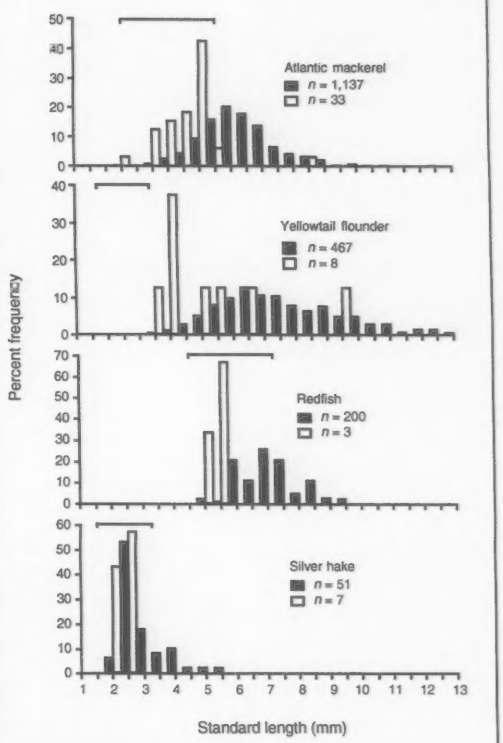

Figure 6

Frequency distribution of the standard length of ethanol-preserved fish larvae in the plankton (black histograms) and in the gut of larval Atlantic mackerel, *Scomber scombrus* (white histograms). Horizontal bars on top of histograms represent the range of hatching length (Fahay, 1983; this study).

in the gut of Atlantic mackerel larvae is unknown. However, assuming a digestion time of 24 hours, a relative daily predation rate (PR, in %/d) was defined as the proportion of all fish larvae of suitable prey size in a sample that was found in the gut of Atlantic mackerel larvae:

$$PR = (NP_g \times 100)/(NP_g + DP),$$

where NP_g = the density of fish larvae in mackerel gut per m^3 of water; and
DP = the density of larvae of suitable prey size in the plankton per m^3.

Predation rate by Atlantic mackerel larvae 3–14 mm long ranged from 7% to 57%/d (average of 31%/d) of the standing stock of the newly hatched fish larvae of suitable prey size (or 2% to 27%/d of all fish larvae). Daily predation declined linearly with increasing density of copepod nauplii (Fig 8A), the only other prey strongly selected for by Atlantic mackerel larvae (Table 4). Sample size for the regression was low (8) because few RMT collections (for which estimates of zooplankton density are available) contained enough Atlantic mackerel larvae to calculate a reliable index. Daily predation was not significantly correlated with the density of copepods (P=0.991) or the combined density of nauplii and copepods (P=0.658). Daily predation on fish larvae of suitable prey size decreased asymptotically as the average number of alternative copepod prey (nauplii + copepodites + adults) consumed by Atlantic mackerel larvae increased (Fig. 8B). The relationship was best described by a reciprocal model; 24% of the variance in daily

Table 4

Prey selectivity (α, Chesson, 1978) in larval Atlantic mackerel, *Scomber scombrus*, sampled southwest of Sable Island (Scotian Shelf) from 18 to 23 July 1991. α was calculated for each Atlantic mackerel larvae and averaged over length classes. A plus sign (+) indicates positive selection for prey ($\alpha > 1/N = 0.2$, where $N = 5$ prey taxa). Only samples containing at least 10 Atlantic mackerel larvae were considered in the calculations.

	Length class (mm)					
Prey taxa	<5	5–<6	6–<7	7–<8	8–<9	≥9
Copepod nauplii	+0.70	+0.33	+0.27	0.06	0.01	—
Copepods[1]	0.02	0.12	0.14	+0.24	+0.32	+0.28
Appendicularians	+0.22	+0.29	0.14	0.14	0.08	0.04
Fish larvae	0.05	+0.26	+0.44	+0.49	+0.53	+0.61
Others[2]	0.01	<0.01	0.01	0.07	0.06	0.07
No. of mackerel larvae	98	203	183	184	113	44

[1] Copepodites and adult copepods.
[2] Includes euphausiids, chaetognaths, gastropods, cladocerans, amphipods, euphausiid nauplii, and crab larvae in order of decreasing frequency.

Table 5

Selectivity for copepod (nauplii, copepodites, and adults) prey size in larval Atlantic mackerel, *Scomber scombrus*, sampled southwest of Sable Island (Scotian Shelf) from 18 to 23 July 1991. α (Chesson, 1978) was calculated for each Atlantic mackerel larva and averaged over length classes. A plus sign (+) indicates positive selection for size ($\alpha > 1/N = 0.2$, where $N = 5$ size categories). Only samples containing at least 10 Atlantic mackerel larvae were considered in the calculations.

	Length class (mm)					
Copepod size (μm)	<5	5–<6	6–<7	7–<8	8–<9	≥9
< 300	+0.94	+0.64	+0.40	0.10	0.01	0.02
300 < 400	0.04	+0.22	+0.26	0.14	0.03	0.04
400 < 500	0.02	0.08	0.12	0.08	0.05	<0.01
500 < 600	—	0.04	0.11	+0.25	0.16	+0.28
≥600	—	0.02	0.11	+0.43	+0.75	+0.66
No. of mackerel larvae	93	165	129	101	61	17

predation rate was explained by the consumption of alternative copepod prey. When one outlier point was removed, the fraction of the variance explained by the model increased to 46% (Fig. 8B).

Discussion

Selectivity for fish larvae in Atlantic mackerel larvae

Over 50% of feeding Atlantic mackerel ≥6 mm had captured at least one fish larva despite the absolute and relative (to other prey) scarcity of fish larvae of suitable prey size in the plankton (on average 0.14 fish larva/m^3 vs. 5,920 nauplii and copepods/m^3). By comparison, copepods were preyed upon in proportion to their relative abundance in the plankton. On the basis of the small percentage of larval fish prey that could be

Table 6

Species composition of larval fish prey found in the gut of larval Atlantic mackerel, *Scomber scombrus*, sampled southwest of Sable Island (Scotian Shelf) from 18 to 23 July 1991. Positive selection for prey ($\alpha > 1/N = 0.25$, where $N = 4$ species of larval fish prey) is indicated by a plus sign (+).

	Silver hake	Yellowtail flounder	Atlantic mackerel	Redfish
Number identified visually	6	3	27	0
Number identified by otoliths	7	6	22	3
Total number identified	13	9	49	3
Percent of grand total	18	12	66	4
Selectivity index	0.18	+0.31	+0.34	0.21

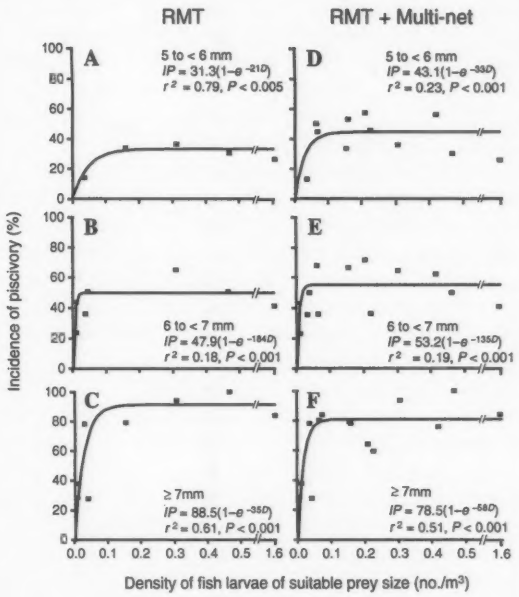

Figure 7

Incidence of piscivory (IP) in larval Atlantic mackerel, *Scomber scombrus*, as a function of the density of fish larvae of suitable prey size (D), by standard-length classes of mackerel larvae. (**A–C**) RMT collections only; (**D–F**) RMT and multi-net collections. The percentage of the variance (r^2) in the incidence of piscivory explained by the Ivlev function (Ivlev, 1961) and the significance level of the regression (P) are given. Note the broken scale on the abscissa.

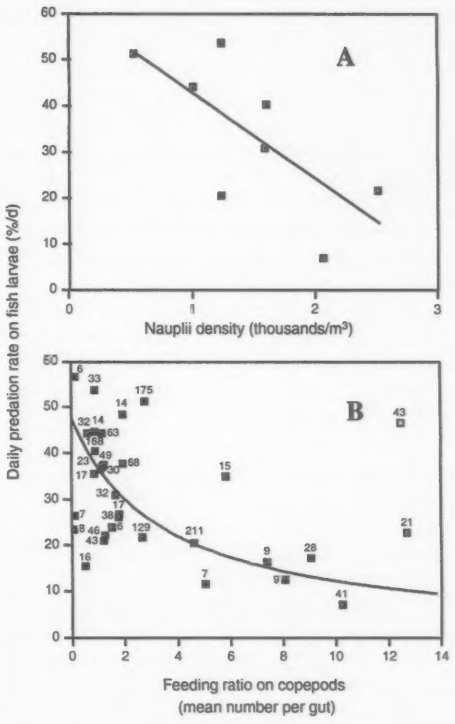

Figure 8

Estimated daily predation rate (PR, see text) of larval Atlantic mackerel, *Scomber scombrus*, on fish larvae of suitable prey size as a function of (**A**) the density of copepod nauplii (*DN*) in the environment ($PR = 61.6 - 0.0189DN$ [n=8, r^2=0.505, F=6.1, P=0.048]), and (**B**) as a function of the feeding ratio of Atlantic mackerel larvae for copepods (*FR*, all developmental stages), ($PR = 1/(2.1 + 0.612FR)$ [n=31, r^2=0.462, F=24.9, P<0.001]). In (B), each data point in the regression was weighted by the number of Atlantic mackerel larvae in the sample (given near each point). The outlier marked by the open symbol was excluded from the analysis.

identified (74 out of 710), Atlantic mackerel larvae exhibited little preference for any of the four dominant species of fish larvae available in July in the area studied.

Despite their relatively low frequency in the diet (2% to 16% by number), fish larvae represented an important fraction of the energy intake of Atlantic mackerel larvae. For example, most of the conspecifics ingested ranged from 3.0 to 5.5 mm in length, which translates into 20 to 200 μg in dry weight (Table 3 in Peterson and Ausubel, 1984). By comparison, the approximate dry weight of copepod prey (0.1–0.6 mm in cephalothorax length) ranged from 0.006 to 2 μg (Cohen and Lough, 1981). Thus, assuming that the nutritional value of copepods is four times that of fish larvae per unit biomass (Gotceitas and Brown, 1993), the energy intake represented by one fish larva corresponded to that of 2.5 to 25 of the largest copepods ingested. Pacific mackerel, *Scomber japonicus*, and Atlantic mackerel larvae are characterized by fast growth, high metabolism, and high food requirements (Hunter and Kimbrell, 1980; Peterson and Ausubel, 1984; Ware and Lambert, 1985). The width of ingested fish larvae closely matches the mouth width of Atlantic mackerel larvae (Ware and Lambert, 1985), and fish larvae are the largest prey ingested (Grave, 1981; Ware and Lambert, 1985; this study). Hence, fish larvae probably represent the most profitable prey available in the plankton to satisfy the high food requirements of Atlantic mackerel larvae.

Piscivores generally select small prey in laboratory experiments and consistently ingest smaller than average prey in field situations, a potential reflection of an inability to capture larger prey (Juanes and Conover, 1994, and references therein). In the

present study, Atlantic mackerel larvae 3–14 mm long preyed primarily on newly hatched fish larvae (conspecifics and others). This suggests that in the days following hatching, fish larvae quickly acquire enough motility to escape attack from Atlantic mackerel larvae in this size range. Thus, the predation rates estimated in the present study (7% to 57%/d of the standing stock of larvae of suitable prey size) would apply only over the relatively short period before the development of an efficient escape response. Growth during this period would determine cumulative predation mortality from co-occurring Atlantic mackerel larvae 3–14 mm in length. In the laboratory, survival to metamorphosis in Pacific mackerel larvae was positively correlated with growth over the period during which sibling cannibalism occurred (Hunter and Kimbrell, 1980).

Effect of prey density on predation by Atlantic mackerel larvae

Surprisingly few studies have related the feeding success of fish larvae in the sea to prey availability (Heath, 1992; Fortier et al., 1995). In the majority of these studies, there are indications that feeding was limited below some threshold density of prey. For example, the feeding ratio of larval Atlantic cod, *Gadus morhua*, was adequately described by an Ivlev equation, with feeding limited at nauplii concentrations <10/L (Ellertsen et al., 1989; Sundby and Fossum, 1990). The same model was used to describe stomach fullness and feeding incidence (proportion of predators with prey in the gut) in larvae of southern bluefin tuna, *Thunnus maccoyii*, as a function of zooplankton settled volume (Young and Davis, 1990; Heath, 1992). In this case, the feeding of larval tuna appeared limited at densities of approximately <0.5 prey/L (Heath, 1992). In ice-covered Hudson Bay, the feeding incidence and feeding ratio of Arctic cod, *Boreogadus saida*, and larvae of sand lance, *Ammodytes* sp. in relation to nauplii density were also adequately modeled by an Ivlev equation (Fortier et al., in press). Feeding was limited at densities <40,000 nauplii/m^2, corresponding approximately to <1.6 nauplii/L. In large enclosures, the growth of larvae of capelin, *Mallotus villosus*, was related to prey biomass by a function resembling an Ivlev function (Frank and Leggett, 1982).

In the present study, there was no indication that predation on copepod nauplii and copepods by Atlantic mackerel larvae was dependent on the density of these prey in the environment. This may indicate that naupliar (261 to 4,134/m^3) and copepod (1,170 to 7,190/m^3) densities were at or above the level at which feeding Atlantic mackerel larvae saturate. However, the relationship between the incidence of predation on fish and the density of fish larvae was adequately described by an Ivlev equation. Limitation began at prey densities <0.1 fish larva of suitable prey size per m^3. This threshold was only slightly less than the mean density of fish larvae of suitable prey size (0.14 larva/m^3), and predation on fish appeared limited in about 40% of our collections. Alternatively, Atlantic mackerel larvae preying on fish larvae appeared swamped by their prey in approximately 60% of the collections. Thus, the contracted production of large numbers of larvae in species such as yellowtail flounder and silver hake may reduce total cumulative predation by Atlantic mackerel larvae. Frank and Leggett (1982) suggested that the synchronized emergence of beach-spawned capelin larvae during onshore wind events in eastern Newfoundland resulted in the saturation of their predators and a reduction of percent predation mortality.

Effect of alternative prey on cannibalism and piscivory by Atlantic mackerel larvae

Controlled studies have invariably reported that the presence of alternative prey provides fish larvae with some protection from larval, juvenile, or small-bodied adult fish predators. In the laboratory, the rate of cannibalism on larvae by juvenile Cape anchovy, *Engraulis capensis*, decreased in the presence of alternative copepod prey (Brownell, 1985). Bay anchovy juveniles preferred newly-hatched (2-d-old) sea bream, *Archosargus rhomboidalis*, but shifted to copepods when the density of the latter increased (Dowd, 1986). The presence of alternative copepod prey strongly protected larval Atlantic mackerel (Kean-Howie et al., 1988) and Atlantic cod (Gotceitas and Brown, 1993) from predation by the three-spine stickleback, *Gasterosteus aculeatus*. The addition of *Daphnia magna* reduced by five to tenfold the predation rate of juvenile bluegill, *Lepomis macrochirus*, on larval white perch, *Morone americana* (Margulies, 1990).

In the present study, we found some evidence that the presence of alternative prey reduced the predation by Atlantic mackerel larvae on fish larvae (Fig. 8). The daily predation rate on fish larvae of suitable prey size (assuming a digestion time of 24 h) declined with increasing density of copepod nauplii (the only other prey, along with fish larvae, selected for by Atlantic mackerel larvae), but not with an increasing density of copepods. The evidence for a reduction of predation was stronger when the actual consumption of alternative prey rather than their density was considered (Fig. 8). On average, the daily predation rate on fish larvae of suitable prey size was reduced from 47% to 12%/d when the average number of copepod prey in the gut of Atlantic mack-

erel larvae increased from 0 to >10 prey. Given that copepods were not selected for, it appears that the time spent manipulating them or the satiation resulting from their ingestion, rather than a switch in prey preference, interfered with the predation by Atlantic mackerel on newly hatched fish larvae.

The noncompensatory nature of cannibalism and piscivory by Atlantic mackerel larvae

Cannibalism and interspecific predation have often been proposed as mechanisms for the density-dependent regulation of marine fish populations (Ricker, 1954; Rothschild, 1986). Because the probability of encounter between Atlantic mackerel larvae should increase with their density, Grave (1981) suggested that cannibalism could be a simple mechanism for the density-dependent (i.e. compensatory) regulation of year-class strength in this species. For compensatory mortality to occur, an increasing fraction of the prey population must be removed per unit of time as the abundance of prey increases. In the present study, the capacity of mackerel larvae 5–14 mm long to prey on conspecifics and other fish larvae increased initially (but at a decreasing rate) and then saturated quickly as prey density increased (Fig. 7). Our results suggest a type-II functional response (Holling, 1959) in which mortality is actually depensatory, a decreasing fraction of the prey population being removed per unit time as prey density increases. This would be the case when mackerel larvae prey on other species of fish larvae. In the case of cannibalism, percent mortality is expected to remain constant (i.e. density-independent) with increasing density of Atlantic mackerel larvae because both prey and predators increase in number.

As predation on other fish larvae appears depensatory and cannibalism seems density-independent, we conclude that piscivory by Atlantic mackerel larvae 3–14 mm long does not contribute to the density-dependent regulation of population size. In the laboratory, cannibalism by Pacific mackerel ceased when schooling developed at the time of metamorphosis (approximately 15.2 mm SL) (Hunter and Kimbrell, 1980). In St. Georges Bay, the longest Atlantic mackerel cannibal observed was 15.2 mm (Ware and Lambert, 1985), but Grave (1981) reported intense cannibalism in early juveniles 13–19 mm SL in the North Sea. Whether piscivory by Atlantic mackerel >14 mm SL is compensatory remains to be determined.

Potential impact of cannibalism and piscivory by Atlantic mackerel larvae on recruitment

While predation on conspecifics and other species of fish larvae by Atlantic mackerel larvae <14 mm is not compensatory, the resulting mortality may nevertheless have some important impact on year-class strength. The latitudinal and vertical distributions of Atlantic mackerel, yellowtail flounder, and silver hake larvae generally coincided on Sable Island Bank, and predation or cannibalism by mackerel larvae could be of significance during the early life of these species. As mentioned earlier, the actual mortality rate attributable to predation by Atlantic mackerel larvae cannot be determined without an estimate of the transit time of fish larvae in the gut. In the laboratory, half the gut content of Pacific mackerel larvae fed *Brachionus plicatilis* was evacuated in 2 h (Hunter and Kimbrell, 1980). In the North Sea, digestion time (from food intake to complete defecation of the last food remains) for Atlantic mackerel larvae 8–14 mm, feeding on copepods, cladocerans, and conspecifics was 8–10 h (Grave, 1981).

In the present study, there were several indications that the digestion of fish larvae by Atlantic mackerel larvae was a relatively slow process. First, a single fish larva was found in the gut of mackerel larvae in 97% of the cases. Second, the frequency of larval fish prey in the gut increased progressively during the day (Fig. 4), an unlikely result if digestion and evacuation were rapid. Third, the proportion of fish larvae in the fore- and midgut of mackerel larvae remained high during the day, suggesting a slow transit time due to the large size of the prey (Fig. 5). Finally, the high frequency of partly or well-digested fish larvae (>90%) in contrast to slightly digested material, also suggested that fish larvae remained for a long time in the gut. All our observations are consistent with a continuous search for fish larvae, saturation of the digestive tractus upon the capture of a larva, slow digestion completed during the night, and evacuation in the early morning. Thus, although the time between capture and complete assimilation of a fish larva could be faster than we estimate, our results suggest a digestion time of 24 h.

The impact of predation by Atlantic mackerel larvae was limited primarily to newly hatched fish larvae. Assuming a conservative 24 h for the time between capture and evacuation, the percent mortality rate of fish larvae of suitable prey size attributable to predation by Atlantic mackerel larvae ranged from 7% to 57%/d (average of 31%/d). A value of 8 h for digestion time (Grave, 1981) would triple these estimates. Recent studies have often reported high mortality rates for the period just before and after yolk resorption when the swimming abilities of the fish are still poorly developed: 80%/d in jack mackerel, *Trachurus symmetricus* (Hewitt et al., 1985), 56% and 60%/d in capelin (Fortier and Leggett, 1985; Taggart and Leggett, 1987). For Atlantic mackerel,

Kendall and Gordon (1981) calculated an average mortality rate of 35%/d (SD=20%/d) for larvae <13 mm, whereas Ware and Lambert (1985) reported a rate of 42%/d for larvae <8 mm. Thus, according to our conservative estimate of digestion time, predation by Atlantic mackerel larvae (average 31%/d) would represent a sizable fraction (>38%) of the total mortality typically experienced by newly hatched larvae in the sea. This is consistent with an estimate of 41% for the fraction of the total mortality of newly hatched bay anchovy that could be attributed to predation by medusae (Purcell et al., 1994). According to our highest estimate (average 93%/d), predation by Atlantic mackerel larvae could wipe out populations of newly hatched co-occurring species in a few days, and all the mortality of newly hatched Atlantic mackerel could be attributed to cannibalism.

Atlantic mackerel larvae can dominate the larval fish assemblage over large areas in spring and early summer. For example, the species represented from 62.2% to 76.9% of the ichthyoplankton in the neritic, transitional, and oceanic zones of the Celtic Sea in the spring of 1980 (Horstman and Fives, 1994). We conclude that, in these areas, predation by Atlantic mackerel larvae could represent a significant survival bottleneck for co-occurring species in the days after hatching.

Acknowledgments

Funding for this research was provided by OPEN (Ocean Production Enhancement Network), one of the 15 networks of Centres of Excellence supported by the Government of Canada through the Natural Sciences and Engineering Research Council of Canada (NSERC). Additional grants from NSERC and Employment and Immigration Canada to L. Fortier were instrumental in completing laboratory analyses. The field work could not have been conducted without the assistance of our colleagues from McGill and Dalhousie Universities. Special thanks are given to L. Natanson for her contribution to this study and T. Miller for videotape measurements of unpreserved larvae. G. Bergeron, G. Chaumillon, L. Michaud, L. Mousseau, A. Potvin, M.-A. Rémillard, M. Simard, and C. Quinonez-Velazquez assisted in the field or the laboratory, or both.

Literature cited

Anderson, J. T.
1988. A review of size dependent survival during pre-recruit stages of fish in relation to recruitment. J. Northwest Atl. Fish. Sci. 8:55–66.

Bailey, K. M., and E. D. Houde.
1989. Predation on eggs and larvae of marine fishes and the recruitment problem. Adv. Mar. Biol. 26:1–83.

Berrien, P. L., N. A. Naplin, and M. R. Pennington.
1981. Atlantic mackerel, *Scomber scombrus*, egg production and spawning population estimates for 1977 in the Gulf of Maine, Georges Bank, and Middle Atlantic Bight. Rapp. P.-V. Reun. Cons. Int. Explor. Mer 178: 279–288.

Brownell, C. L.
1985. Laboratory analysis of cannibalism by larvae of the Cape anchovy *Engraulis capensis*. Trans. Am. Fish. Soc. 114:512–518.

Chesson, J.
1978. Measuring preference in selective predation. Ecology 59:211–215.

Cohen, R. E., and R. G. Lough.
1981. Length-weight relationships for several copepods dominant in the Georges Bank-Gulf of Maine area. J. Northwest Atl. Fish. Sci. 2:47–52.

D'Amours, D., J. G. Landry, and T. C. Lambert.
1990. Growth of juvenile (0-group) Atlantic mackerel (*Scomber scombrus*) in the Gulf of St. Lawrence. Can. J. Fish. Aquat. Sci. 47:2212–2218.

Dowd, C. E.
1986. Predator-prey interactions between juvenile bay anchovy (*Anchoa mitchilli*) and larvae of sea bream (*Archosargus rhomboidalis*). Ph.D. diss., Univ. Miami, Coral Gables, FL, 134 p.

Ellertsen, B., P. Fossum, P. Solemdal, and S. Sundby.
1989. Relation between temperature and survival of eggs and first-feeding larvae of northeast Arctic cod (*Gadus morhua* L.). Rapp. P.-V. Reun. Cons. Int. Explor. Mer 191:209–219.

Fahay, M. P.
1983. Guide to the early stages of marine fishes occurring in the Western North Atlantic Ocean, Cape Hatteras to the southern Scotian Shelf. J. Northwest Atl. Fish. Sci. 4:1–423.

Finucane, J. H., C. B. Grimes, and S. P. Naughton.
1990. Diets of young king and Spanish mackerels off the Southeast United States. Northeast Gulf Sci. 11:145–153.

Fortier, L., and W. C. Leggett.
1985. A drift study of larval fish survival. Mar. Ecol. Prog. Ser. 25:245–257.

Fortier, L., and R. P. Harris.
1989. Optimal foraging and density-dependent competition in marine fish larvae. Mar. Ecol. Prog. Ser. 51:19–33.

Fortier, L., D. Ponton, and M. Gilbert.
1995. The match/mismatch hypothesis and the feeding success of fish larvae in ice-covered Hudson Bay. Mar. Ecol. Prog. Ser. 120:11–27.

Fortier, L., M. Gilbert, D. Ponton, R. G. Ingram, B. Robineau, B., and L. Legendre.
In press. Impact of freshwater on a subarctic coastal ecosystem under seasonal sea ice (southeastern Hudson Bay, Canada). III: Feeding success of marine fish larvae. J. Mar. Syst.

Fossum, P.
1988. A tentative method to estimate mortality in the egg and early fish larval stages, with special reference to cod (*Gadus morhua* L.). Fiskeridir. Skr. Ser. Havunders. 18:329–349.

Frank, K. T., and W. C. Leggett.
1982. Coastal water mass replacement: its effect on zooplankton dynamics and the predator-prey complex associated with larval capelin (*Mallotus villosus*). Can. J. Fish. Aquat. Sci. 39:991–1003.

Gotceitas, V., and J. A. Brown.
1993. Risk of predation to fish larvae in the presence of alternative prey: effects of prey size and number. Mar. Ecol. Prog. Ser. 98:215–222.

Grave, H.
1981. Food and feeding of mackerel larvae and early juveniles in the North Sea. Rapp. P.-V. Reun. Cons. Int. Explor. Mer 178:454–459.

Heath, M. R.
1992. Field investigations of the early life stages of marine fish. Adv. Mar. Biol. 28:1–174.

Hewitt, R. P., G. H. Theilacker, and N. C.-H. Lo.
1985. Causes of mortality in young jack mackerel. Mar. Ecol. Prog. Ser. 26:1–10.

Holling, C. S.
1959. The components of predation as revealed by a study of small-mammals predation of the European pine sawfly. Can. Entomol. 91:293–320.

Horstman, K. R., and J. M. Fives.
1994. Ichthyoplankton distribution and abundance in the Celtic Sea. ICES. J. Mar. Sci. 51:447–460.

Hunter, J. R.
1984. Inferences regarding predation on the early life stages of cod and other fishes. *In* E. Dalh, D. S. Danielssen, E. Moksness, and P. Solemdal (eds.), The propagation of Cod *Gadus morhua* L. Flodevigen Rapportser 1:533–562.

Hunter, J. R., and C. A. Kimbrell.
1980. Early life history of Pacific mackerel, *Scomber japonicus.* Fish. Bull. 78:89–101.

Incze, L. S., and D. E. Campbell.
1989. Estimation of ichthyoplankton (*Theragra chalcogramma*) mortality rates from a patch study: FOCI 1986. Bigelow Laboratory for Sciences, Tech. Rep. 72, 10 + XXXI p.

Ivlev, V. S.
1961. Experimental ecology of the feeding of fishes. Yale Univ. Press, New Haven, CT, 302 p.

Jenkins, G. P., N. E. Milward, and R. F. Hartwick.
1984. Food of larvae of Spanish mackerels, genus *Scomberomorus* (Teleostei: Scombridae), in shelf waters of the Great Barrier Reef. Aust. J. Mar. Freshwater Res. 35: 477–482.

Juanes, F., and D. O. Conover.
1994. Piscivory and prey size selection in young-of-the-year bluefish: predator preference or size-dependent capture success? Mar. Ecol. Prog. Ser. 114:59–59.

Kean-Howie, J. C., S. Pearre Jr., and L. M. Dickie.
1988. Experimental predation by sticklebacks on larval mackerel and protection of fish larvae by zooplankton alternative prey. J. Exp. Mar. Biol. Ecol. 124:239–259.

Kendall, A. W., Jr., and D. Gordon.
1981. Growth rate of Atlantic mackerel (*Scomber scombrus*) larvae in the Middle Atlantic Bight. Rapp. P.-V. Reun. Cons. Int. Explor. Mer 178:337–341.

Leak, J. C., and E. D. Houde.
1987. Cohort growth and survival of bay anchovy *Anchoa mitchilli* larvae in Biscayne Bay, Florida. Mar. Ecol. Prog. Ser. 37:109–122.

Margulies, D.
1990. Vulnerability of larval white perch, *Morone americana*, to fish predation. Env. Biol. Fish. 27:187–200.

Øiestad, V.
1985. Predation on fish larvae as a regulatory force, illustrated in mesocosm studies with large groups of larvae. NAFO Sci. Counc. Studies 8:25–32.

Pearre, S. Jr.
1982. Estimating prey preference by predators: uses of various indices, and proposal of another based on χ^2. Can. J. Fish. Aquat. Sci. 39:914–923.

Peterson, W. T., and S. J. Ausubel.
1984. Diets and selective feeding by larvae of Atlantic mackerel *Scomber scombrus* on zooplankton. Mar. Ecol. Prog. Ser. 17:65–75.

Purcell, J. E., D. A. Nemazie, S. E. Dorsey, E. D. Houde, and J. C. Gamble.
1994. Predation mortality of bay anchovy *Anchoa mitchilli* eggs and larvae due to scyphomedusae and ctenophores in Chesapeake Bay. Mar. Ecol. Prog. Ser. 114:47–58.

Ricker, W. E.
1954. Stock and recruitment. J. Fish. Res. Board Can. 11: 559–623.

Rothschild, B. J.
1986. Dynamics of marine fish populations. Harvard Univ. Press, Cambridge, MA, 277 p.

Sette, O. E.
1943. Biology of the Atlantic mackerel (*Scomber scombrus*) of North America. Part I: Early life history, including growth, drift, and mortality of the egg and larval populations. Fish. Bull. 50:147–237.
1950. Biology of the Atlantic mackerel (*Scomber scombrus*) of North America. Part II: Migrations and habits. Fish. Bull. 51:247–358

Sundby, S., and P. Fossum.
1990. Feeding conditions of Arcto-norwegian cod larvae compared with the Rothschild-Osborn theory on small-scale turbulence and plankton contact rates. J. Plankton Res. 12:1153–1162.

Taggart, C. T., and W. C. Leggett.
1987. Short-term mortality in post-emergent larval capelin *Mallotus villosus*. I: Analysis of multiple in situ estimates. Mar. Ecol. Prog. Ser. 41:205–217

Ware, D. W., and T. C. Lambert.
1985. Early life history of Atlantic mackerel (*Scomber scombrus*) in the southern Gulf of St. Lawrence. Can. J. Fish. Aquat. Sci. 42:577–592

Young, J. W., and T. L. O. Davis.
1990. Feeding ecology of larvae of southern bluefin, albacore and skipjack tunas (Pisces: Scombridae) in the eastern Indian Ocean. Mar. Ecol. Prog. Ser. 61:17–29.

Catchability coefficient for rockfish estimated from trawl and submersible surveys

Kenneth J. Krieger
Michael F. Sigler
Auke Bay Laboratory, Alaska Fisheries Science Center
National Marine Fisheries Service, NOAA
11305 Glacier Hwy., Juneau, Alaska 99801–8626

Abstract.—A bottom-trawl catchability coefficient was estimated for rockfish by comparing trawl catch rates to densities estimated from a manned submersible. A total of 16 comparisons were completed in 1989 and 1991 at depths of 180–283 m. Pacific ocean perch, *Sebastes alutus*, was the target species and accounted for 72% of the rockfish caught in the trawl. The seafloor area sampled by the trawl was calculated from the distance between the wingtips of the net and the distance the net traveled across the seafloor. The seafloor area sampled from the submersible was calculated from the distance the submersible traveled and the lateral range of visibility. A larger volume of water was sampled from the submersible because counts of rockfish included fish to 7 m above the seafloor, whereas the vertical opening of the trawl was 1.8 m; approximately 50% of the rockfish observed from the submersible were >1.8 m above the seafloor. Even though a larger volume of water was sampled from the submersible, catchability coefficients of 0.97 and 1.27 were estimated for minimum and maximum detection probabilities of rockfish from the submersible. Apparently, rockfish dove or were herded horizontally into the opening of the net. Density estimates of rockfish and other groundfish species are feasible from a submersible, and these estimates can be used to determine bottom-trawl catchability coefficients.

Manuscript accepted 7 December 1995.
Fishery Bulletin 94:282–288 (1996).

Bottom-trawl surveys are used to estimate absolute abundance of most groundfish species in Alaska. The method is founded on the basic assumption that catch per unit of effort (CPUE) is a function of stock density. CPUE is converted to biomass from the area swept by the trawl and the sampling efficiency of the gear (catchability coefficient) (Alverson and Pereyra, 1969). The basic equation relating population size to CPUE is

$$P_{ij} = C_{ij} / qf_{ij},$$

where i = time period;
j = location or area;
P = exploitable population size in weight;
C = catch in weight;
q = catchability coefficient; and
f = fishing effort (Alverson and Pereyra, 1969).

Because there is no simple method of measuring catch efficiency, a catchability coefficient of 1.0 is used to convert CPUE data to biomass in bottom-trawl surveys (assuming a 100% catch efficiency across the horizontal spread of the net [wingtip to wingtip]). However, if fish are distributed above the headrope, are buried in the substrate, swim out of the path of the trawl, or escape through the net, the catchability coefficient is <1.0 and abundance is underestimated. Conversely, if fish are herded into the trawl by the bridles and trawl doors and do not escape above or under the net, the catchability coefficient is >1.0 and abundance is overestimated. Catchability coefficients depend on biological factors such as sensory capabilities as well as behavioral responses of the target species, and environmental factors such as light, temperature, and bottom type (see Gunderson, 1993, for an overview). A wide range of catchability coefficients were estimated in studies that monitored efficiency of bottom trawls: Harden-Jones et al. (1977) attached acoustic tags to flatfish and monitored their behavior in response to trawl gear; 61% of the fish in the path of the net were captured. Main and Sangster (1981) observed the catch process of several groundfish species from a towed underwater vehicle; each species responded differently with regard to net avoidance, escapement, and herding by the bridles and doors. Korotkov[1] observed groundfish behavior in front of a bottom trawl from an underwater towed apparatus; catchability coefficients of 0.1 to 0.4 were estimated, depending on trawl rigging and trawl orientation to the bottom. These studies relied on species that could be tagged or on species located at shallow depths where ambient

[1] Korotkov, V. K. 1984. Fish behaviour in a catching zone and influence of bottom trawl rig elements on selectivity. Int. Counc. Explor. Sea, Council Meeting 1984, paper/B:15, 14 p.

light was available for observations. In this study catchability coefficients are estimated for rockfish that inhabit deep depths where ambient light is minimal and that cannot be tagged because of gas bladder expansion when sampled. Catchability coefficients are estimated by comparing trawl catch rates with counts from a manned submersible.

Pacific ocean perch, *Sebastes alutus*, was the target species of this study. Biomass estimates of Pacific ocean perch in the Gulf of Alaska, based on bottom-trawl surveys conducted triennially, were 214,827, 138,003, and 460,755 metric tons for 1987, 1990, and 1993 (Heifetz et al.[2]). These extreme changes in biomass are unlikely, given the slow growth and low mortality rates of *Sebastes* spp. (Heifetz et al.[2]). To improve Pacific ocean perch biomass estimates from bottom-trawl surveys, manned submersibles and bottom trawls have been used since 1988 to study their substrate association and spatial distribution, and the efficiency of bottom trawls for sampling them. Most Pacific ocean perch observed from a submersible were concentrated on smooth substrates in groups of 2–200 fish (Krieger, 1993). Counts of Pacific ocean perch from a manned submersible in 1989 were compared with catch rates from trawl hauls, and a catchability coefficient of 2.1 (SE=0.4) was estimated for the distance between the wingtips of the net. This catchability coefficient was considered preliminary for three reasons: 1) only nine submersible-trawl comparisons were made; 2) no fish were assumed captured while the trawl was retrieved; and 3) all fish were assumed counted within the viewing range from the submersible (Krieger, 1993). The catchability coefficient estimated in this study is based on an increased number of submersible versus trawl comparisons and on improved density estimates from trawl catch rates and submersible counts.

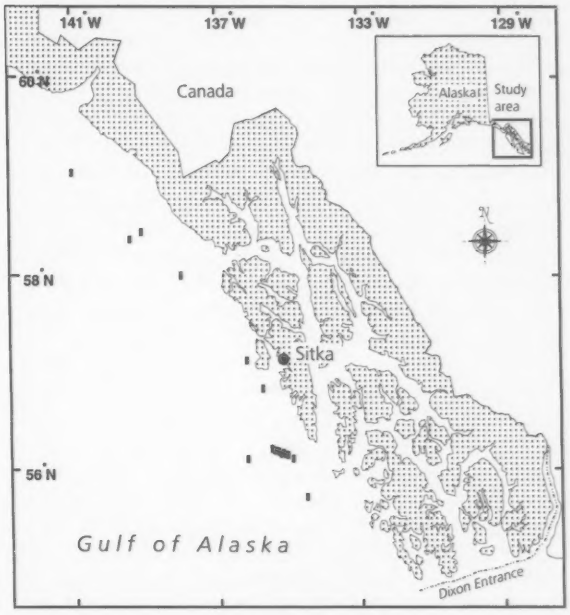

Figure 1

Locations of submersible dive sites that were sampled with bottom trawls in the eastern Gulf of Alaska, 1989 and 1991.

Materials and methods

Sampling of submersible counts and trawl catch rates for Pacific ocean perch were conducted in August 1989 and 1991 on the outer continental shelf in the eastern Gulf of Alaska (Fig. 1). The sampling strategy was to count rockfish from the submersible along four parallel transects, and then intersect the four transects with a bottom trawl. Each transect was determined by following a compass heading for 15 min, and there were 5 min of travel between transects. Trawl hauls were considered successful only if the gear was retrieved intact (no tears in the net or broken cables) and the trawl intersected at least three of the four submersible transects. Submersible dives and bottom trawling were completed during daylight at 180–283 m depths. The time between dives and trawls was <4 h for 13 of the 16 comparisons. Substrates consisted of pebble or sand, interspersed with cobble <0.5 m in diameter and boulders 0.5–5.0 m in diameter.

Submersible

We used the two-man submersible *Delta* chartered by the National Oceanic and Atmospheric Administration, National Undersea Research Center. This battery-powered submersible is 4.7 m long, dives to 365 m, and travels 2–6 km/h for 2–4 h. It is equipped with halogen lights and internal and external video cameras. In addition, it has a magnetic compass, directional gyro compass, underwater telephone, and transponder that allow tracking of the submersible from a surface vessel. The pilot maintained the submersible within 0.5 m of the bottom, while a scien-

[2] Heifetz, J., D. M. Clausen, and J. N. Ianelli. 1994. Slope rockfish. *In* Plan Team for the Groundfish Fisheries of the Gulf of Alaska (eds.), Stock assessment and fishery evaluation report for the groundfish resources of the Gulf of Alaska as projected for 1995, Sect. 5. North Pac. Fish. Manage. Counc., P.O. Box 103136, Anchorage AK 99510.

tist counted rockfish through a starboard porthole 0.5 m above the bottom of the submersible. Rockfish counts and behavior were audio- and video-recorded for subsequent analysis. Rockfish densities were derived from the number of fish counted and the seafloor area searched. This area was calculated from the distance the submersible traveled and the estimated lateral range of visibility from the starboard porthole. The observer estimated that lateral visibility ranged from 3 to 7 m, depending on water clarity. The ability of the observer to estimate distance was tested by three methods: 1) a length of pipe marked at meter intervals was laid on the seafloor and observed on two dives; 2) a hand-held sonar gun provided distance readouts to rock formations located at the maximum visibility range on six dives; and 3) the submersible's sonar provided distance readouts when the seafloor became visible during descents and when the seafloor disappeared from view during ascents. Observer estimates of distance were consistently within 1 m of actual distances. Accuracy to within 1 m was possible because constant illumination was provided entirely by the submersible lights, and water clarity was consistent at each site. The pilot assisted in counting fish >4 m above the seafloor from a panoramic view 2 m above the scientist. The pilot could see at least 10 m above the seafloor.

Identification of Pacific ocean perch from the submersible was not always possible because they look similar to three other red rockfish species: redstripe rockfish, *S. proriger*; sharpchin rockfish, *S. zacentrus*; and harlequin rockfish, *S. variegatus*. Therefore, rockfish density estimates from submersible counts and from trawling include these three species in addition to Pacific ocean perch. Most rockfish observed from the submersible, however, were identified as Pacific ocean perch by their symphyseal knob and body shape. Trawl sampling confirmed their dominance: 72% of the rockfish caught were Pacific ocean perch.

A detection probability (DP) from the submersible was estimated by measuring angles to targets with a clinometer. Clinometer readings were collected from a fixed height above the seafloor to red sea stars, *Luidiaster* spp., on the seafloor; sea stars were selected as targets because their color was similar to red rockfish and they were abundant, stationary targets. The DP was assumed to equal 1.0 near the submersible and to decrease to zero at some distance from the submersible. The DP was computed as the ratio of the observed and expected density of targets. The observed population density was computed as

$$P_i = N_i / D_i,$$

where N_i is the observed count in angle interval i, and D_i is the distance along the seafloor corresponding to angle interval i. The expected density was computed as the average observed density within the full-detection range (the range where the observed density did not decrease).

Bottom trawling

Trawl gear consisted of a 400-mesh Eastern otter trawl equipped with 55-m bridles between the net and 1.5 × 2.1-m doors weighing 386 kg each. The average distance between the wingtips (15.8 m) and the trawl doors (45.0 m) was determined during four trawl hauls by using mensuration gear. Krieger (1993) used a wingtip spread of 14 m, based on previous net measurements of the 400 Eastern trawl, to estimate the preliminary catchability coefficent (NMFS, 1993). A net height (foot-rope to head-rope) of 1.8 m is based on previous mensuration gear measurements of 1.4–1.8 m (NMFS, 1993).

Trawl catches were processed for total number and weight by species. Rockfish density estimates were derived from the number of rockfish captured and the seafloor area swept by the net. The seafloor area swept was the distance trawled multiplied by the horizontal spread of the net. Trawl distances (0.93–1.74 km/haul) and trawl speeds (5.0–6.5 km/h) were calculated from position fixes with a global positioning system (GPS). Trawl periods ranged from 10 to 18 min, depending on trawl speed and trawl distance needed to intersect the submersible transects. At the completion of the 10–18 min trawl period, vessel speed was reduced while the trawl was retrieved. To determine the sampling capabilities of the trawl during retrieval, catch rates from six "standard" trawl hauls were compared with catch rates from seven "retrieval" trawl hauls. A "standard" trawl haul was followed by a "retrieval" trawl haul at randomly selected sites separated by <3 km distance by using the same trawl depths, cable ratios, and vessel speeds as those for trawling at the submersible sites. "Standard" trawl hauls consisted of the net sweeping the seafloor for 10 min at 5.5–6.0 km/h and then being retrieved at reduced vessel speed. "Retrieval" trawl hauls consisted of the net sinking to the seafloor and then being retrieved immediately at reduced vessel speed. A sonar net-sounder was used to determine when the net departed the seafloor. GPS fixes and the rate of cable retrieval were used to determine the speed of the trawl during retrieval.

Data analysis

Rockfish density estimates from submersible counts and trawl catch rates were based on the total sea-

floor area sampled, but were not adjusted for the larger water column sampled from the submersible; submersible personnel surveyed to 10 m above the seafloor, whereas the net sampled to 1.8 m above the seafloor. A catchability coefficient was estimated by comparing the average density from trawl catch rates to the average density from submersible counts. The bootstrap resampling method (Efron, 1982; Efron and Tibshirani, 1986) was used to test the statistical significance of the difference and to estimate a confidence interval for the catchability coefficient. A bootstrap sample was created by sampling 1,000 times with replacement. The statistical significance of the difference (P) between submersible and trawl comparisons was computed by tallying how many of the 1,000 bootstrap replicates were greater than zero; P is for a two-sided test.

Results

Sampling during trawl retrieval

During trawl retrieval, the net remained in contact with the seafloor an additional 7–9 min. The speed of the net along the seafloor during retrieval was 4–5 km/h—a combination of the vessel moving slowly forward and retrieval of the cable. Catch rates for Pacific ocean perch averaged 34.9/1,000 m^2 during "standard" trawling and 29.8/1,000 m^2 during "retrieval" trawling (Table 1) and were not significantly different (2-sided t-test, $P>0.5$). Apparently, the net continued to sample effectively during retrieval; therefore, trawl catch rates included the seafloor area swept during trawl retrieval.

Detection probability from submersible

Observed densities of sea stars began decreasing 3.4 m from the submersible; therefore, the expected density was the average density of targets within the 3.4-m full-detection range. Assuming DP = 1.0 within 3.4 m, we calculated a DP of 0.77 for the entire 5.3-m range of visibility, which implies that about 3/4 of the sea stars were counted within the range of visibility. Sea stars were more difficult to detect than were rockfish because of differences in body shape; the flat bodies of sea stars blended into the seafloor, but the fusiform bodies of rockfish extended above the seafloor. Therefore, the 0.77 DP for sea stars is considered a minimal DP for rockfish and catchability coefficients are calculated for both a 0.77 DP and a 1.0 DP.

Comparison of submersible counts with trawling catch rates

Sixteen dive sites were successfully sampled by bottom trawling (Table 2). The average rockfish densities were 21.7/1,000 m^2 from trawling, and 22.4/1,000 m^2 (DP=0.77) and 17.1/1,000 m^2 (DP=1.0) from submersible counts, resulting in catchability coefficients of 0.97 (95% confidence interval: 0.70–1.32) and 1.27 (95% confidence interval: 0.91–1.73) for the area swept between the trawl wingtips. No significant difference was detected between density estimates from the submersible and trawl for either the 0.77 DP (P=0.95) or the 1.0 DP (P= 0.13).

Discussion

The 0.97 and 1.27 catchability coefficients are considerably less than the 2.1 (SE=0.4) catchability coefficient reported by Krieger (1993), mainly because they include the area sampled during trawl retrieval. The 0.77 DP from the submersible and the increased estimate of net width also contributed to lower estimates of catchability coefficients.

If rockfish did not react to the trawl gear, density estimates from submersible counts would have exceeded those from trawl catch rates because approxi-

Table 1

Number of rockfish caught, distance trawled, and estimated catch rates during standard (10 min + retrieval) and retrieval trawling using a 400 Eastern otter trawl at depths of 180–283 m in the eastern Gulf of Alaska.

	Distance (km)		
Number caught	Trawling (10 min)	Retrieval (7–9 min)	Catch rate (number/1,000 m^2)
2,263	1.10	0.63	82.53
1,267	0.96	0.74	47.02
778	0.93	0.63	31.46
660	1.06	0.65	24.35
416	1.02	0.78	14.58
274	1.15	0.69	9.40
Standard trawling mean = 34.89			
686		0.62	69.81
677		0.74	57.72
304		0.69	27.80
240		0.78	19.41
204		0.63	20.43
131		0.74	11.17
21		0.63	2.10
Retrieval trawling mean = 29.78			

Table 2

Density (number/1,000 m^2) of rockfish estimated from submersible counts and trawl catch rates at 16 sites in the eastern Gulf of Alaska, 1989 and 1991. Submersible densities are for detection probabilities (DP) of 1.0 and 0.77.

	Submersible				Trawl		
			Density (number/1,000 m^2)				
Site	Count	Area (1,000 m^2)	DP=1.0	DP=0.77	Caught	Area (1,000 m^2)	Density (number/1,000 m^2)
1	1,040	12.0	86.7	113.0	2,902	26.3	110.3
2	747	12.3	60.7	79.2	884	26.3	33.6
3	380	13.9	27.3	35.6	1,134	30.2	37.6
4	391	17.3	22.6	29.5	1,419	37.6	37.7
5	230	12.1	19.0	24.8	848	30.2	28.1
6	187	15.3	12.2	15.9	339	30.8	11.0
7	222	16.8	13.2	17.2	1,244	33.4	37.2
8	117	13.7	8.5	11.1	658	35.8	18.4
9	136	12.9	10.5	13.7	426	29.2	14.6
10	79	13.6	5.8	7.6	352	32.9	10.7
11	55	14.4	3.8	5.0	31	34.4	0.9
12	38	13.6	2.8	3.6	158	37.6	4.2
13	16	17.6	0.9	1.2	115	38.3	3.0
14	1	7.1	0.1	0.2	10	33.3	0.3
15	1	5.1	0.2	0.3	6	39.2	0.2
16	0	14.1	0.0	0.0	0	26.3	0.0
Mean			17.1	22.4			21.7

mately 50% of the rockfish were distributed above the 1.8-m height sampled by the net. The similar density estimates imply that rockfish dove to within 1.8 m of the seafloor or were herded horizontally into the net opening by the bridles and doors. Herding of fish by trawl doors and bridles has been documented for several semidemersal species by using acoustic tags (Harden-Jones et al., 1977), direct observations from a towed submersible (Main and Sangster, 1981), and underwater video (Glass and Wardle, 1989). For Pacific ocean perch, herding and diving in response to trawl gear was indicated in studies using sonar and variable bridle lengths. Sonar recordings of Pacific ocean perch indicated that the fish were diving as a fishing vessel passed over them (Kieser et al., 1992) and were diving in response to trawl gear (Nunnallee[3]). Herding was indicated in two studies where increased bridle lengths resulted in increased catch rates of Pacific ocean perch: catch rates increased 2.79- and 3.24-fold when 36.6-m bridles were increased 27.4 m and 54.9 m (Harling and Davenport, 1977), and catch rates were about 2.5 times higher for a net with 33% longer bridles, even though its vertical and horizontal opening was smaller (Wilkins and Weinberg, 1987).

This study demonstrates that estimates of fish density are feasible from a submersible and that these estimates can be used to determine bottom-trawl catchability coefficients. Rockfish were ideal for counting within the illuminated area because they were brightly colored, solitary or loosely grouped, not hidden by rugged habitat, usually motionless, and generally distributed within 7 m of the seafloor (Krieger, 1993). Most rockfish remained oriented into the current while the submersible passed, indicating minimal response to the submersible. The only movements observed were those of individual fish moving out of the direct path of the submersible and those of a few groups moving toward the submersible. Counts of fish within these groups were not hindered, because the fish swam slowly and maintained their spacing and orientation. The pilot observed similar behavior on all sides of the submersible. In addition to rockfish, density estimates appear feasible for numerous invertebrate species and groundfish species, including shortspine thornyhead, *Sebastolobus alascanus*, and several flatfish species.

The value of comparing in situ observations of groundfish with trawl catches has been documented

[3] Nunnallee, E. P. 1991. An investigation of the avoidance reactions of Pacific whiting (*Merluccius productus*) to demersal and midwater trawl gear. ICES Council Meeting 1991, paper/B:5, Sess. U., Fish Capture Committee, 17 p.

in other studies. Uzman et al. (1977) compared submersible counts with trawl catches of fish and invertebrates and concluded that continuous visual assessment of the benthos provides the best approximation of species abundance and diversity. Adams et al. (1995) compared remotely operated vehicle counts with trawl catches of groundfish and concluded that for strongly bottom-associated groundfish, ROV abundance estimates were significantly higher and were less variable than bottom-trawl abundance estimates.

Application to stock assessment

The catchability coefficient estimated in this study with a 400 Eastern trawl may not be directly applicable to Alaska trawl surveys that use a Nor'eastern trawl. The main differences between the Nor'eastern trawl and 400 Eastern trawl are net height and footrope design: the Nor'eastern net height is 6–10 m and roller gear (36–cm rubber bobbins separated by 10-cm rubber disks) is attached to the footrope, whereas the 400 Eastern has a maximum 1.8-m net height with no roller gear on the footrope. The 15–17 m wingtip spread of the Nor'eastern is similar to the 15.8 m average spread of the 400 Eastern trawl, whereas the 47–57 m door spread of the Nor'eastern is wider than the average 45-m door spread of the 400 Eastern. The Nor'eastern trawl is assumed to be more efficient for capturing rockfish because of its higher vertical opening. Roller gear attached to the Nor'eastern trawl may either increase or decrease catch efficiency of rockfish. A repeat of this study using the Nor'eastern trawl is recommended for determining a catchability coefficient for Alaska trawl survey data.

Accurate indexing of Pacific ocean perch seems possible from bottom-trawl surveys because of their substrate preference and susceptibility to bottom-trawl gear. Pacific ocean perch concentrate on trawlable substrates (Krieger, 1993) and were effectively sampled in this study. Assuming that fish occupy the water column above the opening of the trawl and inhabit untrawlable areas, Balsiger et al. (1985) reported that CPUE data from bottom-trawl surveys probably underestimate Pacific ocean perch biomass. Submersible studies, however, indicate Pacific ocean perch biomass may be overestimated from bottom-trawl surveys for two reasons: 1) the catchability coefficient of the survey trawl may exceed 1.0 for the distance between the wingtips; and 2) only trawlable substrates where Pacific ocean perch are concentrated are sampled during surveys, but CPUE from trawlable substrates is applied to untrawlable substrates.

Acknowledgments

We thank the crew of the submersible *Delta*, for safe and successful dives, and the crew and scientists aboard the NOAA ship *John N. Cobb* for their detailed sampling that allowed comparisons of trawl catches with submersible observations. We also thank John Karinen for participating in the submersible diving, and Jon Heifetz, Scott Johnson, Steve Ignell, Richard Carlson, and Sara Kraft for their thorough reviews of this manuscript. The *Delta* was chartered by NOAA's National Undersea Reserch Center.

Literature cited

Adams, P. B., J. L. Butler, C. H. Baxter, T. E. Laidig, K. A. Dahlin, and W. W. Wakefield.
1995. Population estimates of Pacific coast groundfishes from video transects and swept-area trawls. Fish. Bull. 93:446–455.

Alverson, D. L., and W. T. Pereyra.
1969. Demersal fish explorations in the northeastern Pacific Ocean—an evaluation of exploratory fishing methods and analytical approaches to stock size and yield forecasts. J. Fish. Res. Board Can. 26:1985–2001.

Balsiger, J. W., D. H. Ito, D. K. Kimura, D. A. Somerton, and J. M. Terry.
1985. Biological and economic assessment of Pacific ocean perch (*Sebastes alutus*) in waters off Alaska. U.S. Dep. Commer., NOAA Tech. Memo. NMFS F/NWC-72, 210 p.

Efron, B.
1982. The jackknife, the bootstrap and other resampling plans. Society for Industrial and Applied Mathematics, Philadelphia, PA, 92 p.

Efron, B., and R. Tibshirani.
1986. Bootstrap methods for standard errors, confidence intervals, and other measures of statistical accuracy. Stat. Sci. 1:54–77

Glass, C. W., and C. S. Wardle.
1989. Comparison of the reactions of fish to a trawl gear, at high and low light intensities. Fish. Res. 7:249–266.

Gunderson, D. R.
1993. Surveys of fisheries resources. John Wiley & Sons, New York, NY, 221 p.

Harden-Jones, F. R., A. R. Margetts, W. M. Greer, and G. P. Arnold.
1977. The efficiency of the Granton otter trawl determined by sector-scanning sonar and acoustic transponding tags. Rapp. P.-V. Reun. Cons. Int. Explor. Mer 170:45–51.

Harling, W. R., and D. Davenport.
1977. *G. B. Reed* groundfish cruise no. 77-3, August 22 to September 8, 1977. Can. Fish. Mar. Serv. Data Rep. 42, 36 p.

Kieser, R., B. M. Leaman, P. K. Withler, and R. D. Stanley.
1992. *W. E. Ricker* and *Eastward Ho* cruise to study the effect of trawling on rockfish behaviour, October 15–27, 1990. Can. Manuscr. Rep. Fish. Aquat. Sci. 2161, 84 p.

Krieger, K. J.
1993. Distribution and abundance of rockfish determined from a submersible and by bottom trawling. Fish. Bull. 91:87–96.

Main, J., and G. I. Sangster.
1981. A study of the fish capture process in a bottom trawl

by direct observations from a towed underwater vehicle. Scott. Fish. Res. Rep. 23, 23 p.

NMFS (National Marine Fisheries Service).

1993. ADP Code Book. U.S. Dep. Commer., Resour. Assess. and Conserv. Eng. Div., NMFS, Alaska Fish. Sci. Cent., Seattle, 82 p.

Uzmann, J. R., R. A. Cooper, R. B. Theroux, and R. L. Wigley.

1977. Synoptic comparison of three sampling techniques for estimating abundance and distribution of selected megafauna: submersible versus camera sled versus otter trawl. Mar. Fish. Rev. 39(11):11–19.

Wilkins, M. E., and K. L. Weinberg.

1987. Results of a bottom trawl survey of Pacific ocean perch off Washington and Oregon during 1985. *In* B. R. Melteff (coordinator), Proceedings of the international rockfish symposium, p. 241–265. Alaska Sea Grant Rep. 87-2, University of Alaska.

Description of pelagic larval and juvenile stripetail rockfish, *Sebastes saxicola* (family Scorpaenidae), with an examination of larval growth

Thomas E. Laidig
Keith M. Sakuma
Tiburon Laboratory, Southwest Fisheries Science Center
National Marine Fisheries Service, NOAA
3150 Paradise Drive, Tiburon, California 94920

Mary M. Nishimoto
Moss Landing Marine Laboratories
P.O. Box 450, Moss Landing, California 95039
Present address: Marine Science Institute
University of California, Santa Barbara
Santa Barbara, California 93106

Abstract.—Pigmentation, morphometrics, head spination, fin development, and meristic characters were described and illustrated for the developmental series of larval and pelagic juvenile (4.7–38.2 mm standard length) stripetail rockfish, *Sebastes saxicola*. Pigment patterns were sufficiently distinct to differentiate larval and juvenile *S. saxicola* from other *Sebastes* species occurring in the study area (central California). Early larvae of *S. saxicola* were identified by the presence of pigment on the postanal ventral midline and the nape and by the lack of pigment on the lower jaw and the pectoral fins. Late larval *S. saxicola* had areas of intense pigment along the dorsal, lateral, and ventral midlines. Juvenile *S. saxicola* were identified by their distinctive bar pattern and meristic characters. Examination of otolith characters indicated that the extrusion check radius of *S. saxicola* differed from that of other *Sebastes* species examined. Otolith characters, used in combination with pigment patterns, readily separated larval *S. saxicola* from other *Sebastes* species. Calculated growth rates for *S. saxicola* were slower than most previously reported growth rates for other *Sebastes* species.

Manuscript accepted 23 October 1995.
Fishery Bulletin 94:289–299 (1996).

Rockfishes (*Sebastes* spp.) are important to the commercial and recreational fisheries of the northeastern Pacific. In 1993, they accounted for approximately 18% of the commercial groundfish catch in weight (PFMC[1]) and 19.4% of all species in the recreational landings off California, Oregon, and Washington (Witzig et al., 1992). Sixty-one species of rockfish are reported from California alone (Eschmeyer et al., 1983). Management of the fishery has been plagued by taxonomic problems. The need to separate adult rockfish landed by the fishery has long been recognized (Phillips, 1964; Chen, 1971). Larvae and juveniles are far more difficult to separate than are adults, but the need to differentiate them is growing with their use as subjects of biomass estimates and recruitment studies (Moser and Butler, 1987; Hunter and Lo, 1993; Ralston et al.[2]). Here we provide means to identify the larvae and juveniles of *S. saxicola*.

Stripetail rockfish, *Sebastes saxicola*, are small (maximum size 39 cm) and occur on soft bottom at depths of 46–421 m (Eschmeyer et al., 1983). This species accounts for less than 1% of the commercial groundfish catch by weight (Pearson[3]), perhaps because of its small size. It is one of the more abundant groundfish species off Santa Cruz, California (Adams et al., 1995), and is generally common in waters be-

[1] PFMC (Pacific Fishery Management Council). 1994. Status of the Pacific coast groundfish fishery through 1994 and recommended acceptable biological catches for 1995. Pacific Fishery Management Council, Portland, OR, 118 p.

[2] Ralston, S., J. R. Bence, M. B. Eldridge, and W. H. Lenarz. 1993. Estimating the spawning biomass of shortbelly rockfish (*Sebastes jordani*) in the region of Pioneer and Ascension Canyons using a larval production method, 32 p. National Marine Fisheries Service, Southwest Fisheries Science Center, 3150 Paradise Drive, Tiburon, CA 94920.

[3] Pearson, D. E. 1994. National Marine Fisheries Service. 3150 Paradise Drive, Tiburon, CA 94920. Personal commun.

tween 100–149 fathoms off the central California coast (Gunderson and Sample, 1980). This study describes the development of *S. saxicola* from pre-extrusion larvae to the pelagic juvenile stage and describes the age and growth of larval *S. saxicola*.

Methods

Specimens of pelagic larval and juvenile *S. saxicola* were obtained from cruises conducted aboard the NOAA RV *David Starr Jordan* and the Moss Landing Marine Laboratories RV *Ed Ricketts*. Specimens were taken with Manta nets (0.505-mm mesh), bongo nets (0.505-mm mesh), a 5-m^2 Methot-Isaacs-Kidd (MIK) trawl (2-mm mesh and a 0.505-mm codend), and a 26 × 26 m midwater trawl (12.7-mm stretched mesh codend liner). Manta nets were used during surveys in January and February 1992, bongo nets in January and February 1992 and January 1994, MIK trawls in March 1992 and 1993, and midwater trawls in May and June 1990–93. Specimens taken with Manta nets, bongo nets, and MIK trawls were preserved in 95% EtOH, whereas specimens from midwater trawls were frozen. Pre-extrusion larvae were obtained from three adult females in February 1994 and preserved in 95% EtOH. All samples were collected off central California between Cypress Point (36°35'N) and Salt Point (38°35'N).

We examined and measured 197 *S. saxicola* larvae and juveniles from 3.3 mm notochord length (NL) to 43.9 mm standard length (SL). Specimens greater than 19.9 mm SL were identified by meristic characters (Chen, 1986; Matarese et al., 1989; Moreland and Reilly, 1991; Laroche[4]); melanophore patterns were recorded. Specimens less than 20 mm SL were initially identified by pigment patterns developed from a size-series based on pre-extrusion pigment patterns and patterns of the smallest positively identifiable individuals with complete meristic characters. Whenever possible, dorsal-, anal-, and pectoral-fin ray counts and the number of gill rakers on the first gill arch were recorded and subsequently used in identifications. Gill-raker counts were taken only on fish larger then 15 mm SL.

We measured snout to anus length, head length, snout length, eye diameter, body depth at the pectoral-fin base, pectoral-fin length, pectoral-fin base depth, and parietal spine length on 28 specimens from 3.3 mm NL to 20.9 mm SL. Terminology for morphometrics followed Richardson and Laroche (1979).

Eighteen specimens from 6.2 mm NL to 20.9 mm SL were stained with Alizarin Red S and examined for head spination. Terminology for head spination followed Richardson and Laroche (1979).

Otoliths were removed from 58 *S. saxicola* larvae (4.2 mm NL to 19.7 mm SL) and aged according to procedures in Laidig et al. (1991). In addition, otoliths from five species (*S. atrovirens*, *S. auriculatus*, *S. maliger*, *S. rastrelliger*, and *S. semicinctus*) and two species complexes (the copper complex [*S. atrovirens*, *S. carnatus*, *S. caurinus*, and *S. chrysomelas*] and the gopher complex [*S. carnatus* and *S. chrysomelas*]) were removed for comparison of otolith characters with *S. saxicola* (Laidig and Ralston, 1995). These five species and two complexes were chosen for similarity in pigment patterns with preflexion *S. saxicola*; *S. rastrelliger* was also selected for its similar pigmentation in postflexion fish. In addition, otoliths were removed and examined from 15 *Sebastes* larvae of unknown species with pigment patterns similar to *S. saxicola*, but with pigment present on the axillary surface of the pectoral fins.

Results

General development

Larvae were extruded at a size of 3.3–5.2 mm NL. Notochord flexion began at approximately 5.8 mm NL and was completed by 8.0 mm SL. The full adult complement of pectoral-fin rays developed during late-stage flexion and early postflexion (16 rays, Table 1). By 7.0 mm NL, anal-fin rays had begun to form and a full adult complement (7 rays, Table 1) was present in 90% of the fish by 8.0 mm SL. The dorsal, pectoral, and pelvic fins began to form around 7.5 mm NL and a full adult complement (dorsal=12 rays, pectoral=16, pelvic=5, Table 1) was present by approximately 9.0 mm SL. Lateral line pores first appeared around 17 mm SL and a complete series was apparent by approximately 38 mm SL. Because we had only a few specimens above 38 mm SL, we were unable to obtain accurate lateral line pore counts.

Morphometrics

Changes in body shape in *S. saxicola* were related to notochord flexion (Table 2). As the larvae began flexion, they became more stout-bodied, as evidenced by the increase in body depth at the pectoral-fin base. During flexion, the pectoral-fin length increased as the full adult complement of fin rays was attained (Table 2). The parietal spine length increased until approximately 10 mm SL when spine growth ap-

[4] Laroche, W. A. 1987. Guide to larval and juvenile rockfishes (*Sebastes*) of North America. Box 216, Enosburg Falls, VT 05450. Unpubl. manuscr., 311 p.

Table 1

Frequency of occurrence of dorsal-, anal-, and pectoral-fin ray counts and gill-raker counts in larval and juvenile stripetail rockfish, *Sebastes saxicola*.

Character	Count	Frequency of occurrence	Percent occurrence
Dorsal-fin rays	11	2	1.4
	12	136	91.8
	13	10	6.8
Anal-fin rays	6	4	2.5
	7	153	95.0
	8	4	2.5
Pectoral-fin rays	15	14	10.4
	16	117	86.6
	17	4	3.0
Gill rakers	28	2	3.1
	29	6	9.2
	30	15	23.1
	31	15	23.1
	32	22	33.8
	33	3	4.6
	34	2	3.1

peared to cease. All other measurements showed a marked increase after flexion was completed (Table 2).

Head spination

Head spines first began to appear during flexion (Table 3). By 9 mm SL, the postocular, parietal, pterotic, inferior posttemporal, inferior and superior opercular, 1st inferior and 1st superior infraorbital, and all preopercular spines were present. By approximately 10 mm SL, the supracleithral, nuchal, 2nd inferior intraorbital, and nasal spines were formed. By 20 mm SL, the preocular, superior posttemporal, and tympanic spines formed. The cleithral, 3rd superior infraorbital, and 3rd inferior infraorbital spines were not present in larvae less than 21 mm SL. Supraocular and coronal spines did not occur at any size.

Pre-extrusion pigmentation

Pre-extrusion larvae had pigment along the ventral midline extending from the anus to myomere 23 or 24 (second and third most posterior myomeres). This pigment was typically strong, with 2–4 melanophores per myomere (Fig. 1A). Pigment consisting of 6–16 melanophores was also located along the dorsal midline from approximately myomeres 15–23. The dorsal and posterior surfaces of the gut cavity were also heavily pigmented. In addition, in 72% of the larvae very small melanophores (1–5 in number) were observed on the ventral surface of the gut cavity. A single melanophore was located in the nape region of the head in 80% of specimens (Fig. 1A).

Body pigmentation

After extrusion, melanophores along the dorsal midline increased in number and size (Fig. 1B). This increase was most noticeable in the advancement of pigment in the anterior direction (there was little or no advancement posteriorly). At approximately 12 mm SL, the nape and dorsal midline pigments merged to form a solid line along the dorsal body surface. This dorsal body pigment increased in intensity as larvae grew.

A distinct pattern of five body bars (numbered 1–5 from anterior to posterior) was apparent in juveniles greater than 25 mm SL. Body-bar 1 began to appear in the nape region at 13 mm SL (Table 4; Fig. 1D). This bar extended from the dorsal midline to the operculum and was fully formed by approximately 24 mm SL. The next bar to form was body-bar 4 (an inverted triangle under the soft dorsal fin), which appeared at 17 mm SL (Fig. 1E), and was completely developed by approximately 35 mm SL (Table 4; Fig. 1F). Body-bar 2 was the next bar to form (from the spinous dorsal fin to the dorsal surface of the gut), appearing at approximately 19 mm SL and becoming fully developed by 33 mm SL. Body-bars 3 and 5 (from the spinous dorsal fin to the anus and an inverted triangle on the caudal peduncle, respectively) were the last bars to form; both appeared at approximately 20 mm SL and were fully developed at 38 mm SL (Fig. 1F).

The postanal ventral midline melanophores near the anus were lost soon after extrusion (Fig 1B). By 6 mm NL, the anteriormost melanophores were located approximately three myomeres posterior to the anus. The anterior melanophores decreased in number with increased fish length until approximately 10 mm SL. At this size, postanal ventral midline pigment began to advance anteriorly with increased fish size. In addition, pigment intensified to form a very dark area extending from the middle of the anal fin posteriorly to the first few ventral pterygiophores of the caudal fin. In larger juveniles (greater than 25 mm SL), the postanal ventral midline pigment became less intense and only a few melanophores remained near the anal fin articulations (Fig. 1, E and F).

Pigment on the lateral midline began to develop in 6 mm NL fish with a few melanophores near the caudal peduncle (Table 4; Fig. 1B). As fish length increased, the lateral midline pigment increased and became most intense at approximately 20 mm SL,

Table 2

Morphometrics (mm) of stripetail rockfish, *Sebastes saxicola*. Fish undergoing flexion are shown between the dashed lines. — = measurements not taken.

SL (mm)	Snout–anus length	Head length	Snout length	Eye diameter	Body depth	Pect.-fin length	Pect.-fin base depth	Parietal spine length
3.3	1.15	0.70	0.08	0.29	0.51	0.18	0.15	0.00
3.9	1.35	0.74	0.05	0.30	0.47	0.23	0.17	0.00
4.1	1.42	0.71	0.07	0.28	0.48	0.18	0.16	0.00
4.1	1.41	0.76	0.09	0.33	0.50	0.25	0.16	0.00
4.4	1.61	0.79	0.07	0.36	0.63	0.22	0.20	0.00
4.6	1.53	0.72	0.07	0.29	0.57	0.24	0.15	0.00
4.7	1.77	0.88	0.13	0.36	0.64	0.29	0.21	0.00
4.7	1.72	0.85	0.14	0.40	0.71	0.25	0.18	0.00
4.7	1.71	0.85	0.09	0.34	0.62	0.20	0.21	0.00
5.0	1.66	0.85	0.13	0.34	0.63	0.20	0.21	0.00
5.0	1.73	0.80	0.09	0.32	0.52	0.26	0.16	0.00
5.1	1.76	0.90	0.22	0.39	0.73	0.26	0.19	0.00
5.8	—	1.8	0.4	0.7	1.2	—	0.4	0.2
6.2	3.2	2.2	0.6	0.8	1.5	0.4	0.5	0.3
6.9	3.6	2.2	0.6	0.8	1.6	0.6	0.6	0.3
7.3	3.6	2.5	0.7	0.8	1.7	0.7	0.6	—
8.1	4.0	2.5	0.7	0.9	1.8	0.7	0.6	0.4
8.7	4.5	2.8	0.9	1.0	1.9	0.9	0.7	0.5
9.1	5.3	3.0	0.9	1.1	2.4	1.3	0.7	0.5
10.2	6.0	3.5	1.1	1.2	2.9	1.5	0.9	0.5
10.4	6.1	3.7	1.1	1.3	2.8	1.6	0.8	0.3
11.3	6.5	3.9	1.2	1.2	3.0	1.9	0.9	0.4
12.2	7.0	4.2	1.2	1.5	3.2	2.2	1.1	0.3
13.4	7.7	4.5	1.4	1.5	3.7	2.5	1.1	0.5
14.3	8.0	4.9	1.3	1.5	3.9	3.2	1.1	0.4
16.4	9.3	5.5	1.3	1.8	4.5	3.9	1.3	0.4
18.4	10.4	6.3	1.5	2.2	4.9	4.5	1.5	0.4
20.9	12.4	7.5	2.5	2.4	5.4	4.9	1.6	0.3

forming a line stretching from the posterior caudal peduncle (sometimes onto the caudal fin) to the posterior edge of the operculum. After 20 mm SL, pigment on the body intensified (mostly above the lateral midline), causing the lateral midline pigment to become much less evident (Fig. 1E). By 35 mm SL, the lateral midline pigment was virtually indistinguishable as it merged with the body pigment and the five body bars (Fig. 1F).

The hypural region remained mostly unpigmented until approximately 15 mm SL, when pigment formed on the posterior edge of the hypural plates (Fig. 1D). At 20 mm SL, when body-bar 5 became noticeable, the hypural region was highly pigmented (Fig. 1E).

Fin pigmentation

The pelvic and pectoral fins were relatively unpigmented in the larval and pelagic juvenile stages. Pigment was noted in the pelvic fins of only two fish. In these two fish, pigment occurred at the base of the rays of the left pelvic fin. In larger individuals, a few melanophores were noted on the pectoral fin, but these were not in a consistent area of the fin and did not constitute a regular pattern (Table 4). In addition, the axillary surface of the pectoral fin remained unpigmented throughout development.

Pigment on the dorsal fin began appearing at 17 mm SL with a few melanophores on the spinous fin. Melanophores appeared first on the anterior portion of the spinous dorsal fin and spread along the entire fin length as fish size increased. By 25 mm SL, most of the length of the spinous dorsal fin had some pigment, and melanophores were just beginning to appear on the soft dorsal fin (Fig. 1E). By 38 mm SL, the spinous dorsal fin was completely pigmented and the soft dorsal fin had a distinctive pattern. This pattern consisted of two horizontal pigment bands: the first was located just ventral to the tips of the soft fin rays, and the second at the fin ray bases. In addi-

Table 3

Development of head spines in stripetail rockfish, *Sebastes saxicola*. "1" means spine was present and "0" means spine was absent.

	Standard length (mm)																
Spines	6.2	6.9	7.3	8.1	8.5	8.7	9.1	9.7	10.2	10.4	11.3	12.2	13.4	14.3	15.4	16.4	18.4	20.9
Nasal	0	0	0	0	0	0	0	0	0	1	1	1	1	1	1	1	1	1
Preocular	0	0	0	0	0	0	0	0	0	0	0	0	0	1	1	1	1	1
Supraocular	0	0	0	0	0	0	0	0	0	0	0	0	0	0	0	0	0	0
Postocular	1	1	1	1	1	1	1	1	1	1	1	1	1	1	1	1	1	1
Coronal	0	0	0	0	0	0	0	0	0	0	0	0	0	0	0	0	0	0
Tympanic	0	0	0	0	0	0	0	0	0	0	0	0	0	0	0	0	1	1
Parietal	1	1	1	1	1	1	1	1	1	1	1	1	1	1	1	1	1	1
Nuchal	0	0	0	0	0	0	0	1	1	1	1	1	1	1	1	1	1	1
Pterotic	1	1	1	1	1	1	1	1	1	1	1	1	1	1	1	1	1	1
Posttemporals																		
Superior	0	0	0	0	0	0	0	0	0	0	0	0	0	0	0	1	1	1
Inferior	1	1	1	1	1	1	1	1	1	1	1	1	1	1	1	1	1	1
Supracleithral	0	0	0	0	0	0	1	1	1	1	1	1	1	1	1	1	1	1
Cleithral	0	0	0	0	0	0	0	0	0	0	0	0	0	0	0	0	0	0
Operculars																		
Superior	0	1	1	1	1	1	1	1	1	1	1	1	1	1	1	1	1	1
Inferior	0	0	0	0	0	1	1	1	1	1	1	1	1	1	1	1	1	1
Preoperculars																		
1st Anterior	1	1	1	1	1	1	1	1	1	1	1	1	1	1	1	1	1	1
2nd Anterior	1	1	1	1	1	1	1	1	1	1	1	1	1	1	1	1	1	1
3rd Anterior	0	1	1	1	1	1	1	1	1	1	1	1	1	1	1	1	1	1
1st Posterior	0	0	0	0	1	1	1	1	1	1	1	1	1	1	1	1	1	1
2nd Posterior	1	1	1	1	1	1	1	1	1	1	1	1	1	1	1	1	1	1
3rd Posterior	1	1	1	1	1	1	1	1	1	1	1	1	1	1	1	1	1	1
4th Posterior	1	1	1	1	1	1	1	1	1	1	1	1	1	1	1	1	1	1
5th Posterior	0	0	0	0	1	1	1	1	1	1	1	1	1	1	1	1	1	1
Infraorbitals																		
1st Inferior	0	0	1	1	1	1	1	1	1	1	1	1	1	1	1	1	1	1
2nd Inferior	0	0	0	0	0	0	0	1	1	1	1	1	1	1	1	1	1	1
3rd Inferior	0	0	0	0	0	0	0	0	0	0	0	0	0	0	0	0	0	0
1st Superior	0	1	1	1	1	1	1	1	1	1	1	1	1	1	1	1	1	1
2nd Superior	0	0	0	0	0	0	0	0	0	0	0	0	0	0	0	0	1	1
3rd Superior	0	0	0	0	0	0	0	0	0	0	0	0	0	0	0	0	0	0
4th Superior	0	0	0	0	0	1	1	1	1	1	1	1	1	1	1	1	1	1

tion, there was an unpigmented area at the base of the first two soft rays and the last spine (Fig. 1F).

Pigment began appearing on the anal fin at approximately 30 mm SL. Pigment intensified quickly, and by 38 mm SL a pattern had developed, consisting of a band through the middle of the fin and extending from the first anal spine to the last ray (Fig. 1F).

The caudal fin remained unpigmented until approximately 38 mm SL, when pigment began forming near the base of the rays. On the largest fish examined (43.9 mm SL), pigment was observed sporadically on a few fin rays.

Head pigmentation

Pigment on top of the cranium began forming soon after extrusion (Table 4). Four to five melanophores were present by 5 mm NL. The number and size of melanophores increased with increased fish size and by 7 mm NL, the head had become highly pigmented (Fig. 1B). Nape pigment also increased from one melanophore to five or six melanophores by 6 mm NL (Fig. 1B). At around 7 mm NL, nape pigment was overgrown by muscle tissue and became embedded. After flexion, pigment again appeared on the surface of the nape area. This pigment intensified with increased fish size.

At 7 mm NL, pigment began to develop on the anterior portion of the head between the eyes. As fish size increased, more pigment was added to this area. Pigment began forming on the upper jaw at approximately 8 mm SL. By 10 mm SL, pigmentation on the upper jaw and the anterior section of the head was well developed and could not always be differenti-

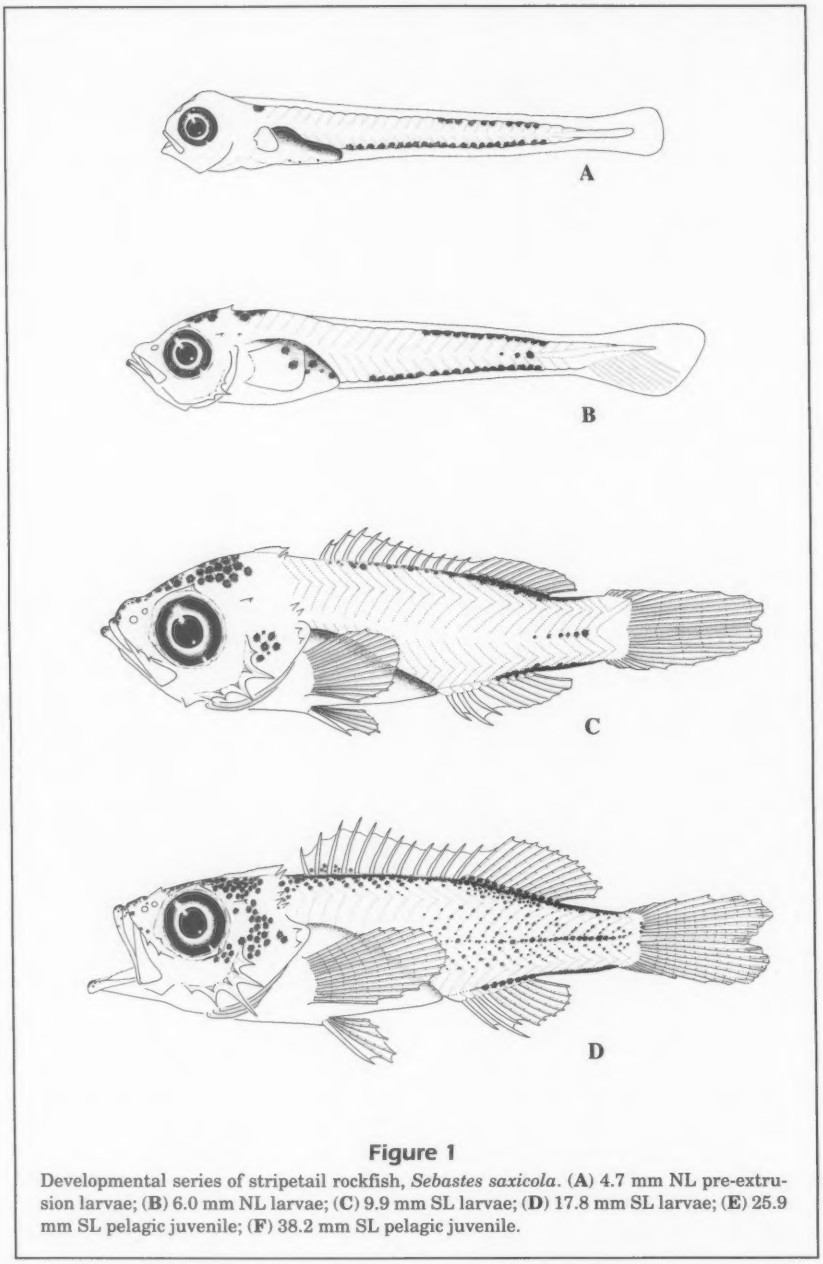

Figure 1

Developmental series of stripetail rockfish, *Sebastes saxicola*. (**A**) 4.7 mm NL pre-extrusion larvae; (**B**) 6.0 mm NL larvae; (**C**) 9.9 mm SL larvae; (**D**) 17.8 mm SL larvae; (**E**) 25.9 mm SL pelagic juvenile; (**F**) 38.2 mm SL pelagic juvenile.

ated (Fig. 1C). At this time, pigment on the cranial region and the anterior section of the head also merged, forming a solid pigment line extending from the upper jaw to the posterior side of the cranium (Fig. 1C).

Pigment began forming on the tip of the lower jaw at approximately 5 mm NL (Table 4). With increased development, pigment spread posteriorly along the jaw. At 30 mm SL, the upper and lower jaw pigments merged to encircle the mouth (Fig. 1F).

Pigment on the operculum began forming at 8 mm SL (Table 4; Fig. 1C). More melanophores were added to this region creating a large area of pigment by 12

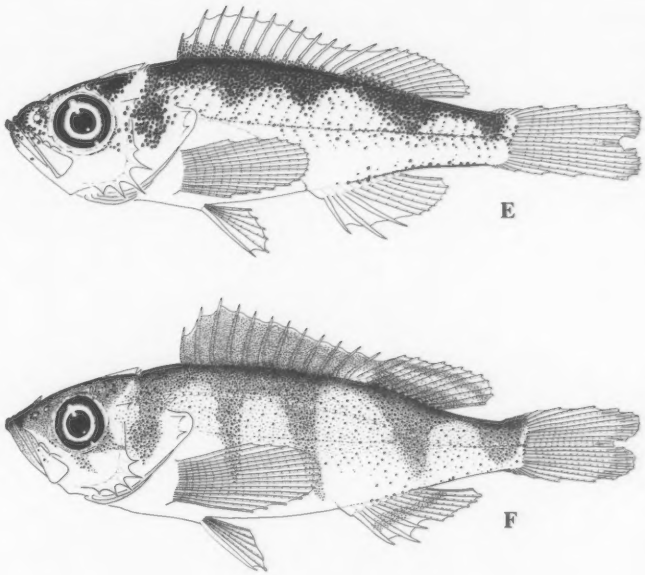

Figure 1 (continued)

mm SL. This pigment area intensified with increased fish size and merged with body-bar 1 at 22 mm SL (Fig. 1F).

Pigment along the ventral and posterior regions of the eye orbit began forming at 12 mm SL (Table 4). This pigment intensified and developed into two cheek bars. The more dorsal cheek bar formed first at 14 mm SL. By 36 mm SL, this bar extended from the eye orbit across the preopercle to the operculum, ending just below the operculum pigment (Fig. 1F). The more ventral cheek bar began forming at 28 mm SL at the base of the eye orbit and extended ventrally. At 44 mm SL, this bar was not completely formed.

Otolith examination

The extrusion check radius for *S. saxicola* ranged from 11.0 to 13.6 μm, averaging 11.9 μm (standard deviation [SD]=0.526 μm)(Fig. 2). The extrusion check radius of *S. saxicola* was not significantly different from the copper (P=0.132; extrusion check radius=10.5 μm; SD=0.354 μm) and gopher complexes (P=0.056; extrusion check radius=10.6 μm; SD=0.288 μm). Three species had extrusion check radii significantly larger (P<0.05) than those of *S. saxicola* (*S. rastrelliger* at 14.0 μm, SD=0.389;

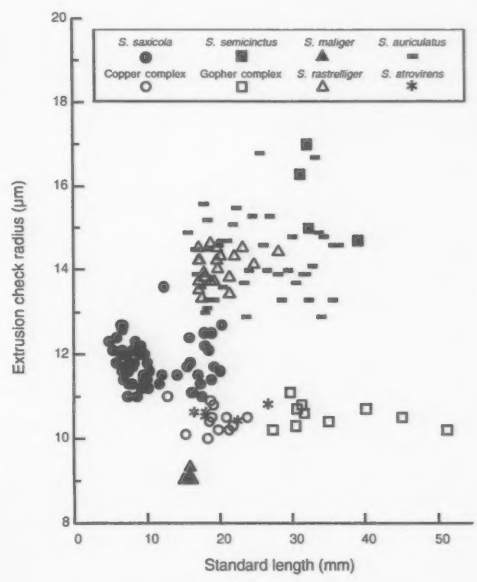

Figure 2

Comparison of extrusion check radius between stripetail rockfish, *Sebastes saxicola*, and other species.

Table 4

Proportions of stripetail rockfish, *Sebastes saxicola*, with melanophores present at various pigment loci averaged over 1.0 mm (range=+/– 0.5 mm) and 2.0 mm (range=+/– 1.0 mm) size bins. SL = standard length in mm. Definitions of pigment loci are given below.

SL	N	LJ	EYE	HEAD	FACE	OPER	CHK	NAPE	DORS	VENT	MID	HYP	DFIN	AFIN	PEC	PEL	B1	B2	B3	B4	B5
4	2	0.0	0.0	0.0	0.0	0.0	0.0	1.0	1.0	1.0	0.0	0.0	0.0	0.0	0.0	0.0	0.0	0.0	0.0	0.0	0.0
5	2	0.5	0.0	1.0	0.0	0.0	0.0	1.0	1.0	1.0	0.5	0.0	0.0	0.0	0.0	0.0	0.0	0.0	0.0	0.0	0.0
6	14	0.4	0.0	1.0	0.3	0.0	0.0	0.7	1.0	1.0	0.3	0.0	0.0	0.0	0.0	0.0	0.0	0.0	0.0	0.0	0.0
7	17	0.5	0.0	1.0	0.9	0.1	0.0	0.3	1.0	1.0	0.9	0.0	0.0	0.0	0.0	0.0	0.0	0.0	0.0	0.0	0.0
8	14	1.0	0.0	1.0	0.9	0.9	0.0	0.6	1.0	1.0	1.0	0.0	0.0	0.0	0.0	0.0	0.0	0.0	0.0	0.0	0.0
9	15	1.0	0.0	1.0	1.0	1.0	0.0	0.7	1.0	1.0	1.0	0.0	0.0	0.0	0.0	0.0	0.0	0.0	0.0	0.0	0.0
10	8	1.0	0.1	1.0	1.0	1.0	0.0	0.9	1.0	1.0	1.0	0.0	0.0	0.0	0.0	0.0	0.0	0.0	0.0	0.0	0.0
11	15	1.0	0.1	1.0	1.0	1.0	0.0	1.0	1.0	1.0	1.0	0.0	0.0	0.0	0.0	0.0	0.0	0.0	0.0	0.0	0.0
12	12	1.0	0.3	1.0	1.0	1.0	0.0	1.0	1.0	1.0	1.0	0.1	0.0	0.0	0.0	0.0	0.1	0.0	0.0	0.0	0.0
13	10	1.0	0.1	1.0	1.0	1.0	0.0	1.0	1.0	1.0	1.0	0.2	0.0	0.0	0.0	0.0	0.2	0.0	0.0	0.0	0.0
14	10	1.0	0.7	1.0	1.0	1.0	0.6	1.0	1.0	1.0	1.0	0.2	0.1	0.0	0.0	0.0	0.2	0.0	0.0	0.0	0.0
15	7	1.0	0.8	1.0	1.0	1.0	0.7	1.0	1.0	1.0	1.0	0.4	0.0	0.0	0.0	0.0	0.4	0.0	0.0	0.0	0.0
16	8	1.0	1.0	1.0	1.0	1.0	0.7	1.0	1.0	1.0	1.0	0.5	0.0	0.0	0.0	0.0	0.1	0.0	0.1	0.1	0.0
17	3	1.0	1.0	1.0	1.0	1.0	0.9	1.0	1.0	1.0	1.0	0.3	0.3	0.0	0.0	0.0	0.7	0.0	0.0	0.3	0.0
18	4	1.0	1.0	1.0	1.0	1.0	1.0	1.0	1.0	1.0	1.0	1.0	0.0	0.0	0.0	0.0	0.3	0.0	0.0	0.3	0.0
19	2	1.0	0.5	1.0	1.0	1.0	1.0	1.0	1.0	1.0	1.0	1.0	0.5	0.0	0.0	0.0	0.5	0.4	0.0	0.5	0.0
20	2	1.0	1.0	1.0	1.0	1.0	1.0	1.0	1.0	1.0	1.0	1.0	0.5	0.0	0.5	0.0	1.0	1.0	0.5	1.0	0.5
22	8	1.0	0.9	1.0	1.0	1.0	1.0	1.0	1.0	1.0	1.0	1.0	0.5	0.0	0.0	0.0	0.5	0.4	0.4	0.5	0.4
24	5	1.0	1.0	1.0	1.0	1.0	1.0	1.0	1.0	1.0	1.0	1.0	1.0	0.0	0.0	0.0	0.6	1.0	0.4	0.6	0.4
26	6	1.0	1.0	1.0	1.0	1.0	1.0	1.0	1.0	1.0	1.0	1.0	1.0	0.0	0.0	0.0	1.0	1.0	0.8	1.0	1.0
28	6	1.0	1.0	1.0	1.0	1.0	1.0	1.0	1.0	1.0	1.0	1.0	1.0	0.2	0.0	0.0	1.0	1.0	1.0	1.0	1.0
30	3	1.0	1.0	1.0	1.0	1.0	1.0	1.0	1.0	1.0	1.0	1.0	1.0	0.7	0.2	0.0	1.0	1.0	1.0	1.0	1.0
32	4	1.0	1.0	1.0	1.0	1.0	1.0	1.0	1.0	1.0	1.0	1.0	1.0	0.8	0.0	0.0	1.0	1.0	1.0	1.0	1.0
34	4	1.0	1.0	1.0	1.0	1.0	1.0	1.0	1.0	1.0	1.0	1.0	1.0	0.8	0.0	0.0	1.0	1.0	1.0	1.0	1.0
36	6	1.0	1.0	1.0	1.0	1.0	1.0	1.0	1.0	1.0	1.0	1.0	1.0	0.8	0.7	0.0	1.0	1.0	1.0	1.0	1.0
38	5	1.0	1.0	1.0	1.0	1.0	1.0	1.0	1.0	1.0	1.0	1.0	1.0	1.0	0.6	0.0	1.0	1.0	1.0	1.0	1.0
40	4	1.0	1.0	1.0	1.0	1.0	1.0	1.0	1.0	1.0	1.0	1.0	1.0	1.0	0.7	0.0	1.0	1.0	1.0	1.0	1.0
44	1	1.0	1.0	1.0	1.0	1.0	1.0	1.0	1.0	1.0	1.0	1.0	1.0	1.0	1.0	0.0	1.0	1.0	1.0	1.0	1.0

LJ=anterior tip of the lower jaw, EYE=posterio-ventral edge of the eye orbit, HEAD=cranial surface, FACE=dorsal surface anterior to the eyes, OPER=operculum, CHK=radiating cheek bars, NAPE=nape pigment, DORS=dorsal body surface, VENT=ventral body surface, MID=along the lateral midline, HYP=hypural region, DFIN=spinous dorsal fin, AFIN=anal fin, PEC=blade of the pectoral fin, PEL=pelvic fin, B1=body-bar 1 (most anterior), B2=body-bar 2, B3=body-bar 3, B4=body-bar 4, B5=body-bar 5 (on peduncle)

S. auriculatus at 14.3 μm, SD=0.939 μm; *S. semicinctus* at 15.8 μm, SD=1.085 μm). The two remaining species had extrusion check radii significantly smaller ($P<0.05$) than that of *S. saxicola* (*S. maliger* at 9.1 μm [SD=0.141 μm] and *S. atrovirens* at 10.6 μm [SD=0.148 μm]).

The extrusion check radius from individuals with axillary pectoral-fin pigment varied from that of *S. saxicola* (Fig. 3). The difference between extrusion check radius in all the larvae with axillary pigment (11.08μm; SD=1.79μm) and *S. saxicola* was not significant. However, when the larvae with axillary pigment were separated into two groups (one with extrusion check radius greater than 13 μm and the other with extrusion check radius less than 11 μm), the extrusion check radius of each group (13.46 μm [SD=0.055 μm] for the larger and 9.89 μm [SD= 0.532 μm] for the smaller) was significantly different from that of *S. saxicola* and from each other ($P<0.001$).

A linear model provided the best fit for the relationship of total otolith radius versus SL ($r^2=0.967$) (Fig. 4). A power curve was used to fit the relationship of SL and age ($r^2=0.927$)(Fig. 5). The model predicted that a fish would be 4.5 mm NL at extrusion (age=0), which is similar to what we observed.

Discussion

Sebastes saxicola have unique pigment patterns which allow them to be distinguished from other *Sebastes* spp. Of the 51 *Sebastes* spp. with published illustrations of pre-extrusion or the recently extruded larvae that occur in the study area, 10 are similar to *S. saxicola* (Morris, 1956; Moser et al., 1977; Stahl-Johnson, 1985; Matarese et al., 1989; Moreno, 1990; Wold, 1991; Sakuma and Laidig, 1995; Laroche[4]). Pre-extrusion *S. saxicola* larvae can be separated

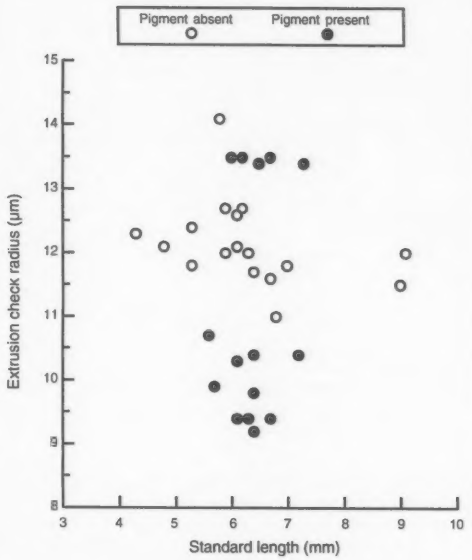

Figure 3

Comparison of extrusion check radius between stripetail rockfish, *Sebastes saxicola* (open circles), which has no axillary pectoral fin pigment, and other *Sebastes* spp. that are similarly pigmented except for the presence of axillary pectoral-fin pigment.

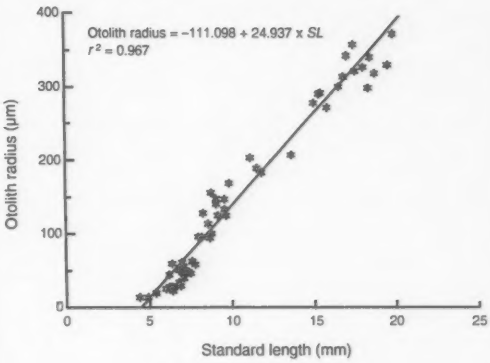

Figure 4

Plot of total otolith radius and standard length of all aged stripetail rockfish, *Sebastes saxicola* (n=58). Solid line indicates predicted values from linear model.

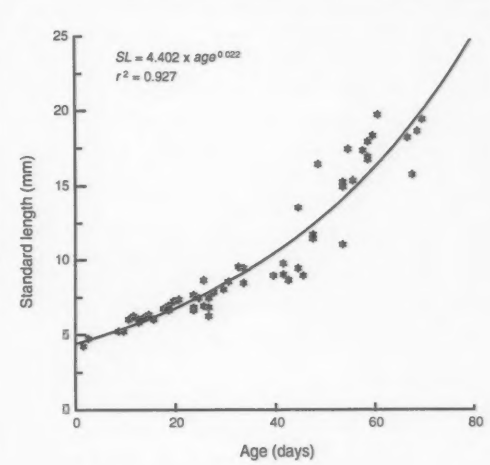

Figure 5

Plot of standard length and age of all aged stripetail rockfish, *Sebastes saxicola* (n=58). Solid line indicates predicted values from model (power curve).

from these 10 species by the extent of pigment along the ventral midline of the tail (i.e. the ventral midline pigment extends almost to the anus), the presence of the single nape pigment, and the absence of pigment on the pectoral fin and lower jaw.

As larval *S. saxicola* increase in length, they become readily distinguishable from most other *Sebastes* species. By early flexion, *S. saxicola* pigment patterns may be confused with only six other rockfish species (*S. atrovirens*, *S. carnatus*, *S. chrysomelas*, *S. maliger*, *S. rastrelliger*, and *S. semicinctus*) (Moreno, 1990; Wold, 1991). The pigment patterns of these six species are not completely described in all larval stages; thus direct comparisons with *S. saxicola* are not possible.

Sebastes saxicola can be separated from these six species on the basis of otolith characters, a technique used by Laidig and Ralston (1995). The size of the extrusion check radius for *S. saxicola* is significantly different from that for *S. atrovirens*, *S. maliger*, *S. rastrelliger*, and *S. semicinctus* (Fig. 2), as well as that for each group of larvae that had axillary pectoral-fin pigment (extrusion check radii greater than 13 µm and less than 11 µm [Fig. 3]). The extrusion check radii of the two groups with axillary pigment correspond well with the copper and gopher complexes (smaller radius) and *S. rastrelliger* (larger radius). Both *S. carnatus* and *S. chrysomelas* have axillary pectoral-fin pigment (Moreno, 1990; Wold, 1991). Thus, the presence of axillary pigment and the difference in size of the extrusion check radius could be used to separate the gopher complex from *S. saxicola*.

Sebastes saxicola can be separated from other *Sebastes* spp. greater than 10 mm SL on the basis of meristic characters and pigment patterns. The average fin ray counts of 12 dorsal rays, 7 anal rays, and 16 pectoral rays (Table 1) are similar to those reported by Moreland and Reilly (1991), who found this combination of meristic counts typical only for *S. saxicola*. The strong lines of pigment on the lateral, dorsal, and ventral midlines help to distinguish late larval *S. saxicola* from other *Sebastes* spp. As the larvae transform into juveniles, the distinctive bar pattern becomes evident (Fig. 1, E and F). In later stage juveniles, body-bars 3 and 4 become quite distinct and allow for field identification.

The growth of *S. saxicola* is similar to that of other *Sebastes* spp. occurring in the study area (Laidig et al., 1991; Woodbury and Ralston, 1991). The growth rate (as determined by the power curve model) for the first 40 days for *S. saxicola* is 0.125 mm/d, which is slightly slower than that reported for other species. Sakuma and Laidig (1995) found that *S. goodei* had a growth rate of 0.135 mm/d for the first 40 days, whereas Laidig et al. (1991) found that the growth rate of *S. jordani* in the first 20 days was approximately 0.165 mm/d. As *S. saxicola* larvae develop, their growth rate increases to 0.367 mm/d (for days 40–70). The change from slower growth to faster growth for *S. saxicola* occurs at approximately 9 mm SL (Fig. 5), which corresponds to the end of flexion. During flexion, the notochord turns up and the hypural plates form, creating the caudal fin. During this period, little growth in length is recorded, but the fish appears to grow in depth (Table 2). This period of slow apparent growth is similar to that found for *S. jordani* (Laidig et al., 1991).

Acknowledgments

We would like to thank the crew of the RV *David Starr Jordan*, scientific personnel who assisted in the collection of samples, and Michael Bowers for the donation of the pre-extrusion larvae. We also thank Brendon Daly, Moss Landing Marine Laboratories, the crew and scientific personnel onboard the RV *Ed Ricketts*, and scientists at Sea Grant (R/F-142) for their contributions. Special thanks are extended to Ralph DeFelice for his excellent illustrations.

Literature cited

Adams, P. B., J. L. Butler, C. H. Baxter, T. E. Laidig, K. A. Dahlin, and W. W. Wakefield.
1995. Population estimates of Pacific coast groundfishes from video transects and swept-area trawls. Fish. Bull. 93:446–455.

Chen, L.
1971. Systematics, variation, distribution, and biology of rockfishes of the subgenus *Sebastomus* (Pisces, Scorpaenidae, *Sebastes*). Univ. California Press, Berkeley, CA, 115 p.
1986. Meristic variation in *Sebastes* (Scorpaenidae), with an analysis of character association and bilateral pattern and their significance in species association. U.S. Dep. Commer., NOAA Tech. Rep. NMFS 45, 17 p.

Eschmeyer, W. N., E. S. Herald, and H. Hammann.
1983. A field guide to Pacific coast fishes. Houghton Mifflin Company, Boston, MA, 336 p.

Gunderson, D. R., and T. M. Sample.
1980. Distributional abundance of rockfish off Washington, Oregon, and California during 1977. Mar. Fish. Rev. 42(3–4):2–16.

Hunter, J. R., and N. C.-H. Lo.
1993. Ichthyoplankton methods for estimating fish biomass introduction and terminology. Bull. Mar. Sci. 53:723–727.

Laidig, T. E., and S. Ralston.
1995. The potential use of otolith characters in identifying larval rockfish (*Sebastes* spp.). Fish. Bull. 93:166–171.

Laidig, T. E., S. Ralston, and J. R. Bence.
1991. Dynamics of growth in the early life history of shortbelly rockfish, *Sebastes jordani*. Fish. Bull. 89:611–621.

Matarese, A. C., A. W. Kendall Jr., D. M. Blood, and B. M. Vinter.
1989. Laboratory guide to early life history stages of northeast Pacific fishes. U.S. Dep. Commer., NOAA Tech. Rep. NMFS 80, 652 p.

Moreland, S. L., and C. A. Reilly.
1991. Key to the juvenile rockfishes of central California. *In* T. E. Laidig and P. B. Adams (eds.), Methods used to identify pelagic juvenile rockfish (genus *Sebastes*) occurring along the coast of central California, p. 59–180. U. S. Dep. Commer., NOAA Tech. Memo. NMFS-SWFSC-166, 180 p.

Moreno, G.
1990. Description of the larval stages of five northern California species of rockfishes (Family Scorpaenidae) from rearing studies. M.S. thesis, California State Univ., Stanislaus, CA, 68 p.

Morris, R. W.
1956. Early larvae of four species of rockfish, *Sebastodes*. Calif. Fish Game 42(2):149–153.

Moser, H. G., and J. L. Butler.
1987. Descriptions of reared larvae of six species of *Sebastes*. *In* W. H. Lenarz and D. R. Gunderson (eds.), Widow rockfish: proceedings of a workshop; Tiburon, California, 11–12 December 1980, p. 19–29. U.S. Dep. Commer., NOAA Tech. Rep. NMFS 48.

Moser, H. G., E. H. Ahlstrom, and E. M. Sandknop.
1977. Guide to the identification of scorpionfish larvae (Family Scorpaenidae) in the eastern Pacific with comparative notes on species of *Sebastes* and *Helicolenus* from other oceans. U.S. Dep. Commer., NOAA Tech. Rep. NMFS Circ. 402, 71 p.

Phillips, J. B.
1964. Life history studies on ten species of rockfish. Calif. Dep. Fish Game, Fish Bull. 126, 70 p.

Richardson, S. L., and W. A. Laroche.
1979. Development and occurrence of larvae and juveniles of the rockfishes *Sebastes crameri*, *Sebastes pinniger*, and *Sebastes helvomaculatus* (Family Scorpaenidae) off Oregon. Fish. Bull. 77:1–46.

Sakuma, K. M., and T. E. Laidig.
1995. Description of larval and pelagic juvenile *Sebastes goodei* with an examination of larval growth. Fish. Bull. 93:720–730.

Stahl-Johnson, K. L.
1985. Descriptive characteristics of reared *Sebastes caurinus* and *S. auriculatus* larvae. *In* A. W. Kendall and J. B. Marliave (eds.), Descriptions of early life history stages of selected fishes, p. 65–76. Can. Tech. Rep. Fish. Aquat. Sci. 1359.

Witzig, J. F, M. C. Holliday, R. J. Essig, and D. L. Sutherland.
1992. Marine recreational fisheries statistics survey, Pacific coast, 1987–1989. National Marine Fisheries Service, Silver Spring, MD, 367 p.

Wold, L.
1991. A practical approach to the description and identification of *Sebastes* larvae. M.S. thesis, California State Univ., Hayward, CA, 88 p.

Woodbury, D. P., and S. Ralston.
1991. Interannual variation in growth rates and back-calculated birthdate distributions of pelagic juvenile rockfishes (*Sebastes* spp.) off the central California coast. Fish. Bull. 89:523–533.

Vertical distribution of euphausiid life stages in waters adjacent to Baja California

Bertha E. Lavaniegos

Centro de Investigación Científica y Educación Superior de Ensenada
Apartado Postal 2732, C.P. 22800, Ensenada, Baja California, México
Present address: Centro de Investigaciones Biológicas del Noroeste
Apartado Postal 128, C.P. 23000, La Paz, Baha California Sur, México

Abstract.—Vertical distribution of euphausiids on opposite sides of Baja California, off Point Eugenia to the west (June 1961) and in the central sector of the Gulf of California to the east (May 1965), are described from day and night sets of samples. Off Point Eugenia, the thermocline was shallow (20 m) toward the coast, characteristic of upwelling in late spring. In the Gulf, the Salsipuedes Channel showed well-mixed water whereas the Guaymas Basin had a stratified profile of temperature and oxygen. Lower abundances of the larger euphausiids during day throughout the water column, compared with night, are attributed to net avoidance. When a thermocline was present, two basic migration patterns were observed: 1) species crossing the thermocline (*Nyctiphanes simplex* and most *Euphausia* spp.) and 2) species remaining at or beneath the thermocline (*Euphausia gibboides* and *Nematoscelis difficilis*). On the basis of distribution at night, the youngest larvae and adults of *N. simplex* were in the mixed layer at the coastal station off Point Eugenia; more advanced stages of development were at mid-depth, between 0 and 50 m, suggesting an upwelling-downwelling cell of circulation. Inside the Gulf, abundant metanauplii and ovigerous females of *N. difficilis* occurred only in the upper layers of Salsipuedes Channel, whereas in Guaymas Basin and Point Eugenia, the youngest larvae were within the thermocline. The decrease of oxygen with depth did not reach the critical values observed in the more tropical eastern Pacific but, in general, where values of [O_2] were <1 mL/L, the abundance of euphausiids was low.

Manuscript accepted 11 December 1995.
Fishery Bulletin 94:300–312 (1996).

Early studies of euphausiids in the California Current showed a coincidence between their vertical distribution and the vertical movement of a mid-depth layer of organisms from which sonic scattering was reflected (the deep scattering layer in Boden, 1950; Barham, 1957). Interaction of this layer with shoaling of the sea floor was described by Isaacs and Schwartzlose (1965). Vertical migration, or lack of it in certain species, has been related to daytime avoidance of nets by euphausiids off California and northern Baja California (Brinton, 1967). For a given species, variation in the extent of vertical migration, and range of nonmigrators, has been related to the depth of the thermocline and distributions of dissolved oxygen (Brinton, 1967, 1979; Youngbluth, 1976). In the margins of the eastern tropical Pacific (ca. 20–22°N), a shoaling oxygen minimum layer constrains the vertical ranges of warm-temperate euphausiid species with a replacement by tropical species tolerant of oxygen deficiency (Longhurst, 1967; Brinton, 1979). Seasonal variability in vertical migratory behavior has been also observed. In La Jolla Bight near San Diego, differences in patterns of vertical migration of *Euphausia pacifica* and the copepod *Calanus pacificus* were observed between upwelling and downwelling periods (Koslow and Ota, 1981).

These and subsequent studies dealing with vertical migration in different taxa have shown variable responses to environmental stimuli. For example, in euphausiids, the influence of light (Boden and Kampa, 1967; Bright et al., 1976), proximity of the bottom (Cochrane et al., 1994), and temperature and salinity (Wiebe and Boyd, 1978) have been described. The selective advantage of remaining at depth during the day is usually considered an adaptation for escape from predators (Zaret and Suffern, 1976; Ohman et al., 1983; Bollens et al., 1992) or an energetic benefit (McLaren, 1963, 1974; Enright, 1977).

The present study describes for the first time the vertical distribution of euphausiids in the central sector of the Gulf of California and off Point Eugenia (28°N) during spring. In the Gulf of California, deep basins, island channels, and, in particular, low [O_2] within subtropical latitudes all suggest possibilities for interesting variability in vertical distribution of fauna. However, information on the subject is restricted to the vertical distribution of euphausiids and pelagic red crab, *Pleuroncodes planipes*, at the entrance of the Gulf, as part of an eastern Pacific transect (Brinton, 1979). Inside the Gulf, only the submergence of the copepod *Calanus pacificus californicus* to depths of 200–300 m during summer has

been reported by Fleminger (in Brinton et al., 1986). Point Eugenia is of biogeographical interest because species of temperate, tropical, and central Pacific regions may occur together relatively near to the coast (Boden et al., 1955; Brinton 1962, a and b).

Methods

Samples used in this study were collected from a three-station transect off Point Eugenia, Pacific coast of Baja California (*Zigpac II* cruise, 12–18 June 1961), and from three stations from the central part of the Gulf of California (*El Golfo II* cruise, 15–20 May 1965) (Fig. 1). In both cruises of RV *Alexander Agassiz*, two series of tows (one during the day and one at night) were made with an opening-closing net as described by Brinton (1967). The net was 1 m in diameter, 2.35 m long, and used 0.505-mm mesh with 0.25-mm mesh in the codend bag as well as a 40-cm long section at the front of it. Off Point Eugenia, nets were hauled horizontally at discrete depths (0, 10, 25, 50, 75, 100, 150, 200, 300, 400, and 500 m) for 30 min. In the Gulf of California, hauls were oblique and nets equipped with flowmeters. In the upper 150 m, five hauls were made through strata of 30 m; below 150 m, five hauls were made through strata of 135 m.

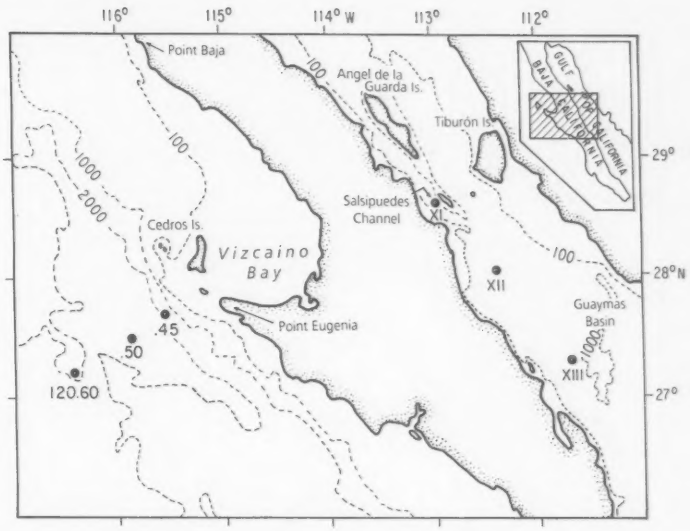

Figure 1

Sampling stations (•) off Point Eugenia, Pacific Coast of Baja California. Isobaths are in fathoms.

Euphausiids were identified, counted, and grouped as adults (males and females), juveniles, and larvae. The entire sample was used except in cases of abundant *Nyctiphanes simplex* and *Euphausia recurva*, where subsamples were obtained with a Folsom splitter. Between 200 and 400 individuals per life phase were typically counted. Larvae of *Nematoscelis difficilis* and *N. simplex* were sorted by developmental stages as defined by Gopalakrishnan (1973) and Lavaniegos (1992). The biogeographic provinces of Brinton (1962a, 1979), based on affinity to water masses, were used in the classification of species.

Abundance at a particular depth is expressed as individuals (ind)/m^3, and total abundance in the water column as ind/m^2 of ocean surface. In horizontal hauls, the depth of tow was taken as the middle depth of the layer. In oblique hauls, the thickness of the layer was the difference between depths of opening and closing of net. Statistical comparisons were not made because of absence of replicate tows. Data on temperature, salinity, and dissolved oxygen were obtained from standard Nansen-bottle casts and processed by California Cooperative Oceanic Fisheries Investigations. Data from the Gulf of California are published (SIO Data Report[1]).

Results

Hydrographic vertical profiles

In the outer coast of Baja California, physical conditions in June 1961 were typical for late spring (Reid et al., 1958; Hickey, 1979; Huyer, 1983). Near the coast (station [st.] 120.45), the mixed layer was 20 m (Fig. 2). The station most distant from the coast (st. 120.60) showed a thicker mixed layer (50–60 m) and warmer temperatures between depths of 20–150 m than did the other stations. Salinity in the surface layer showed low values (33.5–33.8 ppt), influenced by more northern California Current water. Near the coast (st. 120.45), a shallow oxycline and values of salinity >34.0 ppt at 75–100 m depth resulted from the influence of Intermediate Equatorial water.

The Gulf of California is influenced by northerly winds during spring and summer. However, tides,

[1] SIO Data Report. 1967. Physical and chemical data report: CalCOFI Cruise 6505 (*El Golfo* II). SIO Reference 67-16. Scripps Institution of Oceanography, La Jolla, CA, 92093.

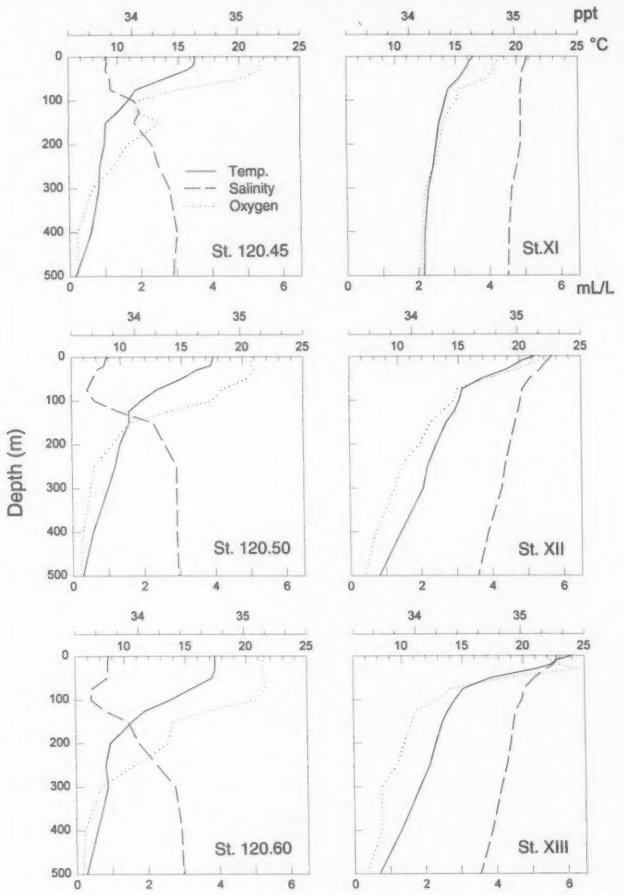

Figure 2

Depth profiles of temperature (°C), salinity (ppt), and dissolved oxygen (mL/L) for Point Eugenia (left) and the Gulf of California (right) stations.

air-sea fluxes, and propagation of internal waves enhance mixing of the water (Roden and Groves, 1959; Badan-Dangon et al., 1985; Bray and Robles, 1991). Strongest tidal currents have been recorded in the Ballenas Channel (west of Angel de la Guarda Island) and Salsipuedes Channel (Fig. 1). Here the water column is well mixed above 500 m during spring tides (Bray and Robles, 1991) as observed in May 1965 (st. XI, Fig. 2). In contrast, the Guaymas Basin profiles (sts. XII and XIII) showed gradients of temperature and oxygen that were particularly strong above 100 m. Temperature in the top 50 m showed differences of 2–4°C among the three sampling stations. Surface salinity showed values >35.0 ppt, characteristic of the Gulf water mass, produced in the northern gulf and flowing and mixing rapidly southward.

Vertical distribution of euphausiids

Off Point Eugenia, the greatest number of species was of the Central Pacific group. These, however, had relatively low abundances, <10 ind/m^2 per species, excepting *Euphausia recurva* and, at one station, *E. hemigibba* (Table 1). This group was absent in the Gulf of California.

The most abundant species in both study regions was *Nyctiphanes simplex* (Tables 1 and 2). This spe-

Table 1

Abundance integrated to surface (ind/m^2) per species off Point Eugenia. (METP = marginal of the eastern tropical Pacific (sensu Brinton 1962a, 1979).

Biogeographic group	Species	St. 120.60		St. 120.50		St. 120.45	
		Night	Day	Night	Day	Night	Day
Transition zone	*Euphausia gibboides*	26	19	123	6	12	4
	Nematoscelis difficilis	1	3	98	10	60	23
	Nyctiphanes simplex	5	1	674	79	836	588
	Thysanoessa gregaria	<1	1	4	3	9	4
METP	*Euphausia eximia*	2	10	13	13	8	3
	Nematobrachion flexipes	1	<1	<1	1	1	<1
	Stylocheiron affine	1	1	2	<1	5	<1
Subarctic	*Euphausia pacifica*	—	—	73	18	20	21
Equatorial	*Nematoscelis gracilis*	<1	—	—	—	—	<1
Central epipelagic	*Euphausia hemigibba*	9	1	1	—	<1	1
	Euphausia mutica	2	—	1	—	<1	—
	Euphausia recurva	33	30	64	1	33	4
	Nematoscelis atlantica	<1	—	<1	—	—	—
	Stylocheiron suhmii	—	<1	—	—	—	—
	Thysanopoda astylata	<1	<1	<1	—	—	<1
Central mesopelagic	*Nematobrachion boopis*	—	<1	—	—	—	—
	Nematoscelis tenella	<1	<1	<1	—	<1	—
	Stylocheiron elongatum	<1	—	<1	<1	—	—
	Stylocheiron longicorne	1	1	2	1	3	1
	Stylocheiron maximum	<1	<1	<1	<1	<1	<1
	Thysanopoda orientalis	<1	—	<1	<1	<1	<1
	Total	79	66	1,054	132	987	650

Table 2

Abundance integrated to surface (ind/m^2) per species in the central sector of the Gulf of California. (METP = marginal of the eastern tropical Pacific, ETP = eastern tropical Pacific (sensu Brinton 1962a,1979).

Biogeographic group	Species	St. XI		St. XII		St. XIII	
		Night	Day	Night	Day	Night	Day
Transition zone	*Nematoscelis difficilis*	324	217	604	178	344	163
	Nyctiphanes simplex	274	619	1,778	1,314	11,082	585
METP	*Euphausia eximia*	—	—	2	—	10	2
	Nematobrachion flexipes	—	—	<1	—	—	—
ETP	*Euphausia distinguenda*	—	—	<1	1	—	1
	Euphausia lamelligera	—	—	<1	1	1	21
	Total	598	836	2,385	1,494	11,437	772

cies is a warm-temperate endemic, occurring typically in nearshore waters of the southern part of the California Current (Brinton, 1962a) and in the Gulf of California (Brinton and Townsend, 1980). Other abundant species of the group identified as the "California Current's transition zone" was *Nematoscelis difficilis*, which was even more abundant in the Gulf than at the California Current stations. *Euphausia gibboides*, *Thysanoessa gregaria* (transition zone), and the subarctic-warm temperate *E. pacifica* were not observed in the Gulf.

Tropical species were scarce along both coasts of the peninsula, as expected during the time of sampling (Brinton, 1979; Brinton and Townsend, 1980). In this group, *E. eximia* and *Nematobrachion flexipes* were common off Point Eugenia and in Guaymas Basin. *Euphausia lamelligera* and *E. distinguenda* were observed in Guaymas Basin only. The tropical-subtropical *Stylocheiron affine* was taken only at Point Eugenia.

Expected trends of low abundances during daytime were observed and are believed to be due to net avoidance during the hours of light. High abundance was usually accounted for by larvae of epipelagic species when most of the population was in the upper 100 m at night. Larvae of *N. simplex* accounted for 90% or more of the euphausiids in the richest samples. Off Point Eugenia their distribution was greater toward the coast and in the upper 50 m (Fig. 3). Night occurrences of calyptopes and early furcilias (C–F_3 in Fig. 3) were almost exclusively at st. 120.45, with most at the surface; the oldest furcilias (F_4–F_6) and juveniles were well represented at st. 120.50, down to 50 m. The old larvae descended to 200 m during daytime. The occurrence of mature adults at the surface at the nearshore station may be associated with nearshore grouping to mate and spawn. Inside the Gulf few larvae of *N. simplex* occurred at Salsipuedes Channel (st. XI, Fig. 4). Moreover, all larval stages were found at Guaymas Basin, where furcilias at st. XII were restricted to the first 30 m during night; the larval calyptopes were dispersed in the upper 100 m. Adults were more abundant at st. XIII, peaking at 30–60 m (there was no sample for 0–30 m) during night and at 135–270 m in the light hours.

Vertical distribution of *Nematoscelis difficilis* larvae off Point Eugenia, as with *Nyctiphanes simplex*, was restricted to coastal stations, with a shallower range nearshore (st. 120.45) than at st. 120.50 (Fig. 5). In contrast to *N. simplex*, *N. difficilis* larvae avoided the upper layer, and juveniles and adults peaked at 100 m depth during nighttime (Fig. 5). Mating and spawning may have occurred in and below the thermocline near the coast, because most of the females with spermatophore attached or carrying external eggs were found between 75 and 200 m during the night (st. 120.45). In the Guaymas Basin, a more extended vertical range, from 55 to 420 m, was observed for adults of this species (Fig. 6). Interestingly, in Salsipuedes Channel, certain of the adults were near the surface, particularly gravid females. These may have been shedding newly hatched metanauplii in the upper layer, where many were found. A progression toward more advanced larval stages from north to south was observed.

Larvae of other species were found only off Point Eugenia. These were of the four most abundant species of *Euphausia* (Fig. 7). Three (*E. gibboides*, *E. recurva*, and *E. eximia*) included larval calyptopes

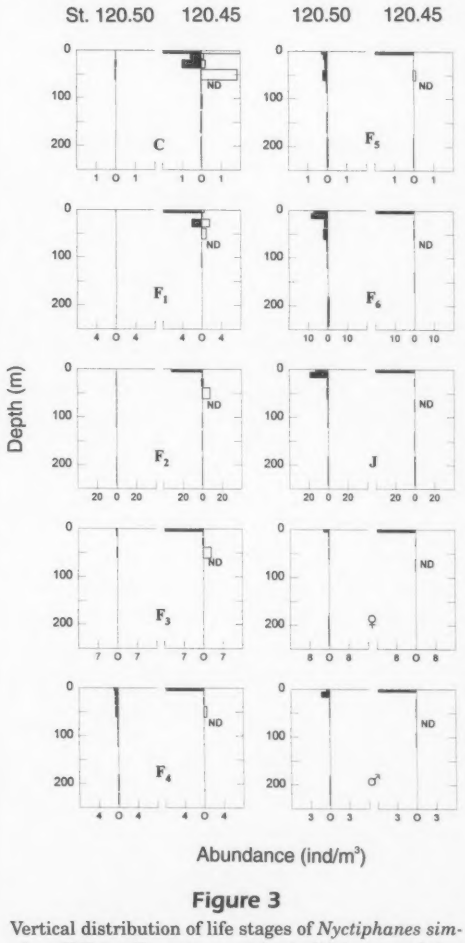

Figure 3

Vertical distribution of life stages of *Nyctiphanes simplex* off Point Eugenia at night (solid bars) and day (open bars). C = calyptopes; F_1–F_6 = furcilia stages; J = juveniles; ND = no data. Note the different scales used for abundance among stages.

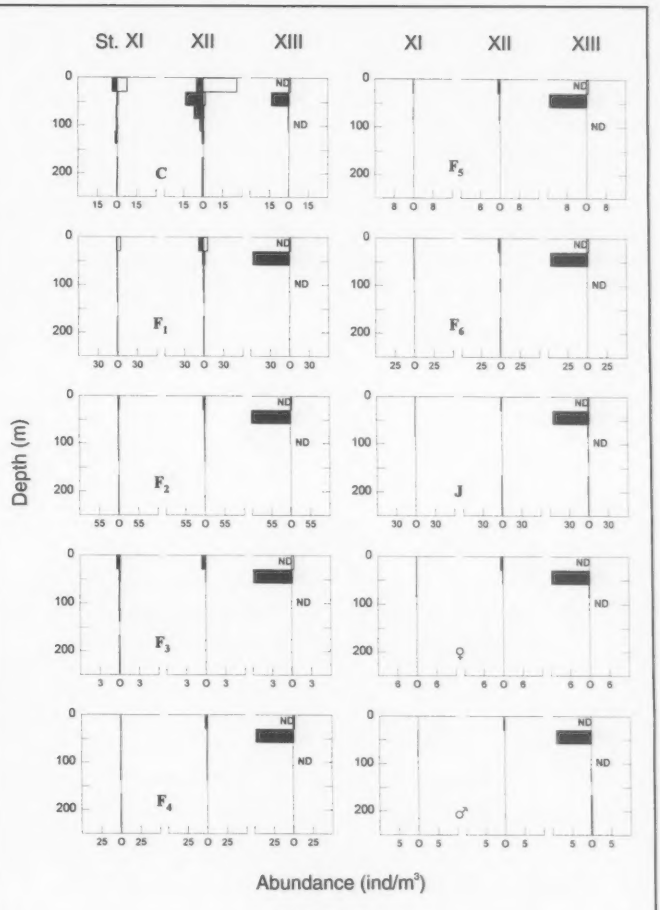

Figure 4

Vertical distribution of life phases of *Nyctiphanes simplex* in the Gulf of California. C = calyptopes; F_1–F_6 = furcilia stages; J = juveniles; ND = no data.

whereas *E. pacifica* larvae were advanced furcilias. Though the larvae of nighttime epipelagic species (*E. recurva*, *E. eximia,* and *E. pacifica*) occupied upper strata during both day and night, larvae of *E. gibboides* showed the same tendency as *N. difficilis* in avoiding the surface layer.

Few postlarvae (juveniles and adults) of epipelagic species were caught during daytime, particularly of *E. gibboides*, making it difficult to compare day and night vertical distributions. However, the other *Euphausia* species (Fig. 7) may have been migrating daily, on the basis of specimens found between 200 and 400 m during daytime, compared with their nighttime presence near the surface (Tables 3 and 4). *Thysanoessa gregaria* and *Stylocheiron affine* did not appear to migrate; they were not present in the upper 100 m during day and night (Fig 8).

The main part of the population of the three mesopelagic species did not occur above 100 m (Fig. 8). Larvae of *Stylocheiron longicorne* and *S. maximum* were at 100 m (except at st. 120.60 during the day) and of *Thysanopoda orientalis* at 200 m (Table 3). Off Point Eugenia and in Guaymas Basin virtually no euphausiids were found below 400 m depth. At those depths, dissolved oxygen was <1 mL/L at both locations (Fig. 2). In Salsipuedes Channel, oxygen values below 400 m was >2 mL/L, and some postlarvae of *N. difficilis* were found as deep as 700–800 m.

Discussion

The vertical distribution of the six most abundant species of euphausiids off Point Eugenia, June 1961, showed differences between day and night. Three of them (*Nyctiphanes simplex*, *Nematoscelis difficilis*, and *Euphausia eximia*) were important species in the central Gulf of California in May 1965. In both regions, when a thermocline was present, two basic kinds of distribution were apparent: 1) species found above and below the thermocline (*Nyctiphanes simplex* and most *Euphausia* species); and 2) species that remain in or below the thermocline (*E. gibboides* and *Nematoscelis difficilis*). In the absence of confirming replicated tows, the differences could also be interpreted as local patchiness. Similar patterns, however, were found during January–February of 1964 (Brinton, 1967) off Pt. Banda (32°N), Dana Pt. (34°N), and Pt. Reyes (38°N). During winter, upwelling is weak and the difference in depth of the thermocline between offshore and onshore stations is less than in summer. Though transects of winter 1964 extended farther offshore than in the present study, the trend of migrating species to be concentrated into depth ranges that were narrower nearshore was observed in both studies. A more northern study, off Cape Mendocino (40°N) and Cape Blanco (43°N) during July–August 1970, also showed this trend (Youngbluth, 1976).

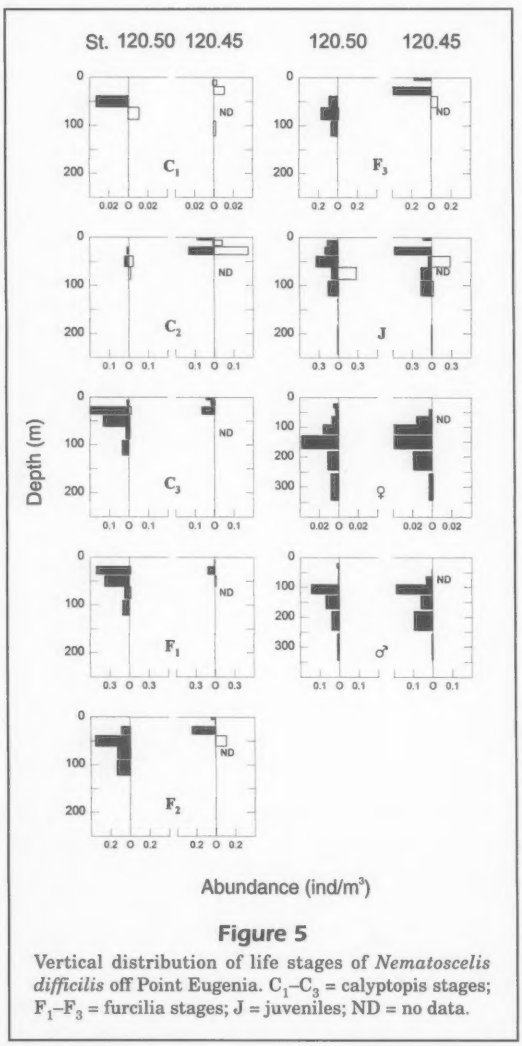

Figure 5

Vertical distribution of life stages of *Nematoscelis difficilis* off Point Eugenia. C_1–C_3 = calyptopis stages; F_1–F_3 = furcilia stages; J = juveniles; ND = no data.

In the Gulf of California, wind-driven upwelling occurs along the mainland coast in winter and on the peninsular coast in summer (Roden and Groves, 1959; Badan-Dangon et al., 1985). However, tides dominate the circulation of water near the midriff islands (Angel de la Guarda and Tiburón), including the Salsipuedes Channel, where currents up to six knots (2.76 m/s) have been measured (Alvarez et al., 1984; Bray and Robles, 1991). In this well-mixed area, the water column is cold, relatively rich in oxygen, and the vertical distribution of *Nematoscelis difficilis* was unique in that many adults were present in the upper 100 m at night. A migratory behavior to mate or shed the hatching metanauplii could be occurring, but an absence of a thermocline, acting as a barrier, could promote this behavior. In the earlier (1964) California Current study, near the coast the juveniles and adults of *N. difficilis* showed a bimodal vertical distribution (a peak near the surface and another in or below the thermocline), whereas offshore, the nocturnal distribution showed only the deep mode (Brinton, 1967). *N. difficilis* was therefore considered a vertical migrant, although a capability of daytime net avoidance was noted. In the congener *N. megalops*, from the northwestern Atlantic, differences between day and night were explained as due to daytime net avoidance (Wiebe and Boyd, 1978; Wiebe et al., 1982). Unfortunately, no replicate data for the Salsipuedes Channel station are available. This appeared to be an important area for reproduction of this species in May 1965; many metanauplii and first larval calyptopes were found in the upper layer, coincident with ovigerous females.

Though larvae of many species were found off Point Eugenia, most were late furcilias. Only the transition-zone group *N. simplex*, *N. difficilis*, and *E. gibboides*; the more tropical *E. eximia*; and the central Pacific *E. recurva* showed evidence of local reproductive activity, as suggested by the abundance of younger larval stages. Of these, differences in vertical distribution were between species with stage

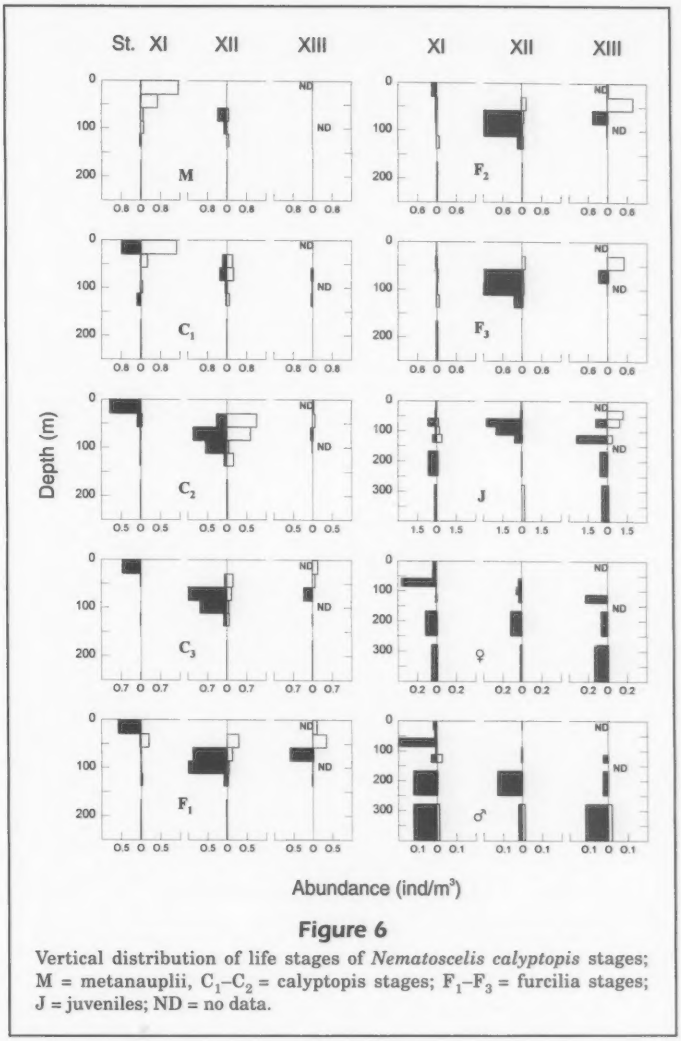

Figure 6

Vertical distribution of life stages of *Nematoscelis calyptopis* stages; M = metanauplii, C_1–C_2 = calyptopis stages; F_1–F_3 = furcilia stages; J = juveniles; ND = no data.

C_1 in the thermocline (*E. gibboides* and *N. difficilis*) and those with C_1 in the mixed layer (*N. simplex*, *E. eximia*, and *E. recurva*). These positions may be near the level of liberation of youngest larvae in species protecting eggs in maternal ovisacs such as done by *N. simplex* and *N. difficilis* (Brinton, 1966; Mauchline and Fisher, 1969). One day or even hours would have elapsed before moulting from metanauplius into C_1 stage. For *Nyctiphanes couchii* in the Celtic Sea, the liberation of mature metanauplii occurred within the euphotic zone, and moulting into calyptopis stage 1 (C_1) occurred in a matter of hours (Williams and Fragopoulu, 1985).

These authors observed in summer a stratified distribution of *N. couchii* during hours of light, with larger euphausiids at greater depths than smaller euphausiids. Similarly, in the northern Benguela Current, during winter, the larval calyptopes of *Nyctiphanes capensis* showed a shallower range of vertical distribution than furcilia (Barange and Pillar, 1992). In the present study the occurrence of older furcilias (F_4–F_6) of *N. simplex* at 200 m off Point Eugenia (Fig. 3) during daytime could indicate, as with *N. couchii* and *N. capensis*, an active daily migration. The restriction of early stages (C_1–F_3) of *N. simplex* to the nearshore station (32 km), exclusively in the surface layers, whereas late furciliar and postlarval stages extended to 64 km from the coast (from the surface into the layer below) may be explained by offshore flows, produced by coastal upwelling. As

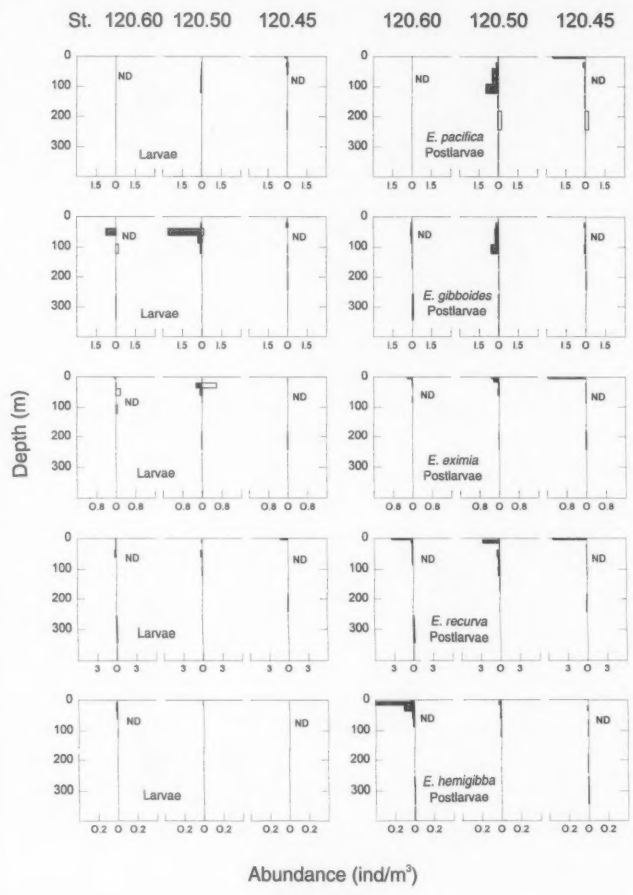

Figure 7

Vertical distribution of *Euphausia* species off Point Eugenia. Note the different scales used for abundance among species. ND = no data.

the larvae grow, they are carried offshore within the surface layers toward a convergence or frontal zone but eventually return to shore at depth by means of onshore flows. A cell of circulation of this kind conforms with the observations of a negative wind stress "curl" or Ekman convergence near the coast between Point Baja and Point Eugenia (Bakun and Nelson, 1977). Evidence for offshore flow in the surface, and onshore flow at 57 m, was found by Walsh et al. (1977) in the adjacent coastal shelf of Point San Hipolito (27°N). Similar conditions, within 28 km from the coast for early larval stages (nauplii and calyptopes) of *N. capensis*, and within 65 km for furcilias, were observed in Möwe Point (Benguela) (Barange and Pillar, 1992). These authors proposed a two-cell cross-shelf circulation to explain the maintenance of *N. capensis* near the coast.

From the same set of samples used in the present study, and from in situ observations in the Santa Barbara Basin (33°N), dense aggregations of stage-V copepodites of *Calanus pacificus californicus* were found (Alldredge et al., 1984). The presence of great abundances of resting copepodites of this species had been previously recorded along southern Baja California in oxygen-deficient water (Longhurst, 1967). Off Point Eugenia the species occupied a stratum near 300 m in offshore stations (120.60 and 120.50) but was found at 0–75 m in the nearshore station 120.45, both day and night. These differences were explained as population diapauses, at depth during

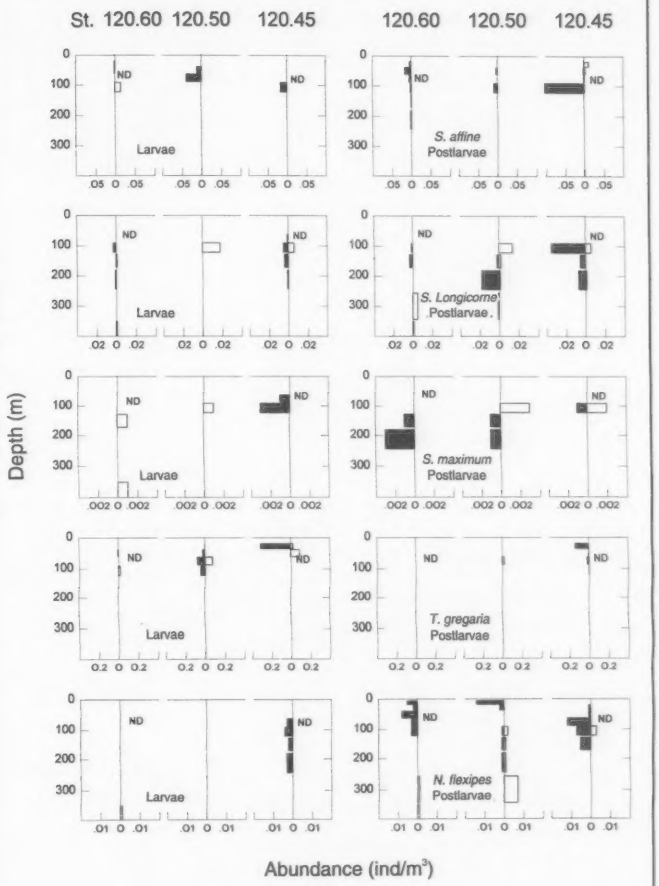

Figure 8

Vertical distribution of *Stylocheiron affine*, *S. longicorne*, *S. maximum*, *Thysanoessa gregaria*, and *Nematobrachion flexipes* off Point Eugenia. ND = no data.

periods of weak upwelling, with descent even to depths lacking oxygen (i.e. Santa Barbara Basin, Alldredge et al., 1984). In the present study, no aggregations of euphausiids analogous to copepods in diapause were found. For some euphausiid species, a low concentration of oxygen might limit migration at depth during daytime. This case apparently occurs in Saanich Inlet (British Columbia), where dense aggregations of *Euphausia pacifica* were observed directly above the anoxic layers (100–150 m) (Mackie and Mills, 1983). Near this site, in the temperate fjord of Dabbob Bay (Washington), a seasonal variation in the vertical migratory range of *E. pacifica* was recorded (Bollens et al., 1992). During the day, larvae of this species occurred deeper in the water column in late summer and fall than in spring. However, they were always above the depth levels of juveniles and adults (50–125 m) during the day, the entire population migrating to the surface at night (Bollens et al., 1992).

The relation between vertical distribution of euphausiids and low oxygen concentration has been discussed for the eastern tropical Pacific (ETP) (Brinton, 1979; Sameoto et al., 1987). In ETP the layer of strongly depleted oxygen (<0.1 mL/L) is present beneath the thermocline, to depths of 300–400 m. The vertically migrating species in the ETP group (*Euphausia lamelligera*, *E. distinguenda*, *E. diomedeae*, and *Nematoscelis gracilis*) tolerate intense O_2-deficiency at their daytime depths and enter the oxygenated mixed layer at night (Brinton,

Table 3

Depth (m) of maximal relative abundance of euphausiid postlarvae (juveniles and adults) of rare species off Point Eugenia, Baja California.

		St. 120.60		St. 120.50		St. 120.45	
Species		Depth	%	Depth	%	Depth	%
Nematoscelis gracilis	Night	200	75	—		—	
	Day	—		—		400	100
Euphausia mutica	Night	0	99	10	47	0	92
	Day	—		—		—	
Nematoscelis atlantica	Night	10	100	25	100	—	
	Day	—		—		—	
Stylocheiron suhmii	Night	—		—		—	
	Day	100	100	—		—	
Thysanopoda astylata	Night	10	100	500	100	—	
	Day	400	100	—		300	100
Nematobrachion boopis	Night	—		—		—	
	Day	400	100	—		—	
Nematoscelis tenella	Night	100	60	400	72	75	100
	Day	400	100	—		—	
Stylocheiron elongatum	Night	200	100	200	100	—	
	Day	—		200	100	—	
Thysanopoda orientalis	Night	—		—		—	
	Day	—		300	100	300	100

Table 4

Layer (m) of maximal relative abundance of euphausiid postlarvae (juveniles and adults) of tropical species in the Guaymas Basin, Gulf of California.

		St. XII		St. XIII	
Species		Layer	%	Layer	%
Euphausia ditinguenda	Night	0–30	50	—	
	Day	285–420	100	30–60	30
Euphausia eximia	Night	0–30	95	30–60	52
	Day	—		150–285	73
Euphausia lamelligera	Night	0–30	68	60–90	30
	Day	285–420	100	285–420	97
Nematobrachion flexipes	Night	285–420	100	—	
	Day	—		—	

1979). In one station in the Costa Rica Dome (9°N, 89.5°W), only *N. gracilis* and *Stylocheiron* spp. were found in water with oxygen below 0.1 mL/L (Sameoto et al., 1987). Off both coasts of central Baja California, the depletion of oxygen is not so strong as in the ETP and therefore it is not restrictive for vertical ranging of the dominant temperate species (*N. simplex* and *N. difficilis*). The relation between the thermocline and vertical migration was more important.

Acknowledgments

Thanks are given to E. Brinton who reviewed the manuscript and provided critical comments. Samples from the *Zigpac II* and *El Golfo II* cruises were collected by A. Fleminger and supplied by the Scripps Institution's plankton collections. Support for this research was provided by the scholarship program at the Consejo Nacional de Ciencia y Tecnologia.

Literature cited

Alldredge, A. L., B. H. Robinson, A. Fleminger, J. J. Torres, J. M. King, and W. M. Hamner.
1984. Direct sampling and in situ observations of a persistent copepod aggregation in the mesopelagic zone of the Santa Barbara Basin. Mar. Biol. 80:75–81.

Alvarez, L. G., A. Badan-Dangon, and J. M. Robles.
1984. Lagrangian observations of near-surface current in Canal de Ballenas. Calif. Coop. Oceanic Fish. Invest. Rep. 25:35–42.

Badan-Dangon, A., C. J. Koblinsky, and T. Baumgartner.
1985. Spring and summer in the Gulf of California: observations of surface thermal patterns. Oceanol. Acta 8(1):13–22.

Bakun, A., and C. S. Nelson.
1977. Climatology of upwelling related processes off Baja California. Calif. Coop. Oceanic Fish. Invest. Rep. 19: 107–127.

Barange, M., and S. C. Pillar.
1992. Cross-shelf circulation, zonation and maintenance mechanisms of *Nyctiphanes capensis* and *Euphausia hanseni* (Euphausiacea) in the northern Benguela upwelling system. Continental Shelf Res. 12(9):1027–1042.

Barham, E.
1957. The ecology of some scattering layers in the Monterey Bay area. Hopkins Mar. Station Tech. Rep. 1.

Boden, B. P.
1950. Plankton organisms in the deep scattering layer. U.S. Navy Electronics Laboratory Rep. 186:1–29.

Boden, B. P., and E. Kampa.
1967. The influence of natural light on the vertical migration of an animal community in the sea. Symposium Zool. Soc. Lond. (Part B) 19:15–26.

Boden, B. P., M. W. Johnson, and E. Brinton.
1955. The Euphausiacea (Crustacea) of the North Pacific. Bull. Scripps Inst. Oceanogr., Univ. Calif. 6(8):287–400.

Bollens, S. M., B. W. Frost, and T. S. Lin.
1992. Recruitment, growth, and diel vertical migration of *Euphausia pacifica* in a temperate fjord. Mar. Biol. 114:219–228.

Bray, N. A., and J. M. Robles.
1991. Physical oceanography of the Gulf of California. *In* J. P. Dauphin and B. R. T. Simoneit (eds.), The Gulf and peninsular province of the Californias, p. 511–553. Am. Assoc. Petroleum Geologists. Mem. 47.

Bright, T., F. Ferrari, D. Martin, and G. A. Franceschini.
1976. Effects of a total solar eclipse on the vertical distribution of certain oceanic zooplankters. Limnol. Oceanogr. 21:296–301.

Brinton, E.
1962a. The distribution of Pacific euphausiids. Bull. Scripps Inst. Oceanogr., Univ. Calif. 8:51–270.
1962b. Variable factors affecting the apparent range and estimated concentration of euphausiids in the North Pacific. Pac. Sci. 16(4):374–408.
1966. Remarks on euphausiacean phylogeny. *In* Symposium on Crustacea; Ernakulam, 1965, vol. 1, p. 255–259. Mar. Biol. Assoc. of India, Ernakulam, India.
1967. Vertical migration and avoidance capability of euphausiids in the California Current. Limnol. Oceanogr. 12(3):451–483.
1979. Parameters relating to the distributions of planktonic organisms, especially euphausiids in the eastern tropical Pacific. Prog. Oceanogr. 8(3):125–189.

Brinton, E., and A. W. Townsend.
1980. Euphausiids in the Gulf of California—The 1957 cruises. Calif. Coop. Oceanic Fish. Invest. Rep. 21:211–236.

Brinton, E., A. Fleminger, and D. Siegel-Causey.
1986. The temperate and tropical planktonic biotas of the Gulf of California. Calif. Coop. Oceanic Fish. Invest. Rep. 27:228–266.

Cochrane, N. A., D. D. Sameoto, and D. J. Belliveau.
1994. Temporal variability of euphausiid concentrations in a Nova Scotia shelf basin using a bottom-mounted acoustic Doppler current profiler. Mar. Ecol. Prog. Ser. 107:55–66.

Enright, J. T.
1977. Diurnal vertical migration: adaptive significance and timing. Part I: Selective advantage: a metabolic model. Limnol. Oceanogr. 22:856–872.

Gopalakrishnan, K.
1973. Development and growth studies of the euphausiid *Nematoscelis difficilis* (Crustacea) based on rearing. Bull. Scripps Inst. Oceanogr., Univ. Calif. 20:1–87.

Hickey, B. M.
1979. The California Current system—hypotheses and facts. Prog. Oceanogr. 8:191–279.

Huyer, A.
1983. Coastal upwelling in the California Current System. Prog. Oceanogr. 12:259–284.

Isaacs, J. D., and R. A. Schwartzlose.
1965. Migrant sound scatterers: interaction with the sea floor. Science (Wash. D.C.) 150:1810–1813.

Koslow, J. A., and A. Ota.
1981. The ecology of vertical migration in three common zooplankters in the La Jolla Bight, April–August 1967. Biol. Oceanogr. 1(2):107–134.

Lavaniegos-E., B. E.
1992. Growth and larval development of *Nyctiphanes simplex* in laboratory conditions. Calif. Coop. Oceanic Fish. Invest. Rep. 33:162–171.

Longhurst, A. R.
1967. Vertical distribution of zooplankton in relation to the eastern Pacific oxygen minimum. Deep-Sea Res. 14:51–63.

Mackie, G. O., and C. E. Mills.
1983. Use of the *Pisces IV* submersible for zooplankton stud-

ies in coastal waters of British Columbia. Can. J. Fish. Aquat. Sci. 40:763–776.

Mauchline, J., and L. R. Fisher.
1969. The biology of euphausiids. Adv. Mar. Biol. 18: 1–454.

McLaren, I. A.
1963. Effects of temperature on growth of zooplankton and the adaptative value of vertical migration. J. Fish. Res. Board Can. 20:685–727.
1974. Demographic strategy of vertical migration by a marine copepod. Am. Natur. 108:91–102.

Ohman, M. D., B. W. Frost, and M. Cohen.
1983. Reverse diel vertical migration: an escape from invertebrate predators. Science (Wash. D.C.) 220:1404–1407.

Reid, J. B., G. I. Roden, and J. G. Wyllie.
1958. Studies of the California Current System. Calif. Coop. Oceanic Fish. Invest. Prog. Rep., 1 July 1956–1 January 1958:28–56.

Roden, G. I., and G. W. Groves.
1959. Recent oceanographic investigations in the Gulf of California. J. Mar. Res. 18(1):10–35.

Sameoto, D., L. Guglielmo, and M. K. Lewis.
1987. Day/night vertical distribution of euphausiids in the eastern tropical Pacific. Mar. Biol. 96:235–245.

Walsh, J. J., T. E. Whitledge, J. C. Kelley, S. A. Huntsman, and R. D. Pillsbury.
1977. Further transition states of the Baja California upwelling ecosystem. Limnol. Oceanogr. 22:264–280.

Wiebe, P. H., and S. H. Boyd.
1978. Limits of *Nematoscelis megalops* in the northwestern Atlantic in relation to Gulf Stream cold core rings. I: Horizontal and vertical distributions. J. Mar. Res. 36(1):119–142.

Wiebe, P. H., S. H. Boyd, B. M. Dais, and J. L. Cox.
1982. Avoidance of towed nets by the euphausiid *Nematoscelis megalops*. Fish. Bull. 80:75–91.

Williams, R., and N. Fragopoulu.
1985. Vertical distribution and nocturnal migration of *Nyctiphanes couchii* (Crustacea: Euphausiacea) in relation to the summer thermocline in the Celtic Sea. Mar. Biol. 89:257–262.

Youngbluth, M. J.
1976. Vertical distribution and diel migration of euphausiids in the central region off the California Current. Fish. Bull. 74:925–936.

Zaret, T. M., and J. S. Suffern.
1976. Vertical migration in zooplankton as a predator avoidance mechanism. Limnol. Oceanogr. 21:804–813

Variability in the population structure of *Lutjanus adetii* (Castelnau, 1873) and *L. quinquelineatus* (Bloch, 1790) among reefs in the central Great Barrier Reef, Australia*

Stephen J. Newman
Australian Institute of Marine Science, P.M.B. No. 3
Townsville, M.C., Queensland, 4810, Australia

and

Department of Marine Biology, James Cook University
Townsville, 4811, Australia
Present address: Western Australia Marine Research Laboratories
Fisheries Department of Western Australia, P.O. Box 20
North Beach, 6020, Western Australia

David McB. Williams
Australian Institute of Marine Science, P.M.B. No. 3
Townsville, M.C., Queensland, 4810, Australia

Garry R. Russ
Department of Marine Biology, James Cook University
Townsville, 4811, Australia

Abstract.—The recent age validation of the tropical snappers *L. adetii* and *L. quinquelineatus* has facilitated the comparison of growth, mortality, and age structures for both these species at the spatial scale of individual reefs. The age structure of both species among reefs within the Great Barrier Reef Marine Park was based on counts of annuli from sectioned otoliths. There was significant variability in growth, mortality, and age structures. Significant differences in mean length, age, and weight (independent of the sex of the fish) were observed for both species among reefs. Peaks in abundance of year classes were variable from reef to reef. Comparisons of the von Bertalanffy growth curves indicated that the pattern of growth in individuals of *L. quinquelineatus* was significantly different among reefs, whereas the pattern of growth in *L. adetii* was not. However, there were no significant differences in the mean length of the early age classes of either species among reefs. The mortality rates and hence survivorship of both *L. adetii* and *L. quinquelineatus* among reefs were highly variable. It is hypothesized that the varying age structures and mortality rates of both of these species at the spatial scale of individual coral reefs are determined by the nonequilibrial balance of variable recruitment interacting with density-independent mortality. Hence the effect of good recruitment years may persist in the age structure of populations over time.

Manuscript accepted 28 September, 1995.
Fishery Bulletin 94:313–329 (1996).

Spatial comparisons of life history parameters of species of the family Lutjanidae have been undertaken only among broad geographic areas (e.g. Nelson and Manooch, 1982). Likewise, the majority of life history studies of species of the Lutjanidae have been based on widespread collections of individuals from broad geographic areas (e.g. Druzhinin and Filatova, 1980; Loubens, 1980; Liu and Yeh, 1991; Davis and West, 1992; Sanders et al.[1]; Mees[2]) and not on an individual reef scale. On the Great Barrier Reef in Australia, the fishing industry and other resource users (e.g. tourists, recreationalists, etc.) are managed under a system which protects marine areas of which individual coral reefs are the primary management unit.[3] To date, a comparison of age and growth parameters of lutjanids among individual reefs within a single geographic area has not been undertaken.

Comparisons of the age structure of lutjanids among a number of

* Contribution 757 of the Australian Institute of Marine Science, Townville, Queensland, Australia.

[1] Sanders, M. J., S. M. Kedidi, and M. R. Hegasy. 1984. Stock assessment for the bigeye snapper (*Lutjanus lineolatus*) caught by trawl in the Gulf of Suez. Food and Agriculture Organization of the United Nations Project for the Development of Fisheries in Areas of the Red Sea and Gulf of Aden, FAO/UNDP RAB/83/023/08, 40 p.

[2] Mees, C. C. 1992. Seychelles demersal fishery: an analysis of data relating to four key demersal species. Technical Report 019, Seychelles Fishing Authority, Victoria, Seychelles, 143 p.

[3] Great Barrier Reef Marine Park Authority. 1985. Zoning the central section. Townsville, Australia.

reefs within a single geographic area of the Great Barrier Reef have been published for only two species: the damselfishes *Pomacentrus moluccensis* and *P. wardi* (Doherty and Fowler, 1994, a and b). A number of studies have compared the abundance and size structure of the serranid *Plectropomus leopardus* between reefs open to fishing and those closed to fishing.[4,5,6] More recently, Ferreira and Russ (1995) have examined the size, age, and sex structure of populations of *P. leopardus* on closed and open reefs in the central Great Barrier Reef region.

The hussar, *Lutjanus adetii,* and the five-line snapper, *L. quinquelineatus,* are both widely distributed along the entire length of the Great Barrier Reef (10°S–24°S) and occur as far as 34°S (Kuiter, 1993). The habitats of both species vary, although they are most commonly associated with hard bottom areas. In the central Great Barrier Reef region, *L. adetii* is common at depths greater than 30 m within the midshelf group of reefs and is known to occur on the outershelf at depths up to at least 99 m, whereas *L. quinquelineatus* is common in both shallow and deep waters on both midshelf and outershelf reefs to a depth of at least 128 m (Newman, 1995). Loubens (1980) has demonstrated that both species are relatively long lived and slow growing in New Caledonia; similar conclusions have been obtained from the central Great Barrier Reef (Newman et al.[7]).

Neither of these lutjanids forms a significant portion of the commercial catch in the central Great Barrier Reef, and they form only a nominal contribution to the recreational catch in this region (Higgs, 1993; Newman, 1995). However, in the southern Great Barrier Reef, *L. adetii* contributes a significant proportion to the commercial lutjanid catch (Newman, 1995) and may become of increasing significance to the recreational line fishery in future years.[8] Relatively little information is available concerning the ecology of these species in Australian waters.

The recent validation (Newman et al.[7]) of age and growth for both *L. adetii* and *L. quinquelineatus* has facilitated the comparison of demographic parameters of both these species at the spatial scale of individual reefs. The aims of this study are to examine spatial variability in growth, mortality, and age structures of populations of *L. adetii* and *L. quinquelineatus* among reefs within the central Great Barrier Reef region (Fig. 1).

Materials and methods

Sampling procedures

Specimens of *L. adetii* (n=355) and *L. quinquelineatus* (n=573) were obtained between October 1991 and December 1993 from fish traps (O-trap design with 40-mm galvanized hexagonal wire mesh [Newman, 1995]) used during a research program investigating the distribution and abundance of lutjanids among reefs in the central Great Barrier Reef region (Newman, 1995; Newman and Williams, 1995). Samples of both species were obtained from four reefs (Rib [RI], John Brewer [JB], Lodestone [LO], and Kelso [KL]); additional samples of *L. quinquelineatus* were obtained from two other reefs (Davies [DV] and Myrmidon [MR]) (Fig. 1). Individual *L. adetii* <17 cm fork length (FL) and *L. quinquelineatus* <10 cm FL were usually not vulnerable to trap fishing and specimens in this size range were therefore not obtained for analysis.

Individuals of each species were measured (FL and standard length [SL]) and weighed (clean weight after removal of the gills and viscera), and sexes were determined by macroscopic examination of the gonads. The sagittal otoliths of individuals were removed and sectioned laterally through the focus with a Beuhler Isomet low-speed jewelry saw, and ages were determined according to the methods described in Newman et al.[7]

Analysis of data

Because a previous study (Newman et al.[7]) indicated significant differential growth between sexes in both species, two-way factorial analyses of variance were used to compare the mean length (FL, mm), age (years), and clean weight (g) of each species both among reefs and between sexes (in order to prevent

[4] Ayling, A. M., and A. L. Ayling. 1984. Distribution and abundance of coral trout species (*Plectropomus* spp.) in the Swain group of reefs. Capricorn section of the Great Barrier Reef Marine Park. Unpubl. report to the Great Barrier Reef Marine Park Authority (GBRMPA; Project 171), Australia.

[5] Ayling, A. M., and A. L. Ayling. 1986. A biological survey of selected reefs in the Capricornia section of the Great Barrier Reef Marine Park. Unpubl. report to the Great Barrier Reef Marine Park Authority (GBRMPA; Project 243 and 269), Australia.

[6] Ayling, A. M., and B. P. Mapstone. 1991. Unpublished data collected for GBRMPA from a biological survey of reefs in the Cairns section of the Great Barrier Reef Marine Park. Unpubl. report to the Great Barrier Reef Marine Park Authority (GBRMPA), Australia.

[7] Newman, S. J., D. McB. Williams, and G. R. Russ. Age validation, growth, and mortality rates of the tropical snappers (Pisces: Lutjanidae), *Lutjanus adetii* (Castelnau, 1873) and *L. quinquelineatus* (Bloch, 1790) from the central Great Barrier Reef, Australia. Submitted to Mar. Freshwater Res. (1996).

[8] Williams, D. McB., and G. R. Russ. 1994. Review of data on fishes of commercial and recreational fishing interest on the Great Barrier Reef, Vol. 1. Great Barrier Reef Marine Park Authority Research Publication 33, 106 p.

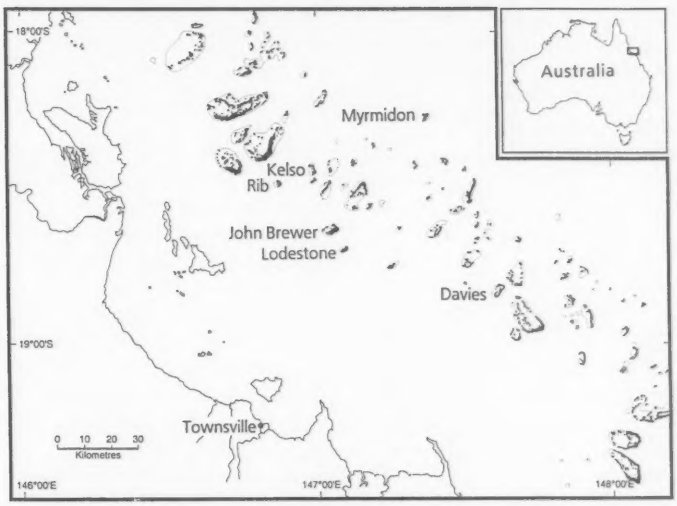

Figure 1

The locations of the reefs sampled for *Lutjanus adetii* and *L. quinquelineatus* from October 1991 to December 1993 in the central region of the Great Barrier Reef, Australia.

confounding differences among reefs with differences between sexes). Both reefs and sexes were treated as fixed and orthogonal factors in the analysis. Multiple comparisons were performed with Tukey's honestly significant difference (HSD) test (α=0.05).

The Kruskal-Wallis one-way analysis of variance by ranks was used to test for differences in the age structures of each species among reefs (Siegel and Castellan, 1988). Multiple pair-wise comparisons were performed, by using Kolmogorov-Smirnov (K-S) tests, to determine differences in the age structure of each species between individual reefs (Zar, 1984).

Growth rates for each species at each reef were also examined. The von Bertalanffy growth function (VBGF) was fitted to lengths at age for each species from each reef by using nonlinear least-squares estimation procedures.[9] The VBGF is defined as follows:

$$L_t = L_\infty (1 - e^{-K(t-t_0)})$$

where L_t = length at time t;
L_∞ = asymptotic length;
K = Brody growth coefficient;
t = age of the fish; and
t_0 = theoretical origin of the growth curve.

Von Bertalanffy growth curves were compared by using the likelihood-ratio test (Kimura, 1980), considered the most robust measure (Cerrato, 1990). A modified analysis of the residual sum of squares (ARSS) was also employed to compare VBGF's among reefs (Zar, 1984; Chen et al., 1992). Further, one-way analysis of variance was used to determine whether there were significant differences in the mean length (FL) of the early age classes of each species among reefs (α=0.05).

Analysis of covariance was used to determine whether there were significant differences in the clean weight at length (FL) relationships among reefs and between sexes for each species. Length and weight data were transformed to a natural logarithm function ($\log_e x$) to satisfy assumptions of normality and homogeneity as detected by Cochran's test (Winer, 1971). Both reefs and sexes were treated as fixed and orthogonal factors in the analysis. Again, multiple comparisons were performed by using Tukey's honestly significant difference (HSD) test.

Estimates of the annual instantaneous rate of total mortality (Z) for each species among individual reefs were obtained by using the age-based catch-curve method of Beverton and Holt (1957) and Ricker (1975). The natural logarithm of the number of fish

[9] Prager, M. H., S. B. Saila, and C. W. Recksiek. 1989. FISHPARM: a microcomputer program for parameter estimation of nonlinear models in fishery science, 2nd ed. Old Dominion University Oceanography Technical Report 87-10.

in each age class (N_t) was plotted against their corresponding age (t), and Z was estimated from the descending slope, b. Estimates of the survival rate of both species on different reefs were then calculated from the Z that was derived from catch curves, because $Z = -\log_e S$ (Ricker, 1975).

Results

There were significant differences in mean length, age, and weight of both species among reefs, and these differences were independent of the sex of the fish (Tables 1 and 2). Tukey (HSD) comparisons showed that, in general, mean length and weight were larger and mean age greater for both species at KL, although the multiple comparisons among reefs were not all definitive (Tables 1 and 2). Significant differences in mean length, age, and clean weight of both species between sexes were the same as those described in Newman et al.,[7] with males larger than females in species (Tables 1 and 2).

Age structures

Age structures of *L. adetii* differed significantly among reefs (Kruskal-Wallis statistic: H=13.85, P<0.01), with the greatest difference being that between RI and JB (Table 3). The relative abundance of older fish (year classes 10–22) at RI was greater than that at JB (Fig. 2). This pattern was seen also at LO and KL, although the overall age structures were not significantly different (Table 3). The pattern of peaks in abundance of year classes was not consistent across all reefs. The small sample size taken from KL may have biased results; however, the sample covered a range of 10 age classes and was similar to the age structure at RI. The age structure at KL was significantly different from that of both JB and LO, and the age structure at JB was significantly dif-

Table 1

Analyses of variance comparing mean length, age, and weight among reefs and between sexes for *Lutjanus adetii* (significant P values are in bold type) and a posteriori multiple comparison of means using Tukey (HSD) analysis (α=0.05; reefs are presented in order of decreasing magnitude). MS = mean square.

Source of variation	df	MS	F	P
Dependent variable: fork length (mm)				
Reefs	3	3106.15	12.912	**< 0.001**
Sex	1	462.23	1.92	> 0.15
Reefs × Sex	3	54.45	0.23	> 0.85
Residual	321	240.56		
Dependent variable: age (years)				
Reefs	3	128.85	8.57	**< 0.001**
Sex	1	43.67	2.90	> 0.05
Reefs × Sex	3	7.24	0.48	> 0.65
Residual	320	15.04		
Dependent variable: clean weight (g)				
Reefs	3	31684.62	14.70	**< 0.001**
Sex	1	23013.95	10.68	**< 0.01**
Reefs × Sex	3	799.39	0.37	> 0.75
Residual	288	2154.85		

Tukey HSD analysis among reefs				
Fork length:	Kelso	Lodestone	Rib	John Brewer
Age:	Kelso	Rib	Lodestone	John Brewer
Clean weight:	Kelso	Lodestone	Rib	John Brewer
Tukey HSD analysis between sexes				
Clean weight:	Males	Females		

ferent from that of LO. JB and LO had strong modes in year class 7, whereas KL suggested a mode in year class 9 (Fig. 2). The abundance of year classes 10–22 at LO was greater than that at JB (Fig. 2).

Age structures of *L. quinquelineatus* also differed significantly among reefs (Kruskal-Wallis statistic: H=21.41, P<0.001). Kolmogorov-Smirnov tests (Table 4) showed that MR and LO were significantly differ-

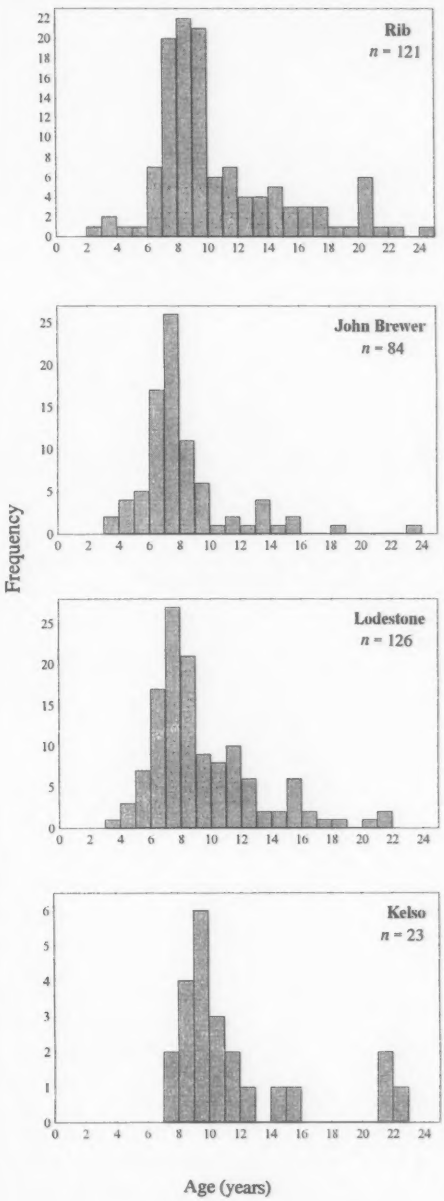

Figure 2

Age-frequency distributions for *L. adetii* among reefs in the central Great Barrier Reef.

Table 2

Analyses of variance comparing mean length, age, and weight among reefs and between sexes for *Lutjanus quinquelineatus* (significant P values are in bold type) and a posteriori multiple comparison of means using Tukey (HSD) analysis (α=0.05; reefs are presented in descending order). MS = mean square.

Source of variation	df	MS	F	P
Dependent variable: fork length (mm)				
Reefs	5	5944.89	25.70	**< 0.001**
Sex	1	19962.29	86.31	**< 0.001**
Reefs × Sex	5	166.94	0.72	> 0.60
Residual	551	231.29		
Dependent variable: age (years)				
Reefs	5	547.00	17.03	**< 0.001**
Sex	1	40.95	1.27	> 0.25
Reefs × Sex	5	41.13	1.28	> 0.25
Residual	550	32.11		
Dependent variable: clean weight (g)				
Reefs	5	28723.22	35.83	**< 0.001**
Sex	1	98157.42	122.45	**< 0.001**
Reefs × Sex	5	1524.81	1.90	> 0.05
Residual	551	801.60		

Tukey HSD analysis among reefs

Fork length:	Kelso	Davies	Rib	John Brewer	Myrmidon	Lodestone
Age:	Kelso	Rib	John Brewer	Davies	Myrmidon	Lodestone
Clean weight:	Kelso	Davies	Rib	John Brewer	Myrmidon	Lodestone

Tukey HSD analysis between sexes

Fork length:	Males	Females
Clean weight:	Males	Females

Table 3

Differences in the distribution of age structures of *Lutjanus adetii* between reefs were determined by using the Kolmogorov-Smirnov test (values of D_{max} are shown, significance level α=0.05, significant results are marked with an asterisk [*]).

	Reef		
Reef	John Brewer	Lodestone	Kelso
Rib	0.38*	0.17	0.19
John Brewer		0.21*	0.56*
Lodestone			0.35*

i.e.	John Brewer	Lodestone	Rib	Kelso

ent from all other reefs. KL was not significantly different from RI, but was significantly different from all other reefs. JB was not significantly different from either DV or RI, whereas DV was significantly different from RI. MR showed a peak in year class 5 and relatively strong year classes 6, 7, and 8 (Fig. 3). However, few fish older than 8 years were represented in catches. LO had relatively strong year classes 2, 3, 4, and 5, but abundance per age class declined rapidly to year 26, except for a strong mode in year class 14 (Fig. 3). DV was somewhat similar, with strong modes in year classes 5 and 6 but with the abundance of subsequent year classes declining approximately exponentially to year 22 (Fig. 3). Data were more limited for KL, which showed relatively even distribution from year classes 2–30 and peaks in year classes 5 and 14. Compared with those from

Table 4

Differences in the distribution of age structures of *Lutjanus quinquelineatus* between reefs were determined by using the Kolmogorov-Smirnov test (values of $D_{max.}$ are shown, significance level α=0.05, significant results are marked with an asterisk [*]).

	Reef				
	John Brewer	Lodestone	Davies	Myrmidon	Kelso
Rib	0.14	0.31*	0.23*	0.43*	0.14
John Brewer		0.27*	0.20	0.43*	0.27*
Lodestone			0.35*	0.30*	0.41*
Davies				0.28*	0.36*
Myrmidon					0.54*

i.e.	Myrmidon	Lodestone	Davies	John Brewer	Rib	Kelso

other reefs, older year classes were relatively dominant at KL. JB and RI had relatively flat age distributions for year classes 2–24 compared with those for LO, DV, and MR. The only pattern that was consistent across all reefs was the strong mode of 5-year-old individuals (Fig. 3), and this may have reflected the age at which these fish attained full recruitment to the sampling gear (fish traps).

Growth models

The von Bertalanffy models of the length-age relationship among reefs for *L. adetii* are shown in Figure 4; the coefficients of determination among reefs ranged from 0.177 to 0.462. The low coefficients of determination were attributable to the absence of younger and smaller fish in the samples. Therefore no point of inflexion was evident in the growth models among reefs. As a result, the parameters of the von Bertalanffy models for *L. adetii* among individual reefs were characterized by large asymptotic standard errors (Table 5), with LO having the best-fitting model. The von Bertalanffy model from LO was similar to that derived from all reefs pooled within the central Great Barrier Reef (Table 5). Despite the absence of small and younger fish caused by the bias in sampling, the von Bertalanffy growth function was the best empirically based assessment of growth in *L. adetii* (Fig. 4). The von Bertalanffy growth curves for *L. adetii* were not significantly different among reefs (likelihood-ratio test, $P>>0.05$; ARSS:F=1.13, $P>>0.05$), and the resulting growth curves (Fig. 4) appeared to be similar. Additionally, there were no significant differences in the mean length (FL) of the early age classes (6+, 7+, 8+, and 9+) of *L. adetii* among reefs (Table 6).

The von Bertalanffy model provided a better description of the length-age relationship among reefs for *L. quinquelineatus* (Fig. 5), with coefficients of determination among reefs ranging from 0.267 to 0.752. The younger and smaller fish were underrepresented in the catch samples from some reefs and this was reflected in the coefficients of determination (Table 5; Fig. 5). The parameters of the von Bertalanffy models for *L. quinquelineatus* among individual reefs were characterized by relatively small asymptotic standard errors (Table 5). The growth curves for *L. quinquelineatus* were significantly different among reefs (likelihood-ratio test, $P<0.01$; ARSS:F=8.401, $P<0.001$). Differences among reefs were observed in values of L_{∞}, K, and t_0 (Table 5). However, there were no significant differences in the mean length (FL) of the early age classes (2+, 3+, 4+, 5+, and 6+) of *L. quinquelineatus* among reefs (Table 7).

Analysis of covariance (ANCOVA) demonstrated that the relationship between weight and length in *L. adetii* was significantly different both among reefs and between sexes and that the among-reef differences were independent of the sex of the fish (Table 8). Similarly, ANCOVA demonstrated that the relationship between weight and length in *L. quinquelineatus* was also significantly different both among reefs and between sexes (Table 8). However, the significant among-reef differences were not independent of the sex of the fish (a significant interaction effect occurred between reefs and sex). The differences among reefs were different for each sex (Table 8).

Mortality

In general, individual *L. adetii* less than 7 years of age did not appear to be fully recruited in the sampled

population and were excluded from the mortality estimates derived from catch curves. For RI, JB, LO, and KL, the reef-specific total annual rate of mortality, Z, of *L. adetii*, was 0.179 (fish aged 8–24 years, r^2=0.729, SE=0.0292), 0.304 (fish aged 7–15 years, r^2=0.512, SE=0.1123), 0.225 (fish aged 7–21 years, r^2=0.781, SE=0.0344) and 0.286 (fish aged 9–15 years, r^2=0.795, SE=0.0726), representing an annual survivorship of approximately 83%, 74%, 80%, and 75%, respectively (Fig. 6). The mortality rates of *L. adetii* among reefs were significantly different (homogeneity of slopes test, P<0.01), and a multiple com-

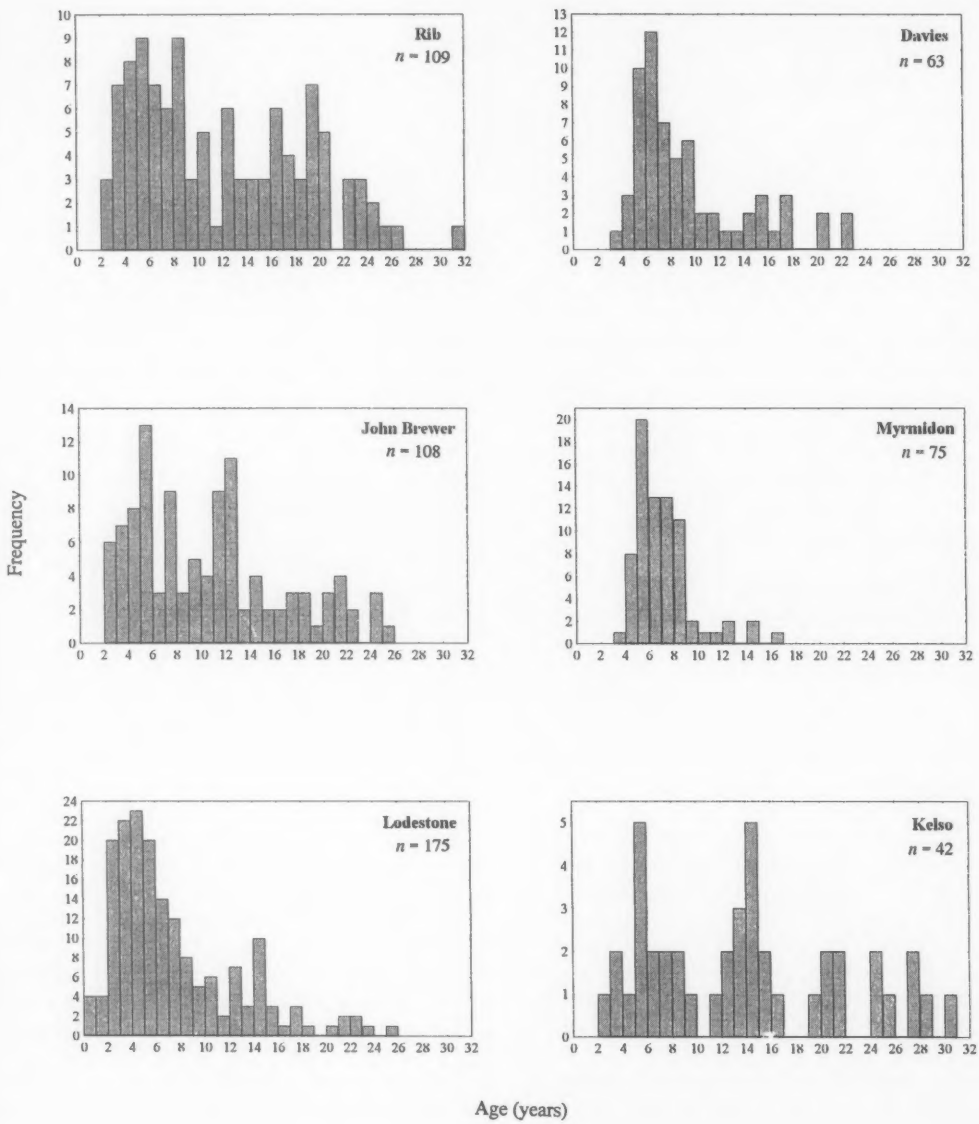

Figure 3

Age-frequency distributions for *L. quinquelineatus* among reefs in the central Great Barrier Reef.

parison of slopes indicated that the mortality rate at Rib Reef was significantly lower than that at all other reefs (RI<[JB=LO=KL]).

Individual *L. quinquelineatus* <5 years of age were usually not fully recruited in the sampled population and were excluded from the mortality estimates derived from catch curves. Estimates of mortality with high coefficients of determination were obtainable from only two reefs, LO and MR. The other reefs had a poor fit to the catch-curve regressions (Fig. 7), and hence mortality rates were not obtained either because there was a persistence of numerous strong

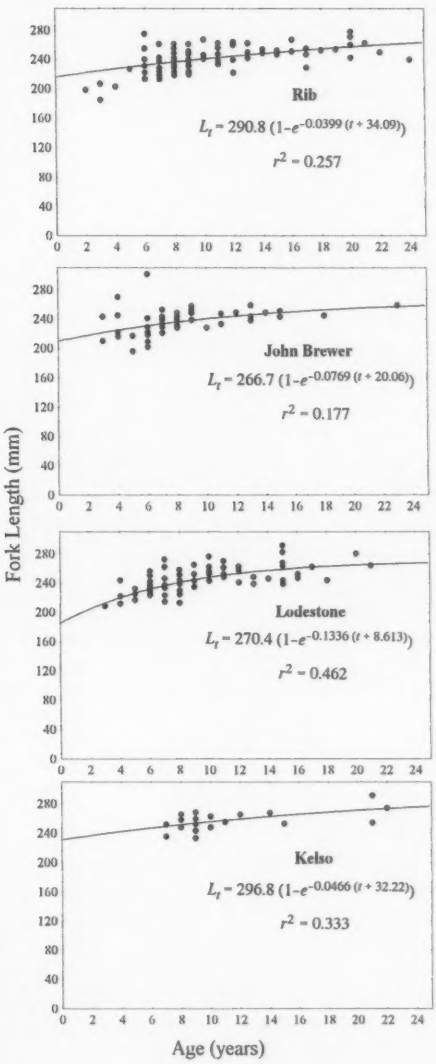

Figure 4

Von Bertalanffy growth curves and observed length at age for *L. adetii* among individual reefs in the central Great Barrier Reef.

Table 5

Growth parameters and asymptotic standard errors (ASE) calculated from the von Bertalanffy growth function, mean fork length (FL, mm), and age (years) for *Lutjanus adetii* and *L. quinquelineatus* among reefs in the central Great Barrier Reef (GBR).

Lutjanus adetii

Parameters	Reefs: Rib (n=122)	John Brewer (n=84)	Lodestone (n=126)	Kelso (n=23)	All reefs pooled central GBR (n=369)
L_∞ (FL)	290.8	266.7	270.4	296.8	265.2
ASE	59.95	34.27	8.93	119.4	4.229
K	0.0399	0.0769	0.1336	0.0466	0.1454
ASE	0.0511	0.0959	0.0484	0.1638	0.0285
t_o	–34.09	–20.06	–8.613	–32.22	–8.077
ASE	31.26	22.10	3.961	94.31	2.132
r^2	0.257	0.177	0.462	0.333	0.390
FL_{mean} (SE)	240.3 (1.48)	234.6 (1.67)	242.0 (1.39)	256.7 (2.59)	241.1 (0.88)
FL_{min}	185	196	209	233	185
FL_{max}	285	301	291	291	301
t_{mean} (SE)	10.24 (0.397)	7.79 (0.350)	8.93 (0.314)	11.17 (0.934)	9.27 (0.206)
t_{min}	2	3	3	7	2
t_{max}	24	23	21	22	24

Lutjanus quinquelineatus

Parameters	Reefs: Rib (n=110)	John Brewer (n=108)	Lodestone (n=175)	Davies (n=63)	Myrmidon (n=75)	Kelso (n=42)	All reefs pooled central GBR (n=577)
L_∞ (FL)	214.1	204.1	198.1	211.5	208.0	220.4	206.9
ASE	5.221	1.665	1.697	2.417	11.26	2.72	0.979
K	0.1125	0.3138	0.4665	0.3048	0.1711	0.2182	0.3064
ASE	0.0433	0.0506	0.0367	0.0694	0.1290	0.0474	0.0174
t_o	–14.12	–2.789	–1.108	–2.313	–8.238	–3.978	–2.587
ASE	5.774	0.8787	0.1942	1.456	7.443	1.588	0.2708
r^2	0.421	0.652	0.745	0.603	0.267	0.752	0.638
FL_{mean} (SE)	198.5 (1.5)	193.2 (1.5)	180.3 (1.9)	199.3 (1.6)	190.5 (1.3)	207.0 (2.8)	191.6 (0.8)
FL_{min}	148	146	60	163	170	155	60
FL_{max}	231	230	230	224	219	233	233
t_{mean} (SE)	11.6 (0.66)	10.2 (0.59)	6.9 (0.39)	9.06 (0.60)	6.65 (0.28)	13.43 (1.21)	9.12 (0.25)
t_{min}	2	2	< 1	3	3	2	< 1
t_{max}	31	25	25	22	16	30	31

year classes or because there were age-varying mortality rates (Fig. 7). The estimates of total mortality rate, Z, of *L. quinquelineatus* at LO and MR were 0.153 (fish aged 4–22 years, r^2=0.711, SE=0.0245) and 0.335 (fish aged 5–16 years, r^2=0.661, SE=0.0703), representing an annual survivorship of approximately 86% and 72%, respectively. Mortality rates of *L. quinquelineatus* between LO and MR reefs were significantly different (homogeneity of slopes test, P<0.01). Figure 7 shows that mortality rates and hence survivorship of *L. quinquelineatus* among reefs is highly variable.

A comparison of mortality rates among successive years (with a relatively large sample size) could be determined only for *L. quinquelineatus* at LO. The total rate of mortality, Z, of *L. quinquelineatus* at LO in 1992 was 0.176 (fish aged 4–17 years, r^2=0.615, SE=0.0402, n=109), representing an annual survivorship of approximately 84% (Fig. 8), whereas the total rate of mortality, Z, of *L. quinquelineatus* at LO in 1993 was 0.155 (fish aged 3–14 years, r^2=0.409, SE=0.0621, n=64), representing an annual survivorship of approximately 86% (Fig. 8). The mortality rates of *L. quinquelineatus* at LO were not significantly different between successive years (homogeneity of slopes test, P>0.05; Fig. 8). The natural mortality rate, M, of both species among reefs is considered equal to total mortality owing to the negligible amount of fishing mortality.

Table 6

Mean length (FL, mm) of early age classes of *Lutjanus adetii* among reefs and analyses of variance comparing the mean lengths of individual age classes among reefs. Number of samples per age class is in parentheses. ns = not significant.

	Reefs					
	Rib	John Brewer	Lodestone			
Age class	Mean FL	Mean FL	Mean FL	df	*F*	*P*
2+	199.0 (1)	— (0)	— (0)	—	—	—
3+	196.0 (2)	226.5 (2)	209.0 (1)	—	—	—
4+	203.0 (1)	238.3 (4)	226.0 (3)	—	—	—
5+	227.0 (1)	212.2 (5)	226.3 (7)	—	—	—
6+	237.1 (7)	228.5 (17)	234.1 (17)	2, 38	0.744	ns
7+	231.3 (20)	233.2 (26)	234.4 (27)	2, 70	0.507	ns
8+	235.3 (22)	239.6 (11)	238.9 (21)	2, 51	0.920	ns
9+	238.3 (21)	245.5 (6)	243.9 (9)	2, 33	1.825	ns

Table 7

Mean length (FL, mm) of early age classes of *Lutjanus quinquelineatus* among reefs and analyses of variance comparing the mean lengths of individual age classes among reefs. Number of samples per age class is in parentheses. ns = not significant.

	Reefs								
	Rib	John Brewer	Lodestone	Davies	Myrmidon	Kelso			
Age class	Mean FL	Mean FL	Mean FL	Mean FL	Mean FL	Mean FL	df	*F*	*P*
1+	—	—	113.0 (8)	—	—	—	—	—	—
2+	163.0 (3)	160.5 (6)	154.3 (20)	—	—	155.0 (1)	3,26	0.523	ns
3+	179.9 (7)	167.6 (7)	166.8 (22)	163.0 (1)	174.0 (1)	172.0 (2)	5,34	1.171	ns
4+	185.0 (8)	179.1 (8)	179.1 (23)	180.0 (3)	181.1 (8)	173.0 (1)	5,45	0.360	ns
5+	188.7 (9)	187.2 (13)	186.8 (20)	191.7 (10)	187.8 (20)	193.6 (5)	5,71	0.984	ns
6+	193.4 (7)	195.7 (3)	188.6 (14)	193.4 (12)	189.4 (13)	193.0 (2)	5,45	0.754	ns

Discussion

The significant differential growth in length and weight of both species among reefs and between sexes indicates that rates of growth in terms of weight at length of both species was variable at the spatial scale of individual reefs. However, statistical and visual comparisons of the VBGF for *L. adetii* indicate that the pattern of growth in individuals among reefs with increasing age was relatively similar. Because only one gear type was used and the distribution of juvenile *L. adetii* was not determined and is presently not known, it was not possible to obtain a sufficient range of sizes to describe the first few years of growth. The growth patterns of *L. quinquelineatus* described by the VBGF were significantly different among reefs. However, no significant differences were detected in the mean lengths of individuals in age classes 2–6 among reefs (Table 6). These results indicate that initial growth rates among reefs were not significantly different and that the significant differences in the overall growth rates among reefs probably reflected the number of young fish available for capture at each reef.

The necessary pooling of size-at-age data over two different years may have biased the resulting growth patterns, if growth was variable among years. There was, however, no evidence to suggest that growth of either species was variable among years. The pooling of data over a number of years was necessary in order to sample a wide cross section of age classes. The inclusion of size-at-age data over a number of years has the advantage of providing a general description of the growth patterns of each species at each reef. However, large sample sizes covering a

range of age classes from a number of consecutive years would be needed to determine if growth rates were variable between years.

The age structures for populations of *L. adetii* and *L. quinquelineatus* among reefs usually showed several strong year classes that were variable among reefs. The occurrence of strong year classes is well documented in the commercial catches of many temperate species (Hjort, 1914; Sissenwine, 1984; Rothschild, 1986) and has recently been observed in a number of tropical species (Doherty and Fowler, 1994b; Ferreira and Russ, 1995). Year-class strength in both temperate and tropical species has been linked to early life history processes (e.g. Hjort, 1914; Sissenwine, 1984;

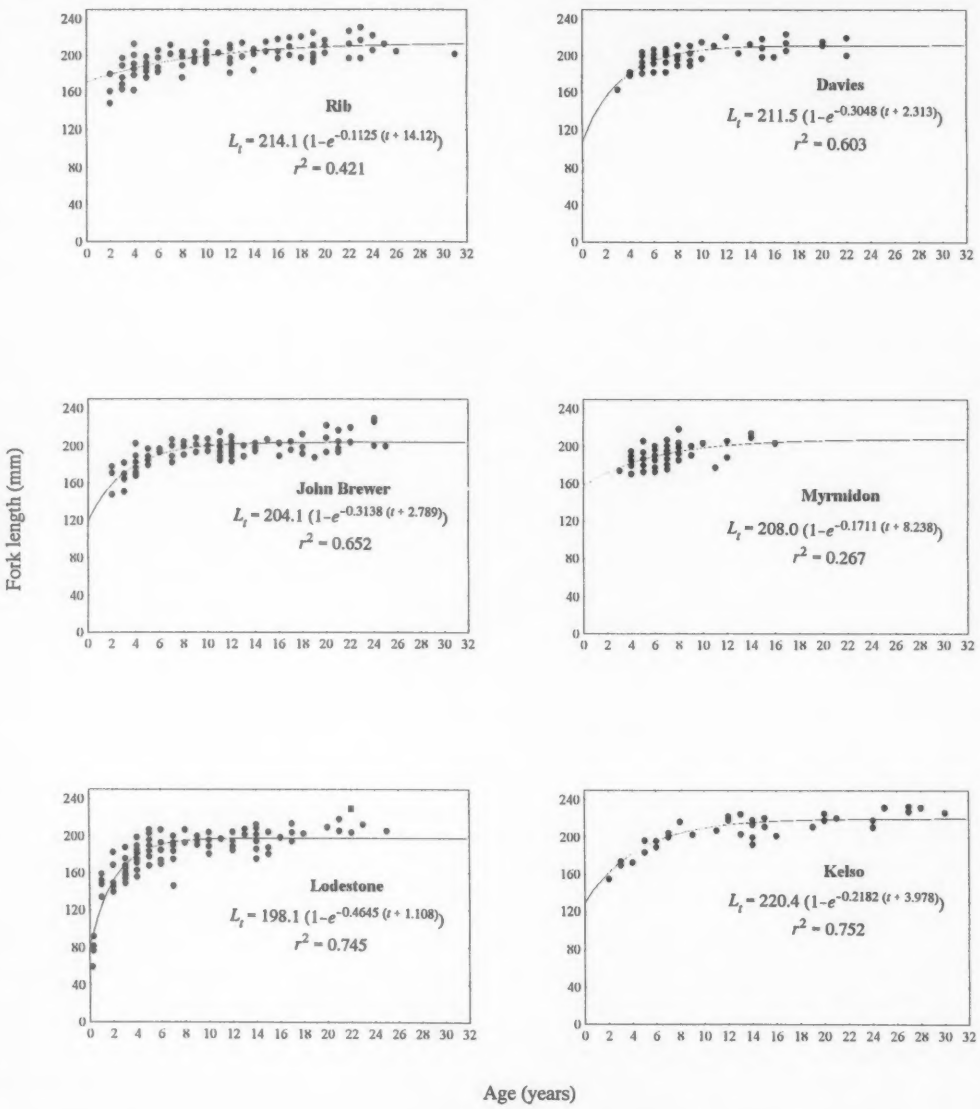

Figure 5

Von Bertalanffy growth curves and observed length at age for *L. quinquelineatus* among individual reefs in the central Great Barrier Reef.

Doherty and Fowler, 1994b). Further, the suggestion that recruitment variability is a major factor influencing both the distribution and local densities of coral reef fishes has been recognized for a number of years (Williams, 1980; Doherty, 1981, 1983, 1991; Victor, 1983; reviews of Doherty and Williams, 1988). Subsequently, Doherty and Fowler (1994b) have shown that for the common tropical damselfish *Pomacentrus moluccensis*, age structures from individual reefs have preserved major temporal variations in the recruitment patterns over at least 10 years, providing empirical evidence of a strong effect of recruitment history on subsequent year-class strength. It is therefore conceivable that the various age structures of both lutjanid species among reefs is a consequence both of variability in recruitment at the localized scale of individual reefs and of good recruitment years persisting in the age structure of populations over time.

Estimates of the rate of natural mortality in fish populations are essential to fishery management (see Ricker, 1975; Gulland, 1983; and Russ, 1991). The mortality rate for *L. adetii* was significantly different among reefs, although these differences were small. The mortality rates for this species in general were low and the rates of survivorship were correspondingly high. Mortality rates for *L. quinquelineatus* were not obtainable from all reefs owing to either the persistence of strong year-class modes, (possibly to nonconstant mortality rates at a number of reefs (although these were not detected among years at Lodestone Reef), or differential mortality of cohorts (as opposed to interannual variability in mean [cross-cohort] mortality rates). The results observed here suggest that interannual variation in recruitment may be retained in the age structure at each reef as found for *P. moluccensis* (Doherty and Fowler, 1994b). Mortality rates derived with the catch-curve method of Beverton and Holt (1957) and Ricker (1975) are based on the assumption that recruitment is constant in the population under con-

Table 8

Analyses of covariance comparing weight at length (transformed to $\log_e$, covariate = length) among reefs and between sexes for *Lutjanus adetii* and *L. quinquelineatus* (significant *P* values are in bold type; note Kelso Reef was not included in the analyses because of the small sample size) and a posteriori multiple comparison of means using Tukey (HSD) analysis (α=0.05).

Source of variation	df	MS	*F*	*P*
L. adetii				
Reefs	2	0.0328	11.917	**< 0.001**
Sex	1	0.0484	17.577	**< 0.001**
Reefs × Sex	2	0.0004	0.127	> 0.85
Residual	266	0.0028	—	—
Tukey HSD analysis among reefs	Lodestone	Rib	John Brewer	
Tukey HSD analysis between sexes	Males	Females		
L. quinquelineatus				
Reefs	4	0.0683	15.647	**< 0.001**
Sex	1	0.0258	5.907	**< 0.05**
Reefs × Sex	4	0.0129	2.948	**< 0.05**
Residual	510	0.0044	—	—
Tukey HSD analysis among reefs				
Male:	Rib	Davies	John Brewer	Myrmidon Lodestone
Female:	Rib	Davies	John Brewer	Myrmidon Lodestone
Tukey HSD analysis between sexes				
Rib:	Males	Females		
John Brewer:	Males	Females		
Lodestone:	Males	Females		
Davies:	Males	Females		
Myrmidon:	Males	Females		

sideration. Mortality estimates derived with the catch-curve regression method are least sensitive to minor violations of this assumption (Ricker, 1975) and this is particularly evident in *L. quinquelineatus*. Despite this, it is evident from Figure 7 that mortality rates of *L. quinquelineatus* are variable among reefs and are similar to those for populations of *L. adetii* in that they are characterized by low rates of total mortality and high rates of survivorship. However, mortality estimates cannot be derived with great confidence from populations where significant recruitment variability is retained in the age structure (e.g. Ferreira and Russ, 1995), and although Ricker (1975) has suggested that irregularities in catch curves caused by variable recruitment can be reduced by combining samples over successive years,

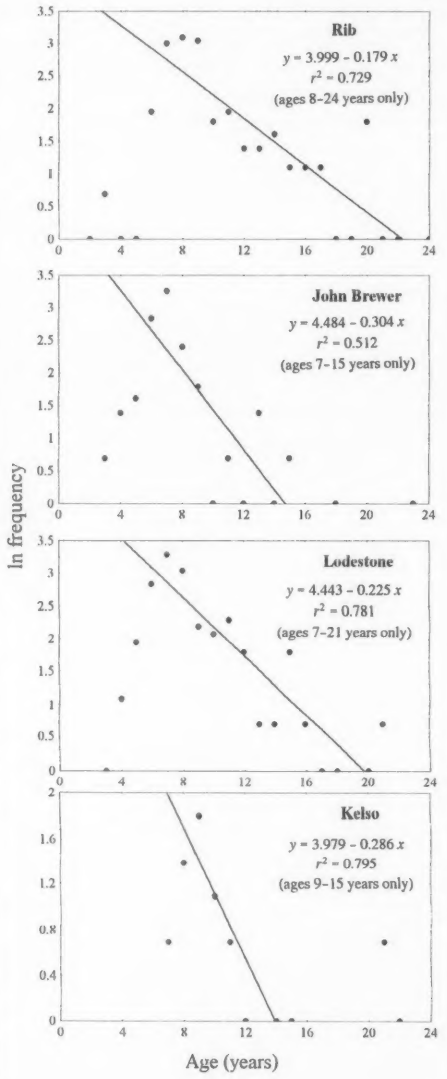

Figure 6

Catch curves for *L. adetii* among reefs, based on observed ages.

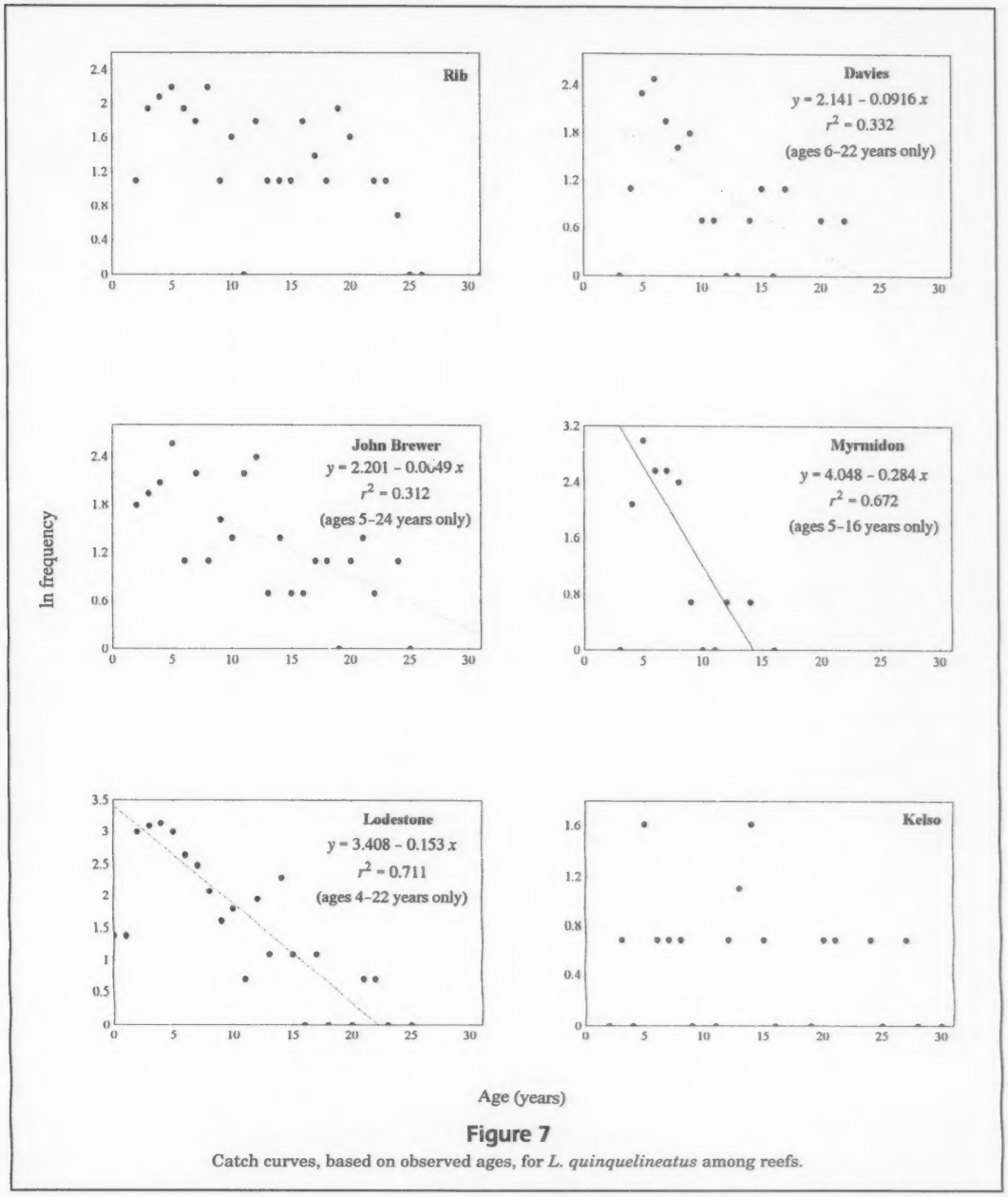

Figure 7

Catch curves, based on observed ages, for *L. quinquelineatus* among reefs.

this method was not expected to reduce variability among age classes in the present study.

However, the mortality rates of *L. quinquelineatus* at Lodestone Reef were not significantly different between successive years (Fig. 8). This result suggests that the variable mortality rates and hence survivorship of these species among reefs may be relatively consistent through time. Similarly, Doherty and Fowler (1994a) suggested that mortality schedules were consistent (not constant) across space and time for two damselfish species from the positive correlations that were present between spatial and temporal variation in recruitment and subsequent abundance. Therefore, the observed differences in mor-

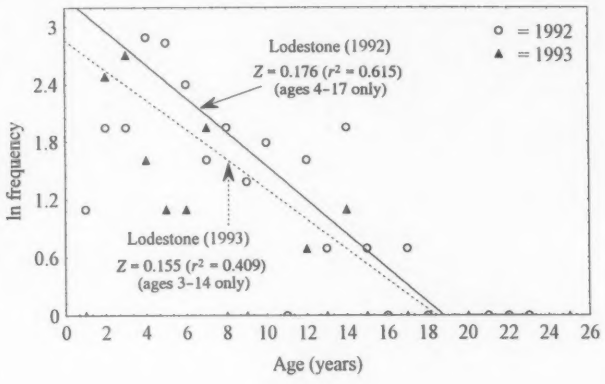

Figure 8

Catch curves for *L. quinquelineatus* from Lodestone Reef between successive years, based on observed ages.

tality rates among reefs for these species are likely to be authentic and not a product of the assumptions inherent in the use of catch curves.

In conclusion, this study demonstrated that significant variability exists in the mortality and age structures of *L. adetii* and *L. quinquelineatus* at the spatial scale of individual reefs. The demography of both these lutjanid species at the spatial scale of individual coral reefs is most likely to be a consequence of the nonequilibrial balance of variable recruitment interacting with density-independent mortality (Doherty and Fowler, 1994b). This spatial variability in demographic parameters among reefs should be considered in the development of management models. The significant differences in mortality rates and age structures for the populations of *L. adetii* and *L. quinquelineatus* among reefs would have more impact on management models than the small differences in growth for these species. Further, greater longevity conveys a selective advantage by increasing the cumulative lifetime fecundity (egg production) of the female parent (see Beverton, 1987). Therefore, in terms of the current management models of the Great Barrier Reef Marine Park, it would be advantageous to protect reefs that are characterized by species with extended longevity and low rates of natural mortality (in comparison with reefs of similar population size but which are characterized by fish with reduced longevity and high rates of natural mortality). The primary advantage of adopting this strategy would be that the spawning biomass of the longer lived fishes would be protected which has the capacity to act as a recruitment source for the surrounding areas that are fished.

Acknowledgments

This work was undertaken while S. J. Newman was a postgraduate fellow at the Australian Institute of Marine Science and contributes in part to the requirements for a Ph.D. degree to S. J. Newman from James Cook University of North Queensland. We gratefully acknowledge financial support from Australian Research Council grants to D. McB. Williams and G. R. Russ and logistical support from the Australian Institute of Marine Science. We thank the crew of the RV *Lady Basten*, the RV *The Harry Messel*, and the RV *Hercules*, as well as volunteers who assisted with fieldwork.

Literature cited

Beverton, R. J. H.
1987. Longevity in fish : some ecological and evolutionary considerations. *In* A. D. Woodhead and K. H. Thompson (eds.), Evolution of longevity in animals: a compariative approach, p. 161–185. Plenum Press, New York, NY.

Beverton, R. J. H., and S. J. Holt.
1957. On the dynamics of exploited fish populations. Fish. Invest. Minist. Agric. Fish. Food (G.B.), Ser. II, 533 p.

Cerrato, R. M.
1990. Interpretable statistical tests for growth comparisons using parameters in the von Bertalanffy equation. Can. J. Fish. Aquat. Sci. 47:1416–1426.

Chen, Y., D. A. Jackson, and H. H. Harvey.
1992. A comparison of von Bertalanffy and polynomial functions in modelling fish growth data. Can. J. Fish. Aquat. Sci. 49:1228–1235.

Davis, T. L. O., and G. J. West.
1992. Growth and mortality of *Lutjanus vittus* (Quoy and Gaimard) from the North West Shelf of Australia. Fish. Bull. 90:395–404.

Doherty, P. J.
1981. Coral reef fishes: recruitment-limited assemblages? Proc. 4th Int. Coral Reef Symp. 2:465–470.
1983. Recruitment surveys of coral reef fishes as tools for science and management. *In* J. T. Baker, R. M. Carter, P. W. Sammarco, and K. P. Stark. (eds.), Proceedings: inaugural Great Barrier Reef conference; Townsville, 28 Aug.–2 Sept. 1983, p. 191–196. JCU Press, Townsville, Australia.
1991. Spatial and temporal patterns in recruitment. *In* P. F. Sale (ed.), The ecology of fishes on coral reefs, p. 261–293. Academic Press, San Diego, CA.

Doherty, P. J., and A. J. Fowler.
1994a. Demographic consequences of variable recruitment to coral reef fish populations: a congeneric comparison of two damselfishes. Bull. Mar. Sci. 54:297–313.
1994b. An empirical test of recruitment limitation in a coral reef fish. Science (Wash. D.C.) 263:935–939.

Doherty, P. J., and D. McB. Williams.
1988. The replenishment of coral reef fish populations. Oceanogr. Mar. Biol. Ann. Rev. 26:487–551.

Druzhinin, A. D., and N. A. Filatova.
1980. Some data on Lutjanidae from the Gulf of Aden area. J. Ichthyol. 20(1):8–14.

Ferreira, B. P., and G. R. Russ.
1995. Population structure of the coralgrouper, *Plectropomus leopardus*, on fished and unfished reefs off Townsville, Central Great Barrier Reef, Australia. Fish. Bull. 93:629–642.

Gulland, J. A.
1983. Fish stock assessment: a manual of basic methods, vol. 1. FAO/Wiley Series on Food and Agriculture, John Wiley and Sons, New York, NY, 223 p.

Higgs, J. B.
1993. Preliminary descriptive analysis of the Great Barrier Reef recreational demersal line fisheries logbook database. M.Sc. thesis, James Cook Univ. North Queensland, Townsville, Australia, 151 p.

Hjort, J.
1914. Fluctuations in the great fisheries of northern Europe viewed in the light of biological research. Rapp. P.-V. Reun. Cons. Perm. Int. Explor. Mer 20:1–228.

Kimura, D. K.
1980. Likelihood methods for the von Bertalanffy growth curve. Fish. Bull. 77:765–776.

Kuiter, R. H.
1993. The complete divers' and fishermen's guide to coastal fishes of south-eastern Australia. Crawford House Press, Bathurst, Australia, 437 p.

Liu, H., and S. Yeh.
1991. Age determination and growth of red emperor snapper (*Lutjanus sebae*) in the Arafura Sea off north Australia. Acta Oceanogr. Taiwan. 26:36–52.

Loubens, G.
1980. Biologie de quelques espèces de poissons du lagon Neo-Caledonian. III: Croissance. Cah. Indo-Pacifique 2:101–153.

Nelson, R. S., and C. S. Manooch III.
1982. Growth and mortality of red snappers in the west-central Atlantic Ocean and northern Gulf of Mexico. Trans. Am. Fish. Soc. 111:465–475.

Newman, S. J.
1995. Spatial variability in the distribution, abundance, growth, mortality and age structures of tropical snappers (Pisces: Lutjanidae) in the central Great Barrier Reef, Australia. Ph.D. diss., James Cook Univ. North Queensland, Townsville, Australia.

Newman, S. J., and D. McB. Williams.
1995. Mesh size selection and diel variability in catch of fish traps on the central Great Barrier Reef, Australia: a preliminary investigation. Fish. Res. (Amst.) 23: 237–253.

Ricker, W. E.
1975. Computation and interpretation of biological statistics of fish populations. Bull. Fish. Res. Board Can. 191, 382 p.

Rothschild, B. J.
1986. Dynamics of marine fish populations. Harvard Univ. Press, Cambridge, England, 277 p.

Russ, G. R.
1991. Coral reef fisheries: effects and yields. *In* P. F. Sale (ed.), The ecology of fishes on coral reefs, p. 601–635. Academic Press, San Diego, CA, 754 p.

Siegel, S., and N. J. Castellan Jr.
1988. Nonparametric statistics for the behavioral sciences, 2nd ed. McGraw-Hill Book Co., New York, NY.

Sissenwine, M. P.
1984. Why do fish populations vary? *In* R. M. May (ed.), Exploitation of marine communities: report of the Dahlem workshop on exploitation of marine communities; 1–6 April, Berlin, p. 59–94. Springer-Verlag, Berlin, Germany. Life Sciences Res. Report 32.

Victor, B. C.
1983. Recruitment and population dynamics of a coral reef fish. Science (Wash. D.C.) 219:419–420.

Williams, D. McB.
1980. Dynamics of the pomacentrid community on small patch reefs in One Tree Lagoon (Great Barrier Reef). Bull. Mar. Sci. 30:159–170.

Winer, B. J.
1971. Statistical principles in experimental design, 2nd ed. McGraw-Hill, Kogakusha, Tokyo, Japan, 907 p.

Zar, J. H.
1984. Biostatistical analysis, 2nd ed. Prentice-Hall Int., Inc., Englewood Cliffs, NJ, 718 p.

Abstract.—Fisheries discard data are often characterized by a smooth distribution of positive amounts of per-set discard but with an extremely large number of zero observations. This discontinuity is difficult to fit with a standard distribution. One approach is to model per-set discard with a mixture of two distributions, with one component representing the zero observations and the other representing the observations of positive discard. In this paper, we describe such a mixture model that is suitable when the discard observations have been rounded to integer amounts. In particular, when "rounded" zeros (representing small amounts of discard) and "true" zeros (representing no discard) are indistinguishable in the data, the mixture model can be used to estimate the proportion of either. We fit this model to tuna discard data collected by observers aboard the U.S. tuna purse-seine fleet in the eastern tropical Pacific Ocean during the years 1989–92. We use the model to estimate discard per set, allowing the model parameters to depend upon fishing strategy and geographic location, and we estimate mean discard per set fisherywide.

Manuscript accepted 26 October 1995.
Fishery Bulletin 94:330–340 (1996).

A mixture model for estimating discarded bycatch from data with many zero observations: tuna discards in the eastern tropical Pacific Ocean

Peter C. Perkins
Elizabeth F. Edwards
Southwest Fisheries Science Center
National Marine Fisheries Service, NOAA
P.O. Box 271, La Jolla, California 92038

Many fisheries catch unwanted individuals of nontarget species in addition to target species. This bycatch is generally discarded and in many fisheries few, if any, individuals survive capture and discard (e.g. Joseph, 1994). Estimating the extent of such discard is increasingly important as fisheries managers contend with situations where unwanted catch in a fishery is desirable in other contexts. For example, bycatch in one fishery may include juvenile members of the target species in the same or another fishery, or individuals from threatened, endangered, or protected species (e.g. Collins and Wenner, 1988; Caillouet et al., 1991).

Despite their increasing importance, bycatch and discard remain relatively unstudied. Few fisheries routinely measure discards so that the amount of discard usually must be estimated rather than reported directly (e.g. Berger et al., 1989). The U.S. tuna purse-seine fishery in the eastern tropical Pacific Ocean (ETP) provides an opportunity to examine this problem because quantitative information on discard of tuna (including both nontarget tuna species and juveniles of target species) has been collected from the fishery since 1988.

A flexible approach is required to model tuna discard from this fishery because the purse-seine vessels capture fish using three distinct fishing strategies. These strategies are defined by the different types of sets involved: "log fishing," "school fishing," and "dolphin fishing." Log fishing catches tuna by setting purse seines around fish associated with floating objects. Log sets usually capture schools of small (30–50 cm) yellowfin tuna, *Thunnus albacares*, or mixed schools of small yellowfin and like-size skipjack tuna, *Katsuwonus pelamis*. School fishing catches tuna by setting purse seines around schools composed purely of tuna (again, usually small fish and either pure schools of yellowfin or mixed schools of yellowfin and skipjack tuna), located by surface disturbances created by the schools. Dolphin fishing catches tuna by first locating surface disturbances created by closely associated dolphins (NRC, 1992) and by setting purse seines around both tuna and dolphins. Tuna associated with dolphins almost always consist of pure schools of large (80–120 cm) yellowfin tuna (IATTC, 1989).

Log fishing generates large amounts of tuna discard in almost every set, whereas school fishing generates

moderate amounts of tuna discard and in a smaller proportion of sets than does log fishing (Joseph, 1994). Dolphin fishing generates small amounts of tuna discard and only infrequently. Thus, tuna discard data from dolphin sets are almost all zero observations, whereas data from log sets are mostly nonzero observations, and school sets are an intermediate case.

In this paper we develop a method for using a single probability distribution to model discard per set for these three disparate types of data and show how to use the model to estimate mean discard per set for each set type. The focus of the present study is development and description of the model as a solution to a common problem in discard estimation. In general, the method presented is applicable to any situation involving analysis of data characterized by subsets with varying proportions of zero observations. Detailed results of applying the model and its implications for the U.S. tuna purse-seine fishery in the ETP are the subject of a future paper.

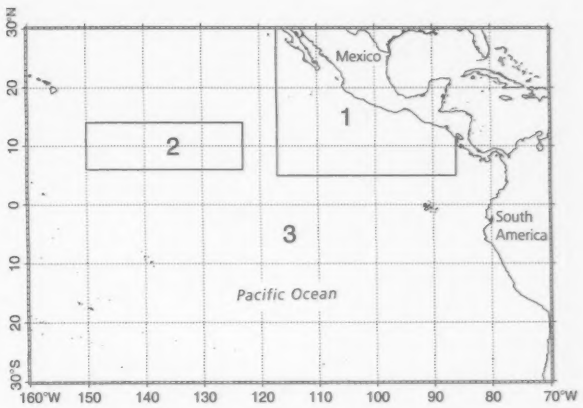

Figure 1

Geographic strata used in developing models to estimate mean discard per set for the U.S. tuna purse-seine fleet fishing in the eastern tropical Pacific Ocean, 1989–92 (Federal Register, 1989). Area 3 includes all ETP not explicitly included in areas 1 and 2.

Methods

Data

The data consisted of per-set estimates of total tons of tuna discarded by the U.S. fleet only. We did not have access to data on species or size composition of tuna discards nor to data on nontuna discards.

Data were collected by National Marine Fisheries Service (NMFS) or Inter-American Tropical Tuna Commission (IATTC) observers placed aboard U.S. tuna purse-seiners during routine fishing trips to the eastern tropical Pacific Ocean (Fig. 1) as part of a bycatch study initiated in 1989 by the IATTC. Observers recorded time and position of all sets made by U.S. vessels fishing in the ETP during the 31-month study period (from 1 September 1989 to 30 March 1992). Observer coverage was 100% during this period. However, during the first eleven months (from 1 September 1989 to 30 July 1990), discard information was recorded only for approximately half of the sets. Observers recorded discards for all sets during the remaining twenty months.

Because it was not feasible to weigh tuna discard directly, observers estimated the discard weight by counting the number of brailers (large fish baskets) used to empty the net after each set, multiplying by an estimated tonnage per brailer, and then multiplying by the estimated fraction of nontarget tuna in the catch. Observers estimated this fraction by observing the composition of brailers or by observing catch sorting on deck. Occasionally the majority of the catch was discarded before being brailed aboard. In these cases, observers estimated discard weight by first estimating the weight of the total catch and then subtracting an estimate of the tonnage loaded by brailer.

Observer estimates of discard tonnage were rounded to integer values, with rounding interval increasing with amount of discard (Fig. 2). There is a systematic tendency toward rounding to the nearest 5 or 10 metric tons (t) for small and medium estimates of discard and to the nearest 25 or 50 t for the largest estimates. For sets with moderately small amounts of discard, observer estimates tended to be more precise because the bycatch, as well as the target fish, were brailed aboard the vessel, then sorted on deck. This allowed the discard to be easily compared with the total catch. For sets with large amounts of discard, the fish may not have been brought on board, making precise estimates more difficult and rounding tendencies greater. For sets with very small amounts of discard, weights were rounded to the nearest ton so that it was not possible to distinguish observations with no discard from those with very small amounts of discard (less than one-half ton). Thus, "zero observations" may correspond to either case.

We did not attempt to account for the uncertainty introduced by these sources of measurement error and rounding. In the absence of data or studies for determining the ground truth of observer estimates

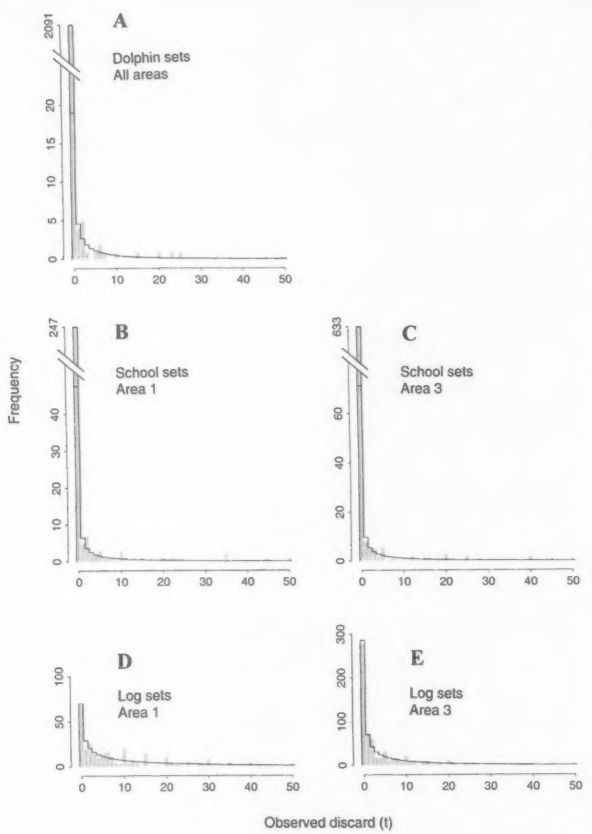

Figure 2

(**A–E**) Observed and fitted per-set tuna discards for school, dolphin, and log sets for the U.S. tuna purse-seine fleet fishing in the eastern tropical Pacific Ocean, 1989–92. Geographic areas are defined in Federal Register (1989) (Fig. 1). Bars indicate observed frequencies, lines indicate fitted frequencies from the negative binomial with added zeros model. Top portion (above horizontal division) of the fitted frequency for the zero bin of dolphin and school set data represents "true zeros," bottom portion represents "rounded" zeros from negative binomial (NB) component. Vertical axes have been cut and scaled to make NB components directly comparable. Not shown: (C) 3 observations >50 tons, (D) 16 observations >50 tons, (E) 12 observations >50 tons.

of discard or in the absence of a plausible model for the measurement errors, we treated the discard weight estimates as exact measurements.

Discard weight was recorded for 59% (2,110 of 3,590, Table 1) of observed dolphin sets, 76% (960 of 1,266) of observed school sets, and 75% (998 of 1,328) of observed log sets. These sets generated 134, 1,098, and 9,819 tons of reported discard, respectively. The relatively small discard totals for school and dolphin sets were due to the large numbers of those sets with zero discard reported. Positive amounts of tuna discard were reported in 65% (650 of 998, Table 1) of log sets for which discard was recorded, but in only 8% (80 of 960) of school sets and only 0.9% (19 of 2,110) of dolphin sets for which discard was recorded. We ignored log and school fishing in area 2 (see next sec-

Table 1

Fishing effort in numbers of sets for the U.S. tuna purse-seine fleet fishing in the eastern tropical Pacific Ocean, 1989–92. Geographic areas are defined according to Federal Register (1989) (Fig. 1). N is the total number of sets in a given area, n is the number of sets for which discard weight was recorded, and n^+ is the number of sets for which strictly positive discard was reported.

Set type	Area	N	n	n^+
Dolphin	1	2,496	1445	10
	2	498	272	5
	3	596	393	4
	Total	3,590	2,110	19
School	1	399	279	32
	2	0	0	0
	3	867	681	48
	Total	1,266	960	80
Log	1	537	326	257
	2	10	4	4
	3	791	672	393
	Total[1]	1,328	998	650

[1] Totals for log sets do not include sets in geographic area 2 because these sets were not included in our analysis. See text for explanation.

tion) for this analysis, because 0 school sets and only 10 log sets (4 with estimated discard) occurred in this area (Table 1). We also omitted 7 sets in which the entire catch (target catch plus discard) was lost owing to equipment failure.

Modelling discard per set

We chose a modified negative binomial (NB) distribution known as the negative binomial with added zeros (NBAZ) (Johnson and Kotz, 1969) to model discard per set. This distribution can accommodate the wide range in the proportion of zero observations, as well as the relatively heavy tails in the observed distributions of discard for all three set types (Fig. 2). (See Discussion section for two other models considered but rejected.)

The NBAZ is a mixture of a NB distribution and a discrete probability mass at zero. Under this model, discard per set is either exactly zero with probability p or has a NB distribution with probability $1-p$. The NB portion of this distribution can be viewed as representing strictly positive amounts of discard rounded to integer values. Thus, zero values that are part of the NB can be interpreted as observations of small amounts of discard rounded down to zero. Zero values from the probability mass can be interpreted as exact zeros. The probability function for this modified NB distribution is

$$\Pr\{Y=y\} = \begin{cases} p+(1-p)\left(\frac{1}{1+a\mu}\right)^{1/a}, & y=0 \\ (1-p)\frac{\Gamma(y+1/a)}{y!\Gamma(1/a)}\left(\frac{1}{1+a\mu}\right)^{1/a}\left(\frac{a\mu}{1+a\mu}\right)^{y}, & y=1,2,\ldots \end{cases} \quad (1)$$

where Y is an individual observation (tons of discard per set), p is the probability of an observation coming from the "true zero" state, $1-p$ is the probability of an observation coming from the NB state, and μ and a are the mean and variance parameters, respectively, of the conditional NB.[1]

The parameter a determines the shape of the distribution. As a approaches zero, the conditional NB distribution in the mixture approaches a Poisson distribution. As a increases, the conditional NB becomes more skewed, with a heavier tail and higher probability of a zero observation. The parameter p is a mixing parameter which controls the relative importance of the NB and the probability mass at zero. When p is one, the distribution is a probability mass at zero. When p is zero, the probability distribution becomes strictly NB and expected discard per set is μ (the NB mean).

The expected value and variance for individual observations from this probability distribution are

$$\mathrm{E}[Y] = (1-p)\mu \quad (2)$$

$$\mathrm{var}[Y] = (1-p)\left(\mu + (a+p)\mu^2\right). \quad (3)$$

We fit the NBAZ model using maximum likelihood and allowing the three model parameters to depend upon set type and geographic area. We also considered using tons of tuna loaded (i.e. commercial catch), time of day, and month as covariates, but rejected them as either unfeasible (due to sampling unbalance) or statistically unimportant. We did not attempt to account for any long-term (i.e. year to year) trend in discard rates because the data included too few years for such an analysis.

A priori, we used the same three geographic areas (Fig. 1) as those currently used to compare U.S. and non-U.S. dolphin mortality rates (Federal Register, 1989). These roughly define the major fishing areas in

[1] The NBAZ can be equivalently reparametized in terms of a "zero-truncated" NB and a probability mass at zero. The parameter corresponding to p would, in that case, denote the probability of a zero observation regardless of source. Thus, that form does not distinguish between "true" and "rounded" zeros.

the system. The total number of sets observed in each area, including sets for which discard was not recorded, represents the actual areal distribution of fishing effort during the study period. However, observation of discard was not proportional to this distribution of total effort (Table 1). In the analysis that follows, it is important to distinguish between the total number of sets, denoted by $N_{i,j}$, and the number of sets for which discard was recorded, denoted by $n_{i,j}$. The former define the actual distribution of fishing effort, whereas the latter simply reflect the sample taken. Because our sample of sets with discard recorded was not proportional to the total effort, ignoring area in the analysis could lead to biased estimates if the mean discard per set differs from area to area for a given set type.

Because there were clear differences between the the three set types in per-set discard, we included set type as a covariate for all three model parameters. Thus, with set type and geographic area as the only covariates, our analysis reduced to fitting the model (Eq. 1) independently for each set type, with p, μ, and a having possibly different values in each area. To determine an appropriate dependence upon area, we used stepwise likelihood-ratio tests to select the simplest model that could not be significantly improved by adding additional terms. We first made initial fits for each set type using no areal dependence, then progressively added dependence for more of the model parameters. At each step, we used a quasi-Newton numerical optimization algorithm to maximize the likelihood and estimate parameters. It should be noted that because this is not a linear model, significance levels (i.e. p-values) from these likelihood-ratio tests are approximate. We used the large-sample normal approximation for MLE's to compute standard errors for p, μ, and a. For comparison, we also computed bootstrap standard errors.

It can be shown from the likelihood equations for the NBAZ that estimates for the parameters a and μ depend solely on the positive observations in the data. The estimate for the parameter p depends on all the data, but most strongly upon the proportion of zero observations. Thus, the precision of the estimates for a and μ can be very poor if the data contain few positive observations, even though the precision of the estimate for p may still be very good.

Estimating mean discard per set

We used Equation 2 and the maximum likelihood estimates for p and μ from the best-fit models to estimate mean discard per set for each set type in each area. We also calculated a "pooled" estimate for each set type as the weighted average of the area-specific estimates, where weightings were proportional to total effort in each area. For example, mean discard per set of type i in area j is estimated as

$$\hat{\mathrm{E}}[Y_{i,j}] = (1 - \hat{p}_{i,j})\hat{\mu}_{i,j}, \tag{4}$$

whereas the "pooled" estimate for all areas combined is estimated as

$$\hat{\mathrm{E}}[Y_i]_{pooled} = \sum_j N_{i,j}\hat{E}[Y_{i,j}] \Big/ \sum_j N_{i,j}, \tag{5}$$

where $N_{i,j}$ is the total effort (in number of sets) of type i occurring in area j. Note that this "pooled" calculation is based on the proportion of total sets (including those for which discard was not recorded) observed in each area. This is an estimate of the mean discard per set over the entire fishery during the study period. However, it is also valid as a prediction of future discard if the proportion of effort (sets) in each area remains constant as the actual number of sets varies, assuming that other factors in the fishery, such as size and species composition of discard and style of fishing, remain the same.

While Equation 4 provides a straightforward way to compute the MLE for the product $(1–p)\mu$, the variance of that product can be difficult to estimate accurately. However, we were able to use the likelihood equations for the NBAZ to derive explicit forms for the MLE of mean discard per set. Specifically, only the product $(1–p)\mu$ need be estimated, and we derived, through algebraic manipulation of the likelihood equations, simple closed-form expressions that do not involve the individual parameter estimates. By the invariance properties of maximum likelihood estimates, these simpler forms give results that are identical to those from using Equation 4.

With no areal dependence, the MLE for the product $(1–p)\mu$ is simply the sample mean:

$$\hat{\mathrm{E}}[Y] = \bar{y} = (1/n)\sum_k y_k, \tag{6}$$

where the set type subscript i is suppressed for clarity. Similarly, with complete areal dependence, the MLE for each area reduces to the sample mean in that area, and the "pooled" estimate is computed by using Equation 5. In both of these cases, the variance for the MLE of $(1–p)\mu$ can be estimated by using the sample variance of the data.

When only the mixing probability p depends on area, the MLE for mean discard per set in area j is slightly more complicated, and reduces to

$$\hat{E}[Y_j] = (n_j^+ / n_j) \sum_k y_k^+ / n^+, \quad (7)$$

where n_j^+ and n_j are the number of positive observations and the total number of observations in area j, the y_k^+ are the positive observations in all areas, and n^+ is the total number of positive observations in all areas. Similarly, when only the NB mean μ depends on area, the MLE for mean discard per set in area j reduces to

$$\hat{E}[Y_j] = (n^+ / n) \sum_k y_{j,k}^+ / n_j^+, \quad (8)$$

where n^+ and n are the number of positive observations and the total number of observations in all areas, the $y_{j,k}^+$ are the positive observations in area j, and n_j^+ is the total number of positive observations in area j. Again, Equation 5 is used to compute "pooled" estimates in these latter two cases. Note that the estimates for different areas are not independent, because both Equations 7 and 8 involve observations from all areas. In particular, the first term in Equation 7 is an area-specific estimate of the probability of a positive observation, whereas the second term is a "pooled" estimate of the mean for positive observations. This is consistent with the areal dependence on which Equation 7 is based, and provides more precise estimates of E[Y] than simply taking the sample mean in each area. A similar interpretation holds for Equation 8.

As a consequence of Equations 6, 7, and 8, the estimate of mean discard per set $(1-p)\mu$ can be much more precise than the estimates of the individual parameters involved in it, because it does not depend solely on either the positive observations or the proportion of zeros.

While variance estimators for Equation 6 are straightforward, there is no simple analytic result for estimating the variance of Equations 7 or 8 (see Discussion). Thus, for consistency, we used bootstrap methods in all cases. Our bootstrap resampling procedure varied slightly for each set type, depending on the particular areal dependence chosen for the model parameters. When no dependence was appropriate, data were resampled across all areas. When dependence was important, data were resampled by area in the same proportions as the original observations.

Results

Modelling discard per set

Based on the results of likelihood-ratio tests, geographic area was a statistically significant predictor of discard per set for only two of the three set types (log and school sets).

Nonzero observations of discard from the third set type (dolphin sets) were reported very infrequently (19 out of 2,110 sets, Table 1). The data provided little statistical information from which to distinguish patterns in discard between geographic areas, and area failed to produce a significant improvement in the fit when included as a covariate for dolphin sets. Therefore, we selected the model with no areal dependence for any of the parameters so that the estimates for p, a, and μ for dolphin sets are fisherywide values (Table 2). The standard error of the mixing parameter p for the dolphin model is small (CV=1.53%), reflecting the high estimate for p dictated by the extremely large number of zero observations of discard. The standard errors of the parameters for the NB portion of the probability distribution (a and μ) are quite large (CV's > 90%, Fig. 3), reflecting the few positive data available for their determination.

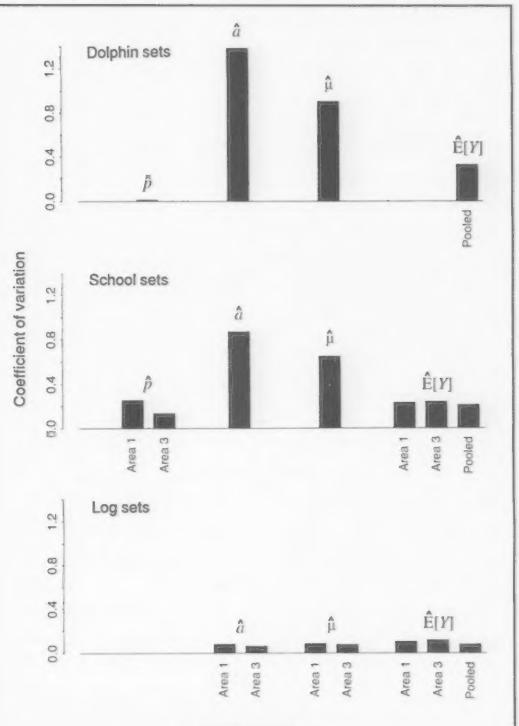

Figure 3

Coefficients of variation for estimates of the model parameters p, a, and μ, and for estimates of mean discard per set for the U.S. tuna purse-seine fleet fishing in the eastern tropical Pacific Ocean, 1989–92. Geographic areas are defined in Federal Register (1989) (Fig. 1). Pooled estimates are fisherywide, across all areas.

Table 2

Parameter estimates from a fit of the negative binomial with added zeros to tuna discard data from the U.S. tuna purse-seine fleet fishing in the eastern tropical Pacific Ocean, 1989–92. p is the mixing parameter, and μ and a are the mean and shape parameters of the conditional negative binomial. Standard errors are in parentheses. Geographic areas are defined according to Federal Register (1989) (Fig. 1).

		School sets		Log sets	
Parameters	Dolphin sets	Area 1	Area 3	Area 1	Area 3
p	0.982 (0.015)	0.715 (0.182)	0.825 (0.111)	0 (0)	0 (0)
μ	3.53 (3.21)	5.53 (3.60)		15.4 (1.3)	7.09 (0.55)
a	3.87 (5.36)	7.20 (6.28)		2.34 (0.19)	3.93 (0.25)

At the other extreme, nonzero discard observations were very frequent for log sets (650 out of 998 sets, Table 1). Using fishing area as a covariate for both the mean and shape parameters μ and a, we improved the fit significantly (p-value <0.001) over simpler models. However, the numerical optimization failed to converge to a positive value for p in either area, producing estimates of zero for p in both areas (Table 2). Thus, the estimated probability distributions effectively collapsed to unmodified NB's. Because positive observations were so abundant, estimated standard errors for the mean and shape parameters (Table 2) were small (CV's <8.5%, Fig. 3).

Discard from school sets presented an intermediate case in which we selected a model which included marginally different estimates for the mixing probability p in areas 1 and 3, but no geographic dependence for a or μ (Table 2). Because there were considerably fewer nonzero observations (80 out of 960 sets, Table 1) for school sets than for log sets, parameter estimates were much less precise. Likelihood-ratio tests indicated that fishing area should be included as a covariate for either the shape parameter a or the mixing probability p, but that including areal dependence for p and a simultaneously, or for μ, did not further improve the fit. Because the approximate p-values for adding areal dependence to the two parameters were fairly similar (0.04 for a, 0.12 for p) and the two parameters have similar effects in the model,[1] there was no clear basis for selecting one parameter over the other. We subsequently decided to include areal dependence only for p for two reasons. First, the small number of positive observations for school sets limits the precision of the shape estimate. Second, the difference in the estimated shape between areas was due mainly to two unusually large observations in area 3. Without these two observations, the difference in estimated shapes was reduced, and the significance levels of the two different models were nearly equal (approximate p-values of 0.09). As was the case for dolphin sets, the predominance of zeros in the school set discard data led to small estimated standard errors for the mixing probability p (CV's <13.5%, Fig. 3) but to large estimated standard errors for the mean and shape parameters (CV's > 65%, Fig. 3).

In our model, p may be interpreted as the probability of exactly zero discard, as opposed to small amounts of discard that have been rounded down to zero in the data. The estimates of p for the three set types imply that essentially all dolphin sets (98%) involve no discard, whereas log sets always involve at least some discard. Observer experience[2] indicates that this result is consistent with generally observed patterns for dolphin and log sets.

The estimated shape parameters varied widely between the three set types (Table 2), but the large standard error estimates for the school and dolphin shape parameters prevent us from making any strong statements about shape as a function of set type. As mentioned above, the estimated shape parameter for school sets was strongly affected by the presence of two unusually large observations (100 and 125 tons of discard) in area 3. Repeating the analysis without these two observations led to a shape estimate of 3.75 (SE=2.10), which is more similar to the shape estimates for log sets (2.94 for area 1, 3.93 for area 3).

We could not use bootstrap methods to compute standard errors for dolphin sets because there were so few sets observed with positive discard recorded (Table 1). In resampling for the bootstrap, approximately one-third of the samples contained too few positive observations for the maximum likelihood algorithm to converge. Therefore, Table 2 includes only the standard errors computed from the analytic approximation formulae.

[1] p and a are similar in the effect they have on the estimated distribution. Increasing either one increases the probability of a zero observation, although increasing a also increases the probability of a large observation.

[2] Jackson, A. 1994. Southwest Fisheries Science Center, Natl. Mar. Fish. Serv., P.O. Box 271, La Jolla, CA 92038. Personal commun.

Estimating mean discard per set

Because the model we fitted for discard from log fishing reduced to a simple NB distribution (with $\hat{p}=0$), the estimates of mean discard per log set in each fishing area are just the corresponding mean parameters μ_j. Mean discard per school or dolphin set was estimated with Equation 4.

Estimates of mean discard per log set were an order of magnitude larger than those for school sets and two orders of magnitude higher than those for dolphin sets (Fig. 4). Most of this difference is due to the wide range in the estimated proportion of sets with zero discard. By comparison (Table 2), estimated mean parameters for the NB component of the model differ by less than a factor of five. Thus, the model that we fitted indicates that, on average, there is a considerable difference among set types in per-set discard, although for sets in which discard actually occurs, there is comparatively less difference in the amount.

Mean discard for log sets was estimated at 10.5 t per set pooled over areas, ranging from 7.1 t per set in area 1 to more than double that value (15.4 t per set) in area 3 (Fig. 4). Mean discard for school sets was estimated at 1.16 t per set pooled over areas, ranging from 1.57 t in area 1 to 0.97 t in area 3. Mean discard per set for dolphin sets was estimated at 0.06 t per set fisherywide. Implications of these results for the fishery are discussed in another study (Edwards and Perkins, in prep.).

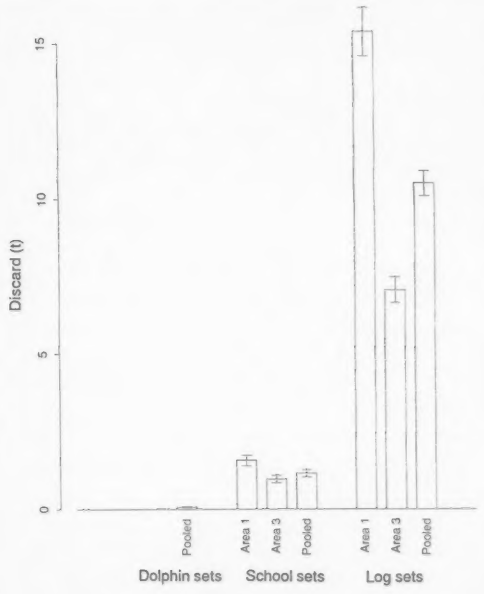

Figure 4

Estimated mean tuna discard per set for the U.S. tuna purse-seine fleet fishing in the eastern tropical Pacific Ocean, 1989–92. Geographic areas are defined in Federal Register (1989) (Fig. 1). Pooled estimates are fisherywide, across all areas. Standard errors are indicated by error bars.

The coefficients of variation (CV's) for the estimates of mean discard per school and dolphin sets (21% and 33%, respectively) are much smaller than those for the individual parameter estimates of α and μ (Fig. 3). As noted in Methods, this is because estimating mean discard per set (i.e. $(1-p)\mu$) is a more robust procedure than estimating the individual parameters. In the case of log sets, the CV's for the estimates of $E[Y]$ and μ differ (Fig. 3), even though in this case the model reduced to a NB distribution where $E[Y] = \mu$. The CV's differ because in estimating variances for the individual parameter estimates we used analytic approximations, while in estimating variances for mean discard, we used bootstrap methods (see Methods).

Where possible (i.e. log and dolphin sets), we estimated variances using the analytic expression in Equation 10 (see Discussion) and found that the results agreed with bootstrap estimates to within about 5%.

Note that the fisherywide estimates for log and school sets are not simply the average of the estimates in each fishing area. This is because the number of sets in each area for which discard was recorded was not proportional to the actual number of sets made in that area. This imbalance was an important reason for including geographic area in the analysis. Nonproportional sampling was not a factor for dolphin sets, because the estimated discard in that case was the same for all fishing areas.

Discussion

Estimating model parameters

Our approach differs somewhat from that of Mangel and Smith (1990), who used the NBAZ to estimate the total biomass of a fish stock. In their analysis, observations of catch from within a stock's geographic range were modelled with the NB component, while the probability mass at zero accounted for observations from outside the range. The sole parameter of interest was the mean μ of the NB component, and fixed values were assumed for the mixing and shape parameters p and α. They reduced the count data to "presence-absence" and derived a likelihood for μ in terms of that reduction. In contrast, we were inter-

ested in estimating the mean of all observations (including "true zeros") and in modelling per-set discard, which requires estimates of p and a. Therefore, we did not follow their approach because we did not have any a priori values for p and a. Reducing counts to simple presence-absence would have decreased the information in the sample such that estimation of the full set of parameters would not have been possible.

Estimating variances for model parameter estimates

The analytic approximation formulae that we used to estimate the variance of the individual parameter estimates are based on the asymptotic normality of MLE's. Since this method uses the estimates for p, a, and μ (rather than their unknown "true" values) in the information matrix, it suffers from the tendency for ML estimates of variance to be biased downwards (e.g. Efron, 1992). We did not attempt to "bias correct" these variance estimates.

When a variance estimate is based on a normal approximation to the sampling distribution of the parameter, the accuracy of the approximation should always be investigated. One way to help validate the normality assumption is to use results from bootstrapping to approximate the sampling distribution. Figure 5 illustrates some examples for the current data. Histograms of the bootstrap replicate parameter estimates for dolphin set data were very skewed. By implication, the normal-approximation variance estimates for the dolphin data, while convenient, are probably not satisfactory. For school set data, histograms of the replicates were slightly skewed because of a small number of unusually large observations. Bootstrap standard errors were consistently higher than the analytic approximations, indicating that the latter may be optimistic. For log set data, histograms were close to normality, and bootstrap standard errors were very similar to those from the analytic approximations. The analytic estimates in this case are probably appropriate.

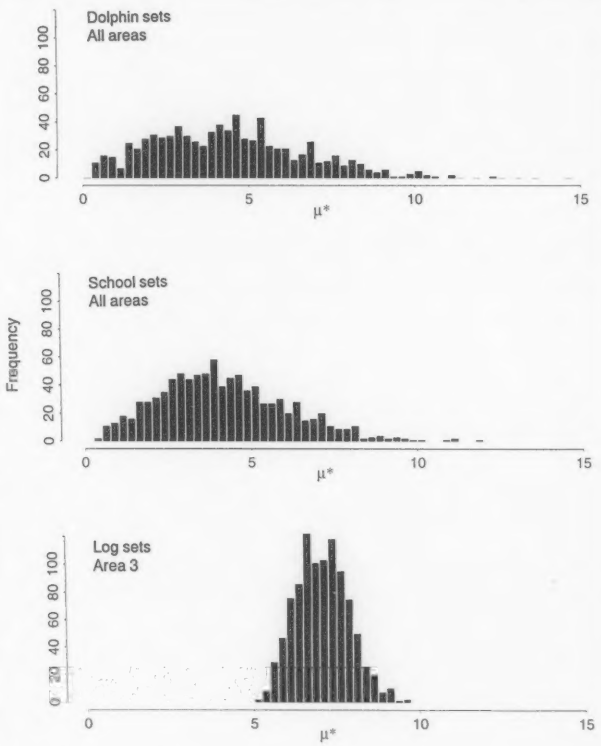

Figure 5

Sample histograms of 1,000 bootstrap replicates of estimates of the negative binomial mean parameter μ, for dolphin, school, and log sets. See text for a complete description of the parameter.

Estimating variances for mean discard per set estimates

In an attempt to derive analytic formulae for the variance of our estimates of E[Y], we manipulated the likelihood equations for the NBAZ and found simplified forms for the MLE of E[Y]. In some cases, the simplified form reduces to the sample mean, Equation 6, and the variance of that estimator is simply (suppressing area and set type subscripts for simplicity)

$$\begin{aligned} \operatorname{var}\left(\hat{\mathrm{E}}[Y]\right) &= (1/n)\operatorname{var}[Y] \\ &= (1/n)(1-p)\left(\mu+(a+p)\mu^2\right), \end{aligned} \tag{9}$$

which can be estimated by substituting MLE's for a, μ, and p. More simply, by using the fact that the estimator is just the sample mean, the minimum variance unbiased estimate of Equation 9 is the sample variance,

$$\hat{\operatorname{var}}\left(\hat{\mathrm{E}}[Y]\right) = \left[\sum_i (y_i - \bar{y})^2\right]/(n-1), \tag{10}$$

where $\bar{y}$ is the sample mean. In other cases, the simplified forms for the MLE of E[Y] are slightly more complex (Eqs. 7 and 8), and Equations 9 and 10 no longer apply. We did derive expressions, analogous to Equation 9, for the variance of Equations 7 and 8 in terms of the three model parameters p, α, and μ. However, these formulae are so complex as to be of no practical use in estimation, and no expression analogous to Equation 10 seems possible.

Rounding errors in the observations

The NBAZ model used in this study comprises two components. As noted in the description of the model, zero values derived from the NB component can be interpreted as observations of small amounts of discard, rounded down to zero, whereas zero values from the probability mass component can be interpreted as exact zeros. This interpretation is based on the assumption of an underlying continuous distribution for positive discard amounts (e.g. a gamma distribution) upon which rounding errors have been superimposed.

One consequence of this interpretation is that the mean amount of discard that should be associated with "true zeros" is zero, and the mean amount that should be associated with "NB zeros" is nonzero. Thus, strict adherence to this interpretation of zeros leads to the conclusion that Equation 4 may be an underestimate of E[Y]. However, if we assume a strictly decreasing underlying distribution for positive discard, symmetric rounding of amounts larger than one-half ton would tend to increase the estimate. In the absence of a specific model for the rounding errors, we did not attempt to correct for any bias due to rounding.

The EM algorithm for maximizing likelihood

We used a quasi-Newton algorithm to maximize likelihood for the parameters p, α, and μ. A useful alternative for mixture models, including "added zero" distributions, uses the EM algorithm to maximize likelihood (e.g, McLachlan and Basford, 1988; Lambert, 1992). In situations with many covariates, it provides a well-behaved alternative to the high-dimensional gradient search required by general optimization algorithms. The algorithm can be implemented by using standard regression techniques for generalized linear models. We applied the EM algorithm to the NBAZ using a combination of logistic regression to maximize likelihood for p and quasi-likelihood NB regression for μ and α (Lawless, 1987). However, the logistic regression failed to converge for the current data because the ML estimate of p for log sets was zero.

Alternative models considered

We considered but rejected two alternatives to the NBAZ model: 1) the Δ-distribution (a mixture of a probability mass at zero with a lognormal [Aitchison, 1955; Pennington, 1983]); and 2) a Γ-distribution mixed with a probability mass at zero (Coe and Stern, 1982). Both have been used in similar cases where the data to be analyzed have contained large numbers of zeros. The Δ-distribution assumes that the natural logs of the positive observations are distributed normally, or can be so transformed, and this assumption was not plausible. The data in this analysis were rounded to the nearest ton and the mode of the positive observations was one ton. Thus, no transformation could bring these data to even approximate normality. The gamma mixture model was not appropriate for the current data because maximum likelihood estimation for a highly skewed gamma distribution depends heavily upon small (near zero) observations. In this study, all observations in that region were rounded to either zero or one, implying a large relative measurement error and therefore potentially poor accuracy. Another more fundamental reason why we rejected these two models was that both models mix a continuous distribution on the positive numbers with a probability mass at zero and assume that observations from each component remain distinguishable. In the current data set, small positive observations are grouped together with zero observations, and using an NB in the mixture allows the model to distinguish between "true zeros" (actual absence of discard) and "rounded zeros" (discard so small that it was ignored or missed).

Conclusions

The methods developed here were used to model fisheries discard data which were rounded to integer values and which included widely varying numbers of zero observations, depending on one or more covariates. The usual models for integer-valued data (e.g. the Poisson distribution) did not fit the data at all well because of the extreme skewness of some of the observed distributions. The NBAZ is more flexible than the standard models and provided a much better fit. In general, the model is applicable to any set of integer-valued data which exhibit a large proportion of zero observations combined with long positive tails. Both categorical and continuous covariates may be used.

Modelling these data with a parametric probability distribution allowed us to describe patterns in the discard in some detail, for example, in estimating the percentage of "true zeros" in the data. Addi-

tionally, we were able to examine whether differences in mean discard were due to different proportions of zero observations or to different distributions of positive observations. In contrast, computing sampling-based estimates of population mean and variance would not give any indication of the patterns in the individual observations. While average or total discard is of significant interest, it is also important to quantify the amount of discard possible for an individual set. Assuming that the parametric model is accepted as appropriate, one can estimate, for example, the probability that, owing to random chance alone, discard from a particular boat will exceed a certain limit in a fixed number of sets. One can also estimate the percentage of zero observations which actually represent small amounts of discard. Finally, a parametric model provides a natural framework for predicting future discard.

Acknowledgments

We thank Al Jackson for his generous help and advice about data collection methods and data form interpretation, Pierre Kleiber for his comments on an earlier version of this manuscript, and the Inter-American Tropical Tuna Commission for making available their data on U.S. tuna vessel tuna discards. We especially thank Cleridy Lennert of the IATTC for her helpful suggestions. We also thank Ronald Hardy and two anonymous reviewers whose helpful suggestions added to the clarity of our manuscript.

Literature cited

Aitchison, J.
1955. On the distribution of a positive random variable having a discrete probability mass at the origin. J. Am. Stat. Assoc. 50:901–908.

Berger, J. D., R. F. Kappenman, L. L. Low, and R. J. Marasco.
1989. Procedures for bycatch estimation of prohibited species in the 1989 Bering Sea domestic trawl fisheries. U.S. Dep. Commer., NOAA Tech. Memo. NMFS-F/NWC-173, 23 p.

Caillouet, C. W., Jr., M. J. Duronslet, A. M. Landry Jr., D. B. Revera, D. J. Shaver, K. M. Stanley, R. W. Heinly, and E. K. Stabenau.
1991. Sea turtle strandings and shrimp fishing effort in the northwestern Gulf of Mexico, 1986–89. Fish. Bull. 89:712–718.

Coe, R., and R. D. Stern.
1982. Fitting models to daily rainfall. J. Appl. Meterol. 21:1024–1031.

Collins, M. R., and C. A. Wenner.
1988. Occurrence of young-of-the-year king, *Scomberomorus cavalla,* and Spanish, *S. maculatus,* mackerels in commercial-type shrimp trawls along the Atlantic coast of the southeast United States. Fish. Bull. 86:394–397.

Efron, B.
1992. Six questions raised by the bootstrap. *In* R. LePage and L. Billard (eds.), Exploring the limits of the bootstrap, p. 99–126. John Wiley and Sons, New York, NY.

Federal Register.
1989. Interim final rule with request for comments;Tuesday, 7 March 1989. Federal Register, Vol. 54(43), Rules and Regulations:9438–9451.

IATTC (Inter-American Tropical Tuna Commission).
1989. Annual Report: 1988. Inter-American Tropical Tuna Commission, La Jolla, CA.

Johnson, N. L., and S. Kotz.
1969. Distributions in statistics: discrete distributions. Houghton Mifflin, Boston, MA, 187 p.

Joseph, J.
1994. The tuna-dolphin controversy in the eastern Pacific Ocean: biological, economic, and political impacts. Ocean Developments and International Law 25:1–30.

Lambert, D.
1992. Zero inflated Poisson regression, with an application to defects in manufacturing. Technometrics 34(1):1–14.

Lawless, J. F.
1987. Negative binomial and mixed Poisson regression. Can. J. Stats. 15(3):209–225.

Mangel, M., and P. E. Smith.
1990. Presence-absence sampling for fisheries management. Can. J. Fish. Aquat. Sci. 47(10):1875–1887.

McLachlan, G. J., and K. E. Basford.
1988. Mixture models: inference and applications to clustering. Marcel Dekker, New York, NY, 253 p.

NRC (National Resource Council).
1992. Dolphins and the tuna industry. National Academy Press, Washington, D.C., 176 p.

Pennington, M.
1983. Efficient estimators of abundance for fish and plankton surveys. Biometrics 39(1):281–286.

Demographic analysis of the sandbar shark, *Carcharhinus plumbeus*, in the western North Atlantic*

Thomas R. Sminkey

Florida Marine Research Institute, Department of Environmental Protection
100 Eighth Avenue SE, St. Petersburg, Florida 33701

John A. Musick

Virginia Institute of Marine Science, School of Marine Science
College of William and Mary, Gloucester Point, Virginia 23062

Abstract.—The sandbar shark, *Carcharhinus plumbeus*, is the most common large coastal shark in Virginia waters and is an important component of recreational and commercial fisheries along the east coast of the United States. Sandbar shark demographic analyses, using known and estimated life history parameters, including fishing mortality (F) at ages and levels estimated in a recent stock assessment, were used to estimate potential population growth and exploitation. Life history tables were constructed by using best estimates of natural mortality (M) of 0.11 or 0.07 for maximum ages of 30 or 60 yr, respectively. Natality was fixed at 2.1 female pups/yr. Fishing mortality (F=0.05, 0.10, 0.15, 0.20, or 0.25) was simulated to begin at age 8, 10, 15, 20, or 29. The annual population growth rate was highest under a "best-case" scenario of M=0.05 (½ best estimate) and maximum age of 30 yr, but was only 11.9%/yr. At M=0.11 for all ages, the population increase rate was 6.4%/yr, and the generation time was about 20 years. At higher juvenile mortality rates, the population growth rate decreased to 2.6%/yr. Adding fishing mortality at immature ages caused the population to decline unless F levels were <0.10 and 0.05 at maximum age = 30 and 60, respectively. It is apparent that sandbar shark populations will decline under any substantial fishing mortality on immature ages and that mature fish can be exploited only at very low levels.

Manuscript accepted 4 December 1995.
Fishery Bulletin 94:341–347 (1996).

The sandbar shark, *Carcharhinus plumbeus*, ranges from Cape Cod to Brazil in the western North Atlantic (Bigelow and Schroeder, 1948; Springer, 1960; Garrick, 1982) and is the most common large coastal shark in Virginia waters (Musick et al., 1993). It comprises 20% of the large-shark fauna of the U.S. east coast and is an important component of recreational and commercial fisheries (Hoff, 1990; Musick et al., 1993; Anonymous[1]). Age and growth (Casey et al., 1985; Casey and Natanson, 1992; Sminkey and Musick, 1995), seasonal distribution (Bigelow and Schroeder, 1948; Springer, 1960; Musick et al., 1993), and reproductive biology (Colvocoresses and Musick[2]) of the sandbar shark have been studied, but population studies have been limited to a time series of relative abundance in Virginia waters (Musick et al., 1993) and to a demographic analysis based on previously published life history parameters (Hoff, 1990).

The recent increase in fishing pressure on sandbar sharks and subsequent decline in abundance (Musick et al., 1993), revised age and growth studies (Casey and Natanson, 1992; Sminkey and Musick, 1995), and a reexamination of fecundity data presented in Colvocoresses and Musick[2] have provided updated parameters necessary for a demographic analysis of the sandbar shark. This analysis uses estimates of longevity, age-specific survival, and age-specific natality to construct a life history table which generates estimates of the net reproductive rate per generation, the generation time, and the intrinsic rate of increase of the population (Krebs, 1985). These parameters are useful for management purposes and for input into population models (Krebs, 1985; Hoenig and Gruber, 1990). The objective of this study is to provide an updated demographic analysis of the sandbar shark by estimating population parameters under varying conditions of natural mortality and fishing mortality (i.e. mortality caused by fishing).

* Contribution 1983 of the Virginia Institute of Marine Science, School of Marine Science, College of William and Mary, Gloucester Point, VA 23062.

[1] Anonymous. 1992. Fishery management plan for sharks of the Atlantic Ocean. U.S. Dep. Commer., NMFS, NOAA, 10 December 1992.

[2] Colvocoresses, J. A., and J. A. Musick. 1989. Reproductive biology of the sandbar shark, *Carcharhinus plumbeus*, in the Chesapeake Bight. Abstract, 69th annual meeting, Am. Soc. Ichthyology and Herp.; 17–23 June 1989, San Francisco, CA.

Materials and methods

Based on size at maturity (Springer, 1960; Sminkey, 1994) and von Bertalanffy growth equations for sandbar sharks determined by Sminkey and Musick (1995), age at 100% maturity was determined to be 15 years. Casey and Natanson (1992) determined age at maturity to be ca. 29 years on the basis of a von Bertalanffy growth equation derived from tag and recapture information and a similar size at maturity. For this demographic analysis, 15 and 29 years therefore were used in separate trials as conservative estimates of the age at which 100% of females were mature.

The age-specific natality was determined from a reexamination of the data from 50 pregnant sandbar sharks collected from 1974 to 1986 (Colvocoresses and Musick[2]) and from 3 additional females collected during 1990–92. Results similar to those reported by Colvocoresses and Musick[2] were obtained. The relationship between maternal size and number of pups was very weak (Fig. 1; r^2=0.25), with the average number of pups per litter equal to 8.4 (n=53, SD=2.3). Sandbar sharks produce a litter once every 2 years (Branstetter[3]; Musick, unpubl. data) with a sex ratio not significantly different from 1:1. Thus, age-specific natality was fixed at 2.1 female pups per year beginning with age of maturity.

[3] Branstetter. S. 1994. Gulf and South Atlantic Fisheries Development Foundation, Tampa, FL 33609. Personal commun.

The probable maximum age for sandbar sharks differs between the von Bertalanffy growth equation derived from vertebral data (Sminkey and Musick, 1995) and the growth equation from tag and recapture data (Casey and Natanson, 1992). The latter study reported tagged sandbars estimated to be 22 (155 cm fork length, FL), 32 (157 cm FL), and over 40 years old (185 cm FL) at recapture; the 22-year-old was determined to be immature. The first 2 of these ages were estimated on the basis of length at release, a vertebrally derived growth equation (sexes combined) of Casey and Natanson (1992), and on time at liberty. Regarding the 40+ year old shark, Casey and Natanson (1992) stated "since length at first maturity is 150 cm FL, it is reasonable to assume that this individual was over 30 yr old at tagging and over 40 yr at recapture." Casey and Natanson (1992) then suggested that sandbar sharks may live in excess of 50 years. Sminkey and Musick (1995) reported that the oldest individual examined (175 cm FL) was 24 years old (determined by vertebral counts). On the basis of vertebral data of Sminkey and Musick (1995), it seems reasonable to consider the maximum age for sandbar sharks to be about 30 years. For the life history tables, 30 and 60 years were considered as maximum ages in separate trials.

To examine the effects of fishing mortality (F) on the demography of the sandbar shark, the survivorship function was modified in several trials to include fishing mortality. Values of F included 0.25,

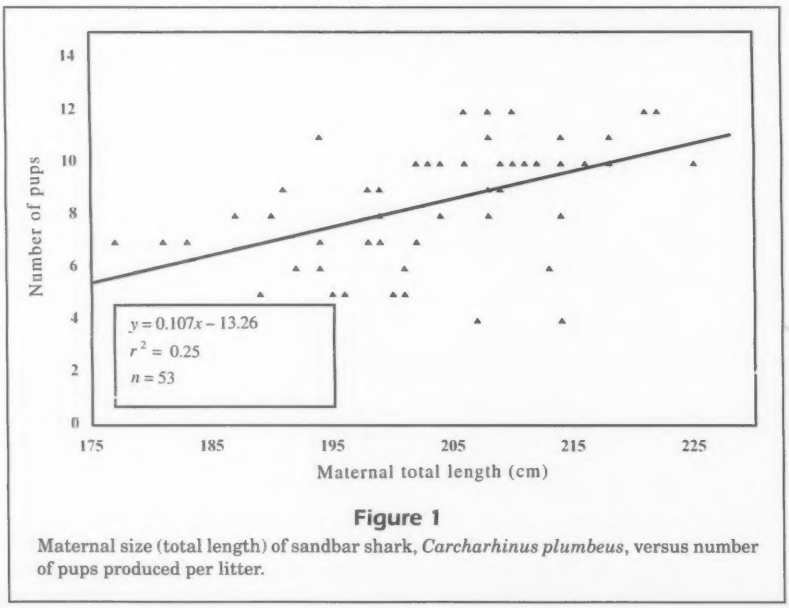

Figure 1

Maternal size (total length) of sandbar shark, *Carcharhinus plumbeus*, versus number of pups produced per litter.

0.20, 0.15, 0.10, and 0.05. $F = 0.25$ was the approximate level of mortality on large coastal sharks in the fishery from 1986 to 1991 and is the recommended F for maximum sustainable yield (Anonymous[1]). The mean carcass size of all large coastal sharks in the 1986–91 fishery was approximately 24 lb (Anonymous[1]), but the mean carcass size landed for sandbar sharks only was approximately 40 lb (Branstetter[3]). Based on two sandbar shark growth models, 24 and 40 lb correspond to ages 8 and 12 years, respectively (Sminkey and Musick, 1995; Musick, unpubl. data) or 15 and 24 years, respectively (Casey and Natanson, 1992). Considering that a mean is a measure of central tendency, then nearly 50% of the catch was younger than these ages. Therefore, fishing mortality was simulated to begin at 8, 10, 15, 20, and 29 years, which are conservative estimates based on mean carcass sizes.

Annual survival including natural mortality was estimated to be only 0.90 (max. age=30) and 0.93 (max. age=60) following the method of Hoenig (1983), which related maximum age attained to instantaneous total mortality rate (Z). If the maximum age attained was estimated from unexploited or lightly exploited stocks, Z approximates the instantaneous natural mortality rate (M). However, it has been suggested that survival of young-of-year sandbar sharks may be lower (Hoff, 1990). Increased mortality on neonate and age-1 sharks would primarily result from predation by larger sharks (Springer, 1960; Branstetter, 1990). Therefore, natural mortality during the first two years of life was varied in the life history tables. But, the population of large predatory sharks in coastal Virginia waters has been severely depleted (Musick et al., 1993), potentially reducing the mortality rate on juvenile sandbar sharks. Following Hoff (1990), a best-case life history table was constructed with survival equal to 0.95 (one-half of estimated mortality rate).

The net reproductive rate (R_0), the generation time (G), and the intrinsic rate of increase of the population (r) were calculated (Krebs, 1985) for each trial.

The effects of exploitation can be assessed from the value and sign of the intrinsic rate of increase. Based upon the outcome, an appropriate minimum size (age) and fishing mortality level (F) for sandbar sharks may be recommended to maintain a viable, reproducing population.

Results

Using the growth model for sandbar sharks calculated by Sminkey and Musick (1995) and the best estimate of annual survival rate (0.90) with no increased juvenile mortality, the population will increase at 6.4% per year (Table 1). If natural mortality were lower ("best-case" scenario, survival=0.95), the population could increase at a rate of nearly 12%/yr (Table 2). If there was increased mortality of neonates and age-1 sharks, the population increase rate would range from 2.1%/yr to 7.2%/yr (Table 2). These rates all suggest healthy and increasing populations without fishing. Population replacement (r=0.0) was attained with annual survival rates of 0.70 for neonates and 0.85 for age 0+ fish, and 0.50, 0.70, and 0.88 for ages 0, 1, and 1+, respectively (Table 2). Any greater mortality would lead to population declines.

If age at maturity and maximum age are set at 29 and 60 years, respectively, and annual survival is 0.93, the population increase rate will be 3.5%/yr (Table 2). If natural mortality is 0.1 for all ages (annual survival=0.9), the population will decrease at 0.1%/yr (Table 2). With decreased juvenile survival (0.70 for age 0, and 0.50 and 0.70 for ages 0 and 1), the population increase rates are only 2.7% and 1.1%/yr, respectively (Table 2). With similar juvenile mortality rates, population equilibrium is obtained when postjuvenile survival is 0.91 and 0.92 (Table 2).

When fishing mortality is added at the recommended level for maximum sustainable yield [MSY] (F=0.25; Anonymous[1]), age of maturity is fixed at 15 years, and age at first capture is set at 8 years, the population would decrease by >7%/yr (Table 3). Assuming these ages of first maturity and first capture, we conclude that fishing mortality would have to be reduced to F=0.10 to maintain a growing population (Table 3). If a minimum-size limit equivalent to a 15-year-old sandbar shark (135 cm precaudal length, 148 cm fork length, or 178 cm total length) were imposed, fishing mortality could remain at F=0.25 and still support an increasing population (Table 3). However, population doubling time (= $\ln(2)/r$) would be about 33 years.

Under an age of maturity of 29 years and a maximum age of 60 years, the population increases at all levels of F up to 0.25, if fishing does not begin until age 29. Population doubling time, however, would increase dramatically as F increased, ranging from 27.7 years if F=0.05 to 693 years if F=0.25. If fishing begins before age 29, the population could increase only at very low fishing mortality rates (Table 3). The generation time (G) is the period between the birth of the parents and the birth of the offspring. When offspring are produced over a period of time, G is the mean period between the parent's birth and the birth of each offspring. As fishing mortality increases, survival of parents decreases, leading to fewer offspring later in life, therefore G decreases. This result does not suggest more rapid population replacement.

Table 1

Life history table for sandbar shark, *Carcharhinus plumbeus*, using best estimate of natural mortality only, no increased juvenile natural mortality, age at maturity = 15, and maximum age = 30. Column symbols are as follows: X = age in years; l_x = survivorship (annual survival = 90%); m_x = natality (no. of female pups/yr); $X \times l_x \times m_x$ = age-specific reproductive rate; R_0, net = reproductive rate per generation; G = generation time (yr); r = intrinsic rate of population increase; and % = population increase rate (%/yr).

X	l_x	m_x	$l_x \times m_x$	$X \times l_x \times m_x$	R_0	G	r	%
0	1.00				3.54	20.37	0.062	6.4
1	0.90							
2	0.81							
3	0.73							
4	0.66							
5	0.59							
6	0.53							
7	0.48							
8	0.43							
9	0.39							
10	0.35							
11	0.31							
12	0.28							
13	0.25							
14	0.23							
15	0.21	2.1	0.43	6.51				
16	0.19	2.1	0.39	6.25				
17	0.17	2.1	0.35	5.98				
18	0.15	2.1	0.32	5.70				
19	0.14	2.1	0.28	5.41				
20	0.12	2.1	0.26	5.13				
21	0.11	2.1	0.23	4.85				
22	0.10	2.1	0.21	4.57				
23	0.09	2.1	0.19	4.30				
24	0.08	2.1	0.17	4.04				
25	0.07	2.1	0.15	3.79				
26	0.07	2.1	0.14	3.55				
27	0.06	2.1	0.12	3.32				
28	0.05	2.1	0.11	3.10				
29	0.05	2.1	0.10	2.89				
30	0.04	2.1	0.09	2.69				

Discussion

Demographic analysis using life history tables is a useful tool for fishery managers to evaluate potential population changes under various conditions of fishing mortality (Hoenig and Gruber, 1990). In this study, the demographic analyses indicate that if fishing mortality continues to target small sandbar sharks, beginning with 8-year-old sharks, at the level of fishing estimated for 1986–91 (F=0.25; Anonymous[1]), the population will decrease by >7% per year. The population of sandbar sharks along the mid-Atlantic coast declined to about 15% of its previous level over a 13-year span (Musick et al., 1993; Musick et al.[4]), suggesting that this demographic study may be an accurate estimate of potential population changes as a result of excessive fishing mortality. The potential population increase rates reflect an evolutionary strategy not well adapted to sudden and severe population depletions, particularly if applied to many age classes simultaneously or persisting over several years.

Natural mortality is difficult to estimate directly for any fish population; therefore we chose to use the longevity relationship of Hoenig (1983) to estimate this parameter. Additionally, following the example of Hoff (1990), we reduced the natural mortality by half to examine the "best-case" population under the conditions of the vertebrally derived growth model. This simulation may indicate the maximum poten-

[4] Musick, J. A., S. Branstetter, and T. R. Sminkey. 1994. Trends in shark abundance from 1974 to 1993 for the Chesapeake Bight region of the U.S. mid-Atlantic coast. Contrib. SB-19, Shark evaluation workshop, 14–18 March 1994, Southeast Fisheries Science Center, Natl. Mar. Fish. Serv., Miami, FL 33149, 16 p.

Table 2

Life history parameters for sandbar shark, *Carcharhinus plumbeus*, under two growth models (Sminkey and Musick [1995]: age at maturity = 15, max. age = 30; and Casey and Natanson [1992]: age at maturity = 29, max. age = 60) with varying natural mortality only. Natality is 2.1 female pups/yr. R_0 = net reproductive rate per generation; G = generation time (yr); and r = intrinsic rate of population increase. Negative values are in bold.

Annual survival (%/yr)						
Age 0	Age 1	Age 2+	R_0	G	r	Population increase rate
Age at maturity = 15						
0.70	0.90	0.90	2.76	20.37	0.050	5.1
0.50	0.70	0.90	1.53	20.37	0.021	2.1
0.70	0.85	0.85	1.00	19.44	0.000	0.0
0.50	0.70	0.88	1.00	19.95	0.000	0.0
0.95	0.95	0.95	11.20	21.45	0.113	11.9
0.50	0.70	0.95	5.01	23.16	0.070	7.2
Age at maturity = 29						
0.93	0.93	0.93	3.79	39.05	0.034	3.5
0.90	0.90	0.90	0.97	36.88	**-0.001**	**-0.1**
0.70	0.93	0.93	2.84	39.05	0.027	2.7
0.50	0.70	0.93	1.52	39.05	0.011	1.1
0.50	0.70	0.92	1.00	38.28	0.000	0.0
0.75	0.91	0.91	1.00	37.20	0.000	0.0

Table 3

Life history parameters for sandbar shark, *Carcharhinus plumbeus*, under varying rates of fishing mortality and two growth models (Sminkey and Musick [1995]: age at maturity = 15, max. age = 30; and Casey and Natanson [1992]: age at maturity = 29, max. age = 60). Natality is 2.1 female pups/yr in both models. Age_i = age at which F starts; R_0 = net reproductive rate per generation; G = generation time (yr); r = intrinsic rate of population increase. Negative values are in bold.

Instantaneous fishing mortality					
Age_i	F	R_0	G	r	Population increase rate (%/yr)
Age at maturity = 15					
Annual survival = 0.90					
8	0.25	0.25	17.29	**-0.080**	**-7.7**
8	0.20	0.40	17.68	**-0.051**	**-5.0**
8	0.15	0.66	18.17	**-0.023**	**-2.2**
8	0.10	1.12	18.77	0.006	0.6
8	0.05	1.95	19.50	0.034	3.5
10	0.25	0.42	17.29	**-0.051**	**-5.0**
10	0.20	0.60	17.68	**-0.029**	**-2.8**
10	0.15	0.90	18.17	**-0.006**	**-0.6**
10	0.10	1.37	18.77	0.017	1.7
10	0.05	2.16	19.50	0.039	4.0
15	0.25	1.45	17.29	0.021	2.2
15	0.20	1.64	17.68	0.028	2.8
15	0.15	1.90	18.17	0.035	3.6
15	0.10	2.26	18.77	0.043	4.4
15	0.05	2.77	19.50	0.052	5.4
Age of maturity = 29					
Annual survival = 0.93					
15	0.25	0.03	31.66	**-0.109**	**-10.4**
15	0.20	0.07	32.23	**-0.081**	**-7.8**
15	0.15	0.18	33.06	**-0.052**	**-5.1**
15	0.10	0.45	34.29	**-0.023**	**-2.3**
15	0.05	1.23	36.19	0.006	0.6
20	0.25	0.11	31.66	**-0.070**	**-6.8**
20	0.20	0.20	32.23	**-0.050**	**-4.9**
20	0.15	0.37	33.06	**-0.030**	**-2.9**
20	0.10	0.74	34.29	**-0.009**	**-0.9**
20	0.05	1.58	36.19	0.013	1.3
29	0.25	1.04	31.66	0.001	0.1
29	0.20	1.20	32.23	0.006	0.6
29	0.15	1.44	33.06	0.011	1.1
29	0.10	1.82	34.29	0.017	1.8
29	0.05	2.47	36.19	0.025	2.5

tial for population growth in the absence of fishing mortality. The annual population increase rate of nearly 12% is modest when compared with teleost reproductive potential (Hoff, 1990) and probably is not actually attainable in sandbar shark populations.

The Casey and Natanson (1992) growth model assumes the maximum age attained is 60 years, resulting in an estimate of $M = 0.07$. However, if natural mortality was 0.10, the life history table predicts a population decrease rate of 0.1% in the absence of any increased neonate mortality or fishing mortality (Table 2). This indicates a nonviable population under natural mortality levels, particularly if neonate and juvenile mortality were higher. Therefore, if sandbar sharks are assumed to grow according to this model, it seems reasonable to accept the lower estimate of natural mortality.

There is great uncertainty regarding age-specific natural mortality during the first two years of life when juvenile sandbar sharks are vulnerable to predation by large coastal sharks. The trials with increased mortality during these years demonstrate the sensitivity to natural mortality estimates in the life history table. If age at maturity is 15 years and mortality is >0.10, the population increase rate is considerably reduced (2.1%–5.1%/yr), suggesting that the population may be near equilibrium (r=0.0) under these conditions (Table 2). However, Musick et al. (1993) and Musick et al.[4] suggest that the apparent stable abundance of juvenile sandbar sharks in

the Chesapeake Bay is the result of a marked decrease in the large coastal shark population. In this case juvenile survival is probably less dependent upon predation and may be age-independent (M=0.10 for all ages). Assuming this natural mortality level, the population increases at 6.4%/yr (Table 1).

The life history parameters generated by the two growth models with the best estimates for natural mortality, suggest similar population increase potential but on two different time scales. The intrinsic rates of population increase are 0.062 and 0.034 for the growth models of Sminkey and Musick (1995) and Casey and Natanson (1992), but the generation times are 20.37 and 39.05 years, respectively, and population doubling times are 11.2 and 20.4 years, respectively. The life history tables with the vertebral growth model agree well with the results of Hoff (1990), although he used an age-fecundity relationship.

The effects of fishing mortality on the intrinsic rate of increase with both growth models demonstrate the detrimental effect of exploitation on immature fish (Table 3). At fishing mortality levels >0.10, the population will decline. The ages used for these estimates (8 and 15) correspond to the mean carcass size in the 1986–91 large coastal shark fishery and are based upon the most recent data available. At the currently estimated fishing mortality level (0.25) these populations are not viable and will eventually collapse. The recent analyses of Musick et al. (1993) and Musick et al.[4] report that the adult coastal stock has already been reduced to only 15% of its abundance in 1980–81. Clearly the sandbar shark, with a slow growth and low net reproductive rate typical of most elasmobranchs, cannot withstand even a low rate of fishing mortality on immature individuals.

Cailliet (1992) used demographic analyses to examine population growth in the leopard shark, *Triakis semifasciata*, including fishing mortality to begin at several ages. The population would replace itself (r=0) if fishing began at age 4 at the estimated rate (F=0.084) and would slowly increase (0.4–6.4%/yr) if fishing did not begin until later ages (5, 10, 15, 21 years). However, it was demonstrated that if fishing mortality doubled (F=0.168), the age at which F starts must be >12 to produce a growing population. Although females first mature at age 17, Cailliet (1992) concluded that a size limit of 110 cm TL (approximately 13 years) would ensure population replacement at this moderately low fishing level.

A demographic analysis of the Pacific angel shark, *Squatina californica*, examined the effects of low fishing mortality rates (F=0.05, 0.10, 0.20, 0.22) simulated to begin at age 10 yr (Cailliet et al., 1992). This age was the estimated age of entry into the fishery as well as the approximate age of first maturity. Cailliet et al. (1992) concluded that the population would grow very slowly (0.4%/yr) at F=0.20, would decrease at higher F, and that a size limit above the size of first maturity should be imposed in the absence of better estimates of natural and fishing mortality.

Demographic analyses of the Atlantic sharpnose shark, *Rhizoprionodon terranovae*, classified as a "small coastal" species in the Fishery Management Plan (FMP) for sharks of the Atlantic Ocean, indicated that, in the absence of fishing mortality, the population would increase by only about 4.5%/yr (Cortés, 1995). This best estimate is considerably below the rate derived for "small coastal" sharks of the Atlantic Ocean (e^r=1.91; 91%/yr) (Parrack[5]). Furthermore, if fishing mortality continues at the estimated rate for 1986–90 (F=0.43) (Anonymous[1]), a size limit of about 97 cm TL (nearly 6 years old) would have to be imposed just to allow population replacement (Cortés, 1995). Cortés (1995) demonstrates that extreme modification of the reproductive and survival parameters was required to attain the population increase rate derived by Parrack[5] and concluded that management of the Atlantic sharpnose under the FMP was based on unrealistic biological parameters.

This demographic analysis of sandbar sharks provides additional life history information on acceptable levels of exploitation. If the current FMP recommendation of F=0.25 for MSY (Anonymous[1]) is implemented in an unrestricted fishery, the sandbar shark population will not recover. This level of fishing would be acceptable for a healthy population if a minimum size limit of 135 cm precaudal length or about 23 kg carcass weight (size at first maturity) were imposed and juvenile survival remained high. But, with the current severe depletion of the sandbar shark population of the western North Atlantic, far more restrictive fishing mortality levels must be implemented to allow the population to rebuild itself. Such a conservative approach would also provide a buffer against natural perturbations during the crucial recovery phase.

Acknowledgments

This research formed part of a dissertation submitted by the senior author to the School of Marine Science, The College of William and Mary, in partial fulfillment of the requirements for the degree of Doctor of Philosophy. We thank S. Branstetter for his

[5] Parrack, M. L. 1990. A preliminary study of shark exploitation during 1986–1989 in the U.S. FCZ. Contrib. MIA-90-493, Southeast Fisheries Science Center, Natl. Mar. Fish. Serv., Miami, FL 33149, 23 p.

assistance and advice throughout this project and for reviewing an early draft of this manuscript. This research was funded by grants from the U.S. Fish and Wildlife Service (Wallop-Breaux Program, administered through the Virginia Marine Resources Commission) and the U.S. Sea Grant program.

Literature cited

Bigelow, H. B., and W. C. Schroeder.
1948. Sharks. *In* J. Tee-Van, C. M. Breder, S. F. Hildebrand, A. E. Parr, and W. C. Schroeder (eds.), Fishes of the western North Atlantic, part 1, vol. 1, p. 59–546. Mem. Sears Foundation for Marine Research, Yale Univ., New Haven, CT.

Branstetter S.
1990. Early life-history implications of selected carcharhinoid and lamnoid sharks of the northwest Atlantic. *In* H. L. Pratt Jr., S. H. Gruber, and T. Taniuchi (eds.), Elasmobranchs as living resources: advances in the biology, ecology, systematics, and the status of the fisheries, p. 17–28. U.S. Dep. Commer., NOAA Tech. Rep. NMFS 90.

Cailliet, G. M.
1992. Demography of the central California population of the leopard shark (*Triakis semifasciata*). Aust. J. Mar. Freshwater Res. 43:183–193.

Cailliet, G. M., H. F. Mollet, G. G. Pittingewr, D. Bedford, and L. J. Natanson.
1992. Growth and demography of the Pacific angel shark (*Squatina californica*), based upon tag returns off California. Aust. J. Mar. Freshwater Res. 43:1313–1330.

Casey, J. G., and L. J. Natanson.
1992. Revised estimates of age and growth of the sandbar shark (*Carcharhinus plumbeus*) from the western North Atlantic. Can. J. Fish. Aquat. Sci. 49:1474–1477.

Casey, J. G., H. L. Pratt Jr., and C. E. Stillwell.
1985. Age and growth of the sandbar shark (*Carcharhinus plumbeus*) from the western North Atlantic. Can. J. Fish. Aquat. Sci. 42:963–975.

Cortés, E.
1995. Demographic analysis of the Atlantic sharpnose shark, *Rhizoprionodon terraenovae*, in the Gulf of Mexico. Fish. Bull. 93:57–66.

Garrick, J. A. F.
1982. Sharks of the genus *Carcharhinus*. U.S. Dep. Commer., NOAA Tech. Rep. NMFS Circ. 445.

Hoenig, J. M.
1983. Empirical use of longevity data to estimate mortality rates. Fish. Bull. 82:898–903.

Hoenig, J. M., and S. H. Gruber.
1990. Life-history patterns in the elasmobranchs: implications for fisheries management. *In* H. L. Pratt Jr., S. H. Gruber, and T. Taniuchi (eds.), Elasmobranchs as living resources: advances in the biology, ecology, systematics, and the status of the fisheries, p. 1–16. U.S. Dep. Commer., NOAA Tech. Rep. NMFS 90.

Hoff, T. B.
1990. Conservation and management of the western North Atlantic shark resource based on the life history strategy limitations of sandbar sharks. Ph.D. diss., Univ. Delaware, Newark, DE, 149 p.

Krebs, C. J.
1985. Ecology: the experimental analysis of distribution and abundance, 3rd ed. Harper and Row, New York, NY, 800 p.

Musick, J. A., S. Branstetter, and J. A. Colvocoresses.
1993. Trends in shark abundance from 1974 to 1991 for the Chesapeake Bight region of the U.S. mid-Atlantic coast. *In* S. Branstetter (ed.), Conservation biology of elasmobranchs, p. 1–18. U.S. Dep. Commer., NOAA Tech. Rep. NMFS 115.

Sminkey, T. R.
1994. Age, growth and population dynamics of the sandbar shark, *Carcharhinus plumbeus*, at different population levels. Ph.D. diss., The College of William and Mary, Gloucester Point, VA, 99 p.

Sminkey, T. R., and J. A. Musick.
1995. Age and growth of the sandbar shark, *Carcharhinus plumbeus*, before and after population depletion. Copeia 1995:871–883.

Springer, S.
1960. Natural history of the sandbar shark, *Eulamia milberti*. Fish. Bull. 61:1–38.

Contribution to the biology of the grooved and triangle Tanner crabs, *Chionoecetes tanneri* and *C. angulatus*, in the eastern Bering Sea

David A. Somerton
Alaska Fisheries Science Center
National Marine Fisheries Service, NOAA
7600 Sand Point Way NE, Seattle, Washington 98115

William Donaldson
Alaska Department of Fish and Game
211 Mission Road, Kodiak, Alaska 99615

Abstract.—Populations of the grooved Tanner crab, *Chionoecetes tanneri*, and the triangle Tanner crab, *C. angulatus*, were surveyed along the continental slope of the eastern Bering Sea with a bottom trawl. Over the depth range sampled (100–1,000 m), the relative abundance of the two species was about equal. Mature male and female *C. tanneri* occurred at the same depths, but for *C. angulatus*, males were found at significantly shallower depths than were females. Carapace widths at 50% maturity for males and females were 118.7 mm and 79.2 mm for *C. tanneri* and 91.4 mm and 57.8 mm for *C. angulatus*. Fecundity of *C. tanneri* did not increase with carapace width (CW, mm) and averaged 86,500 eggs over the sizes sampled. Fecundity of *C. angulatus* increased with carapace width according to the following formula: eggs = $-65{,}600 + 1660 \times CW$. Mean egg diameter was 0.75 mm for *C. tanneri* and 0.74 mm for *C. angulatus*. The relationship between body weight (gm) and carapace width did not differ between species: weight = $1.219/10^4 \times CW^{3.183}$.

Manuscript accepted 17 November 1995.
Fishery Bulletin 94:348–357 (1996).

The continental slope of the North Pacific Ocean is inhabited by several species of crabs in the genus *Chionoecetes* that are similar in size to their shallower, commercially harvested relatives *C. bairdi* and *C. opilio* but are immediately distinguishable by their brilliant orange or red color and slender legs. In the eastern North Pacific Ocean there are two species: the grooved Tanner crab, *C. tanneri*, ranging from northern Mexico to Kamchatka, and the triangle Tanner crab, *C. angulatus*, ranging from Oregon to the Sea of Okhotsk (Hart, 1982). In the western North Pacific there is a single species, *C. japonicus*, which occurs in the Sea of Japan (Sinoda, 1982). Although the potential for commercial fisheries for *C. tanneri* has been recognized for quite some time (Pereyra, 1967), commercially successful fishing ventures have occurred only recently (Jamieson, 1990). In contrast, *C. japonicus* has been commercially fished since the mid-1960's (Sinoda, 1982). The primary impediment to the development of commercial fisheries for *C. tanneri* and *C. angulatus* has been that the large supply of other *Chionoecetes* species on the world market has kept the price too low to offset the high costs of fishing in deep water. Fisheries for other slope-dwelling species, however, have developed when the catches of shallower, related species have declined. For example, in Japan the fishery for *C. japonicus* developed after the local stocks of *C. opilio* declined (Sinoda, 1982). In Alaska, the fishery for the slope-dwelling king crab *Lithodes aequispina* developed after the decline in abundance of the shelf-dwelling king crabs *Paralithodes camtschaticus* and *P. platypus* (Somerton and Otto, 1986). This pattern may be reflected in Alaskan *Chionoecetes* because as *C. bairdi* and *C. opilio* populations in the Bering Sea have declined, landings of *C. tanneri* have increased from a negligible amount in 1992 to 360 metric tons in 1993, and to 414 metric tons in 1994.[1]

Although aspects of the biology of *C. tanneri* have been documented in areas off Oregon (Pereyra, 1966, 1968; Tester and Carey, 1986) and British Columbia (Jamieson et al., 1990), only information on size dis-

[1] 1995. Alaska Department of Fish and Game, 211 Mission Road, Kodiak, AK 99615. Unpubl. data.

tribution (Hughes, 1981; Alton, 1986) has been reported for Alaskan waters. Furthermore, nothing about the biology of *C. angulatus* has ever been reported. We collected information on both species on a 1982 Japan-U.S. cooperative trawl survey of the continental slope of the eastern Bering Sea. Here we summarize these data, focusing on the depth and size distributions, sizes at maturity, weight-size relationships, and various aspects of the reproductive biology of both species.

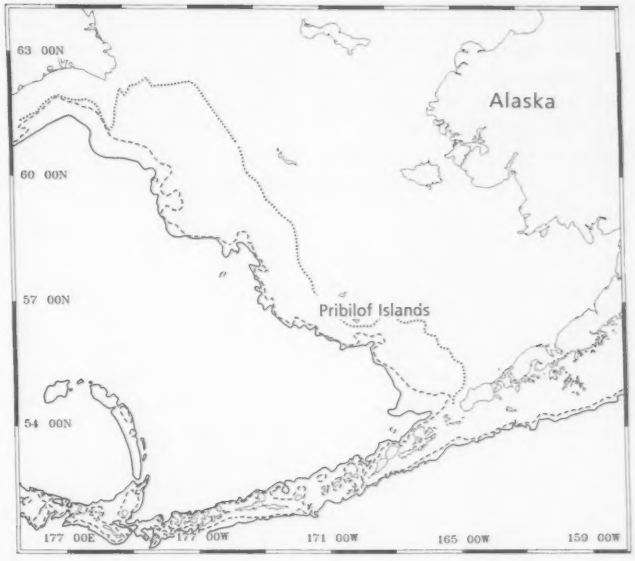

Figure 1

Area surveyed during the Japan-U.S. cooperative survey of the slope of the eastern Bering Sea. The 100-m (dotted line), 200-m (dashed line), and the 1,000-m (solid line) isobaths are shown for the eastern Bering Sea.

Materials and methods

Sampling of *C. tanneri* and *C. angulatus* was conducted from the Japanese stern-trawler, *Ryujin Maru No. 8*, on the continental slope of the eastern Bering Sea between 58.3°N and 60.9°N latitude (Fig. 1). Crabs were captured with a bottom trawl that measured 23 m between the wings, had a codend consisting of three layers of 90-mm mesh, and had a footrope equipped with 55-cm diameter steel bobbins. The study was divided into two parts: from 11 July to 4 August 1982, scientists from the Alaska Fisheries Science Center collected data on all of the biological parameters described below; from 8 August to 25 August, Japanese scientists collected only carapace width data. For both parts, species identification was based on characteristics provided in Garth (1958).

Maximum carapace width of all crabs was measured with vernier calipers to the nearest 1.0 mm, excluding lateral spines. In the first part of the study, both sexes were evaluated for shell condition and females were additionally evaluated for reproductive condition. Shell condition was rated on a 4-point scale, based on hardness, color, and wear of the exoskeleton (see Somerton, 1982), which represents the approximate time interval since the last molt. Briefly, the characteristics of each shell-condition category and its assumed postmolt interval (PMI) are as follows:

1 carapace pliable (PMI <2 wk);
2 carapace hard, little wear on tips of dactyli, few scratches (2 wk <PMI <1 yr);
3 carapace hard, conspicuous wear on tips of dactyli, abundant scratches (1 yr <PMI <2 yr);
4 same as condition 3, except that wear on dactyli is more pronounced (PMI >2 yr).

Reproductive condition was rated on a 5-point scale. Characteristics of each reproductive condition category are as follows:

1 immature—narrow flattened abdomen;
2 nonovigerous—no embryos or empty egg cases attached to the pleopod setae;
3 uneyed embryos—embryos without conspicuous dark eyes;
4 eyed embryos—embryos with clearly visible dark eyes;
5 empty egg cases—empty egg cases and funiculi attached to the pleopod setae.

Whenever possible, one or more of the following types of data were also collected:

- height of the right chela of males (excluding males with partially regenerated right-hand chela) measured to the nearest 0.1 mm according to the definition in Jamieson et al. (1990);
- total wet body weight of intact males measured to the nearest gram on a triple-beam balance;
- uneyed egg masses from ovigerous females (stored in formalin diluted to 10% with seawater).

Egg masses were processed as follows: mean egg diameter was estimated by randomly selecting 10 eggs from each of 10 randomly selected egg masses and measuring the diameters to the nearest 0.1 mm with an ocular micrometer. Fecundity was estimated

by first air drying the egg masses and, after separating the eggs from the pleopods and setae, weighing them to the nearest 0.1 mg. Two subsamples of about 200 eggs from each dried egg mass were randomly selected, weighed, and counted. Fecundity was then estimated by dividing the total weight of an egg mass by the average of the two estimates of individual egg weight.

Male functional maturity (Conan and Comeau, 1986) was determined from chela allometry. The procedure used is based on the observation that, for *Chionoecetes*, when chela measurements are plotted against carapace measurements on log-log axes, the data conform to two, nearly parallel, straight lines, one representing immature individuals and the other representing individuals that have undergone a puberty molt and have acquired the secondary sexual characteristic of enlarged chelae (Hartnoll, 1978; Somerton, 1980; Conan and Comeau, 1986). We determined with which line an individual observation was associated by using the computer algorithm described in Somerton (1980) to reassign observations iteratively to the two lines until the residual sum of squares was minimized. The carapace width at 50% maturity (W_{50}) for both males and females was estimated by fitting a logistic regression model to the maturity and carapace width data by using generalized linear modeling (Chambers and Hastie, 1992). W_{50} and the variance of W_{50} were then estimated from the parameters of the fitted model with formulas provided in Somerton (1980). In addition to W_{50}, we also calculated the mean carapace width of mature individuals (W_m) as an alternative measure of the size at maturity for comparative purposes.

Weight and carapace width relationships for males of each species were estimated by nonlinear regression (Chambers and Hastie, 1992) to fit a power function to weight and carapace width data. A between-species difference in these relationships was tested by making the relationships linear with a log transformation of the data, and by using analysis of covariance to test whether species-specific relationships fit the data significantly better than a single, combined relationship.

Results and discussion

The 205 trawl hauls that were successfully completed were distributed evenly over the latitudinal range of the survey area (Fig. 2), but fewer hauls were made at greater depths. Over the survey area, both species displayed patchy distributions; much of the catch came from relatively few sampling sites (Fig. 2). *Chionoecetes tanneri* occurred at 47 sites and had a mean CPUE (catch in numbers per kilometer of towed distance) at these sites of 1.9; *Chionoecetes angulatus* occurred at 50 sites and had a mean CPUE of 2.6. The difference in CPUE was not significant (t-test, P=0.418).

Size distribution

Chionoecetes tanneri males ranged 42–170 mm in carapace width (CW); females ranged 38–126 mm CW (Fig. 3). The maximum size of females was similar to maximum sizes reported off Oregon (126 mm, Pereyra, 1966; 122 mm, Tester and Carey, 1986), whereas the maximum size of males fell between the maximum sizes reported for Oregon (181 mm, Pereyra, 1966; 162 mm, Tester and Carey, 1986). *Chionoecetes angulatus* males ranged 25–160 mm CW; females ranged 35–104 mm CW. The maximum sizes of both sexes were slightly larger than the reported maximum sizes of *C. japonicus* in the Sea of Japan (males 150 mm, females 90 mm, Watanabe and Suzuuchi, 1983).

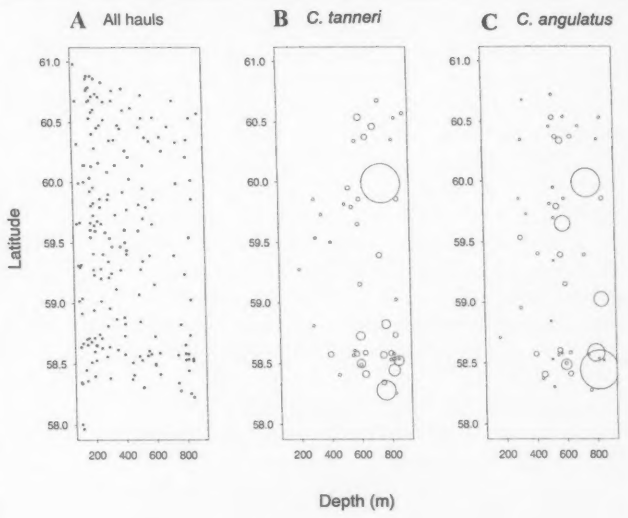

Figure 2

Distribution of all successful trawl hauls (**A**), positive *Chionoecetes tanneri* hauls (**B**), and positive *C. angulatus* hauls (**C**), with respect to latitude and depth in meters. For both species, the size of the circle is proportional to the total catch in numbers per kilometers of towed distance.

Depth distribution

Both species occurred in the deeper portion of the survey area; few individuals of either species were encountered shallower than 300 m (Fig. 4). For *C. tanneri*, the mean depth of mature males (752 m) was not significantly different from the mean depth of mature females (709 m; *t*-test, P=0.38). This is in contrast to the summertime depth distributions of *C. tanneri* reported off British Columbia (males 580–670 m, females 670–720 m, Jamieson et al., 1990) and off Oregon (males 640–686 m, females 503–549 m, Pereyra, 1966) where mature males were found at distinctly shallower depths than those for mature females. Thus in the eastern Bering Sea, *C. tanneri* does not show a clear depth segregation of males and females as is seen in more southerly latitudes, and the depths occupied by both sexes are greater.

For *C. angulatus*, the mean depth for mature males (647 m) was significantly less than the mean depth for mature females (748 m; *t*-test, P<0.001), indicating that this species does appear to have the same pattern of sexual segregation by depth as that displayed by *C. tanneri* in more southerly latitudes (Pereyra, 1966). The depth distribution reported for *C. japonicus* (Yosho and Hayashi, 1994) indicates that the greatest abundance of both sexes occurs at about 1,000 m. Although this finding suggests that *C. japonicus* may occur deeper than *C. angulatus*, it is clear (Fig. 4) that the distribution of *C. angulatus* extends into deeper water than was covered in our survey and that our estimates of mean depth are low (*C. angulatus* has been reported as deep as 2,974 m [Hart, 1982]; in fact, the type specimen of *C. angulatus* was taken quite near our sampling site in 2,549 m [Rathbun, 1932]).

Juvenile male *C. tanneri* were found in significantly shallower waters than were mature males (*t*-test, P<0.001), whereas juvenile male *C. angulatus* were not significantly different (P=0.30) in mean depth from mature males. This is in contrast to the depth distribution reported for *C. tanneri* from British Columbia to Oregon where there is a strong depth segregation by size, where juveniles are found in deeper water than are adults (Pereyra, 1968; Jamieson et al., 1990). The observed between-area difference in vertical distribution indicates that the factors producing the size variation with depth at more southerly latitudes do not function similarly in the Bering Sea. Pereyra (1968) hypothesized that *C. tanneri* larvae are advected offshore by Ekman transport and settle to the bottom in deep water. The strong variation in size with depth then results from a shoreward ontogenetic migration of the young crabs. In the region where we surveyed, however, advection of the near-surface water is either quite weak or onshore,[2] rather than strongly offshore. Thus the difference in the observed size variation with depth between the Bering Sea and Oregon may be due to differences in the local oceanographic conditions.

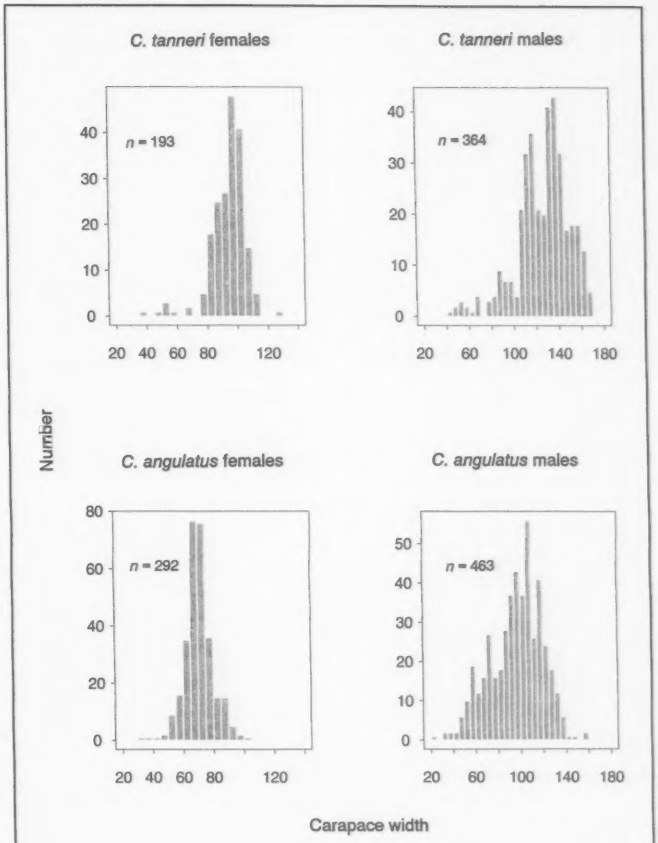

Figure 3

Carapace width distribution for male and female *Chionoecetes tanneri* and *C. angulatus*. The total number of individuals measured (n) in each category is indicated for each sex and species.

[2] Pease, C. 1995. Pacific Marine Environmental Laboratory, Seattle, Washington. Personal commun.

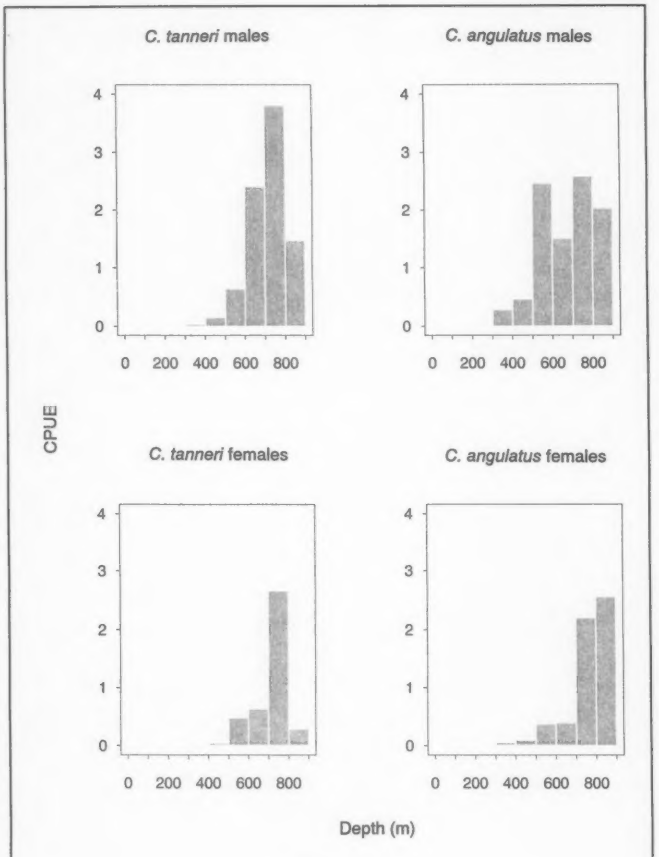

Figure 4

Depth distribution is shown for *Chionoecetes tanneri* and *C. angulatus*, by sex, expressed as mean catch in numbers per kilometer of towed distance (CPUE) within 100-m depth intervals.

Size at maturity

Estimates of the carapace width at 50% maturity, W_{50}, for both male and female *C. tanneri* (Figs. 5 and 6) were not significantly different from reported values of W_{50} off Oregon (Table 1). Likewise, the estimate of the mean carapace width of mature individuals, W_m, for females was not significantly different from the estimate of W_m for Oregon, but the estimate of male W_m was significantly smaller than the estimate for Oregon (Table 1). Although there may be a slight change in size at maturity from Oregon to the Bering Sea, compared with the large spatial variation in size at maturity observed for the shallow-water species *C. bairdi* and *C. opilio* on the Bering Sea shelf (W_m changes by up to 17% over distances of 200 km, Somerton, 1981a), the constancy of size at maturity over the latitudinal range of *C. tanneri* is remarkable. Such constancy has been documented before (Tester and Carey, 1986) and has been attributed to the uniformity of water temperature over great distance at the depths inhabited by this species. For *C. angulatus*, the observed estimates of W_{50} (Figs. 5 and 6; Table 1) were similar to values of W_{50} for *C. japonicus* in the Sea of Japan.

Reproduction

Fecundity of *C. tanneri* did not increase significantly with carapace width (P=0.89, n=29; Fig. 7), primarily because of the large variability in fecundity at size. Over the carapace widths sampled (83–113 mm), mean fecundity was 86,500 eggs. Fecundity of *C. angulatus* displayed much less variability and increased significantly with carapace width (fecundity = –65,608 + 1,664 × CW, P<0.001, R^2=0.55, n=24). For *C. japonicus*, Ito (1976) reported that 70-mm females have about 40,000–50,000 eggs, approximately the same as the fecundity predicted for *C. angulatus* at the same size (Fig. 7). Mean egg diameter was 0.75 mm (SE=0.04) for *C. tanneri* and 0.74 mm (SE=0.04) for *C. angulatus*. Although these estimates are not significantly different from the estimates reported for *C. japonicus* (0.68 mm, Ito, 1976; 0.74 mm, Fukutake, 1965), they are significantly larger than the estimates reported for both of the shallow-water species *C. bairdi* (0.56 mm) and *C. opilio* (0.66 mm, Haynes et al., 1976).

Most mature females of both species carried eggs in the same stage of development (Table 2); therefore it appears that both species have synchronous and seasonal reproduction, in other words, all reproductively active females mate and extrude eggs at about the same time of year. Seasonal reproduction has been previously reported for *C. tanneri* (Pereyra, 1966; Jamieson et al., 1990) and *C. japonicus* (Ito, 1976). However, it has also been reported that *C. japonicus* has a 2-year reproductive cycle (Ito, 1976) and therefore does not have synchronous spawning. If this is true for either *C. tanneri* or *C. angulatus*, one would expect to find more heterogeneity in the observed stages of egg development, unless our macroscopic evaluation of reproductive condition failed to detect differences in embryonic development between the first and second year of a 2-year cycle.

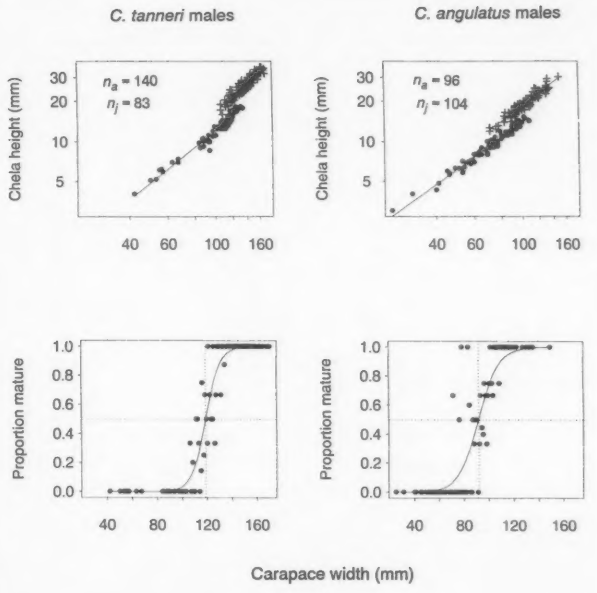

Figure 5

Size at 50% maturity (W_{50}) for male *Chionoecetes tanneri* and *C. angulatus*. Upper graphs show the assignment of chela height and carapace width data to juvenile (dot) and adult (plus) categories. The number of observations in each category (n_a for adults, n_j for juveniles) is indicated in the appropriate graph. Lower graphs show the fit of a logistic model (solid line) to the proportion mature within 1-mm size categories. Dotted lines show the carapace width associated with a 0.50 proportion mature.

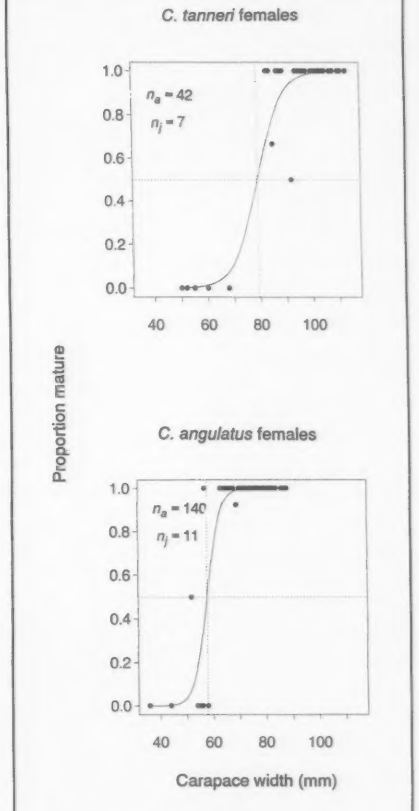

Figure 6

Size at 50% maturity (W_{50}) for female *Chionoecetes tanneri* and *C. angulatus*. For each species is shown the fit of a logistic model (solid line) to the proportion mature within 1-mm size categories. Dotted lines show the carapace width associated with a 0.50 proportion mature. Number of adults and juveniles sampled are indicated in each graph.

Synchronous seasonal reproduction is not necessarily the norm for slope-dwelling crabs. For example, the two species of king crabs that also inhabit the eastern Bering sea slope, *Lithodes aequispina* and *L. couesi*, have asynchronous and nonseasonal reproduction (Somerton, 1981b; Somerton and Otto, 1986) as evidenced by a wide variation among adult females in the developmental stages of their embryos. These king crab species also have eggs that are more than twice the diameter of eggs from shallow-water king crabs, such as *Paralithodes camtschaticus*, and have exceptionally large larvae provisioned with a greater amount of yolk (Somerton, 1981b). Such larvae may be lecithotrophic (i.e. nonfeeding) and therefore remain at depth throughout their development. This larval strategy could, in turn, reduce or eliminate larval dependency on the seasonal production of food and thus obviate the need for seasonal reproduction (Somerton, 1981b). For *C. tanneri* and *C. angulatus*, however, the mean egg diameter is only slightly larger than that for the shallow-water species *C. bairdi* and *C. opilio*, indicating that *C. tanneri* and *C. angulatus* probably have planktotrophic larvae which must migrate to feed in surface waters where prey concentrations are greater. Although such ontogenetic vertical migrations by the larvae of deep-sea fauna were once considered improbable, it is now known that a variety of taxa, from depths even greater than those for *C. tanneri* or *C. angulatus*, possess vertically migratory planktotrophic larvae (Young, 1994).

Molting

For mature female *C. tanneri* and *C. angulatus*, relative abundance of the four shell-condition categories

Table 1

Carapace width at 50% maturity (W_{50}) and mean carapace width of mature individuals (W_m), in millimeters, by species, sex, and area. Standard errors are shown in parentheses. Estimates for W_{50} for *C. japonicus* were interpolated from a figure in the noted source and are therefore approximate.

Species	Sex	W_{50}	W_m	Area	Source
C. tanneri	male	118.7 (1.26)	137.9 (1.25)	Bering Sea	This study
	female	79.2 (4.82)	99.5 (1.25)	Bering Sea	This study
	male	118.0	142.7	Oregon	Tester and Carey (1986)
	female	85.0	102.0	Oregon	Tester and Carey (1986)
	male		148.9	Oregon	Pereyra (1966)
	female		102.5	Oregon	Pereyra (1966)
C. angulatus	male	91.4 (1.64)	105.2 (1.58)	Bering Sea	This study
	female	57.8 (1.46)	72.2 (0.52)	Bering Sea	This study
C. japonicus	male	~95		Japan	Watanabe and Suzuuchi (1983)
	female	~55		Japan	Watanabe and Suzuuchi (1983)

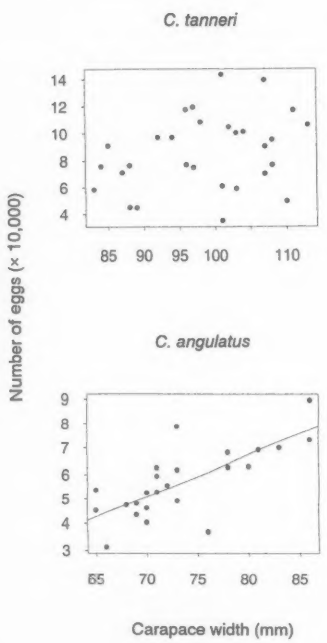

Figure 7

Fecundity is shown as a function of carapace width for female *Chionoecetes tanneri* (upper graph) and *C. angulatus* (lower graph). The number of eggs was not significantly related to size for *C. tanneri*, but it was significant for *C. angulatus* and the regression line is shown.

Table 2

Number and percentage of individuals examined in each of three reproductive conditions for mature female *C. tanneri* and *C. angulatus*.

Reproductive condition	*C . tanneri*	*C. angulatus*
3 (uneyed eggs)	33 (79%)	121 (86%)
4 (eyed eggs)	0	2 (1%)
2, 5 (no eggs)	9 (21%)	17 (12%)

did not differ significantly between species (Table 3; χ^2=0.27, P=0.53). Most mature females were scored as having shell condition 3 (Table 3), indicating that they probably had not molted for at least 1 year and likely have a terminal molt similar to that of the shallower water species *C. bairdi* and *C. opilio*. Some individuals of both species had molted so recently that their exoskeletons were still pliable. Because the puberty molt is usually associated with mating, some mating must have occurred as late as July. However, the primiparous (shell conditions 1 and 2) females also had a surprisingly high percentage of barrenness (*C. tanneri*—60%; *C. angulatus*—76%) compared with multiparous (shell condition 3) females (*C. tanneri*—16%; *C. angulatus*—3%). For *C. bairdi* and *C. opilio*, primiparous females are rarely barren because mating and egg extrusion quickly follow the puberty molt (Watson, 1970). Perhaps for *C. tanneri* and *C. angulatus*, egg extrusion does not follow a molt as closely as it does for shallower species, and

Table 3

Number and percentage of individuals examined in each shell condition category for adult female and male *C. tanneri* and *C. angulatus*.

Shell condition	*C. tanneri*	*C. angulatus*
Females		
1	1 (2%)	4 (3%)
2	4 (10%)	11 (8%)
3	37 (88%)	121 (88%)
4	0	2 (1%)
Males		
1	5 (5%)	20 (21%)
2	123 (88%)	63 (65%)
3	12 (9%)	14 (14%)
4	0	0

the high incidence of barrenness was due simply to our sampling between times of molting and egg extrusion.

For mature male *C. tanneri* and *C. angulatus*, the relative abundance of the four shell condition categories differed significantly between species (χ^2=21.4, P<0.001), primarily because there were considerably more *C. angulatus* males in a recently molted condition (Table 3). The high incidence of recently molted *C. angulatus* males was not due to the chance capture of a large molting aggregation, because recently molted individuals were found at many of the sampling sites. Therefore, it is likely that the timing of the male molting season differs between species.

For both species, however, the relative abundance of the four shell conditions differed between sexes (*C. tanneri*, χ^2=104.1, P<0.001; *C. angulatus*, χ^2=130.0, P<0.001) primarily because males had lower shell-condition scores than did females. Such between-sex differences in shell condition scores could reflect differences in the timing of the molt relative to sampling, differences in preferred habitat, or differences in adult mortality rate. Alternatively, such differences in shell condition could indicate that mature males have molted more recently, on average, than adult females, raising the question of whether males cease molting at maturity. Jamieson et al. (1990) believed that male *C. tanneri* undergo a terminal puberty molt and are therefore similar to *C. opilio*, for which a male terminal molt has been clearly established (Conan and Comeau, 1986). However, Tester and Carey (1986) also found a between-sex difference, similar to our study, in the index of postmolt age for *C. tanneri* off Oregon; mature males exhibited considerably lower incidence of exoskeleton damage from chitonoclastic bacteria than did mature females. This sexual difference in exoskeleton damage was interpreted as an indication that male *C. tanneri* continue to molt after maturity. Although our shell-condition data were consistent with the observations of Tester and Carey (1986), we are not convinced that this indicates that males contintue to molt.

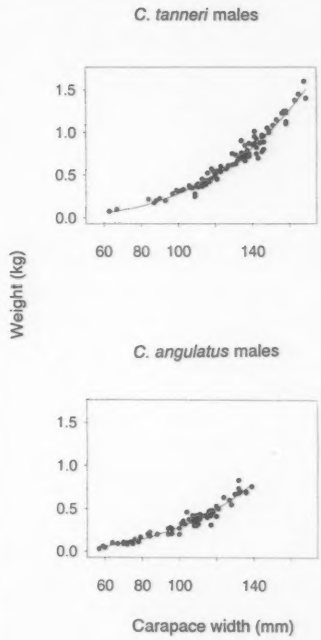

Figure 8

Weight-length relationships for *Chionoecetes tanneri* and *C. angulatus* and the fitted power curves.

Weight–carapace-width relationship

The increase in male body weight with carapace width (Fig. 8) was not significantly different between the two species (ANCOVA, P=0.92; Table 4), therefore a single function was fitted to the combined data. This similarity in the weight-width relationship reflects a remarkable similarity in the shape of *C. tanneri* and *C. angulatus* compared with shallow-water species of *Chionoecetes*. For example, the predicted weight at 120 mm CW is 505 gm for both *C. tanneri* and *C. angulatus* males. The weight of a similar-size *C. japonicus*, another slope-dwelling species, is 588 gm (Watanabe and Suzuuchi, 1983), fairly close to *C. tanneri* and *C. angulatus*. However, the

Table 4

Parameter estimates for the fitted equation weight (gm) = a (carapace width in mm)^b, number of data (n), and goodness of fit (R^2) for male *C. tanneri* and *C. angulatus*, and for both species combined.

	a	b	n	R^2
C. tanneri	1.186×10^{-4}	3.189	101	0.96
C.angulatus	2.244×10^{-4}	3.054	76	0.94
Combined	1.219×10^{-4}	3.183	177	0.97

weight of a similar-size *C. opilio* from the shelf of the eastern Bering Sea is 739 gm (Somerton, 1981c), considerably heavier than the slope species. The likely explanation for this is that slope species of *Chionoecetes*, like slope species of king crabs, have proportionately thinner legs than shelf species (Somerton, 1981b). The evolutionary significance of such depth-related changes in shape is unclear, but for other deep-water crustacea, reduced musculature is assumed to be an adaptation for energy efficiency in a habitat where food is scarce (Childress, 1971).

Similarity of *C. angulatus* and *C. japonicus*

Repeatedly throughout the foregoing discussion, we have compared various distributional or life history characteristics reported from other studies of *C. japonicus* with those determined for *C. angulatus* from our samples because we suspect that the two species actually are either taxonomically identical or that *C. japonicus* is a subspecies of *C. angulatus* (3 years after Rathbun [1932] described *C. japonicus*, Derjugin and Kobjakowa [1935] described *C. angulatus bathyalis* on the basis of specimens that were also collected near Japan). We base our question not only on the similarity of the various biological features that we examined (e.g. size and depth distribution, size at maturity) but also on the high degree of similarity in shape between the two species. We recommend that the validity of the separation of *C. angulatus* and *C. japonicus* be re-examined by qualified systematists.

Acknowledgments

We thank Allen Shimada for help in sampling, William Meyers for laboratory analysis of the fecundity samples, and Bob Otto, Bob McConnaughey, and Gerard Conan for reviewing the manuscript.

Literature cited

Alton, M.
1986. Fish and crab populations of the Gulf of Alaska seamounts. *In* R. H. Uchida, S. Hayes, and G. W. Boehlert (eds.), Environment and resources of seamounts in the North Pacific, p. 45–51. U.S. Dep. Commer., NOAA Tech. Rep. NMFS 43.

Chambers, J. M., and T. J. Hastie.
1992. Statistical models in S. Wadsworth and Brooks/Cole, Pacific Grove, CA, 608 p.

Childress, J. J.
1971. Respiratory rate and depth of occurrence of midwater animals. Limnol. Oceanogr. 16:104–106.

Conan, G. Y., and M. Comeau.
1986. Functional maturity and terminal molt of male snow crab, *Chionoecetes opilio*. Can. J. Fish. Aquat. Sci. 43:1710–1719.

Derjugin, K. M., and S. Kobjakowa.
1935. Zur Dekapodenfauna des Japonishen Meeres. Zoologischer Anzeiger 112:141–147.

Fukatake, I.
1965. Number of ovarian eggs of the deep sea edible crab, *Chionoecetes japonicus*, in the Japan Sea. Bull. Jpn. Sea Reg. Fish Res. Lab. 15:95–97. J. Fish. Res. Board Canada Trans. Ser. 1192.

Garth, J. S.
1958. Brachyura of the Pacific Coast of America. Oxyrhyncha. Allan Hancock Pacific Exped. 21, 854 p.

Hart., J. F. L.
1982. Crabs and their relatives in British Columbia. British Columbia Prov. Mus. Handbk. 40, 266 p.

Hartnoll, R. G.
1978. The determination of relative growth in crustacea. Crustaceana 34:281–293.

Haynes, E., J. F. Karinen, J. Watson, and D. J. Hopson.
1976. Relation of number of eggs and egg length to carapace width in the brachyuran crabs *Chionoecetes bairdi* and *C. opilio* from the southeastern Bering Sea and *C. opilio* from the Gulf of St. Lawrence. J. Fish. Res. Board Can. 33:2592–2595.

Hughes, S. E.
1981. Initial U.S. exploration of nine Gulf of Alaska seamounts and their associated fish and shellfish resources. Mar. Fish. Rev. 42(1):26–33.

Ito, K.
1976. Maturation and spawning of the queen crab *Chionoecetes japonicus* in the Japan Sea with special reference to the reproductive cycle. Bull. Jpn. Sea Reg. Fish. Res. Lab. 27:59–74. [In Japanese.]

Jamieson, G.
1990. Development of a fishery for *Chionoecetes tanneri* on the continental slope off British Columbia: management considerations. *In* Proceedings of the international symposium on king and Tanner Crabs; Nov. 1989, Anchorage, Alaska, p. 587–592.

Jamieson, G., G. Heritage, and N. Noakes.
1990. Life history characteristics of *Chionoecetes tanneri* off British Columbia. *In* Proceedings of the international symposium on king and Tanner crabs; Nov. 1989. Anchorage, Alaska, p. 153–162.

Pereyra, W.
1966. The bathymetric and seasonal distribution and reproduction of adult Tanner crabs, *Chionoecetes tanneri* Rathbun, off the northern Oregon Coast. Deep Sea Res. 13:1185–1205.

1967. Tanner crab—untapped Pacific resource. Natl. Fisherman. 48(4):16

1968. Distribution of juvenile Tanner crabs, *Chionoecetes tanneri* Rathbun, life history model and fisheries management. Proc. Natl. Shellfish Assoc. 58:66–70.

Rathbun, M. J.

1932. Preliminary descriptions of new species of Japanese crabs. Proc. Biol. Soc. Wash. 45:29–38.

Sinoda, M.

1982. Fisheries for the genus *Chionoecetes* in southwest Japan Sea. *In* Proceedings of the international symposium on the genus *Chionoecetes*, p. 21–39. Alaska Sea Grant Rep. 82–10.

Somerton, D.

1980. A computer technique for estimating the size of sexual maturity in crabs. Can. J. Fish. Aquat. Sci. 37:1488–1494.

1981a. Regional variation in the size of maturity of two species of Tanner crab (*Chionoecetes bairdi* and *C. opilio*) in the eastern Bering Sea, and its use in defining management subareas. Can. J. Fish. Aquat. Sci. 38:153–174.

1981b. Contribution to the life history of the deep-sea king crab, *Lithodes couesi*, in the Gulf of Alaska. Fish. Bull. 79:259–269.

1981c. Life history and population dynamics of two species of Tanner crab, *Chionoecetes bairdi* and *C. opilio*, in the eastern Bering Sea with implications for the management of the commercial harvest. Ph.D. diss., Univ. Washington, Seattle, WA, 220 p.

1982. Estimating the frequency of molting in adult male *Chionoecetes bairdi* in the eastern Bering Sea. Proceedings of the international symposium on the genus *Chionoecetes*. Alaska Sea Grant Rep. 82-10.

Somerton, D., and R. Otto.

1986. Distribution and reproductive biology of the golden king crab, *Lithodes aequispina*, in the eastern Bering Sea. Fish. Bull. 84:571–584.

Tester, P., and A. Carey.

1986. Instar identification and life history aspects of juvenile deepwater spider crabs, *Chionoecetes tanneri* Rathbun. Fish. Bull. 84:973–980.

Watanabe, Y., and T. Suzuuchi.

1983. On the queen crab *Chionoecetes japonicus* off the Western Coast of Hokkaido of Japan Sea. 2: Relative growth off the south-western coast. J. Hokkaido Fish. Exp. Station (Hokusuishi Geppo) 40:187–199.

Watson. J.

1970. Maturity, mating and egg laying in the spider crab, *Chionoecetes opilio*. J. Fish. Res. Board Can. 27:1607–1616.

Yosho, I., and I. Hayashi.

1994. The bathymetric distribution of *Chionoecetes opilio* and *C. japonicus* (Majidae: Brachyura) in the western and northern areas of the Sea of Japan. Bull. Jpn. Sea Natl. Res. Inst. 44:59–71.

Young, C. M.

1994. A tale of two dogmas: the early history of deep-sea reproductive biology. *In* C. M. Young and K. J. Eckelbarger (eds.), Reproduction, larval biology and recruitment of the deep-sea benthos, p. 1–25. Columbia Univ. Press, New York, NY.

Biology and distribution of arrowtooth, *Atheresthes stomias*, and Kamchatka, *A. evermanni*, flounders in Alaskan waters

Mark Zimmermann
Pamela Goddard
Alaska Fisheries Science Center
National Marine Fisheries Service, NOAA
7600 Sand Point Way NE, Seattle, Washington 98115-0070

Abstract.—The biology and distribution of arrowtooth, *Atheresthes stomias*, and Kamchatka, *A. evermanni*, flounder were examined in Alaskan waters to determine whether there were sufficient differences to justify treating them as separate species in resource assessment surveys conducted by the National Marine Fisheries Service. Geographic ranges of the two flounder species overlap in Alaska waters; both occur in the eastern Bering Sea and western Aleutian Islands region. However, only arrowtooth flounder occur throughout the eastern Aleutian Islands region and the Gulf of Alaska. Arrowtooth flounder were abundant over a wide range of depths (76–450 m) and were more abundant than Kamchatka flounder in catches shallower than 325 m. Kamchatka flounder were abundant only in deep trawl hauls (226–500 m) and were more abundant than arrowtooth flounder in catches at depths greater than 375 m. Arrowtooth flounder were also abundant over a wide range of bottom-water temperatures (2.1°–4.6°C), whereas Kamchatka flounder were abundant in a much narrower range of bottom temperatures (3.8°–4.2°C). By percentage, females dominated the arrowtooth flounder population in the eastern Bering Sea (68.6%) and Aleutian Islands region (59.6%), whereas the Kamchatka flounder population was 55.9% and 47.5% female, respectively. The females of both species attained greater length at age than did the males. The difference in growth between the sexes was greater among arrowtooth flounder and may account for the preponderance of females in the arrowtooth flounder population.

Manuscript accepted 9 January 1996.
Fishery Bulletin 94:358–370 (1996).

Arrowtooth flounder, *Atheresthes stomias*, and Kamchatka flounder, *A. evermanni*, were not always treated as separate species in resource assessment bottom trawl surveys of the Alaska Fisheries Science Center (AFSC) prior to 1991 because of their similarity in appearance, lack of commercial importance, and the limited abundance of Kamchatka flounder in comparison with arrowtooth flounder. They were both grouped as arrowtooth flounder and possible differences between them were not thoroughly documented. Most of the previous research conducted on *Atheresthes* spp. has treated them as a species complex. The few comparative studies of *Atheresthes* spp., based on morphometrics (Norman, 1934; Wilimovsky et al., 1967; Yang, 1988), genetics (Ranck et al., 1986), diet (Yang and Livingston, 1986), and geographic distribution (Shuntov, 1965; Wilimovsky et al., 1967; Allen and Smith, 1988), have documented few differences between the two species.

Arrowtooth flounder accounts for 55% of the flatfish biomass in the western Gulf of Alaska (Brown[1]); it is the dominant flatfish of that area, and yet it has not supported a large fishery. Arrowtooth flounder have been caught commercially in small fisheries off the Pacific coast of Canada and off the Washington and Oregon coasts for use in animal feeds as well as for human consumption (Kabata and Forrester, 1974). Softening of the flesh, probably caused by an enzyme released from a myxosporean parasite (Greene and Babbitt, 1990), has limited the marketability of arrowtooth flounder as food. Recent work, however, has shown promise in producing marketable flounder products, such as arrowtooth flounder fillets (Greene and Babbitt, 1990), arrowtooth flounder surimi (Wasson et al., 1992; Porter et al., 1993; Reppond et al., 1993), and Kamchatka flounder surimi (Haga et al.[2]). Potentially, a fishery targeting arrowtooth flounder in Alaskan waters could have an effect on the Alaskan population of Kamchatka flounder. Knowledge of the biology of the two species may provide crucial information needed for their proper management and conservation. Therefore, since 1991, these species have been considered as two separate

[1] Brown, E. S. 1994. Alaska Fisheries Science Center, Resource Assessment and Conservation Engineering Division, 7600 Sand Point Way NE, Seattle, WA 98115. Personal commun.

[2] Haga, H., R. Shigeoka, and T. Yamauchi. 1980. Method for processing fish contaminated with sporozoa. U.S. Patent 4,207,354, Jun. 10.

species during resource assessment surveys conducted by the AFSC.

The purpose of the present work was to document the geographical overlap of the two flounder species in Alaskan waters and to describe the ecological differences, such as length at age, sex-ratios, and depth and temperature preferences that allow such externally similar species to coexist. Incorporation of this information into future AFSC surveys may prove essential for the management of the two species.

Materials and methods

Data were obtained from bottom trawl surveys conducted from research vessels over the continental shelf (<200 m) and slope (200–800 m) of the eastern Bering Sea and off the Aleutian Islands (<500 m). The surveys were conducted from June through September 1991. Sample design, fishing gear and methods, catch sampling procedures, and data analyses are described by Goddard and Zimmermann[3] for the eastern Bering Sea shelf and slope and by Harrison (1993) for the Aleutian Islands. The bottom trawl used in the Bering Sea shelf survey was different from that used in the Bering Sea slope and Aleutian Islands region. The bottom trawl used on the Bering Sea shelf had smaller meshes in the net wings and body and was used without roller gear; therefore it fished heavily on the bottom. The bottom trawl used on the Bering Sea slope and in Aleutian Islands region was used with bobbin roller gear and had larger meshes in the net wings and body. Additional data were incorporated from the western Gulf of Alaska bottom trawl survey (<500 m) conducted in 1993 but were used only for defining geographic ranges. Nets were towed at approximately 5.5 km/hr (3 knots) for 30 minutes, covering a distance of 2.8 km (1.5 nmi). Mean net width, as measured with SCANMAR net mensuration gear, was multiplied by the distance traveled to calculate the area swept by the net. Catch per unit of effort (CPUE) was calculated for each species for each tow in kilograms per hectare (kg/ha). Either micro-bathythermograph probes fixed to the net or expendable bathythermograph probes dropped at the haul sites recorded bottom temperatures (±0.1°C).

Arrowtooth and Kamchatka flounders were distinguished by the position of their upper eyes. The upper eye of arrowtooth flounder interrupts the profile of the head and can be seen from the blind side. The upper eye of the Kamchatka flounder does not interrupt the head profile. Fish whose upper eye was not located with any certainty or which had a damaged upper eye were distinguished by number of gill rakers (Yang, 1988). After sorting, each species was weighed separately. Fish size was recorded as fork length, and the sex of each fish was determined by making an incision posterior to the abdomen on the blind side and by visually inspecting the gonadal tissue.

Comparisons were made between the abundance of the two species in CPUE (kg/ha) by depth interval and water temperature interval. When there were a sufficient number of hauls, depth was divided into 25-m intervals and temperature into 0.1°C intervals. When there were few hauls, catches were grouped into 100-m depth intervals and 1.0°C intervals. For trawl hauls in which both species were caught, a logistic model was developed to show the relationship between the proportion of arrowtooth flounder in the total *Atheresthes* catch and depth;

$$(\ln(p/1-p) = \alpha + \beta x),$$

where p is the proportion of arrowtooth flounder in the total *Atheresthes* catch rate, $1-p$ is the proportion of Kamchatka flounder in the total *Atheresthes* catch rate, α and β are constants, and x is the depth in meters.

The geographic distributions of both species were described from our thorough but depth-limited bottom trawl survey data, supplemented by data supplied by the Fishery Observer Program of the AFSC, which also supplied species composition data on catches from deep waters in the Gulf of Alaska. Nonlinear regressions related mean length of arrowtooth and Kamchatka flounder by haul to depth;

$$L = L_{\infty} - Ae^{BM},$$

where L is estimated length, L_{∞} is theoretical maximum length, M is depth in meters, and A and B are constants.

Initial observations indicated an unusually high percentage of females in the arrowtooth flounder population. Juvenile fish from which the sex could not be determined, generally less than 20 cm in length, were not included in the analysis. The percentage of females in the arrowtooth flounder population was compared against the percentage of females in the Kamchatka flounder population for both the Aleutian Islands and the eastern Bering Sea. Comparisons were also made against the other major flatfish species in the eastern Bering Sea to de-

[3] Goddard, P., and M. Zimmermann. 1993. Distribution, abundance, and biological characteristics of groundfish in the eastern Bering Sea based on results of the U.S. bottom trawl survey during June–September 1991. AFSC Processed Rep. 93-15, 342 p. Alaska Fisheries Science Center, Natl. Mar. Fish. Serv., NOAA, 7600 Sand Point Way NE, Seattle, WA 98115-0070.

termine whether the unusually high percentage of females in the arrowtooth flounder population, seemingly an odd occurrence, was also typical of the other species from the same area caught in the same survey. Additional comparisons could not be made from data gathered in the Aleutian Islands because of the limited number of sex determinations of other flatfish species.

The unusually high percentage of females in the arrowtooth flounder population prompted us to analyze the data in different ways to look for trends in percentages of females. The percentage of females was calculated from individual trawl hauls in which the sex was determined from a minimum of 10 fish. Percent-female values for arrowtooth flounder were examined geographically to determine whether there were regions where male arrowtooth flounder were abundant. Percent-female values were also regressed against bottom temperature and depth. By searching for trends in percent-female values, we hoped to identify areas where high proportions of arrowtooth flounder males may have occurred but were not sampled or were underrepresented in our survey.

For fish from the eastern Bering Sea slope, sagittal otoliths were collected from up to three fish per sex per centimeter interval for ageing and were stored in a glycerol-thymol solution. Because previous methods for preparing the otoliths for ageing did not clearly reveal the annular rings, researchers at the AFSC developed a new technique (Scott[4]). Otoliths were cut along their dorsal-ventral axis through the nucleus and evenly heated in a muffle furnace at 270°C for 5 to 10 min. If the annular rings were not sufficiently darkened, the otoliths were burned in an alcohol flame. When cool, oil was applied to the otolith surface and the cut surface read with a binocular dissecting scope.

Von Bertalanffy growth curves were calculated for the age and length data by using nonlinear regression to provide estimates of L_∞, K, and t_0. To determine whether growth differed significantly between sexes or between species, the residual sum of squares (RSS) from a combined model was compared by using an approximate F-test (Draper and Smith, 1981):

$$F = \frac{(RSS_{TOTAL} - (RSS_1 + RSS_2))/3}{(RSS_1 + RSS_2)/N - 6},$$

where N is equal to the number of otoliths aged, and 1 and 2 are either male and female arrowtooth or male and female Kamchatka flounder. Kimura (1990) showed that this approximation of the test statistic, which tests for differences between all growth curve parameters simultaneously, can be useful for testing von Bertalanffy growth parameters. The test statistic was compared against values from the F-distribution at the α=0.05 level of significance. The von Bertalanffy parameters were then used to provide estimates of length at age for the range of ages found for each species and sex group.

Results

Atheresthes spp. were caught in 492 of the 779 trawl hauls. Neither species was caught in the shallowest trawl hauls (<25 m), whereas catch rates for both species were low in the deepest trawl hauls (700 m to 800 m). Arrowtooth flounder were abundant from 76 m to 450 m, with mean CPUE ranging from 3.3 to 13.6 kg/ha (Fig. 1). Kamchatka flounder were abundant from 226 m through 500 m, with mean CPUE ranging from 3.8 to 12.8 kg/ha. Arrowtooth flounder catch rates showed a bimodal distribution in relation to depth, with high catch rates in both shallow (76 m to 225 m) and deep (226 m to 450 m) trawl hauls. Kamchatka flounder catch rates were weakly bimodal, with only low catch rates in shallow waters and all the highest catch rates in deeper waters.

A comparison of the percent of the total *Atheresthes* CPUE by species for each depth interval shows that arrowtooth flounder were more abundant in the shallower depth intervals (≤250 m) (Fig. 2). There was a zone of transition between the two species from 251 m to 425 m. Finally, Kamchatka flounder were more abundant than arrowtooth flounder from 426 m to 800 m. For trawl hauls in which both species were caught, a logistic regression relating percentage of arrowtooth flounder of the total *Atheresthes* CPUE against depth (Fig. 3) showed a significant, negative relationship (df=277, F=98.8, P<0.001, R^2=0.26). The model was

$$3.47 - 0.009(Depth) = \ln(p/1-p),$$

where p = Arrowtooth flounder CPUE/*Atheresthes* CPUE.

Data on the water temperature distribution of *Atheresthes* spp. were recorded from 252 of the 492 trawl hauls in which *Atheresthes* spp. were caught. *Atheresthes* spp. were caught only in temperatures between 0.3° and 5.9°C (Fig. 4), whereas the survey temperatures ranged from −1.5° to 11.7°C. Arrowtooth flounder were abundant at a wide range of bottom temperatures, but they were most abundant at temperatures of 2.1° to 4.6°C. While the total range

[4] Scott, K. 1994. Alaska Fisheries Science Center, Resource Ecology and Fisheries Management Division, 7600 Sand Point Way NE, Seattle, WA 98115. Personal commun.

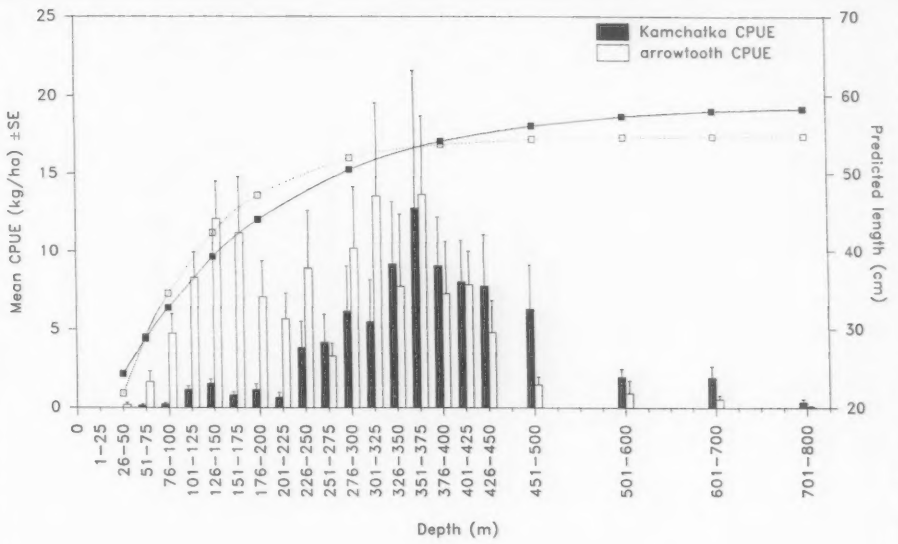

Figure 1

Mean catch per unit of effort (CPUE) in kg/ha (±1 SE) in relation to depth interval for the *Atheresthes* species. Length-at-depth curves are superimposed over the bar graph.

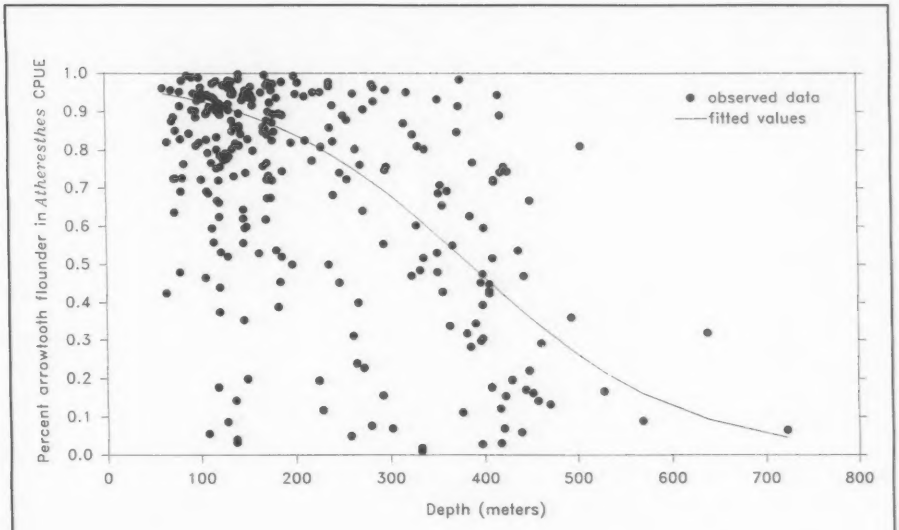

Figure 2

Percent by species of the total *Atheresthes* catch per unit of effort (CPUE) in relation to depth interval.

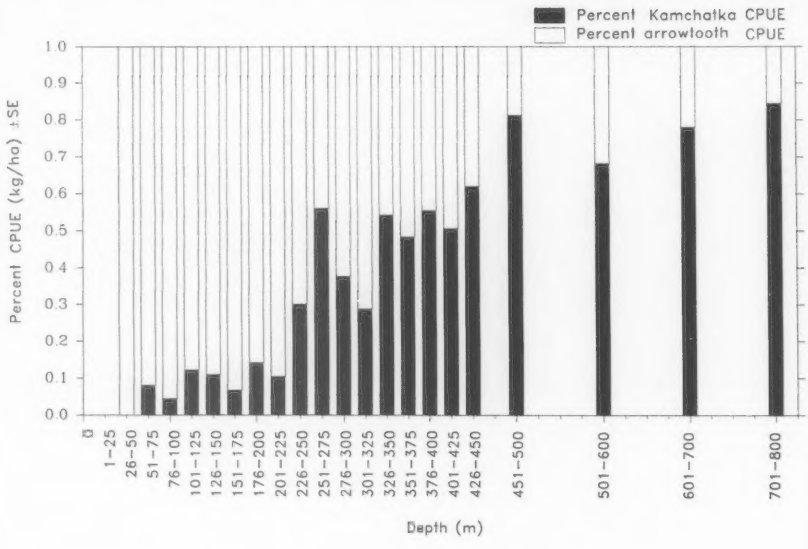

Figure 3

Logistic model relating percentage of arrowtooth flounder of the total *Atheresthes* catch rate to depth.

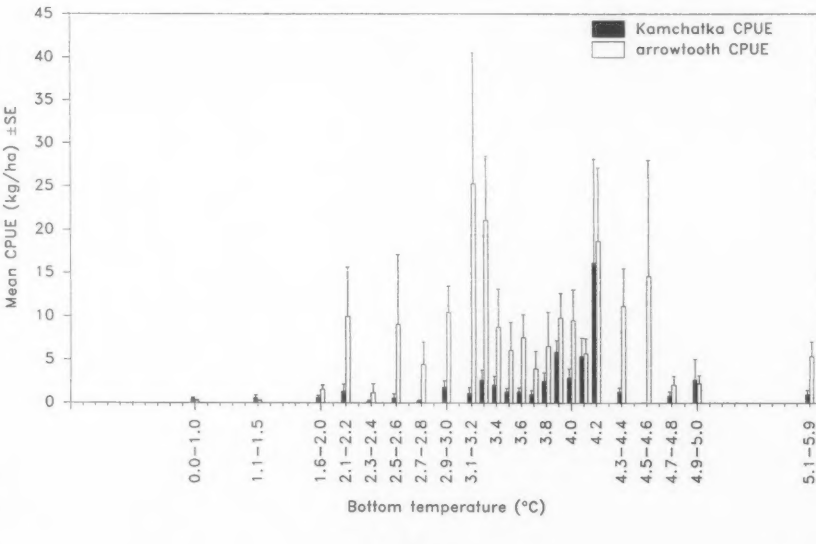

Figure 4

Mean catch per unit of effort (CPUE) in kg/ha for the *Atheresthes* species in relation to bottom temperature.

of water temperatures for Kamchatka flounder (0.7° to 5.9°C) was similar to the range for arrowtooth flounder (0.3° to 5.9°C), the highest catch rates of Kamchatka flounder were distributed over a narrower temperature range (3.8° to 4.2°C).

Arrowtooth flounder catch rates were high on the eastern Bering Sea continental shelf (7.3 kg/ha), especially in waters between 100 m and 200 m (17.7 kg/ha), on the eastern Bering Sea continental slope (8.8 kg/ha), and the fish occurred throughout the Aleutian Islands (Fig. 5). The Kamchatka flounder geographic distribution was similar to that of arrowtooth flounder (Fig. 6), except that Kamchatka flounder were not caught along the Alaska Peninsula, nor in the Gulf of Alaska. Kamchatka flounder were much less abundant than arrowtooth flounder in the eastern Bering Sea, especially on the shelf (1.2 kg/ha), and about half as abundant as arrowtooth flounder on the slope area (4.6 kg/ha). However, in the deepest half of the slope area (500 m to 800 m), the catch rate of Kamchatka flounder (1.5 kg/ha) was about twice that of arrowtooth flounder (0.7 kg/ha). Kamchatka flounder occurred on the northwest tip of the eastern Bering Sea shelf, whereas arrowtooth flounder were absent from that area. Arrowtooth flounder catch rate was high along the north side of the easternmost Aleutian Islands bordering the southern Bering Sea (16.4 kg/ha), where more than half of the total biomass for the entire Aleutian Islands occurred (Harrison, 1993). Kamchatka flounder generally decreased in abundance from west to east along the Aleutian Islands (Harrison, 1993). The easternmost Aleutian Islands were the southeastern border of their distribution, where the catch rate was low (0.7 kg/ha). In the rest of the Aleutian Islands area, Kamchatka flounder had a slightly higher catch rate (3.1 kg/ha) than arrowtooth flounder (2.9 kg/ha), particularly in the 300 m to 500 m depth interval (10.8 vs. 2.0 kg/ha, Harrison, 1993).

Data provided from the Fishery Observer Program of the AFSC indicated the presence of Kamchatka flounder in the Gulf of Alaska as far east as 154°26'W, but in limited numbers and at great depths (Conrad[5]). The identification of Kamchatka flounder oc-

[5] Conrad, M. 1994. Alaska Fisheries Science Center, Fishery Observer Program, 7600 Sand Point Way NE, Seattle, WA 98115. Personal commun.

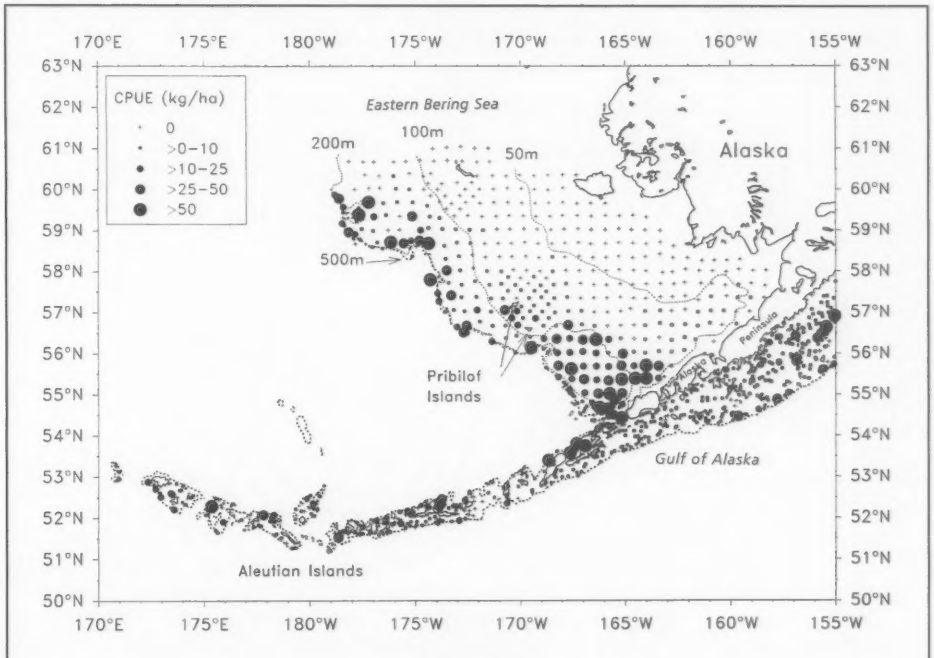

Figure 5

Map of arrowtooth flounder, *Atheresthes stomias*, CPUE (kg/ha) over the eastern Bering Sea shelf and slope, in waters off the Aleutian Islands, and in Gulf of Alaska areas. The 50-, 100-, and 200-m bathymetric contours are not included in the Aleutian Islands and Gulf of Alaska areas owing to complicated bottom topography.

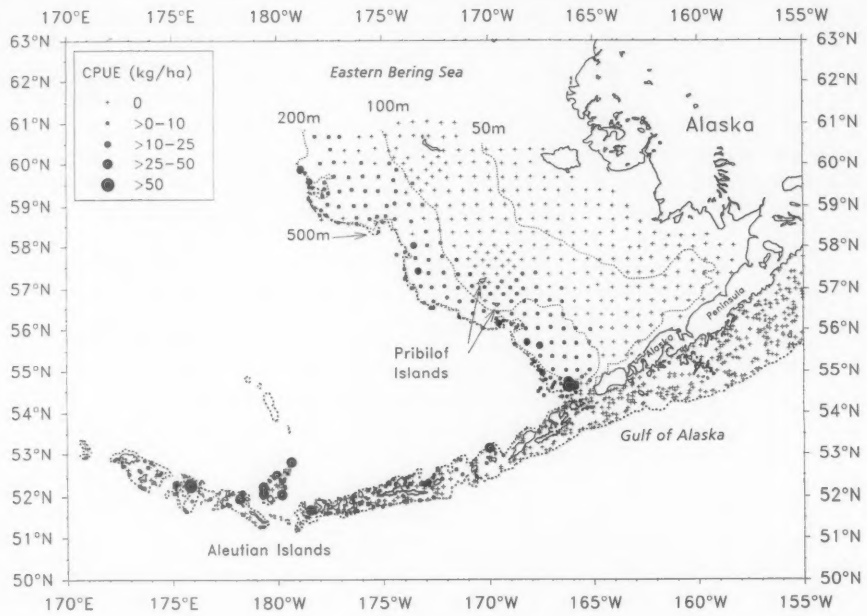

Figure 6

Map of Kamchatka flounder, *Atheresthes evermanni*, CPUE (kg/ha) over the eastern Bering Sea shelf and slope, in waters off the Aleutian Islands, and in Gulf of Alaska areas. The 50-, 100-, and 200-m bathymetric contours are not included in the Aleutian Islands and Gulf of Alaska areas owing to complicated bottom topography.

curring in the Gulf of Alaska was confirmed by meristic data recorded from three specimens. These rare occurrences of Kamchatka flounder in the Gulf of Alaska (length range 56–65 cm) were in depths (549–686 m) outside the depth range covered during the Gulf of Alaska bottom trawl survey.

The mean length of both *Atheresthes* flounders increased with depth, and asymptotic, curvilinear models were fitted to the data

$$\textit{arrowtooth flounder length} = 54.8 - 53.8e^{-0.0098\textit{depth}},$$

(df=131, F=3618.8, P<0.001, R^2=0.80);

$$\textit{Kamchatka flounder length} = 58.8 - 45.9e^{-0.0057\textit{depth}},$$

(df=64, F=2123.3, P<0.001, R^2=0.75).

The models show that for much of the size range (~30 cm to ~50 cm) for both species, Kamchatka flounder of the same length as arrowtooth flounder occur at a greater depth (superimposed on Fig. 1). Kamchatka flounder attain a greater length at depth than do arrowtooth flounder in depths greater than 400 m.

The relationship between length and water temperature was more complex and could be adequately described only in combination with geographic and depth relationships. The combined results from the eastern Bering Sea and Aleutian Island regions are presented in Table 1. A comparison of the depth and temperature differences between size groups and between species by statistical analyses was difficult because of lack of independence of the samples (both species were often taken together). Although the differences could not be tested, different size groups appeared to be associated with different depth zones and temperatures.

Catches of small arrowtooth flounder (<30 cm FL) were associated with shallow areas near the Pribilof Islands, the Alaska Peninsula, and the region north of the eastern Aleutian Islands. Medium-size arrowtooth flounder (from ≤30 to <40 cm FL) were grouped mostly between the 100 m and 200 m isobaths on the eastern Bering Sea shelf and around the central Aleutian Islands. The largest arrowtooth flounder

Table 1

Mean depth and mean temperature of trawl hauls from the eastern Bering Sea and Aleutian Islands region for small (<30 cm), medium (≥30 to <40 cm), and large (≥40 cm) arrowtooth, *Atheresthes stomias*, and Kamchatka, *A. evermanni*, flounder. Standard errors (±1) are in parentheses.

	Length group					
	Small	*n*	Medium	*n*	Large	*n*
Arrowtooth flounder						
Mean depth (m)	74.1 (3.11)	26	121.4 (2.64)	109	255.0 (10.41)	110
Mean temperature (°C)	4.5 (0.30)	16	3.4 (0.12)	48	3.7 (0.09)	70
Kamchatka flounder						
Mean depth (m)	—		135.1 (3.96)	37	351.4 (13.36)	66
Mean temperature (°C)	—		3.7 (0.19)	15	3.8 (0.09)	50

(≥40 cm FL) were caught near the edge of the Bering Sea shelf, in the Bering Sea slope area, and throughout the Aleutian Islands regions.

There was a difference in the temperature regimes of the Aleutian Islands and eastern Bering Sea regions. In waters off the Aleutian Islands, where collection of length data combined with bottom temperature data was scant (n=18), there was a significant, negative relationship between length and bottom temperature (df=16, F=13.5, P=0.002, R^2=0.46): smaller fish were present in the shallowest and warmest water (~5° to 6°C) whereas larger fish were found in deeper, cooler water, approaching 4°C. On the Bering Sea shelf and slope, there was a more complex relationship between fish size and bottom temperature, described by a large number (n=116) of observations. As fish size increased with depth, the bottom temperature dropped from 4.1°C (<30 cm FL, n=10) to 3.3°C (from ≤30 to <40 cm FL, n=43), and to 2.4°C (≥40 cm FL, n=12) near the shelf edge, though the largest fish were located where the bottom temperature increased (3.9°C, n=51) in the slope area.

For Kamchatka flounder, the group of smaller size fish was eliminated from analysis because it was represented by only five hauls, and for only two of those hauls had bottom temperatures been recorded. The groups of medium- and large-size Kamchatka flounder had geographic distributions similar to groups of comparable-size arrowtooth flounder. The medium-size (from ≤30 to <40 cm FL) Kamchatka flounder were found on the Bering Sea shelf generally between the 100 m and 200 m isobaths; however, they did not extend along the Alaska Peninsula nor near the eastern Aleutian Islands as did arrowtooth flounder. The group of large-size Kamchatka flounder (≥40 cm FL) was found along the edge of the Bering Sea shelf, the Bering Sea slope, and throughout waters off the Aleutian Island chain, similar in geographic range to arrowtooth flounder. However, they were absent from the eastern islands. The bottom temperature data for the Kamchatka flounder was similar to that of the arrowtooth flounder, except that there were fewer data.

Arrowtooth flounder catches typically had a high percentage of females, whereas the Kamchatka flounder catches taken from the same trawl hauls generally had an equal sex ratio (our observations). In the eastern Bering Sea, the arrowtooth flounder population had a greater percentage of females (68.6%) than did the Kamchatka flounder population (55.9% female) (Table 2). Arrowtooth flounder also had a greater percentage of females than did *Hippoglossoides* spp. (51.7% female), Alaska plaice (*Pleuronectes quadrituberculatus*, 42.3% female), rock sole (*P. bilineatus*, 48.9% female) and yellowfin sole (*P. asper*, 54.2% female).

In the Aleutian Islands, arrowtooth flounder also had a higher percentage of females (59.6% female) than did Kamchatka flounder (47.5% female) and rock sole (52.6% female), the only species encountered in sufficient numbers in trawl hauls for comparison.

Plotting female percentage values of arrowtooth flounder geographically did not indicate any large areas where the percentage of females was low. Nor did it indicate areas where the population had a low percentage of females but was either undersampled or outside of the sampled area. The percentage of females was not significantly related to depth

($P>0.05$). The percentage of females was, however, significantly related to mean bottom-water temperature (df=121, $F=9.3$, $P=0.003$), but the relationship was very poor ($R^2=0.07$).

Otoliths were read from 187 arrowtooth and 120 Kamchatka flounder (Table 3). Computer generated estimates of L_∞, K, and t_0 were accepted except for the L_∞ estimates for arrowtooth flounder females. Our length measurement data indicated that the computer estimate was about 40 cm too long, therefore the relationship was forced, with L_∞ set to 85 cm. The von Bertalanffy growth curve was significantly different ($F=42.8$, $P<0.001$) between arrowtooth flounder males ($n=53$, range 3 to 9 years old) and females ($n=134$, range 4 to 12 years old, Fig. 7A). The growth curve was also significantly different ($F=10.6$, $P<0.001$) between Kamchatka flounder males ($n=57$, range 3 to 10 years old) and females ($n=63$, range 4 to 33 years old, Fig. 7B). Most of the Kamchatka flounder females were between the ages of 4 and 13 years, and just two fish were aged as 30 and 33 years old (not shown in Fig. 7B). All analyses were performed with and without the 30- and 33-year-old Kamchatka flounder females, with no change in results. The females of both species attained a longer length at age than did the males. For example, at age 9, female Kamchatka flounder were estimated to be 5 cm longer than male Kamchatka flounder and at age 9, female arrowtooth flounder were estimated to be 13 cm longer than the males.

The growth curves of arrowtooth flounder females and Kamchatka flounder females were significantly different ($F=25.0$, $P<0.001$), indicating that female arrowtooth flounder attain a greater length at age than Kamchatka flounder females (Fig. 7). For example, at age 9, female arrowtooth flounder were 7 cm longer than female Kamchatka flounder. The growth curve parameters of arrowtooth flounder males and Kamchatka flounder males were not significantly different ($P>0.05$).

Table 2

Percentage of females in the populations of the major flatfish species surveyed in the eastern Bering Sea in 1991.

Species	Percent female	Fish sampled	Trawl hauls
Arrowtooth flounder (*Atheresthes stomias*)	68.6	14,437	142
Kamchatka flounder (*A. evermanni*)	55.9	3,443	71
Yellowfin sole (*Pleuronectes asper*)	54.2	33,387	289
Flathead sole and Bering flounder (*Hippoglossoides* spp.)	51.7	25,872	342
Rock sole (*P. bilineatus*)	48.9	29,677	281
Alaska plaice (*P. quadrituberculatus*)	42.3	10,283	205

Discussion

In areas where the two species are found together, Kamchatka flounder occupy deeper water than arrowtooth flounder. The percent of arrowtooth flounder in the total *Atheresthes* catch was negatively related to depth. Even though the biomass of Kamchatka flounder was much smaller than that of arrowtooth flounder in the study area, their catch rates were actually higher than those for arrowtooth flounder in deep waters. For fish of similar size, Kamchatka flounder occurred at greater depths than arrowtooth flounder. The rare catches of small-size

Table 3

Parameters of the von Bertalanffy growth curves for arrowtooth, *Atheresthes stomias*, and Kamchatka, *A. evermanni*, flounder by sex, based on age readings from otoliths and length data from the 1991 AFSC bottom trawl survey of the eastern Bering Sea slope.

Group	Number of age readings	Age range (yr)	Length range (cm)	Parameters			Forced parameters
				L_∞	K	t_0	
Arrowtooth flounder							
Male	53	3–9	33–51	57.932	0.172	–2.172	none
Female	134	4–12	36–75	85.000	0.161	0.812	L_∞
Kamchatka flounder							
Male	57	3–10	33–55	62.344	0.157	–1.411	none
Female	63	4–33	38–91	93.880	0.085	–1.519	none

and infrequent catches of medium-size Kamchatka flounder in the study area made it impossible to compare the catch rates of both species across the shallow end of the depth distribution. Whether this situation was a sampling artifact, year-class artifact, or an accurate representation of the Kamchatka flounder depth distribution, it increased the Kamchatka flounder's apparent preference for greater depths.

Comparison of the water temperature distribution of both species may also have been confounded by the limited catches of small- and medium-size Kamchatka flounder in the study area. For arrowtooth flounder, the more common catches on the Bering Sea shelf of small-size (warmest bottom temperature) and medium-size (coldest bottom temperature) arrowtooth flounder broadened the temperature range for the species. Thus the few trawl catches of small- and medium-size Kamchatka flounder on the Bering Sea shelf might have narrowed the temperature distribution of Kamchatka flounder.

The peculiar relationship of bottom-water temperature with mean fish size (i.e. medium-size fish at moderate depths but coldest water) may be explained by the unusual bottom-water temperature distribution of the eastern Bering Sea. The coldest bottom temperatures in the eastern Bering Sea in 1991 were on the mid-shelf area (Goddard and Zimmermann[3]), as is typically the case (Kinder and Schumacher, 1981). These mid-shelf waters are a cold-water remnant of the previous winter's ice cover (Takenouti and Ohtani, 1974). In contrast to the coastal waters, the mid-shelf waters do not increase in temperature with the spring and summer increase in solar radiation (Kinder and Schumacher, 1981). The depths of the mid-shelf waters are too great to permit wind- or tidal-driven mixing, and a thermocline develops that increases the stability of the water column. No strong currents bring warmer waters from the Gulf of Alaska into this area, and the relatively warm slope waters, which are not as affected by the winter ice cover, are fortified with warm waters from the deep (Schumacher[6]).

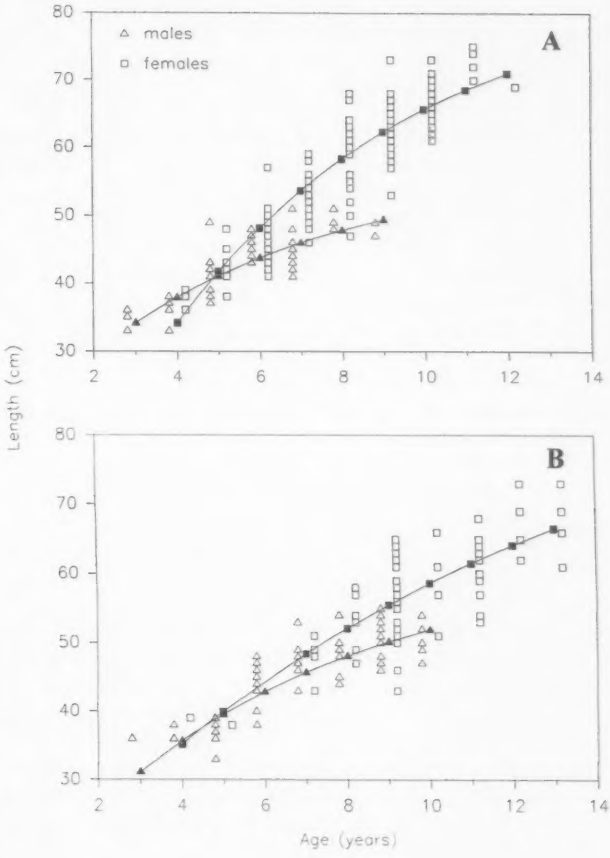

Figure 7

Individual length-at-age data (empty symbols) and von Bertalanffy estimates of mean length at age (filled symbols) for arrowtooth flounder, *Atheresthes stomias* (**A**), and Kamchatka flounder, *A. evermanni* (**B**).

The temperature data collected off the Aleutian Islands show a more typical relationship with depth; shallow bottom temperatures were warm and bottom temperature decreased, approaching 4°C, as depth increased. Most of the temperature data collected, however, came from the eastern Bering Sea shelf and slope.

Studies have shown that the geographic ranges of *Atheresthes* species do overlap in the north Pacific Ocean (Shuntov, 1965; Wilimovsky et al., 1967; Allen and Smith, 1988). The extent of the overlap and the southeastern boundary of the Kamchatka flounder distribution, however, had not been clearly defined. Kamchatka flounder has been reported to be the

[6] Schumacher, J. D. 1994. Pacific Marine Environmental Laboratory, 7600 Sand Point Way NE, Seattle, WA 98115. Personal commun.

dominant species on the northwestern side of the Pacific Ocean, and arrowtooth flounder the dominant species on the northeastern side of the Pacific Ocean (Wilimovsky et al., 1967).

Kamchatka flounder occurs along the eastern shores of Japan from as far south as 38°N (Moiseev, 1953), in the Sea of Japan (Allen and Smith, 1988), along the eastern and western shores of the Kamchatka Peninsula, and along the eastern coast of Siberia north to Cape Navarin (Shuntov, 1965). Shuntov (1965) also reported that Kamchatka flounder occurs in the eastern Bering Sea, Commander Islands region, throughout the Aleutian Islands, and into the Gulf of Alaska as far east as Shelikof Strait.

On the western side of the Pacific Ocean, arrowtooth flounder occurs along the eastern shore of the Kamchatka Peninsula north to Cape Navarin (Shuntov, 1965). It occurs in the Commander Islands region (Shuntov, 1965), the eastern Bering Sea, throughout waters off the Aleutian Islands chain, in the Gulf of Alaska, and down the West Coast of North America to San Simeon, California, 40°N (Allen and Smith, 1988).

The geographic distribution and overlap of *Atheresthes* species in Alaskan waters were more clearly defined than had been previously reported (Shuntov, 1965; Wilimovsky et al., 1967; Allen and Smith, 1988). The arrowtooth flounder population was less abundant in the Aleutian Islands than in the southern Bering Sea area. The absence of arrowtooth flounder from the northwest tip of the eastern Bering Sea shelf perhaps also indicates the decreasing abundance of arrowtooth flounder from east to west in the eastern Bering Sea. The waters around the easternmost Aleutian Islands marked the general southeastern border of the Kamchatka flounder population. Our bottom trawl survey data show a smaller geographic range for Kamchatka flounder than that reported by Shuntov (1965). Data collected by the Fishery Observer Program of the AFSC were supported by the findings of Shuntov (1965), indicating that the Kamchatka flounder distribution also extends into the Gulf of Alaska, but only in limited numbers and in deep water. Future bottom trawl hauls in deeper waters (>500 m) during AFSC Gulf of Alaska surveys may extend the Kamchatka flounder's known range farther east.

Although large-size Kamchatka flounder were reported from deep waters in the Gulf of Alaska (Conrad[5]), the lack of any Kamchatka flounder in our Gulf of Alaska survey may indicate that this is not a self-sustaining population. These large-size Kamchatka flounder may have ventured into the Gulf of Alaska from the Aleutian Islands or eastern Bering Sea areas. The westerly flowing currents in the Gulf of Alaska do not foster retention of larvae in this area (Schumacher[6]), which might make it more difficult for larval Kamchatka flounder spawned in the Gulf to remain there.

The observed high percentage of females in the arrowtooth flounder population clearly distinguishes this species from Kamchatka flounder. The overabundance of females in the arrowtooth flounder population is an unusual occurrence among the major flatfish species in the eastern Bering Sea. The possibility that the sampling gear undersampled males, either by not catching them or by not retaining them as well as it did females, remains a possible explanation that was not examined. Many other possible sources of error were explored to determine whether the number of arrowtooth flounder females was overestimated. There was no indication that areas high in percentages of males were excluded from the trawl surveys. The possibility that fishery biologists conducting the surveys might have consistently made incorrect sex determinations seems highly unlikely because females are determined by the presence of ovarian tissue, whereas males are often designated males simply because no gonadal tissues were found. Any error made because of improper sex determination should have overestimated the number of males in the population. An explanation for the overabundance of female arrowtooth flounder in our observations may come from the length-at-age results.

The difference in length at age between male and female arrowtooth flounders was significant and indicated that for fish over 5 years old, female arrowtooth flounder were larger than male arrowtooth flounder. Our results were supported by earlier AFSC surveys for the eastern Bering Sea (Smith and Bakkala, 1982; Bakkala et al., 1985; Sample et al., 1985; Walters et al., 1988) and Aleutian Islands (Ronholt et al., 1994). These studies show that growth curves for arrowtooth flounder males and females diverge as early as three to five years of age and that females are larger than males. It is doubtful, however, that in past surveys arrowtooth and Kamchatka flounder were regularly separated for otolith collections, because they were not consistently separated for other purposes. Our results differ from the length-at-age data collected from arrowtooth flounder in British Columbian waters, which showed no separation in growth curves between sexes until age 9 (Kabata and Forrester, 1974).

Our findings that female arrowtooth flounder attain a greater size at age than do male arrowtooth founder was supported by sexual maturity studies. Fifty-percent maturity occurs at a larger size in female arrowtooth flounder than in males off both the Washington (37 cm vs. 28 cm, respectively, Rickey, 1995) and Oregon coasts (44 cm vs. 29 cm, Hosie and

Barss[7]). Growth rates of males may decline as they become mature, whereas females, to support the greater reproductive burden of egg production, continue their rapid growth rate and become mature at a larger size (see Roff, 1982).

Difference in size gives arrowtooth flounder females a survival advantage over males because larger fish are better able to avoid predation. Larger fish are also better able to capture and consume larger items of prey, such as walleye pollock, *Theragra chalcogramma*, which are an important part of their diet (Yang and Livingston, 1986). Perhaps this size difference accounts for the high percentage of females in the arrowtooth flounder population.

Although the possibility of cannibalism influencing the sex ratio of arrowtooth flounder cannot be ignored, it is unlikely because cannibalism is uncommon in arrowtooth flounder (Kabata and Forrester, 1974; Yang and Livingston, 1986).

Although the von Bertalanffy growth curve parameters tested as significantly different between male and female Kamchatka flounder, the difference in length at age between the sexes was less than the difference for arrowtooth flounder and perhaps did not afford a significantly higher survival rate for the females. There were no length-at-age results for Kamchatka flounder previously reported in the literature.

The unusually high percentage of females in the arrowtooth flounder population, the greater length at age of female arrowtooth flounder over female Kamchatka flounder, the greater depth preference of Kamchatka flounder over arrowtooth flounder, and the geographic boundaries of the two species defined in the study area all indicate significant interspecies differences. We therefore recommend that arrowtooth and Kamchatka flounder be treated as separate species in resource assessment surveys and for management purposes. Additional information should be gathered on possible differences in mortality of the male and female arrowtooth flounder, the reason for the greater depth preference of Kamchatka flounder, and whether or not the Kamchatka flounder population in the study area is successfully reproducing, or whether it is migrating into the area from the west.

Acknowledgments

We thank the many individuals involved in the bottom trawl surveys, both in the collection of data at sea and in the editing of the data into its final format. We express our thanks to the captains and crews aboard the *Alaska, Ocean Hope 3, Miller Freeman, Ocean Hope 1, Green Hope, Argosy,* and *Alsea* for providing safe and efficient platforms from which to conduct our operations. We thank Mark Conrad and Ren Narita from the Fishery Observer Program of the AFSC for providing data on catch occurrences of Kamchatka flounder in the Gulf of Alaska. Kent Scott and Julie Lyons of the Age and Growth Unit of the AFSC improved upon the previous method of ageing *Atheresthes* otoliths. Comments and suggestions from several co-workers, greatly improved the quality of this manuscript. Finally, thanks go to Jim Ianelli, Dan Kimura, Peter Munro, and Steve Syrjala for their statistical assistance with our data analysis.

Literature cited

Allen, M. J., and G. B. Smith.
1988. Atlas and zoogeography of common fishes in the Bering Sea and northeastern Pacific. U.S. Dep. Commer., NOAA Tech. Rep. NMFS 66, 151 p.

Bakkala, R. G., J. J. Traynor, K. Teshima, A. M. Shimada, and H. Yamaguchi.
1985. Results of cooperative U.S.-Japan groundfish investigations in the eastern Bering Sea during June–November 1982. U.S. Dep. Commer., NOAA Tech. Memo. NMFS F/NWC-87, 448 p.

Draper, N. R., and H. Smith.
1981. Applied regression analysis, 2nd ed. John Wiley and Sons, Inc., New York, NY.

Greene, D. H., and J. K. Babbitt.
1990. Control of muscle softening and protease-parasite interactions in arrowtooth flounder, *Atheresthes stomias*. J. Food Sci. 55(2):579–580.

Harrison, R. C.
1993. Data report: 1991 bottom trawl survey of the Aleutian Islands area. U.S. Dep. Commer., NOAA Tech. Memo. NMFS-AFSC-12, 144 p.

Kabata, Z., and C. R. Forrester.
1974. *Atheresthes stomias* (Jordan and Gilbert, 1880) (Pisces: Pleuronectiformes) and its eye parasite *Phrixocephalus cincinnatus* Wilson 1908 (Copepoda: Lernaeoceridae) in Canadian Pacific waters. J. Fish. Res. Board Can. 31:1589–1595.

Kimura, D. K.
1990. Testing nonlinear regression parameters under heteroscedastic, normally distributed errors. Biometrics 46:697–708.

Kinder, T. H., and J. D. Schumacher.
1981. Hydrographic structure over the continental shelf of the southeastern Bering Sea. *In* D. W. Hood and J. A. Calder (eds.), The eastern Bering Sea shelf: oceanography and resources, vol. 1, p. 31–52. U.S. Dep. Commer., NOAA, Office of Marine Pollution Assessment, Juneau, Alaska.

Moiseev, P. A.
1953. Cod and flounders of far-eastern waters. [Fisheries Research Board of Canada, Trans. Series 119] Izvestiya TINRO, vol. 40, p. 1–287.

[7] Hosie, M. J., and W. H. Barss. 1977. Age and length at maturity of arrowtooth flounder, *Atheresthes stomias*, in Oregon waters. Oregon Dept. of Fish and Wildlife, Marine Field Laboratory, P.O. Box 5430, Charleston, OR 97420. Unpubl. manuscr., 9 p.

Norman, J. R.
1934. A systematic monograph of the flatfishes (Heterosomata). Vol. I: Psettodidae, Bothidae, Pleuronectidae. Br. Mus. (Nat. Hist.), Lond., 459 p. [Reprinted, 1966 by Johnson Reprint, NY]

Porter, R. W., B. J. Kouri, and G. Kudo.
1993. Inhibition of protease activity in muscle extracts and surimi from Pacific whiting, *Merluccius productus*, and arrowtooth flounder, *Atheresthes stomias*. Mar. Fish. Rev. 55(3):10–15.

Ranck, C., F. Utter, G. B. Milner, and G. B. Smith.
1986. Genetic confirmation of specific distinction of arrowtooth flounder, *Atheresthes stomias*, and Kamchatka flounder, *A. evermanni*. Fish. Bull. 84:222–226.

Reppond, K. D., D. H. Wasson, and J. K. Babbitt.
1993. Properties of gels produced from blends of arrowtooth flounder and Alaska pollock surimi. J. Aquat. Food Prod. Technol., vol. 2(1):83–98.

Rickey, M. H.
1995. Maturity, spawning, and seasonal movement of arrowtooth flounder, *Atheresthes stomias*, off Washington. Fish. Bull. 93:127–138.

Roff, D. A.
1982. Reproductive strategies in flatfish: a first synthesis. Can. J. Fish. Aquat. Sci. 39:1686–1698.

Ronholt, L. L., K. Teshima, and D. W. Kessler.
1994. The groundfish resources of the Aleutian Islands region and southern Bering Sea 1980, 1983, and 1986. U.S. Dep. Commer., NOAA Tech. Memo. NMFS-AFSC-31, 351 p.

Sample, T. M., K. Wakabayashi, R. G. Bakkala, and H. Yamaguchi.
1985. Report of the 1981 cooperative U.S.-Japan bottom trawl survey of the eastern Bering Sea continental shelf and slope. U.S. Dep. Commer., NOAA Tech. Memo. NMFS F/NWC-88, 338 p.

Shuntov, V. P.
1965. Distribution of the Greenland halibut and arrowtoothed halibuts in the north Pacific. [Translated by Isr. Program Sci. Transl., 1968. *In* P. A. Moiseev (ed.), Soviet fisheries investigations in the northeast Pacific, part 4, p. 147–156. [Available from U.S. Dep. Commer., Natl. Tech. Inf. Serv., Springfield, VA, as TT 67-51206.]

Smith, G. B., and R. G. Bakkala.
1982. Demersal fish resources of the eastern Bering Sea: Spring 1976. U.S. Dep. Commer., NOAA Tech. Rep. NMFS SSRF-754, 129 p.

Takenouti, A. Y., and K. Ohtani.
1974. Currents and water masses in the Bering Sea: a review of Japanese work. *In* D. W. Hood and E. Kelly (eds.), Oceanography of the Bering Sea, p. 39–57. Inst. Mar. Sci., Univ. Alaska, Fairbanks, Occasional Publ. 2.

Walters, G. E., K. Teshima, J. J. Traynor, R. G. Bakkala, J. A. Sassano, K. L. Halliday, W. A. Karp, K. Mito, N. J. Williamson, and D. M. Smith.
1988. Distribution, abundance, and biological characteristics of groundfish in the eastern Bering Sea based on results of the U.S.-Japan triennial bottom trawl and hydroacoustic surveys during May–September, 1985. U.S. Dep. Commer., NOAA Tech. Memo. NMFS F/NWC-154, 400 p.

Wasson, D. H., K. D. Reppond, J. K. Babbitt, and J. S. French.
1992. Effects of additives on proteolytic and functional properties of arrowtooth flounder surimi. J. Aquat. Food Prod. Technol., vol. 1(3/4):147–165.

Wilimovsky, N. J., A. Peden, and J. Peppar.
1967. Systematics of six demersal fishes of the north Pacific Ocean. Fish. Res. Board Can., Tech. Rep. 34, 52 p.

Yang, M. S.
1988. Morphological differences between two congeneric species of pleuronectid flatfishes: arrowtooth flounder, *Atheresthes stomias*, and Kamchatka flounder, *A. evermanni*. Fish. Bull. 86:608–611.

Yang, M. S., and P. A. Livingston.
1986. Food habits and diet overlap of two congeneric species, *Atheresthes stomias* and *Atheresthes evermanni*, in the eastern Bering Sea. Fish. Bull. 82:615–623.

Size-dependent predation risk in larval fishes: mechanistic inferences and levels of analysis

Douglas F. Bertram*

Friday Harbor Laboratories, University of Washington
620 University Road, Friday Harbor, Washington 98250-9299

In any ecological study, the level of observation, as well as the aggregation and analysis of data, affects the inferences that can be drawn. In fisheries science, many studies, covering a wide range of levels of analysis, have examined size-dependent processes, particularly predation, as a primary source of mortality for larval fish (reviewed by Bailey and Houde, 1989; Bertram and Leggett, 1994; Leggett and Deblois, 1994). A general result from those studies is that mortality rate declines as body size increases both across (e.g. Peterson and Wroblewski, 1984) and within species (e.g. van der Veer and Bergman, 1987). However, the use of that general result to forecast survival probabilities at lower levels of aggregation and analysis (e.g. for individual larvae) could lead to erroneous predictions (Pepin and Miller, 1993). Several recent studies have questioned the validity of the generality that increasing larval size reduces predation risk when analyses were conducted at the level of the individual and when the effects of prey size on vulnerability to predation were examined independently of age effects (Litvak and Leggett, 1992; Pepin et al., 1992; Bertram and Leggett, 1994).

The results of Pepin et al. (1992) show that the effect of larval size inversely affects vulnerability to predation, depending on the level at which the information is aggregated and analyzed. Contrasting patterns of larval mortality caused by predation within and between mesocosmic (2.7 m^3 circular tanks) trials were observed in the predation of yolk-sac and first-feeding capelin larvae, *Mallotus villosus*, by threespine sticklebacks, *Gasterosteus aculeatus* (Pepin et al., 1992). Prey age ranged from 1 to 5 d (median post-emergence) and prey size ranged from 5 to 5.8 mm. In each experimental trial, single naive predators were offered a cohort of 500 similar-age prey for 24 h. Comparisons between experiments indicated that greater mean size and age of larvae in the mesocosm reduced mortality due to predation. However, within experiments, larger larvae suffered higher mortality than did smaller individuals of the same age (see also Litvak and Leggett, 1992). Resolving the discrepancy between these results is important because the conclusions differ depending upon the level of observation and analysis. Large size and age were beneficial to larval survival when mean values for each trial were compared over the full range of available prey sizes (i.e. between trial comparisons). Conversely, large size at age was detrimental to larval survival at a lower level of observation and analysis (i.e. within trials) when a reduced range of prey sizes was examined. Patterns and generalizations based on observations from higher levels of aggregation (e.g. cohorts, populations, species) and extended ranges of data, although conceptually appealing, may be misleading for gaining insights into the mechanistic processes that affect larval survival at the level of the individual, where selection acts (Pepin and Miller, 1993). Moreover, to achieve an understanding of the mechanisms that determine overall survival, information from several levels of observation must be integrated (Crowder et al., 1992; Pepin and Miller, 1993). In this study I use fundamental foraging theory to examine an underlying mechanism that could have produced both of the observed mortality patterns in Pepin et al.'s (1992) results at low and higher levels of analysis, within and between trials, respectively.

Pepin et al. (1992) argued that the within- versus between-trial differences occurred because predators actively selected larger larvae within trials ("because of greater encounter or attack probabilities due to greater activity or longer perception distance [i.e. the distance that larvae were visible to the predator] relative to smaller prey") but as the average size of prey increased between trials, the average predation rate decreased owing to greater avoidance capabilities of the larger, older larvae. In accordance with foraging theory (e.g. Stephens and Krebs, 1986), the predators in Pepin et al.'s (1992) study may also have actively selected larger larvae because of their higher caloric value and hence their profitability to a predator within trials (prey handling time was likely to be size-independent in the study system; energetic costs of attack were also assumed to be independent of prey size). Furthermore, the consistently high profitability

* Send reprint requests to Department of Biological Sciences, Simon Fraser University, Burnaby, B.C., V5A 1S6 Canada.

Manuscript accepted 11 October 1995.
Fishery Bulletin 94:371–373 (1996).

of large larvae to a predator may have more than compensated for the fact that fewer larvae were captured as prey size increased, between trials.

I evaluated this proposition by estimating the total mass of prey that were consumed by predators in each of the 23 predation trials conducted by Pepin et al. (1992). I estimated the total number of prey ingested for each trial in two ways. First, as an estimate of the maximum number of prey ingested, I used the difference between the number of prey present at the beginning and end of each trial (Pepin, unpubl. data). Second, I calculated an estimate for the minimum number of prey ingested by using Equation 2 from Pepin et al. (1992). For each trial I estimated the total mass of prey consumed by multiplying the number of prey ingested by the mass of a capelin larva whose length was equal to the mean of prey lengths used in that trial. To calculate the mass of larvae of average length, I used a general allometric length-weight relationship for capelin (Pepin, 1995). The results demonstrate that the maximum total number of prey consumed per predator decreased significantly with increasing prey length between trials (Fig. 1A; F=22.1, df=1,21, P=0.0001, for the pooled data set). Moreover, the total maximum mass of prey consumed increased significantly with increasing prey length (Fig. 1B; F=52.8, df=1,21, P<< 0.001; see also Fig. 9 in Pepin et al., 1992). The latter result also held within all three categories of prey and predator length ratios.

It is worth noting that the group of triangles below the regression lines (Fig. 1, A and B) represent five trials from an experiment that employed the smallest predators (mean=38.4 mm vs. 50.6 mm for all 18 trials in other experiments; t=3.5, df=21, P=0.002) and the lowest temperatures (mean=11.6°C vs. 13.2°C for all other trials; t=2.6, df=21, P=0.016). It is likely that the low number of prey consumed during those trials (mean=393 vs. 474 for all other trials; t=7.9, df=21, P<<0.001) resulted from the small predator size and low temperature, because smaller predators consume fewer prey (Pepin et al., 1992) and activity and ingestion rates are generally reduced at low temperatures.

The minimum total number of prey consumed also decreased significantly with increasing prey length between trials (F=20.8, df=1,21, P=0.0002, for the pooled data set). The mass of prey consumed also increased with prey length within each prey and predator length category when the minimum number of prey consumed were used. When the results from each prey and predator length category were pooled, the relationship between prey consumption and prey length was not significant owing to the low prey consumption values for the five trials with anomalous temperatures and predator lengths (see above). There was a highly

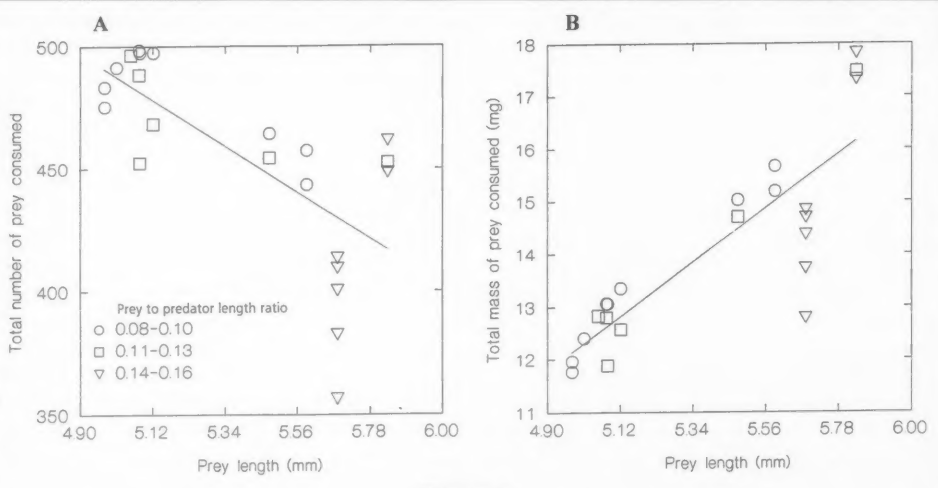

Figure 1

The total mass and number of larval capelin, *Mallotus villosus*, consumed by threespine stickleback, *Gasterosteus aculeatus*. Estimates of the maximum total number (**A**) (y=918–85.9x) and mass (**B**) (y=–11.1+4.7x) of prey consumed by sticklebacks versus the mean length of capelin larvae from 23 predation trials conducted by Pepin et al. (1992). The categories of prey and predator length ratio were assigned arbitrarily (on the basis of unpubl. data from P. Pepin). Regression equations were based on the pooled data set.

significant positive relationship between the minimum mass of prey consumed and prey length when those five trials were excluded from the analysis (F=43.9, df=1,16, P<<0.001). Thus, both estimates of prey consumption indicate a positive relationship between prey length and total mass of prey consumed.

My analysis is consistent with the interpretation that predators actively select the largest, most profitable prey to maximize both the mass of prey consumed and the caloric gain from an attack, as predicted by foraging theory. Because of this pattern of prey selection, predators consumed significantly more biomass as prey size increased, between trials, despite a decline in average predation mortality. More generally, the result confirms that larger larvae may be subject to higher rates of predation notwithstanding that their overall vulnerability to predation is inversely related to length. A future challenge will be to incorporate this result from several levels of analysis into longitudinal studies that examine the effects of mortality caused by predation on the size structure of cohorts of growing prey.

The above arguments on prey profitability are consistent with the interpretation of Pepin et al. (1992) that predators actively select larger prey because of greater encounter or attack probabilities that result from greater activity or a longer perception distance (i.e. the distance that a larva is visible to a predator) relative to smaller prey. Indeed predators may have selected larger prey because of the combined effects of higher profitabilities and encounter rates for larger prey. It is noteworthy, however, that prey encounter rates and profitability may not always increase in unison with increasing prey size because encounter rates will be dependent on prey behavior and the perception capabilities and size of the predator. Separating the general effects of prey encounter rate and profitability on predator size-selectivity (see also Juanes and Conover, 1994) will require mechanistic studies and modelling efforts that address prey behavior, profitability of the prey to a predator, as well as encounter, attack, and capture rates, all of which will require corresponding information on predator foraging technique and perception capabilities over a broad range of prey sizes and prey-to-predator size ratios.

Acknowledgments

I thank D. A. Roff for the discussion which prompted the analysis presented herein. P. Pepin graciously provided unpublished data. T. J. Miller, W. C. Leggett, P. Pepin, and three anonymous reviewers helped to improve the paper. Support was provided by a Natural Sciences and Engineering Research Council of Canada post doctoral fellowship.

Literature cited

Bailey, K. M., and E. D. Houde.
1989. Predation on eggs and larvae of marine fishes and the recruitment problem. Adv. Mar. Biol. 25:1–83.

Bertram, D. F., and W. C. Leggett.
1994. Predation risk during the early life history periods of fishes: separating the effects of size and age. Mar. Ecol. Prog. Ser. 109:105–114.

Crowder, L. B., J. A. Rice, T. J. Miller, and E. A. Marschall.
1992. Empirical and theoretical approaches to size-based interactions and recruitment variability in fishes. *In* D. L. DeAngelis, and L. J. Gross (eds.), Individual-based models and approaches in ecology: populations, communities, and ecosystems, p. 237–255. Chapman and Hall, New York, NY.

Juanes, F., and D. O. Conover.
1994. Piscivory and prey size selection in young-of-the-year bluefish: predator preference or size-dependent capture success? Mar. Ecol. Prog. Ser. 114:59–69.

Leggett, W. C., and E. Deblois.
1994. Recruitment in marine fishes: Is it regulated by starvation and predation in the egg and larval stages? Neth. J. Sea Res. 32:119–134.

Litvak, M. K., and W. C. Leggett.
1992. Age and size-selective predation on larval fishes: the bigger-is-better hypothesis revisited. Mar. Ecol. Prog. Ser. 81:13–24.

Pepin, P.
1995. An analysis of the length-weight relationship of larval fish: limitations of the general allometric model. Fish. Bull. 93:419–426.

Pepin, P., and T. J. Miller.
1993. Potential use and abuse of general empirical models of early life history processes in fish. Can. J. Fish. Aquat. Sci. 50:1343–1345.

Pepin, P., T. H. Shears, and Y. de Lafontaine.
1992. Significance of body size to the interaction between a larval fish (*Mallotus villosus*) and a vertebrate predator (*Gasterosteus aculeatus*). Mar. Ecol. Prog. Ser. 81:1–12.

Peterson, I., and J. S. Wroblewski.
1984. Mortality rate of fishes in the pelagic ecosystems. Can. J. Fish. Aquat. Sci. 41:1117–1120.

Stephens, D. W., and J. R. Krebs.
1986. Foraging theory. Princeton University Press. Princeton, NJ, 247 p.

van der Veer, H. W., and M. J. N. Bergman.
1987. Predation by crustaceans on a newly settled 0-group plaice *Pleuronectes platessa* population in the western Wadden Sea. Mar. Ecol. Prog. Ser. 35:203–215.

Stomach contents of juvenile cobia, *Rachycentron canadum*, from the northern Gulf of Mexico

James S. Franks
Gulf Coast Research Laboratory
P.O. Box 7000
Ocean Springs, Mississippi 39566-7000

Nikola M. Garber
Gulf Coast Research Laboratory
P.O. Box 7000
Ocean Springs, Mississippi 39566-7000
Present address: Bowling Green State University
313 Harshman–Bromfield
Bowling Green, Ohio 43403

James R. Warren
Gulf Coast Research Laboratory
P.O. Box 7000
Ocean Springs, Mississippi 39566-7000

The cobia, *Rachycentron canadum*, is a monotypic member of the family Rachycentridae. It is a migratory pelagic fish that occurs worldwide in tropical, subtropical, and warm temperate seas, except in the central and eastern Pacific Ocean (Shaffer and Nakamura, 1989). In the western Atlantic, the cobia occurs from Massachusetts and Bermuda to Argentina (Briggs, 1958) but is most common in the Gulf of Mexico (Migdalski and Fichter, 1983), ranging from Key West, Florida, along the Gulf coast to Campeche, Mexico (Dawson, 1971).

Some individual cobia are seasonal migrants, moving from wintering grounds near the Florida Keys into the Gulf of Mexico during spring, generally entering northern Gulf waters from April through May and returning to the wintering grounds during late fall and early winter (Franks et al., 1991; Biesiot et al., 1994). The timing of these migrations may relate to the availability of important prey species (Darracott, 1977).

A few observations on the food habits of adult *R. canadum* from the Gulf (Gulf of Mexico) have been reported. Knapp (1951) listed the stomach contents of 24 cobia taken near Port Aransas, Texas, and Miles (1949) briefly discussed the foods of 11 cobia from Aransas Bay, Texas. Reid (1954) mentioned the stomach contents of a single adult taken in the vicinity of Cedar Key, Florida, and Boschung (1957) remarked on the prey in four cobia collected off coastal Alabama. Christmas et al.[1] reported the prey of 11 adult cobia taken off Mississippi. A brief review of reported foods of cobia was presented by Shaffer and Nakamura (1989). Stomach contents of 287 cobia caught by hook and line in the northern Gulf of Mexico recreational fishery, mostly adults taken off Mississippi, were reported by Meyer and Franks (1996). None of these studies identified which prey, if any, were specifically consumed by juvenile cobia, rather, these observations were reported either for adults, for a size range comprising both juveniles and adults, or for cobia "in general." This paper represents the first study describing specifically the diet of juvenile *R. canadum*.

Knowledge of the feeding habits of juvenile cobia is necessary for understanding the role of diet in the recruitment processes of this economically important species and is a necessary prerequisite for management of this resource. The specific objective of this study was to analyze quantitatively the diet of juvenile cobia from the northern Gulf of Mexico.

Methods

Juvenile cobia were collected by trawl during fisheries resource surveys conducted in the northern Gulf of Mexico by the National Marine Fisheries Service (NMFS), Southeast Fisheries Science Center, Pascagoula, Mississippi. Fish were collected in July (n=7) and September (n=40) 1993 and in March (n=2) 1994 north of lat. 28°32'N and between long. 85°40'W and long. 93°55.4'W (Fig. 1). Most of the specimens (71%) were collected during September 1993 off Mississippi and Alabama. Bottom water depth ranged from 9 to 6 m.

Collection gear included a 28-m high-profile fish trawl with 0.6-cm codend mesh; a 19-m "western jib" shrimp trawl with 4-cm codend mesh; a 17-m "mongoose" shrimp trawl with 4-cm codend mesh; and

[1] Christmas, J. Y., A. Perry, and R. S. Waller. 1974. Investigations of coastal pelagic fishes. Gulf Coast Research Laboratory, P.O. Box 7000, Ocean Springs, MS 39566-7000. Completion Rep. to the U.S, Bur. Comm. Fish, Proj. 2-128-R, 105 p.

Manuscript accepted 13 December 1995.
Fishery Bulletin 94:374–380 (1996).

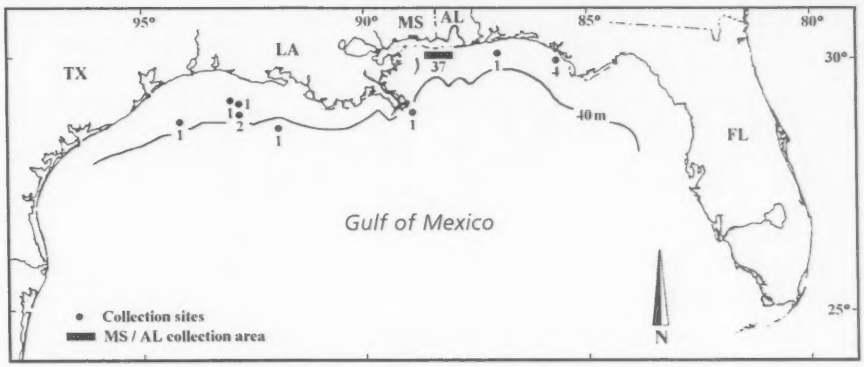

Figure 1

Collection sites and sample sizes of juvenile cobia, *Rachycentron canadum*, from the northern Gulf of Mexico. The MS/AL collection area comprised 17 collection sites.

a 13-m otter trawl with 4-cm codend mesh. Towing speed was 2.5 knots, and the duration of tows ranged from 0.25 to 1 h. Time and location were recorded for each tow. Juveniles were collected in 25 net hauls (18 by day; 7 at night). Whole specimens were frozen aboard the research vessel, generally <0.5 h following capture. In our laboratory, specimens were thawed, measured to the nearest mm fork length (FL), and weighed to the nearest 0.1 g total weight (TW). Stomachs were removed, opened, and designated either as containing food or as empty. Stomach contents were fixed in 10% buffered formalin and then placed in 50% ethanol. A cursory examination revealed that intestinal contents were too digested to be identified; thus, intestines were separated from stomachs at their confluence and discarded.

Stomach contents were placed onto a 0.840-mm mesh screen sieve and gently washed with fresh water. Prey were identified to the lowest taxa possible, counted, weighed (blotted wet weight) to the nearest 0.1 g, and measured volumetrically to the nearest 0.1 mL by water displacement in a graduated cylinder. Prey too digested for unequivocal identification were assigned to one of the appropriate principal prey categories (fish, crustaceans, or cephalopods) as "remains" and included in the determination of the contributions of those principal categories to the diet.

Stomach-content data were pooled for all stomachs and analyzed for percent numeric abundance (%*N*), percent of total volume (%*V*), and percent frequency of occurrence (%*F*) of prey items to describe quantitatively the diet, where %*N* = (number of individuals of one prey taxon divided by total number of all prey individuals) × 100; %*V* = (volume of one prey taxon divided by total volume of all prey) × 100; and %*F* = (number of stomachs containing prey of one taxon divided by total number of stomachs that contained any prey items) × 100. These methods have been reviewed by Windell (1971) and Hyslop (1980). These values were used to calculate an index of relative importance (*IRI*) (Pinkas, 1971), where the importance of an item is directly related to the size of the value:

$$IRI = (\%N + \%V) \times \%F.$$

Percent *IRI* (%*IRI*) was also calculated and consisted of the *IRI* value of each prey taxon divided by the sum of the *IRI* values (Eggleston and Bochenek, 1989). Empty stomachs were excluded from the above computations.

A small number of other items found in stomachs (e.g. mollusc shells and both larval and postlarval crustaceans and parasitic worms) were considered miscellaneous or nonfood items probably ingested incidentally in normal feeding. These were not used in calculating percentages or indices describing relationships of food items in the diet.

A stomach fullness index was calculated by dividing the total prey weight of each cobia by its total body weight × 100 (Sullivan and Gillman, 1993; Rooker, 1995). Stomach fullness was tested between daytime and nighttime captures, and to further examine diel feeding periodicity based on stomach fullness, cobia were grouped by time of capture into 6, 4-h periods: 0000–0400 (n=2); 0400–0800 (including dawn) (n=5); 0800–1200 (n=15); 1200–1600 (n=10); 1600–2000 (including dusk) (n=8); and 2000–2400 (n=9). A one-way analysis of variance (ANOVA) was used to test for differences in mean fullness between time intervals.

Chi-square (χ^2) 2 × 2 contingency table analyses and Fisher's exact test were used to test for differences in frequency occurrence of principle prey cat-

egories (fish, crustaceans, and cephalopods) between two size (FL) groups of juvenile cobia, small (236–338 mm) and large (340–440 mm), that represented all juveniles with food in their stomachs. The χ^2 test and Fisher's exact test were used to identify significant differences in frequency occurrence of principle prey categories between two geographic areas of juvenile collection (east of long. 89°W; west of long. 89°W), essentially described as east and west of the Mississippi River delta. The diet was also examined for seasonal differences in the occurrence of principal prey.

Results

Stomach contents of 49 juvenile *R. canadum* ranging from 236 to 440 mm FL (mean 335 mm) and from 0.08 to 0.81 kg TW (mean 0.34 kg) were examined. Thirty-nine of the 49 (80%) stomachs examined contained prey. The diet comprised three principal categories: fish, crustaceans, and cephalopods (Table 1).

Fishes occurred in 31 (79.5%*F*) of the stomachs containing food and represented 40.9% of the total number of prey and 37.7% of the total volume of prey (Fig. 2). The fish category dominated the *%IRI* (60.0%) (Fig. 2). Fish prey were represented by nine species (Table 1). Other fishes, owing to various states of digestion, could be identified only to genus (*Anchoa* sp. and *Symphurus* sp.) or family (Serranidae).

Anchovies were by far the predominant fish prey items, accounting for 19.7%*N* and 18.4%*V* of all items in the diet (Table 1). The striped anchovy, *Anchoa hepsetus*, was the dominant species by %*V* (9.2), *IRI* (163.8), and %*IRI* (4.9). The bay anchovy, *Anchoa mitchilli*, exhibited the highest numeric percentage (8.4) among fish in the diet; however, all specimens of *A. mitchilli* occurred in one stomach. The dominance of anchovies would be even greater if one considered that unidentifiable fish remains (15.1%*N*, 6.9%*V*, and 74.4%*F*) were primarily anchovies.

Crustaceans ranked first in importance numerically (42.7%*N*) and second by volume (37.4%*V*) and occurred in 59.0% of the stomachs (Fig. 2). Decapods were the most common crustaceans encountered (Table 1). The roughback shrimp, *Trachypenaeus similis*, was the dominant food item in the diet on the basis of %*N* (19.2), but all of these specimens occurred in only two stomachs. Other decapod species were brown rock shrimp, *Sicyonia brevirostris*, lesser rock shrimp, *Sicyonia dorsalis*, and iridescent swimming crab, *Portunus gibbesii*. Other decapods were identifiable only to Portunidae, Xanthidae, or Brachyura. *Sicyonia brevirostris* and *P. gibbesii* contributed 9.1%*V* and 5.9%*V* to the total diet, respectively (Table 1). Decapod remains (2.2%*V*) were categorized as being either those of shrimp (11.8%*N*, 33.3%*F*) or crab (0.8%*N*). The mantis shrimp, *Squilla empusa* (Stomatopoda), contributed 6.4%*V* but only 2.1%*N* to the diet.

Cephalopods were present in 17.9% of the stomachs and comprised 16.3%*N* and 24.9%*V* of prey organisms (Fig. 2). This group was represented by two species, the slender inshore squid *Loligo plei*, and the longfin inshore squid, *Loligo pealei*. Overall, *Loligo plei* dominated the diet among identifiable prey (17.0%*V*, 15.4%*F*, 494.3 *IRI* and 14.9% *IRI*) and was the second most important food item based on %*N* (15.1) (Table 1). *Loligo pealei* was the fifth ranking food item by volume, contributing 7.7%.

The proportion of empty stomachs was significantly greater for juveniles collected during the night (40%) than during the day (12%) (χ^2=3.518, df=1, P<0.05). Mean stomach fullness was found to vary significantly (with 95% confidence) between daytime (3.13) and nocturnal (0.92) collections (ANOVA, df=1, P<0.05) (Fig. 3). When further measured for specific time intervals of capture, mean fullness values were 0.08 (0001–0400), 2.00 (0400–0800), 3.29 (0800–1200), 2.45 (1200–1600), 3.70 (1600–2000), and 0.73 (2000–2400)

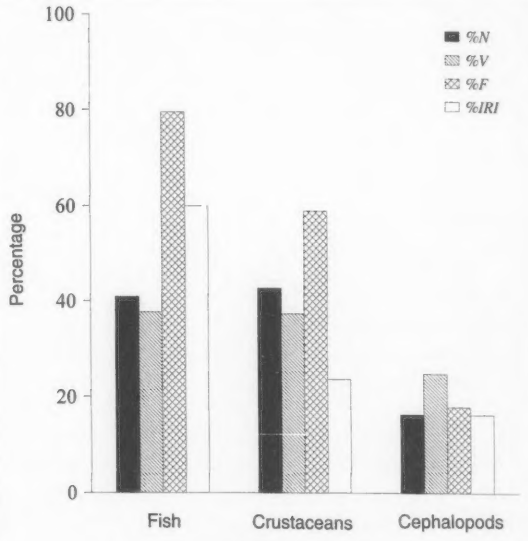

Figure 2

Percent numerical abundance (%*N*), percent total volume (%*V*), percent frequency of occurrence (%*F*), and percent index of relative importance (%*IRI*) for primary prey categories in the diet of juvenile *Rachycentron canadum* from the northern Gulf of Mexico.

(Fig. 4); however, the difference between these means was not statistically significant (ANOVA, df=5, $P>0.05$).

Comparison of the percent occurrence of principal prey categories between the diets of two groups of juvenile cobia based on length (group 1=236–338 mm FL; group 2=340–440 mm FL, Fig. 5) showed that the smaller juveniles fed primarily on crustaceans and fish, whereas fish were the primary foods of group 2. Crustaceans were found in 21 of 25 (84%) stomachs of fish in group 1 but in only 5 of 14 (36%) stomachs of fish in group 2. This indicated a highly significant ($\chi^2=8.469$, df=1, $P<0.05$) difference in diet and was directly related to the greater frequency occurrence of shrimp (including shrimp remains) in the diet of group-1 fish. Fish were important prey for both groups of juveniles (Fig. 5), and although we encountered fish more frequently in the stomachs of group-2 fish, fish occurrence between the two

Table 1

Prey items occurring in the stomachs of 39 juvenile cobia, *Rachycentron canadum*, from the northern Gulf of Mexico, 1993–94. % Frequency of occurrence is based on stomachs containing food (n=39). Unid = unidentified.

Prey	Number of individual prey items	% Number	Volume (mL)	% Volume	% Freqnency of occurrence	Index of relative importance (IRI)	% IRI
Class Osteichthyes							
Anchoa hepsetus	16	6.7	36.0	9.2	10.3	163.8	4.9
Anchoa mitchilli	20	8.4	29.0	7.4	2.6	41.1	1.2
Anchoa sp.	11	4.6	7.0	1.8	12.8	81.9	2.5
Saurida brasiliensis	2	0.8	7.0	1.8	2.6	6.8	0.2
Prionotus rubio	1	0.4	8.5	2.2	2.6	6.8	0.2
Centropristis philadelphica	2	0.8	5.0	1.3	2.6	5.5	0.2
Unid. serranid	3	1.3	0.5	0.1	2.6	3.6	0.1
Stenotomus caprinus	1	0.4	12.5	3.2	2.6	9.4	0.3
Abudefduf saxatilis	1	0.4	1.0	0.2	2.6	1.6	0.1
Trichiurus lepturus	1	0.4	1.0	0.2	2.6	1.6	0.1
Symphurus plagiusa	2	0.8	10.5	2.7	5.1	17.9	0.5
Symphurus sp.	2	0.8	3.0	0.7	5.1	7.7	0.2
Fish remains	36	15.1	27.0	6.9	74.4	1,636.8	49.5
Class Crustacea							
Stomatopoda							
Squilla empusa	5	2.1	25.0	6.4	7.7	65.5	2.0
Squilla chydaea	3	1.3	1.5	0.4	2.6	4.4	0.1
Squilla sp.	2	0.8	1.0	0.3	5.1	5.1	0.2
Decapoda							
Trachypenaeus similis	46	19.2	44.5	11.4	5.1	156.1	4.7
Sicyonia brevirostris	3	1.3	35.5	9.1	5.1	53.0	1.6
Sicyonia dorsalis	2	0.8	4.0	1.0	2.6	4.7	0.1
Portunus gibbesii	7	3.0	23.0	5.9	2.6	23.1	0.7
Unid. portunid	2	0.8	1.5	0.4	2.6	3.1	0.1
Unid. xanthid	1	0.4	0.5	0.1	2.6	1.3	0.1
Unid. brachyuran	1	0.4	1.0	0.2	2.6	1.6	0.1
Shrimp remains	28	11.8	8.5	2.1	33.3	462.9	13.9
Crab remains	2	0.8	0.5	0.1	5.1	4.6	0.1
Class Cephalopoda							
Loligo plei	36	15.1	66.5	17.0	15.4	494.3	14.9
Loligo pealei	2	0.8	30.0	7.7	5.1	43.4	1.3
Squid remains	1	0.4	1.0	0.2	2.6	1.6	0.1
Total	239		392.0			3,309.2	
Total stomachs analyzed	49						
No. (%) containing food	39 (80%)						
No. (%) empty	10 (20%)						

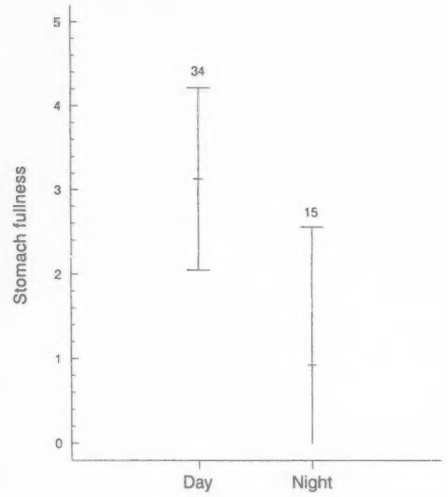

Figure 3

Comparison of day and night mean stomach fullness values (±95% CL) for juvenile *Rachycentron canadum* from the northern Gulf of Mexico. Number of fish sampled is given for each time period. Stomach fullness = prey weight/predator weight·100.

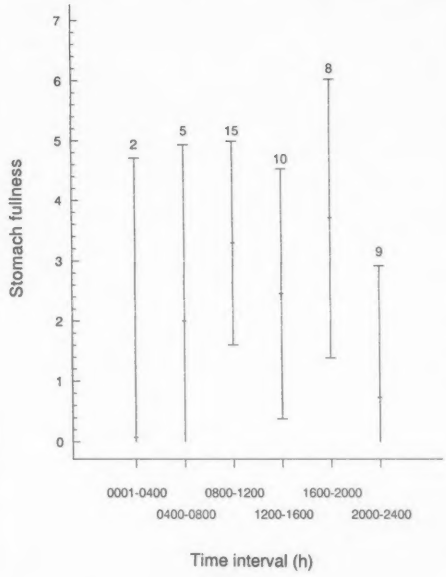

Figure 4

Diel feeding periodicity based on mean stomach fullness (±95% CL) for juvenile *Rachycentron canadum* from the northern Gulf of Mexico. Numbers over each series of values are sample sizes. Stomach fullness = prey weight/predator weight·100.

groups was not statistically different. The percent occurrence of cephalopods (squid) was low for both groups and differed insignificantly.

Chi-square contingency analysis suggested that geographic location did not significantly affect the diet, although we did observe that cephalopods (squid) were absent in the stomachs of all juveniles (n=6) collected west of the Mississippi River. The stomachs of the 2 cobia collected in March (spring) contained, collectively, the only specimens of sea bass (Serranidae, n=3) and xanthid crab (n=1) encountered in the study. The only other prey found in the stomachs of the juveniles collected in March were anchovies which, notably, were the predominant fish prey among the summer (July and September) cobia. A larger sample size is needed to assess accurately any geographic or seasonal variations in diet.

Discussion

We found that juvenile cobia captured by trawl in the northern Gulf of Mexico during fall 1993 and early spring 1994 were carnivorous and fed exclusively on small fish, crustaceans, and squid. Fish, crustaceans, and cephalopods also comprised the diet of adult cobia collected in the northcentral Gulf of Mexico (Meyer and Franks, 1996). On the basis of the frequency occurrence of prey in the diet of cobia caught near Aransas Bay, Texas, Knapp (1951) reported the predominance of fishes (83%), followed by stomatopods (58%), penaeid shrimps (46%), portunid crabs (42%), and squid (17%). Meyer and Franks (1996) reported that the percent frequency of occurrence and numeric percentage of crustaceans (79.1%F, 77.6%N) dominated that of fishes (58.5%F, 20.3%N) and cephalopods (13.2%F, 2.2%N). Our results showed that fish and crustaceans were present in the diet in approximately equal volumes, and, as reported by Miles (1949) and Christmas et al.)[1] for cobia taken off Texas and Mississippi, respectively, occurred in nearly equal numbers; however, we found that fish occurred in the diet with somewhat greater frequency than did crustaceans. Based on *IRI* calculations, the relative importance of fishes (*IRI*=1,984.5) as prey items was approximately three times that of shrimp (*IRI*=676.7) and three and one-half times that of squid (*IRI*=539.3).

In our study, anchovies were the dominant prey among the fish consumed and were major contributors to the diet. Unidentified fish remains, probably anchovies, occurred in almost 75% of the stomachs

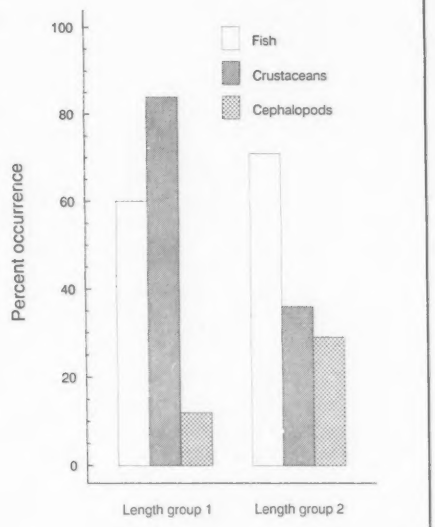

Figure 5

Principal prey of two length groups of juvenile *Rachycentron canadum*: Group 1 (236–338 mm FL, n=25) and Group 2 (340–440 mm FL, n=14), expressed as percent frequency of occurrence.

and were demonstrably important in the overall diet, exhibiting the highest *IRI* (1,636.8) and *%IRI* (49.5) of all food items. We observed that anchovies occurred in 36% of group-1 juveniles, whereas only 14% of the stomachs of group-2 juveniles contained anchovies. Because anchovies were rarely encountered (0.3%*F*) in the diet of northern Gulf adult cobia (Meyer and Franks, 1996), our findings may suggest a possible ontogenetic shift in feeding between juveniles and adults.

Trachypenaeus similis was a key component of the juvenile cobia diet on the basis of numeric and volumetric percentages, and our data show that shrimp, including shrimp remains, occurred in more than 41% of the stomachs, exceeded only by fish in percent frequency occurrence of prey. We found that crustaceans, primarily shrimp, occurred at a significantly higher frequency in the stomachs of smaller juveniles (84%) than in larger juveniles (36%). In contrast, Meyer and Franks (1996) reported that crustaceans, primarily portunid crabs, were the primary foods of adult cobia, based on percent occurrence, and essentially dominated the adult diet.

Loligo plei was one of the most important identified prey consumed by juvenile cobia. This species of squid is abundant in the northern Gulf of Mexico, particularly in shallower Gulf waters during spring and fall of the year (Hixon, 1980). Knapp (1951) reported the percent occurrence for *Loligo* in the diet of cobia as 17%. We report a similar percentage (18%) for *Loligo* and a percent occurrence of 21% for all loliginids combined. Meyer and Franks (1996) reported the percent occurrence of loliginids as ~12%.

Evaluation of diel feeding periodicity based on stomach fullness showed that juvenile cobia feed primarily during daylight. Although fullness peaked during the day, notably during late afternoon through dusk, there was no significant difference in fullness between daytime collection time intervals, including those containing dawn, noon, or dusk. Diana (1979) remarked that when fish with diel feeding cycles are collected at different intervals of time, some stomachs should be empty. We found that 20% of the stomachs we examined were empty.

Field observations in this study did not include reference to regurgitation of prey (i.e. everted stomachs or partially digested food in the mouth). Bowman (1986) stated that undetected regurgitation relative to fish food studies could produce severe underestimation of prey consumption, and he[2] reported that regurgitation is frequently observed in fishes trawled from depths exceeding 100 m. In our study only two cobia were collected at depths >40 m (i.e. 56 m and 66 m), and the stomach of each contained food. Incidentally, the juvenile from the 66-m site contained the second highest volume of food measured from all juvenile stomachs. Most cobia in our study (94%) were trawled from waters <30 m in depth. Even though somewhat limited by the small sample size of stomachs with prey, we were able to observe that increasing size (length) in juveniles appeared to influence an apparent ontogenetic shift from crustacean to piscine prey. Diet composition of juvenile cobia showed no marked changes in prey taxa between seasons or geographic locales.

Cobia are strong swimmers, quick enough to catch fish, squid, and decapod crustaceans. Personal observations, made by the senior author of cobia in culture systems and in natural habitats, reveal that *R. canadum* is a very aggressive feeder and quite capable of catching motile prey. Interestingly, prey species in this study demonstrate considerable diversity in the foraging behavior of juvenile cobia. Anchovies and squid are important components of the open-water nekton. Portunid crabs are both nektonic and benthic organisms. The shrimps and the Brachyuran crab, though capable of swimming, are

[2] Bowman, R. E. 1981. Examination of known and potential causes of variation in fish feeding studies. Northeast Fisheries Science Center, Natl. Mar. Fish. Serv., NOAA, 166 Water St., Woods Hole, MA 02543. Woods Hole Lab. Ref. Doc. 81-23, 29 p.

predominantly benthic inhabitants. Other prey, such as the blackwing searobin, *Prionotus rubio*, rock sea bass, *Centropristis philadelphica*, Atlantic cutlassfish, *Trichiurus lepturus*, longspine porgy, *Stenotomus caprinus*, and blackcheek tonguefish, *Symphurus plagiusa*, are essentially demersal. The variety of the diet in this study suggests that juvenile cobia often feed in the water column and possibly near the surface but primarily on or near the sea floor, exhibiting opportunistic feeding behavior comparable to that reported for adults (Meyer and Franks, 1996).

Acknowledgments

Special thanks go to Ian Workman, Dan Foster, Rob Caylor, and Mark Grace of the National Marine Fisheries Service, Pascagoula, Mississippi, for providing the specimens of juvenile cobia, as well as the field collection data, examined in this study. We thank Dianne Scott and Amber Garber for their assistance in the processing of stomachs. Appreciation is extended to Robin Overstreet, Harriet Perry, Gabriele Meyer, and Guillermo Sanchez for their help in the identification of stomach contents. Lisa Engel assisted in data entry. We also thank Robin Overstreet, Chet Rakocinski, and Patricia Biesiot for reviewing earlier versions of the manuscript and offering helpful comments. We also greatly appreciate the constructive comments and suggestions of two anonymous reviewers. Funding for this study was provided by the Gulf Coast Research Laboratory, the Mississippi Department of Marine Resources, and the Department of the Interior, U.S. Fish and Wildlife Service, Federal Aid for Sportfish Restoration Project F-91.

Literature cited

Biesiot. P. M., R. M. Caylor, and J. S. Franks.
1994. Biochemical and histological changes during ovarian development of cobia, *Rachycentron canadum*, from the northern Gulf of Mexico. Fish. Bull. 92:686–696.

Boschung, H. T., Jr.
1957. The fishes of Mobile Bay and the Gulf coast of Alabama. Ph.D. diss., Univ. of Alabama, Tuscaloosa, AL, 633 p.

Bowman, R. E.
1986. Effect of regurgitation on stomach content data of marine fishes. Environ. Biol. Fishes 16:171–181.

Briggs, J. C.
1958. A list of Florida fishes and their distribution. Bull. Fla. State Mus., Biol. Sci. 2:221–318.

Darracott, A.
1977. Availability, morphometrics, feeding and breeding activity in a multi-species, demersal fish stock of the western Indian Ocean. J. Fish. Biol. 10:1–16.

Dawson, C. E.
1971. Occurrence and description of prejuvenile and early juvenile Gulf of Mexico cobia, *Rachycentron canadum*. Copeia 1971:65–71.

Diana, J. S.
1979. The feeding and daily ration of young lemon sharks, *Negaprion brevirostris*, and the main effect of ration size on their growth and conversion efficiency. M.S. thesis, Univ. Miami, Coral Gables, FL, 129 p.

Eggleston, D. B., and E. A. Bochenek.
1989. Stomach contents and parasite infestation of school bluefin tuna *Thunnus thynnus* collected from the middle Atlantic Bight, Virginia. Fish. Bull. 88:389–395.

Franks, J. S., M. H. Zuber, and T. D. McIlwain.
1991. Trends in seasonal movements of cobia, *Rachycentron canadum*, tagged and released in the northern Gulf of Mexico. J. Miss. Acad. Sci. 36(1):55.

Hixon, R. F.
1980. Growth, reproductive biology, distribution and abundance of the three species of loliginid squid (Myopsida, Cephalopoda) in the northwest Gulf of Mexico. Ph.D. diss., Univ. Miami, Coral Gables, FL, 233 p.

Hyslop, E. J.
1980. Stomach content analysis—a review of methods and their application. J. Fish. Biol. 17:411–429.

Knapp, F. T.
1951. Food habits of the sergeantfish, *Rachycentron canadus*. Copeia 1951:101–102.

Meyer, G. H., and J. S. Franks.
1996. Food of cobia, *Rachycentron canadum*, from the northcentral Gulf of Mexico. Gulf Res. Rep. 9(3):161–167.

Migdalski, E. C., and G. S. Fichter.
1983. The fresh and salt water fishes of the world, p. 225–226. Crown Publishers, Inc., New York, NY.

Miles, D. W.
1949. A study of the food habits of the fishes of the Aransas Bay area. M.S. thesis, Univ. Houston, Houston, TX, 70 p.

Pinkas, L.
1971. Bluefin tuna habits. *In* L. Pinkas, M. S. Oliphant, and I. K. Iverson (eds.), Food habits of albacore, bluefin tuna, and bonito in California waters, p. 47–63. Calif. Dep. Fish Game, Fish. Bull. 152.

Reid, G. K., Jr.
1954. An ecological study of the Gulf of Mexico fishes, in the vicinity of Cedar Key, Florida. Bull. Mar. Sci. Gulf Caribb. 4:1–94.

Rooker, Jay R.
1995. Feeding ecology of the schoolmaster snapper, *Lutjanus apodus* (Walbaum), from southwestern Puerto Rico. Bull. Mar. Sci. 56(3):881–894.

Shaffer, R. V., and E. L. Nakamura.
1989. Synopsis of biological data on the cobia *Rachycentron canadum* (Pisces: Rachycentridae). FAO Fisheries Synop. 153 (NMFS/S 153). U.S. Dep. Commer., NOAA Tech. Rep. NMFS 82, 21 p.

Sullivan, K. M., and D. Gilliam.
1993. Diet and feeding habits of the southern stingray, *Dasyatis americana*, in the central Bahamas. Bull. Mar. Sci. 52(3):1007–1013.

Windell, F. T.
1971. Food analysis and rate of digestion. *In* W. E. Ricker (ed.), Methods for assessment of fish production in fresh waters, p. 215–226. Blackwell Sci. Publ., Oxford, England.

Winter capture of a harbor porpoise in a pelagic drift net off North Carolina

Andrew J. Read
Woods Hole Oceanographic Institution
Woods Hole, Massachusetts 02543
Present address: Duke University Marine Laboratory
135 Duke Marine Laboratory Road
Beaufort, North Carolina 28516-9721

John R. Nicolas
Northeast Fisheries Science Center
National Marine Fisheries Service, NOAA
Woods Hole, Massachusetts 02543

James E. Craddock
Woods Hole Oceanographic Institution
Woods Hole, Massachusetts 02543

Harbor porpoise, *Phocoena phocoena*, of the Bay of Fundy and Gulf of Maine are among the best-studied small cetaceans owing to their coastal nature, frequent encounters with commercial fisheries, and subsequent accessibility to researchers. Unfortunately, our knowledge of these animals is limited primarily to observations made during summer. In autumn most porpoises leave these coastal waters, and their winter distribution is unknown. Various hypotheses have been constructed to explain the apparent disappearance of these animals during the winter months, including that of migration to offshore banks or to a southern coastal area (Gaskin, 1984). Information on the winter distribution of harbor porpoises in the northwest Atlantic is needed to understand better the effects of human activities on this population, which is subject to large removals in coastal gill nets during the spring, fall, and summer (Read et al., 1993).

Existing information on the winter distribution of porpoises comes from strandings and a small number of dedicated surveys. From January to May, porpoises strand on the coasts of Massachusetts to North Carolina (Polacheck et al., in press), but most of these individuals are very young. Stranded adults are seldom encountered. Winter surveys are hampered by poor sighting conditions and so far have failed to find any significant concentrations of porpoises (Palka[1]). In this report, we document the incidental capture of a harbor porpoise in a pelagic drift net off the coast off North Carolina, during winter. The record is significant for two reasons. First, it is the southernmost incidental capture of a harbor porpoise in the northwest Atlantic. Second, observations of the stomach contents of this specimen suggest that the ecology of this population may be quite different in winter than in summer months.

The porpoise was captured on 25 February 1993, 75 km east of Nag's Head, North Carolina, at 35°55'N and 74°47'W, in water 229–293 m deep. Surface water temperature was 12–13°C. The net was set the previous evening and hauled early (0630–0830 h) in the morning. The float line was approximately 10 m below the surface of the water, and the porpoise was entangled near the top of the net. The porpoise was examined at sea by an observer, who noted that the porpoise had been killed recently "because the insides were steaming." Also in the net were a basking shark (*Cetorhinus maximus*), 2 ocean sunfish (*Mola mola*), 2 swordfish (*Xiphias gladius*) and 3 bluefish (*Pomatomus saltatrix*).

The porpoise was male, with a standard length of 129 cm and mass of 28.5 kg. Measurements of girth and blubber thickness indicated that the animal was healthy and robust. The observer collected life history tissues (teeth, stomach, and reproductive tract) from the carcass and transported them to Woods Hole. The age of the porpoise was estimated in the laboratory from counts of dentinal growth layers in thin, decalcified, and stained sections of teeth. Two independent estimates of the age of the animal were made, both indicating that the porpoise was born between April and June 1991. One testis measured $5.3 \times 2.4 \times 1.2$ cm and weighed 11 g without the epididymis. Histological examination of the testis and epididymis (Read and Hohn, 1995) revealed that the porpoise was sexually immature.

The forestomach contained the remains of many small mesoplagic prey not recorded from other harbor porpoises in the northwest Atlantic (Smith and Gaskin, 1974; Recchia and Read, 1989; Fontaine

[1] Palka, D. 1995. Preliminary cruise report of the spring distribution survey of harbor porpoises in the mid-Atlantic. Northeast Fisheries Science Center, Natl. Mar. Fish. Serv., Woods Hole MA 02543.

Manuscript accepted 26 October 1995.
Fishery Bulletin 94:381–383 (1996).

et al., 1994). Approximately 99% of the contents (145 g wet weight) comprised partially digested remains of a single species of lanternfish, *Ceratoscopelus maderensis*. Other prey were represented only by hard parts, such as otoliths and squid beaks. Cephalopod prey remains included 7 upper and one lower beak of *Selenoteuthis scintillans* and 2 lower beaks of *Loligo pealei*. In total, 1,994 otoliths from at least 8 fish species were recovered from the stomach (Table 1). The state of digestion of stomach contents suggested that the porpoise had been feeding mostly at night and in the early morning on small-bodied fish and squid.

Of the prey items we identified from this porpoise, only silver hake, *Merluccius bilinearis*, are common prey of harbor porpoises in the Gulf of Maine. In summer, harbor porpoises in the Bay of Fundy and Gulf of Maine feed primarily on Atlantic herring, *Clupea harengus*, augmenting this with silver hake and other demersal species (Smith and Gaskin, 1974; Recchia and Read, 1989). Recent analyses of the stomach contents of harbor porpoises from the southern Gulf of Maine indicate a shift to smaller-bodied prey, such as pearlside, *Maurolicus weitzmani*, during autumn (Read et al.[2]).

These observations lead us to suggest that harbor porpoises in the northwest Atlantic are not tied to shallow nearshore waters during winter. The stomach contents of this specimen indicate that porpoises can forage successfully on midwater prey in deep water. Similar prey remains have been recovered from the stomach of a harbor porpoise taken in Irish waters (Rogan and Berrow[3]). Porpoises can dive to depths of more than 225 m (Westgate et al., 1995), although deep-feeding excursions would not be necessary if mesopelagic prey are taken at night when they migrate toward the surface. Adult *Ceratoscopelus maderensis*, for example, are found at depths of 33–250 m at night (Scott and Scott, 1988). If porpoises are able to use the shelf edge and slope waters during winter, a large expanse of suitable habitat is available from the Grand Banks to Cape Hatteras. This hypothesis is supported by the observations of Stenson and Reddin,[4] who reported the incidental capture of harbor porpoises in experimental drift nets set during winter and spring off the slope of the Grand Banks outside the 1,000 m isobath.

A largely offshore winter distribution of harbor porpoises would explain the paucity of sightings of this species outside the summer and fall months. The Gulf of Maine population of harbor porpoises is believed to number more than 45,000 individuals (Palka, in press); such a large number of animals would have been detected in coastal waters, even during winter. We hypothesize that the population disperses to the south during winter and is found in low densities over the shelf and slope waters, possibly mixing with porpoises that summer in the Gulf of St. Lawrence and Labrador. Molecular genetic techniques are being used to address the question of stock mixing during winter (Rosel[5]). The many young porpoises that strand along the mid-Atlantic coast during this season, most of which are less than a year old, may have been segregated from the remainder of the population after they were weaned from their mothers.

We recognize that it is difficult to test this hypothesis of offshore dispersion during winter. Traditional visual census techniques are ineffective with very low densities of harbor porpoises, particularly given the weather conditions that prevail during this season. Few fisheries that might capture harbor porpoises are operative during this season; pelagic driftnet fishing effort is currently limited to only a few

[2] Read, A. J., J. E. Craddock, and D. Gannon. 1994. Life history of harbor porpoises and pilot whales taken in commercial fishing operations off the Northeast United States. Northeast Fisheries Science Center, Natl. Mar. Fish. Serv., Woods Hole, MA 02543. Final Contract Rep. 50-EANE-2-00082.

Table 1

Fish remains in the stomach of a harbor porpoise, *Phocoena phocoena*, killed in a pelagic drift net off Cape Hatteras on 25 February 1993.

Family	Species	Number of otoliths
Ophichthidae	*Myrophis punctatus*	2
Myctophidae	*Ceratoscopelus maderensis*	1,920
	Ceratoscopelus warmingii	1
	Myctophum affine	2
	Hygophum hygomii	4
Moridae	*Laemonema* sp. (?)	29
Merlucciidae	*Merluccius bilinearis*	4
Percomorph	Unidentified	32

[3] Rogan, E., and S. D. Berrow. 1995. Aspects of the biology of the harbour porpoise, *Phocoena phocoena*, in Irish waters. Paper SC/47/SM40 presented at the 47th meeting of the Scientific Committee of the International Whaling Commission, Dublin, Ireland.

[4] Stenson, G. B., and D. G. Reddin. 1991. Incidental catches of small cetaceans in drift nets during salmon tagging experiments in the Northwest Atlantic. *In* Harbor porpoise in eastern North America: status and research needs; workshop held 5–8 May 1992 at Northeast Fish. Sci. Cent., Natl. Mar. Fish. Serv., Woods Hole, MA 02543.

[5] Rosel, P. 1995. Department of Zoology, Univ. New Hampshire, Durham NH 03824. Personal commun.

trips each winter. Instead, alternative techniques, such as tracking the movements of individual porpoises by satellite telemetry and the use of nontraditional census techniques (e.g. acoustic surveys), may reveal where these animals spend their winter months.

Acknowledgments

We thank the observer, Dianne Borgaard, for her careful observations and meticulous dissection at sea. Damon Gannon identified the cephalopod prey remains, Eugenia Bohlke identified the worm eel, Stephanie Fernandez prepared the tooth sections, and Aleta Hohn read the tooth and testis sections. This research was supported by Contract 50-EANE-2-00082 from the Northeast Fisheries Science Center, NMFS/NOAA.

Literature cited

Fontaine, P. M., M. O. Hammill, C. Barette, and M. C. S. Kingsley.
1994. Summer diet of the harbour porpoise *(Phocoena phocoena)* in the estuary and the northern Gulf of St. Lawrence. Can. J. Fish. Aquat. Sci. 51:172–178.

Gaskin, D. E.
1984. The harbour porpoise *Phocoena phocoena* (L.): regional populations, status, and information on direct and indirect catches. Rep. Int. Whaling Comm. 34:569–586.

Palka, D.
In press. Abundance estimate for the Gulf of Maine harbor porpoise. Rep. Int. Whaling Comm. Spec. Issue 16.

Polacheck, T., F. Wenzel, and G. Early.
In press. What do stranding data say about harbor porpoise (*Phocoena phocoena*)? Rep. Int. Whaling Comm. Spec. Issue 16.

Read, A. J., and A. A. Hohn.
1995. Life in the fast lane: the life history of harbor porpoises from the Gulf of Maine. Mar. Mamm. Sci. 11:423–440.

Read, A. J., S. D. Kraus, K. D. Bisack, and D. Palka.
1993. Harbor porpoises and gill nets in the Gulf of Maine. Conserv. Biol. 7:189–193.

Recchia, C. A., and A. J. Read.
1989. Stomach contents of harbour porpoises, *Phocoena phocoena* (L.), from the Bay of Fundy. Can. J. Zool. 67:2140–2146.

Scott, W. B., and M. G. Scott.
1988. Atlantic fishes of Canada. Can. Bull. Fish. Aquat. Sci. 219, 731 p.

Smith, G. J. D., and D. E. Gaskin.
1974. The diet of harbour porpoises (*Phocoena phocoena* (L.)) in coastal waters of eastern Canada, with special reference to the Bay of Fundy. Can. J. Zool. 52:777–782.

Westgate, A. J., A. J. Read, P. Berggren, H. N. Koopman, and D. E. Gaskin.
1995. Diving behaviour of harbor porpoises, *Phocoena phocoena.* Can. J. Fish. Aquat. Sci. 52:1064–1073.

Erratum

Erratum: Fishery Bulletin 94(1), p. 173.

Lang, Kathy L., Frank P. Almeida, George R. Bolz, and Michael P. Fahay.

The use of otolith microstructure in resolving issues of first year growth and spawning seasonality of white hake, *Urophycis tenuis*, in the Gulf of Maine–Georges Bank region.

Correction: Text and Figure 4 (page 173) should read as follows:

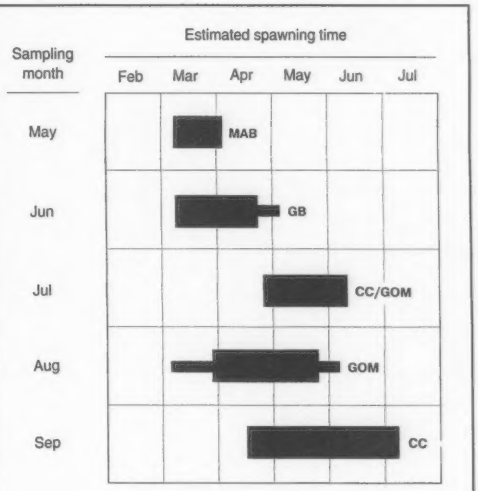

Figure 4

Back-calculated spawning times of juvenile white hake, *Urophycis tenuis*. Narrow bars indicate single observations. (MAB = mid-Atlantic Bight; GB = Georges Bank; CC = Cape Cod; and GOM = Gulf of Maine.)

Back-calculated spawning dates indicated that peak spawning occurred in the spring for fish collected from the mid-Atlantic Bight and Georges Bank (smaller, younger individuals), whereas peak spawning occurred in late spring/early summer (May–June) for fish collected along coastal New England (larger, older individuals) (Fig. 4).

Superintendent of Documents **Subscriptions** Order Form

***5178**

☐ **YES,** enter my subscription(s) as follows:

_____ subscriptions to ***Fishery Bulletin (FB)***
for $32.00 per year ($40.00 foreign).

The total cost of my order is $_____. Prices include regular domestic postage and handling and are subject to change.

_____
(Company or Personal Name) (Please type or print)

_____
(Additional address/attention line)

_____
(Street address)

_____
(City, State, ZIP Code)

_____
(Daytime phone including area code)

_____
(Purchase Order No.)

Charge your order. It's Easy!

MasterCard

VISA

S3S

For privacy protection, check the box below:
☐ Do not make my name available to other mailers

Please choose method of payment:
☐ Check Payable to the Superintendent of Documents
☐ GPO Deposit Account ☐☐☐☐☐☐☐ – ☐
☐ VISA or MasterCard Account
☐☐☐☐☐☐☐☐☐☐☐☐☐☐☐☐
☐☐☐☐ (Credit card expiration date)

To fax your orders (202) 512–2233

Thank you for your order!

_____
(Authorizing Signature)

Mail To: Superintendent of Documents
P.O. Box 371954, Pittsburgh, PA 15250–7954

Fishery Bulletin
Guide for Contributors

Preparation

Title page should include authors' full names and mailing addresses and the senior author's telephone and FAX number.

Abstract should not exceed one double-spaced typed page. It should state the main scope of the research but emphasize its conclusions and relevant findings. Because abstracts are circulated by abstracting agencies, it is important that they represent the research clearly and concisely.

Text must be typed double-spaced throughout. A brief introduction should portray the broad significance of the paper; the remainder of the paper should be divided into the following sections: **Materials and methods**, **Results**, **Discussion** (or **Conclusions**), and **Acknowledgments**. Headings within each section must be short, reflect a logical sequence, and follow the rules of multiple subdivision (i.e. there can be no subdivision without at least two items). The entire text should be intelligible to interdisciplinary readers; therefore, all acronyms, abbreviations, and technical terms should be spelled out the first time they are mentioned. The scientific names of species must be written out the first time they are mentioned; subsequent mention of scientific names may be abbreviated. Follow the *U.S. Government Printing Office Style Manual* (1984 ed.) and the *CBE Scientific Style and Format* (6th ed.) for editorial style, and the most current issue of the American Fisheries Society's *Common and Scientific Names of Fishes from the United States and Canada* for fish nomenclature. Dates should be written as follows: 11 November 1991. Measurements should be expressed in metric units, e.g., metric tons as (t); if other units of measurement are used, please make this fact explicit to the reader. The numeral one (1) should be typed as a one, not as a lower-case el (l).

Text footnotes should be numbered with Arabic numerals. Footnote all personal communications, unpublished data, and unpublished manuscripts with full address of the communicator or author, or, as in the case of unpublished data, where the data are on file. Authors are advised to avoid references to nonstandard (gray) literature, such as internal, project, processed, or administrative reports. Where these references are used, please include whether they are available from NTIS (National Technical Information Service) or from some other public depository.

Literature cited comprises published works and those accepted for publication in peer-reviewed literature (in press). Follow the name and year system for citation format. In the text, cite as follows: Smith and Jones (1977) or (Smith and Jones, 1977). If there is a sequence of citations, list chronologically: Smith, 1932; Smith and Jones, 1985; Smith and Allen, 1986. Abbreviations of serials should conform to abbreviations given in *Serial Sources for the BIOSIS Previews Database*. Authors are responsible for the accuracy and completeness of all citations.

Tables should not be excessive in size and must be cited in numerical order in the text. Headings should be short but ample enough to allow the table to be intelligible on its own. All unusual symbols must be explained in the table legend. Other incidental comments may be footnoted with italic numerals. Use the asterisk only to indicate probability in statistical data. Because tables are typeset, they need only be submitted typed and formatted, with double-spaced legends. Zeros should precede all decimal points for values less than one.

Figures include line illustrations and photographs (or slides) and must be cited in numerical order in the text. Unless photographs are submitted on glossy paper with good contrast, we cannot guarantee a good final printed copy. Figures are to be labeled with author's name and number of figure. Use Times Roman font (boldface) to label divisions within figures. Zeros should precede all decimal points for values less than one. Figures may be submitted as computer software files, as photomechanical transfers (PMT's), or as high quality photographic prints. Figures submitted as software files must be saved in the software program with which they were created. Do not submit them as EPS files. Send only xerox copies of figures to the Scientific Editor; original figures will be requested later when the manuscript has been accepted for publication. Figure legends should explain all symbols and abbreviations and should be double-spaced on a separate page at the end of the manuscript.

Copyright law does not cover government publications; they fall within the public domain. If an author reproduces any part of a government publication in his work, reference to source is considered correct form.

Submission

Send printed copies (original and two copies) to the Scientific Editor:

Dr. John B. Pearce, Scientific Editor
Northeast Fisheries Science Center
National Marine Fisheries Service
166 Water Street
Woods Hole, MA 02543-1097

Once the manuscript has been accepted for publication, you will be asked to submit a software copy of your manuscript to the Managing Editor. The software copy should be submitted in *WordPerfect* text format (or in standard ASCII text format if *WordPerfect* is unavailable) and should be placed on a 5.25-inch or 3.5-inch disk that is double-sided, double or high density, and that is compatible with either DOS or Apple Macintosh systems.

Copies of published articles and notes are available free of charge to the senior author (50 copies) and to his or her laboratory (50 copies). Additional copies may be purchased in lots of 100 when the senior author receives page proofs.

☆ U.S. Gov. Printing Office 1996
790-016/20006